ISSN 2095-3933
CN 33-1377/R

JOURNAL OF ELECTROCARDIOLOGY AND CIRCULATION

心电与循环

钱江 15th QICC | 心血管会议
Qianjiang International Cardiovascular Conference

XIN DIAN YU XUN HUAN

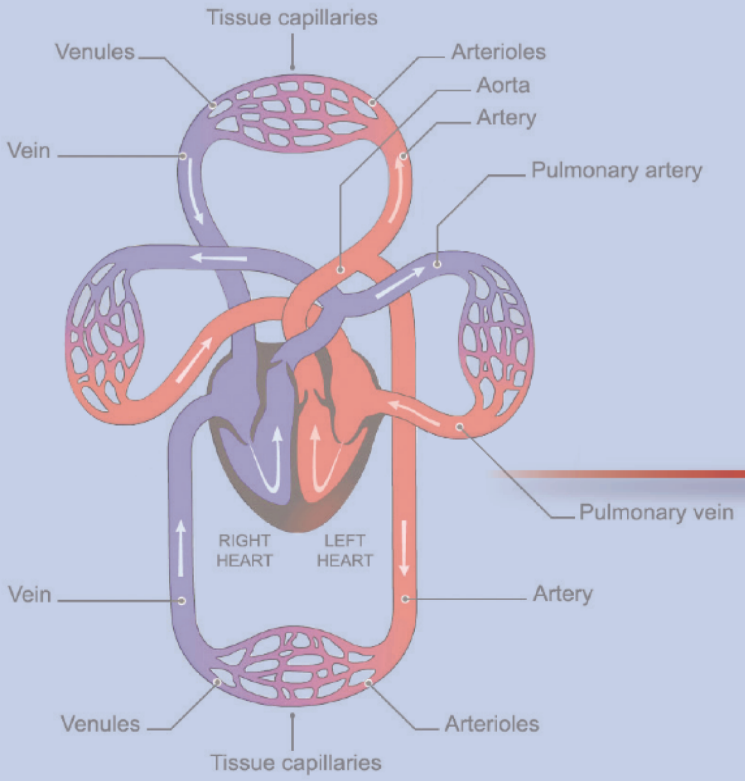

第十五届钱江国际心血管病会议

THE 15TH QIANJIANG INTERNATIONAL CARDIOVASCULAR CONFERENCE

论 文 汇 编

第40卷 增刊 第2期
2021·9
浙 江 省 医 学 会

心电与循环

JOURNAL OF ELECTROCARDIOLOGY AND CIRCULATION

双月刊 1982年9月创刊 第40卷 增刊第2期 2021年 9 月 22 日出版

浙出增刊备案号（331377202102）

主 管
浙江省卫生健康委员会
310006，杭州市庆春路216号

主 办
浙江省医学会
310003，杭州市武林广场
浙江省科协大楼

编 辑
《心电与循环》编辑部
310003，杭州市武林广场
浙江省科协大楼
电话：0571-87567813，87567809
官网：www.xdyxh.com
微信公众号：xdyxhzzs
E-mail：xdyxh@vip.126.com

主 编
王建安

出 版
浙江《心电与循环》杂志社
310003，杭州市武林广场
浙江省科协大楼

广告发布登记证号
浙市监广发Z-034号

印 刷
杭州日报报业集团
盛元印务有限公司

发 行
国内：浙江省报刊发行局
国外：中国出版对外贸易总公司
（北京782信箱，100011）

订 阅
全国各地邮局
邮发代号32-61

定 价
25.00元

中国标准连续出版物号
ISSN 2095-3933
CN 33-1377 / R

目 次

英文摘要

病例分析

责任编辑　马雯娜　沈昱平　杨丽　陈丹　严玮雯　李媚　陈丽　俞骏文　孙家衍

编辑部启事

1. 本刊官网网址为 www.xdyxh.com，欢迎作者进行在线投稿。
2. 欢迎广大读者、作者关注本刊微信公众号。

●英文摘要

The long–term prognosis of Culotte vs. different Crush strategies procedures in unprotected left main bifurcation coronary lesions: a systematic review and meta–analysis

WANG Hailong　PANG Xiaohua

Chongqing University Three Gorges Hospital, Chongqing 404040, China

[Abstract] **Background** Culotte and different Crush strategies are still controversial in patients with PCI treatment for PCI treatment in the unprotected left main bifurcation coronary lesions(UPLMBCLs). **Methods** We systematically searched the PubMed, Embase, Medline and Wanfang databases, and the search time was set from the establishment of the database to June 2021. We reviewed all the studies on the prognosis of different Crush and Culotte strategy in PCI. We analyzed all included studies, reviewed the quality of the study, and analyzed publication bias and heterogeneity. **Results** A total of 8 studies included 1 283 patients (710 patients with 4 different Crush strategies, 573 patients with Culotte strategy). Comprehensive analysis found that the incidence of major adverse cardiac event (MACE) in the Mixed–Crush group was higher than that in the Cullote group ($P<0.05$), the Culotte group was higher than the DK–Crush group ($P<0.01$), and there was no statistically significant difference between Mini–Crush and Cullote ($P>0.05$). The incidence of target lesion revascularization (TLR) in the Cullote group was significantly higher than that in the DK–Crush group ($P<0.01$), there was a similar incidence of TLR between the Mini–Crush group and the Cullote group ($P>0.05$), and there was a similar incidence between the Nano–Crush group and the Cullote group ($P>0.05$). The incidence of myocardial infarction (MI) in the Cullote group was higher than that in the DK–Crush group ($P<0.05$), and there was a similar incidence between Mini–Crush and Cullote groups ($P>0.05$). The incidence of cardiogenic death (CD) in the DK–Crush group was similar to that in the Cullote group ($P>0.05$), and there was a similar incidence between the Mini–Crush and Cullote groups ($P>0.05$). **Conclusion** We conclude that for the PCI management strategy for UPLMBCLs, patients receiving DK–Crush have the greatest long–term benefit, and those receiving Mixed–Crush have the least long–term benefit. The long–term benefits of Mini–Crush, Nano–Crush and Culotte strategy are similar, so we recommend that patients undergoing PCI with UPLMBCLs should use the DK–Crush strategy.

[Key words] Culotte strategy; Different Crush strategies; Unprotected left main bifurcation coronary lesions

Exogenous rDLK1 improves neovascularization after hindlimb ischemia

YOU Yayu　ZHANG Ning　XIE Xiaojie

The Second Affiliated Hospital Zhejiang University School of Medicine, Hangzhou 310009, China

[Abstract] **Objective** To determine whether delta–like non–canonical Notch ligand 1(DLK1) could affect angiogenesis and blood flow recovery after critical limb ischemia. **Methods** Mouse model of hindlimb ischemia created by femoral artery ligation was performed on 6–8 weeks old male C57BL/6 mice. From Day 0, Mice were injected intravenously with recombinant DLK1(rDLK1) (0.1 mg/kg) or vehicle every 3 days for 14 days. Hindlimb blood flow was sequentially measured before and at 0, 3, 7, and 14 days after surgery. Angiogenesis was detected by CD31 staining,

and mature blood vessel was assessed by α–SMA staining. In addition, flow cytometry was used to evaluate the endothelial progenitor cell (EPC) ($CD34^+$/KDR+) mobilization from bone marrow to ischemic muscles. **Results** rDLK1–treated mice showed better recovery than vehicle control–treated mice at days 3 and 7 post–surgery. This result was further supported by increased CD31+ and a–SMA+ vessels in the ischemic muscles of rDLK1–treated mice compared to the vehicle group. In addition, The rDLK1 group exhibited significantly enhanced EPC mobilization from bone marrow to ischaemic tissue during the progression of hindlimb ischemia. **Conclusion** These findings suggested that rDLK1 repletion may inhibit ischemia–induced damage by promoting EPC mobilization, thus improve angiogenesis and tissue repair. This benefit of rDLK1 may lead to a new therapeutic approach for critical hindlimb ischemia.

[Key words] Peripheral arterial disease; Delta–like non–canonical Notch ligand 1; Hindlimb ischemia

Decellularized porcine pericardium with double network hydrogel coating to improve the biological properties of bioprosthetic heart valves

CHENG Si LIU Xianbao Wang Jian'an

The Second Affiliated Hospital Zhejiang University School of Medicine, Hangzhou 310009, China

[Abstract] **Objective** To confirm whether combining decellularization with the synergistic effect of double network hydrogel improves these above–mentioned biological properties of bioprosthetic heart valves (BHVs). **Methods** In in–vitro tests, attenuated total reflection fourier transform infrared spectroscopy (ATR–FTIR), scanning electron microscope (SEM), energy dispersive spectroscopy (EDS), ematoxylin–eosin (HE) staining, Masson staining and immunofluorescence staining were utilized to confirm the morphologies and chemical characterization of decellularized glutaraldehyde–treated porcine pericardium(dCell–PP), hyaluronic acid hydrogel–coated dCell–PP (HA–PP), polyacrylamide hydrogel–coated dCell–PP (PAAm–PP) and PAAm/HA double network hydrogel–coated dCell–PP (P/H–PP). The tests of water contact angle, protein adsorption, platelet adhesion, hemolysis and arteriovenous shunt (AV–shunt) assay were applied to assess hemocompatibility. Endothelialization was observed by human umbilical vein endothelial cells (HUVECs) viability assay, HUVECs proliferation assay and HUVECs migration assay. Inflammation was observed by cell viability assay of RAW 264.7 Cells, enzyme linked immunosorbent assay (ELISA) assay and immunofluorescence staining. After accelerated calcification treatment, EDS mapping and alizarin red staining were utilized to evaluate the ability of anti–calcification. Collagenase, elastase, glycosaminoglycans degrading enzymes (GAGase) degradation tests were were used to observe component stability. Biomechanical properties were assessed by uniaxial tensile test, anti–suture tearing test, pulsatile flow test and accelerated fatigue test. After implanted subcutaneously in rats for 30 days, materials stability and biocompatibility in vivo were evaluated by using of histological analysis, immunohistochemistry staining, immunofluorescence, Masson staining, victoria blue staining, alcian blue staining, alizarin red staining and Von kossa staining. **Results** In vitro, it was confirmed that the decellularization process was successful and the hydrogel existing outside the porcine pericardium did conform to the chemical composition and structure of HA and PAAm. In terms of hemocompatibility, we found that P/H–PP adsorbed less protein than Glut–PP and had an effective anti–platelet adhesion ability than Glut–PP. After circulation of rabbit AV–shunt assay for 2 h, the section and surface images showed that the lumen of P/H–PP was almost clean, with a few small thrombi on the surface, while the lumen of the dCell–PP and Glut–PP was completely blocked and numerous thrombus formed on the surface. In the aspect of endothelialization, dCell–PP without hydrogel coating was unable to support the growth of HUVECs, and on the contrary, P/H–PP could facilitate the adhesion, proliferation and migration of HUVECs. As to inflammation responses, P/H–PP did not trigger inflammation

compared with other groups. In the aspect of calcification,numerous nodules of calcium deposits were observed in the Glut–PP, dCell–PP and HA–PP, but no visible calcification was detected in the PAAm–PP and P/H–PP. To assess the stability of extracellular matrix (ECM), collagenase, elastase and glycosaminoglycans degradation enzyme were used to treat the specimens. P/H–PP, PAAm–PP, and Glut–PP showed significantly lower weight–loss ratios compared with that of dCell–PP and HA–PP. We further evaluated the biomechanical properties, the ultimate tensile strength (UTS) and Young's modulus of P/H–PP were significantly higher than that of dCell–PP. Under different cardiac outputs, heart rate and mean arterial pressure, effective orifice area (EOA) and total regurgitant fraction of P/H–PP all conformed the requirements of ISO 5480. As to the durability, after 150 million cycles, EOA and total regurgitant fraction of P/H–PP still met the requirements of ISO 5480. In vivo, after implanted subcutaneously in rats for 30 days, P/H–PP showed better ECM stability, mitigated inflammation response, and reduced calcification than Glut–PP and dCell–PP. **Conclusion** All these results indicate that we develop a novel approach based on decellularized porcine pericardium with double network hydrogel coating to improve the biological properties of BHVs, such as the effects of extending durability, accelerating endothelialization, anti–coagulation, anti–inflammation and anti–calcification. In the future, this strategy has the potential for creating a variety of double network hydrogel–coated hybrid biomaterials.

[Key words] Bioprosthetic heart valves; P/H–PP; Human umbilical vein endothelial cells

Tanyu Tongzhi Formula enhances atherosclerotic plaque stabilization by promoting M2 macrophage polarization via AKT/ERK and PPARγ signaling in ApoE knock–out Mice

MA Lan MAO Wei

The First Affiliated Hospital of Zhejiang Chinese Medical University, Hangzhou 310006, China

[Abstract] Our previous studies have demonstrated Tanyu Tongzhi Formula (TTF) could significantly alleviate the clinical symptoms of patients with coronary heart disease (CHD), lower the level of serum lipids and inflammatory factors of CHD patients and AS model rats. We aim to assess the effect of TTF on atherosclerotic plaque in $ApoE^{-/-}$ mice and explore the underlying mechanisms involved in macrophage polarization in this study. 40 male $ApoE^{-/-}$ mice were divided randomly into 4 groups. Mice in the control group were fed with a regular diet, while mice in the HFD, TTF–L, and TTF–H group were fed with high fat diet (HFD) and received either saline or TTF at concentration of 0.60, 2.25 g/mL by daily oral gavage for 16 weeks. Our results showed that, in TTF–L and TTF–H groups, the levels of serum cholesterol (CHOL), triglyceride (TG), IL–1β, IL–6, and tumor necrosis factor–(TNF–) α of mice significantly decreased, the content of lipids decreased and percent area of collagen increased in atherosclerotic plaque compared with the HFD group. Moreover, TTF remarkably promoted the expression of M2 macrophage markers (Fizz1, Arg1, Mrc), suppressed the expression of M1 macrophage markers (TNF–α, IL–1β, IL–6) by increasing PPARγ expression, and inhibiting AKT/ERK activation. We further found that M2 polarization is reduced when the PPARγ is inhibited or AKT/ERK pathway is activated. Thus, TTF stabilized and delayed atherosclerotic plague progression by promoting M2 polarization via increasing PPARγ and inhibiting AKT/ERK phosphorylation, which could provide more theoretical basis for its clinical application.

[Key words] Tanyu Tongzhi Formula; Atherosclerosis;M2 macrophage polarization; PPARγ

Current status and considerations of clinical experience in the treatment of atherosclerosis from the perspective of phlegm

MA Lan

The First Affiliated Hospital of Zhejiang Chinese Medical University, Hangzhou 310006, China

[Abstract] Atherosclerosis is characterized by lipid core composed of atherosclerotic lipid and necrotic substance, and fibrous cap composed of focal fibrous thickening of intima. Phlegm is mostly formed by stagnation of fluid, which can be distributed throughout the body with the rise and fall of Qi. The phlegm production in the vascular tract is closely related to the formation of atherosclerotic plaque and is the key driving factor in each link of its pathophysiology. Therefore, by reviewing the ancient and modern literature, the author analyzed the relationship between phlegm and different disease stages of atherosclerosis from the aspects of etiology, pathogenesis, clinical manifestations and treatment, so as to provide more theoretical basis for the treatment of atherosclerosis from phlegm.

[Key words] Phlegm; Retardance the vascular; Atherosclerosis; Staging; Chinese medicine

Endostar, a modified recombinant human endostatin, suppresses angiogenesis through inhibition of Wnt/β–catenin signaling pathway

XU Xiaoming

The First Affiliated Hospital of Zhejiang Chinese Medical University, Hangzhou 310006, China

[Abstract] Endostar, a novel modified recombinant human endostatin, is now widely studied for the treatment of diseases that are characterized or caused by pathological angiogenesis. However, its molecular mechanism remains unclear. In this study, we investigated the effects of Endostar on the Wnt/β–catenin signaling pathway, which has emerged as an important aspect of angiogenesis. We showed that Endostar significantly inhibited the proliferation, migration, invasion, and capillary–like tube formation of human umbilical vascular endothelial cells in a dose–dependent manner. Using a luciferase reporter assay, we also demonstrated that Endostar suppressed β–catenin–dependent T cell factor transcriptional activity in increasing doses. Moreover, we found that Endostar treatment also restricted the stabilized mutant β–catenin–mediated increase in transcriptional activity, suggesting that Endostar exerts its inhibitory influence on Wnt/β–catenin signaling by targeting β–catenin or its downstream molecules. Western blot and immunofluorescence results revealed that Endostar significantly decreased nuclear and total β–catenin levels. Finally, we discovered that Endostar down–regulated cyclin D1 and VEGF, two proteins that are known as the downstream targets of Wnt/β–catenin signaling and that also play important roles in angiogenesis. Our findings suggested that Endostar suppressed Wnt/β–catenin pathway activity in angiogenesis. These results support the use of Endostar in further clinical applications.

[Key words] Endostar; Wnt/β–catenin signaling pathway; Cyclin D1; VEGF

Angiogenesis inhibitor endostar prevents vasa vasorum neovascularization in the swine atherosclerosis model

XU Xiaoming

The First Affiliated Hospital of Zhejiang Chinese Medical University, Hangzhou 310006, China

[Abstract] **Objective** Vasa vasorum neovascularization is a key feature of atherosclerosis and is strongly associated with inflammatory infiltration, lipid deposition, intraplaque hemorrhage, and hemosiderin deposit. Here we investigate the effects of Endostar, a strong anti-angiogenic drug, on vasa vasorum neovascularization in the experimental porcine model of early atherosclerosis. **Methods** Eighteen adult male Ba-Ma mini pigs were randomly divided into three groups, with six animals in each group. The pigs in the normal (N) group were fed a normal diet for 18 weeks without balloon injury surgery. The animals in the atherosclerotic (AS) control group and the AS+Endostar group were fed a hypercholesterolemic diet for 12 weeks after balloon injury surgery, and received either saline or Endostar treatment for an additional six weeks, while remaining on the hypercholesterolemic diet. The atherosclerotic abdominal aorta and levels of serum lipids, TNF-α, IL-6 and hs-CRP were analyzed at 18 weeks. **Results** The AS group had significantly higher body weight and serum lipid concentration levels than the N group ($P<0.05$), attesting to the success of the hypercholesterolemic diet. However, no statistical differences were noted between the AS and AS+Endostar groups. Histopathology results revealed that vasa vasorum density and intima-media thickness (IMT) had also increased in the AS group, as compared with the N group ($P<0.05$). Endostar treatment significantly alleviated atherosclerosis with decreased vasa vasorum density and IMT (AS vs. AS+Endostar, $P<0.05$). The results from Western blot analysis indicated that the expression of VEGF, β-catenin and TNF-α in the atherosclerotic abdominal aorta was considerably reduced by the Endostar treatment. In addition, immunohistochemistry results showed that the angiogenesis markers VEGF and β-catenin were predominately localized in endothelial cells of adventitial vasa vasorum. The levels of serum inflammatory markers TNF-α, hs-CRP and IL-6 were significantly higher in the AS group compared with the N group ($P<0.05$), but showed no significant difference during the Endostar treatment, suggesting that local inhibition of angiogenesis was not accompanied by a change in serum inflammatory markers and the inhibitive effect of Endostar on local TNF-α expression may be due to the prevention of vasa vasorum neovascularization. **Conclusion** Our results demonstrated that Endostar treatment inhibited vasa vasorum neovascularization and AS progression in the experimental porcine model of early atherosclerosis, thus supports the role of vasa vasorum neovascularization in the development of atherosclerosis and the therapeutic potential of anti-angiogenesis intervention in atherosclerosis.

[Key words] Atherosclerosis; Vasa vasorum; Neovascularization; Endostar; Swine

Farnesoid X receptor agonist attenuates atherosclerosis development by repressing macrophage apoptosis and PCSK9 gene in APOE$^{-/-}$ mice

DAI Jin

The First Affiliated Hospital of Zhejiang Chinese Medical University, Hangzhou 310006, China

[Abstract] Farnesoid X receptor (FXR), a member of the nuclear receptor superfamily of ligand-activated transcription factors, plays an important role in the regulation of lipid homeostasis. Activation of FXR has been reported

to attenuate atherosclerosis development. However, its molecular mechanism remains unclear. In this study, we analyzed the effects of the FXR agonist GW4064 on macrophage apoptosis in atherosclerosis. We showed that GW4064 significantly improved plasma blood LDL–C levels and reduced atherosclerosis development by HE staining. Moreover, we found by that GW4064 reduced macrophage infiltration and repressed macrophage apoptosis both in vitro by flow cytometry and in atherosclerosis plaques with APOE–/mice. Western blot and real time PCR results revealed that GW4064 significantly decreased Fas/FasL levels, which are involved in plaque instability in humans. Finally, we discovered that GW4064 downregulated PCSK9 and upregulated LDLR levels, which also play important roles in LDL–C regulation and macrophages apoptosis. In summary, our findings demonstrated that GW4064 attenuated the atherosclerosis development, which was related with the repressed macrophages apoptosis and down–regulated of PCSK9 expression.

[Key words] Farnesoid X receptor; Atherosclerosis; Macrophage apoptosis; Proprotein convertase subtilisin/kexin type 9

Protective effects of tanshinone IIA on endothelial progenitor cells injured by tumor necrosis factor–α

YANG Jinxiu

The First Affiliated Hospital of Zhejiang Chinese Medical University, Hangzhou 310006, China

[Abstract] Tanshinone IIA (Tan IIA) is a traditional Chinese herbal medicine often used for prevention and treatment of cardiovascular disorders such as atherosclerosis. Endothelial dysfunction and associated inflammatory processes play an important role in the development of atherosclerosis. Endothelial progenitor cells (EPCs) constitute one aspect of the endothelial repair process. The aim of the present study was to evaluate the putative protective effect of Tan IIA on EPCs injured by tumor necrosis factor–α (TNF–α). EPCs were cultured from bone marrow derived mononuclear cells. EPC proliferation ability and migration capacity were determined using the MTT assay and transwell chamber assay, respectively. An EPC adhesion assay was performed by replating the cells on fibronectincoated dishes and then counting the adherent cells. Endothelial tube formation was assessed with the use of Matrigel assay. The level of monocyte chemoattractant protein–1 (MCP–1), interleukin–6 (IL–6) and soluble CD40 ligand (sCD40L) was measured in cell culture supernatant by enzyme–linked immunosorbent assay (ELISA). It was found that TNF–α impaired EPCs proliferation, migration, adhesion capacity, in vitro vasculogenesis ability and promoted EPCs secretion of inflammatory cytokines including MCP–1, IL–6 and sCD40L. Tan IIA could reverse these effects. These findings show that Tan IIA has the potential to protect EPCs against damage induced by TNF–α. The findings of this study may shed light on the pharmacological basis for the use of traditional Chinese medicine in the treatment of atherosclerosis relevant to EPC and ultimate EC damage.

[Key words] Endothelial progenitor cell; Migratio; Paracrine; Tanshinone ⅡA; Tumor necrosis factor–α; Vasculogenesis

Activation of extracellular signal–regulated kinase 1/2 and Sp1 may contribute to the expression of tissue inhibitor of metalloproteinases–1 induced by transforming growth factor–β 1 in HPASMCs

YANG Jinxiu

The First Affiliated Hospital of Zhejiang Chinese Medical University, Hangzhou 310006, China

[Abstract] **Background** Tissue inhibitor of metalloproteinases–1 (TIMP–1) is important in the development of pulmonary arterial hypertension (PAH). However, the molecular regulatory mechanisms of TIMP–1 in the pulmonary arteries were not very clear, especially in the human pulmonary arterial smooth muscle cells (HPASMCs). The present study investigated the signaling pathway involved in the regulation of TIMP–1 in HPASMCs induced by transforming growth factor (TGF)–β 1. **Methods and Results** Cultured HPASMCs were incubated with different concentrations of TGF–β 1 (0–40 ng/mL) for 24 h, or with 10 ng/mL TGF–β 1 for different time (1–48 h). Western blot, real–time PCR and ELISA analysis showed that TGF–β 1 time– and dose–dependently enhanced the expression and secretion of TIMP–1. Furthermore, TGF–β 1 could phosphorylate two of the three mitogen–activated protein kinases (MAPK), extracellular signal–regulated kinase 1/2 (ERK1/2) and p38, but not c–Jun NH2–terminal kinase (JNK). Of these kinases, only the inhibition of ERK 1/2 by U0126, which was a specific inhibitor of MAPK/ERK kinase1/2, effectively blocked the TGF–β 1–induced expression of TIMP–1. Mithramycin, an inhibitor of Sp1 transcription factor, also significantly inhibited the expression of TIMP–1. Additionally, EMSA showed that TGF–β 1 could up–regulate the DNA–binding activity of Sp1, and that U0126 and mithramycin could effectively inhibit these events. **Conclusion** TGF–β 1 could time– and dose–dependently stimulate the expression and secretion of TIMP–1 in HPASMCs, and ERK1/2 and Sp1 signaling pathways might be involved in these activities.

[Key words] Human pulmonary arterial smooth muscle cells; Tissue inhibitor of metalloproteinases–1; Transforming growth factor –β 1; Extracellular signal–regulated kinase 1/2; Sp1

Catheter ablation of ventricular arrhythmia originating from isolated outflow tract diverticulum: two cases and literature review

ZHOU Bin

The First Affiliated Hospital of Zhejiang Chinese Medical University, Hangzhou 310006, China

[Abstract] Congenital ventricular diverticulum is a rare cardiac malformation with a prevalence of about 0.26% in unselected adult patients during other diagnostic procedures. We present two cases of arrhythmogenic isolated outflow tract diverticulum incidentally revealed by cardiac angiography during catheter ablation for ventricular arrhythmia. The isolated outflow tract diverticulums in both cases were found to be the origins of the arrhythmia. Catheter ablation was successfully performed for one patient while a conservative observation strategy was chosen for another. Both patients have no cardiac event during observational follow–up for 12 months. The paper also included a comprehensive review of the literature.

[Key words] Catheter ablation;Ventricular arrhythmia originating; Isolated outflow tract diverticulum

Catheter ablation versus medical rate control for persistent atrial fibrillation in patients with heart failure:a PRISMA–compliant systematic review and meta–analysis of randomized controlled trials

ZHOU Bin

The First Affiliated Hospital of Zhejiang Chinese Medical University, Hangzhou 310006, China

[Abstract] **Background** The effectiveness of restoring the sinus rhythm by catheter ablation relative to that of medical rate control for persistent atrial fibrillation (AF) patients with heart failure (HF) remains to be defined. **Methods** We systematically searched Embase, Pubmed, the Cochrane Library, and ClinicalTrials.gov for articles that compared the outcomes of interest between catheter ablation and medical rate control therapy in persistent AF patients with HF and left ventricular systolic dysfunction (LVSD). The primary endpoint was the change in the left ventricular ejection fraction (LVEF) following catheter ablation or medical rate control therapy relative to baseline. Other endpoints included changes in cardiac function and exercise capacity, including the New York Heart Association (NYHA) class, the brain natriuretic peptide (BNP) level, the peak oxygen consumption (peak VO_2), the 6–minute walk test (6MWT) results, and quality of life (QOL). **Results** Three randomized controlled trials (RCTs) with 143 patients were included. At the overall term follow–up, catheter ablation significantly improved the LVEF ($P<0.05$) and peak VO2 ($P<0.01$) and reduced the NYHA class ($P<0.01$) and the Minnesota Living with Heart Failure Questionnaires (MLHFQ) scores ($P<0.05$) compared with the medical rate control for persistent AF patients with HF. Alterations in parameters, such as the BNP level, 6MWT, and Short form–36 (SF–36) questionnaire scores also revealed trends that favored catheter ablation therapy, although these differences were not significant. **Conclusion** Catheter ablation resulted in improved LVEF, cardiac function, exercise capacity, and QOL for persistent AF patients with HF compared with the medical rate control strategy.

[Key words] Atrial fibrillation; Catheter ablation; Heart failure; Medical rate control

Different effects of Thiazolidinediones on in–stent restenosis and target lesion revascularization after percutaneous coronary intervention: a meta–analysis of randomized controlled trials

ZHOU Bin

The First Affiliated Hospital of Zhejiang Chinese Medical University, Hangzhou 310006, China

[Abstract] **Objective** To evaluate the effects of Thiazolidinediones (TZDs) in the prevention of in–stent restenosis (ISR) and target lesion revascularization (TLR) after percutaneous coronary intervention (PCI) and to further investigate the differences between rosiglitazone and pioglitazone. **Methods** We systematically searched Embase, Pubmed, the Cochrane Library, and ClinicalTrials.gov through January 2017. Randomized controlled trials (RCTs) investigating the effects of TZDs for ISR after PCI were identified. The primary outcomes were rates of ISR and TLR. Secondary outcomes included major adverse cardiac events (MACE) and late lumen loss (LLL), minimum lumen diameter (MLD) and percentage stenosis (PS) during follow–up. **Results** Fourteen RCTs with a total of 1 350 patients were finally included. At the overall term follow–up, TZDs treatment is associated with significantly reduced risk of TLR (*RR*=0.45, 95%*CI*: 0.30

– 0.67, $P<0.05$ for pioglitazone, *RR*=0.68, 95%*CI*: 0.46 – 1.00, $P<0.05$ for rosiglitazone). Pioglitazone is associated with significantly reduced risks of ISR (*RR*=0.47, 95%*CI*: 0.27 – 0.81, $P<0.01$), and MACE (*RR*=0.44, 95%*CI*: 0.30 – 0.64, $P<0.05$). Pioglitazone also resulted in less LLL, greater MLD and lower PS (all $P<0.05$). No significant relationship was found between rosiglitazone and ISR (*RR*=0.91, 95%*CI*: 0.39 – 2.12, $P>0.05$) and MACE (*RR*=0.73, 95%*CI*: 0.53 – 1.00, $P>0.05$). **Conclusion** TZDs treatment is associated with significant reduction in ISR, TLR, MACE for patients after PCI. Pioglitazone treatment seems to have more beneficial effects than rosiglitazone and no significantly increased cardiovascular risk was detected for both agents.

[Key words] Thiazolidinediones; In–stent restenosis; Target lesion revascularization

Nitric oxide may be the key factor linking CD40 pathway to endothelial progenitor cell dysfunction

PAN Yanyun

The First Affiliated Hospital of Zhejiang Chinese Medical University, Hangzhou 310006, China

[Abstract] Endothelial progenitor cells (EPCs) were reported to repair the injured endothelium. However, they are vulnerable to the inflammatory environment represented by most vascular diseases including atherothrombosis and pulmonary arterial hypertension. Elevated plasma concentrations of pro–inflammatory mediator soluble CD40 ligand (sCD40L) were one of the features of those inflammation–related diseases. Activation of CD40 pathway can reduce the numbers and impair the activities of EPCs, but the key mechanisms are still elusive. What is more, CD40 pathway was found to play a significant role in regulating nitric oxide (NO) bioavailability which was gaining widespread attention for its role in modulating various physiological processes of EPCs. We review recent work on how CD40 pathway influences EPC functions and NO bioavailability, discuss their internal relations, and hypothesize that NO may be the key factor linking CD40 pathway to EPC dysfunction. Our hypothesis brings a new insight into the therapeutic function of NO in inflammatory conditions. Moreover, it may suggest us a new concept for the further clinical development of EPC transplanting therapy.

[Key words] Endothelial progenitor cells; CD40; Nitric oxide

Interruption of CD40 pathway improves efficacy of transplanted endothelial progenitor cells in monocrotaline induced pulmonary arterial hypertension

PAN Yanyun

The First Affiliated Hospital of Zhejiang Chinese Medical University, Hangzhou 310006, China

[Abstract] Transplantation of endothelial progenitor cells (EPCs) plays a therapeutic role in pulmonary arterial hypertension (PAH). Meanwhile, recruitment of progenitors has potential inflammatory effects and exaggerates vascular injury. CD40 pathway is identified as a major player in vascular inflammatory events. In this study, we investigated the role of CD40 pathway in regulating early outgrowth EPC functions, and searched for improvements in PAH cell therapy. **Methods** EPCs were isolated from rat bone marrow and cultured for 7 days. After treatment with soluble CD40 ligand (sCD40L) for 24 hours, EPC migration, adhesion, proliferation and vasculogenesis functions were tested.

Rat PAH model was founded by subcutaneous injection of monocrotaline (MCT). Control EPCs or lentivirus vectors (Lv)–shRNA–CD40 EPCs were infused via tail vein at day 7, 14, and 21 after MCT injection. Therapeutic effects were evaluated at day 28. **Results** sCD40L dose–dependently impaired EPC migration, adhesion, proliferation and vasculogenesis functions. However, paracrine effects of soluble inter–cellular adhesion molecule–1, vascular endothelial growth factor and interleukin–6 were dose–dependently improved by sCD40L. Control EPC–derived conditioned medium protected endothelial cell in vitro vasculogenesis, while sCD40L–pretreated ones showed detrimental effects. After monocrotaline injection, sCD40L levels in rat serum increased gradually. Other than in vitro results, benefits of both two EPC treatments were obvious, even taken at day 21. Benefits of control EPCs wore off over time, but those of Lv–shRNA–CD40 EPCs were more effective and enduring, as characterized by both ameliorated rat hemodynamic and reversed vascular remodeling. Furthermore, Lv–shRNA–CD40 EPCs integrated into endothelium better, rather than into adventitia and media. **Conclusion** sCD40L impaired protective effects of EPCs. Traditional EPC treatments were limited in PAH, while interruption of CD40 pathway of transplanted cells could apparently improve the therapeutic efficacy.

[Key words] Transplantation of endothelial progenitor cells; Pulmonary arterial hypertension; CD40

The effect of early vasopressin use on patients with septic shock: a systematic review and meta–analysis

HUANG Haijun

The First Affiliated Hospital of Zhejiang Chinese Medical University, Hangzhou 310006, China

[Abstract] Background The effect of early vasopressin initiation on clinical outcomes in patients with septic shock is uncertain. A systematic review and meta–analysis was performed to evaluate the impact of early start of vasopressin support within 6 h after the diagnosis on clinical outcomes in septic shock patients. **Methods** We searched the PubMed, Cochrane, and Embase databases for randomized controlled trials (RCTs) and cohort studies from inception to the 1st of February 2021. We included studies involving adult patients (> 16 years)with septic shock. All authors reported our primary outcome of short–term mortality and in the experimental group patients in the studies receiving vasopressin infusion within 6 h after diagnosis of septic shock and in the control group patients in the studies receiving no vasopressin infusion or vasopressin infusion 6 h after diagnosis of septic shock, clearly comparing with clinically relevant secondary outcomes use of renal replacement therapy (RRT), new onset arrhythmias, ICU length of stay and length of hospitalization). **Results** Five studies including 788 patients were included. The primary outcome of this metaanalysis showed that short–term mortality between the two groups was no difference (*OR*= 1.09, 95%*CI*: 0.80 – 1.48, $P > 0.05$, χ^2=0.83, I^2=0%). Secondary outcomes demonstrated that the use of RRT was less in the experimental group than that of the control group (*OR*=0.63, 95%*CI*: 0.44–0.88, $P < 0.01$, χ^2=3.15, I^2=36%). The new onset arrhythmias between the two groups was no statistically significant difference (*OR* =0.59, 95%*CI*: 0.31–1.10, $P > 0.05$, χ^2=4.7, I^2=36%). Therewas no statistically significant difference in the ICU length of stay (*MD*=0.16, 95%*CI*: −0.91–1.22, $P > 0.05$, χ^2=6.08, I^2=34%) and length of hospitalization (*MD*=−2.41, 95%*CI*: −6.61–1.78, $P > 0.05$, χ^2= 8.57, I^2 = 53%) between the two groups. **Conclusion** Early initiation of vasopressin in patients within 6 h of septic shock onset was not associated with decreased short–termmortality, new onset arrhythmias, shorter ICU length of stay and length of hospitalization, but can reduce the use of RRT. Further large–scale RCTs are still needed to evaluate the benefit of starting vasopressin in the early phase of septic shock.

[Key words] Vasopressin; Septic shock; Effect

CTRP9 activation of Nrf2/HO−1 reduces inflammation and improves ventricular remodeling after myocardial infarction in rats

HUANG Haijun

The First Affiliated Hospital of Zhejiang Chinese Medical University, Hangzhou 310006, China

[Abstract] **Objective** To investigate the effect of CTRP9 on ventricular remodeling after myocardial infarction in rats and its possible mechanism. **Methods** Eighty male SD rats were randomly divided into sham operation group (Sham group), myocardial infarction group (MI group), normal saline group (NC group), green fluorescent protein adenovirus group (Ad−GFP+MI group) and CTRP9 adenovirus group(Ad−CTRP9+MIgroup). The model of myocardial infarction in SD rats was established by ligating the anterior descending branch of the left coronary artery. The recombinant adenovirus vector carrying CTRP9 gene (Ad−CTRP9) was injected into the myocardium. The indexes of cardiac function, myocardial infarction area, myocardial injury markers, inflammation markers and stress indexes were evaluated. QPCR and Western blot were used to detect the expression of nuclear factor NF−E2 related factor (Nrf2) and heme oxygenase−1 (HO−1). **Results** After injection of Ad−CTRP9, the LVEF, + dp/dt max, −dp/dt max, SOD and GSH−Px were significantly increased (all $P<0.05$), the LVEDP, CK, LDH, CK−MB and MDA were significantly decreased, the survival rate and myocardial infarction area were significantly decreased, the inflammatory response indexes MPO, TNF− α, IL−6 were significantly decreased, and IL−10 was significantly increased (all $P<0.05$). The mRNA expression of Nrf2 and HO−1 in myocardial tissue was significantly increased by qPCR. The protein expression of Nrf2 and HO −1 in myocardial tissue was significantly increased by Western blot. **Conclusion** CTRP9 can not only reduce cardiomyocyte injury and oxidative stress after myocardial infarction in rats, but also activate Nrf2/HO−1 signal pathway to reduce inflammation and improve ventricular remodeling after myocardial infarction in rats. It is of great development value in clinical treatment of myocardial infarction.

[Key words] CTRP9; NF−E2 related factor; Heme oxygenase−1

Lower versus standard intensity warfarin in old asian patients receiving radiofrequency catheter ablation for atrial fibrillation

XU Buyun PAN Jie LOU Yuanqing XU Chao XING Yangbo

Shaoxing People's Hospital, Shaoxing 312000, China

[Abstract] **Objective** To explore the optimal intensity warfarin during the perioperative period of radiofrequency catheter ablation for atrial fibrillation in old Asian patients. **Methods** This is a prospective randomized study. Old Asian patients (age ⩾70 years) preparing to receive radiofrequency catheter ablation for atrial fibrillation were enrolled. Participants were randomized to two Groups. Warfarin was adjusted to maintain international normalized ratios at 1.5−2.0 and 2.0−2.5 in group A and B, respectively, for at least four weeks before ablation. Endpoints were assessed from time of randomization to three months after ablation. Primary efficacy endpoints were thromboembolic complications and intra−cardiac thrombosis. Primary safety endpoint was defined as major bleeding. Second endpoints included new asymptomatic cerebral emboli and minor bleeding. **Results** A total of 226 patients were enrolled and included in analysis set (group A: 115, group B: 111). Intra−cardiac thrombosis was detected before ablation in one patients

in group A. And only one patient suffered a stroke after ablation in group B. Two patients in Group B suffered major bleeding events. The incidence of new asymptomatic cerebral emboli lesions was similar between the two groups (10.2% vs. 8.7%, $P>0.05$). Lower intensity warfarin was associated with significantly less minor bleeding (1.9% vs. 9.1%, $P<0.05$). **Conclusion** Compared with standard intensity warfarin (international normalized ratio:2.0–2.5), low–intensity warfarin (international normalized ratio:1.5–2.0) might have comparable efficacy in preventing perioperative thromboembolic complications and was associated with less perioperative bleeding events, in old Asian patients receiving radiofrequency catheter ablation for atrial fibrillation.

[Key words] Atrial fibrillation ; Asian ; Elderly ; Warfarin

Bone marrow mesenchymal stem cell–derived exosomal microRNA–133a restrains myocardial fibrosis and epithelial–mesenchymal transition in viral myocarditis rats

LI Qiming

The Fourth Affiliated Hospital of Zhejiang University School of Medicine, Yiwu 322000, China

[Abstract] Myocarditis is a disease characterized by localized or diffuse inflammation of the myocardium without efficient treatment. This study explored the regulatory mechanism of microRNA–133 (miR–133) secreted from bone marrow mesenchymal stem cell–derived exosome (BMSC–Exo) on myocardial fibrosis and epithelial–mesenchymal transition (EMT) in viral myocarditis (VMC) rats through regulating mastermind–like 1 (MAML1). BMSCs in rats were isolated and cultured to identify their immune phenotype and osteogenic and adipogenic ability, and BMSC–Exo were extracted and identified. Exosomes were obtained through ultracentrifugation, which were identified by transmission electron microscope and western blot analysis. The rats were injected with Coxsackie B3 virus for preparation of VMC model, and cardiomyocytes were isolated, cultured and grouped in the same way as animal experiments (NCExo, Ad–miR–133aExo, Adas–miR–133aExo). In vivo and in vitro experiments were conducted to figure out the roles of exosomal miR–133a and MAML1 in inflammation, apoptosis, EMT, fibrosis, and cell viability. The targeting relationship between miR–133a and MAML1 was verified by dual luciferase reporter gene assay. BMSC–Exo raised miR–133a expression in VMC rats, and effectively improved the VMC rat cardiac function and myocardial fibrosis, increased cardiomyocyte viability and inhibited the EMT process. Elevated miR–133a in exosomes strengthened the improvements. Silenced miR–133a effectively reversed the effects of BMSC–Exo on VMC rats. miR–133a targeted MAML1. Inhibition of MAML1 improved cardiac function and myocardial fibrosis in VMC rats, and could reverse the effect of miR–133a–silenced exosomes on VMC rats. Study suggests that elevated exosomal miR–133a suppresses myocardial fibrosis and EMT in rats with VMC via down–regulating MAML1, thereby inhibiting the progression of myocarditis.

[Key words] Myocarditis;miR–133;EMT

Pim–2 kinase inhibits inflammatory by suppressing mTORC1 pathway in atherosclerosis

HU Feng CHENG Xiaoshu

The Second Affiliated Hospital of Nanchang University, Nanchang 330001, China

[Abstract] **Background** Inflammatory immunity theory has rasied considerable concern in the pathogenesis of

atherosclerosis. Proviral integration site of murine (Pim) kinases are a distinct class of serine/threonine-specific kinases consisting of Pim-1, Pim-2 and Pim-3. Pim-2 is known to function in apoptosis pathways and anti-inflammatory response. Here, we investigated whether Pim-2 kinase inhibits atherosclerotic inflammation by suppressing mTORC1 pathway. **Methods** Atherosclerosis animal model was established by feeding with a high-fat diet in ApoE$^{-/-}$ mice. THP-1-derived macrophages were subjected to an ox-LDL (50 μg/mL, 24 h) condition in vitro mimicking the in vivo situation. **Results** Found that the protein expression of Pim-2 was upregulated in ox-LDL-treated THP-1-derived macrophages and atherosclerotic mice model. In addition, ox-LDL up-regulated the protein expression of p-mTOR, p-S6K1 and p-4EBP1, intracellular lipid droplets, free cholesterol and cholesterylester and the mRNA expression of inflammatory cytokines including IL-6, MCP-1, TLR-4 and TNF-α in THP-1-derived macrophages. Functionally, the overexpression of Pim-2 (Pim-2 OE) obviously attenuated atherosclerotic inflammation associated with mTORC1 signaling pathway in vitro and in vivo, whereas the knockdown of Pim-2 (Pim-2 KD) markedly promoted atherosclerotic inflammation associated with upregulation of mTORC1 signaling pathway. The plaque areas and lesions in the whole aorta and aortic root sections were alleviatived in ApoE$^{-/-}$ mice with Pim-2 OE, whereas aggravated with Pim-2 KD. Moreover, mTOR agonist (MHY1485) could counteract the anti-inflammatory effect of Pim-2 in ox-LDL-treated THP-1-derived macrophages after Pim-2 OE, whereas rapamycin rescued the atherosclerotic inflammation in ox-LDL-treated THP-1-derived macrophages after Pim-2 KD. Furthermore, si-mTOR and si-Raptor alleviated the atherosclerotic proinflammatory effect in ox-LDL-treated THP-1-derived macrophages under the background of Pim-2 KD. **Conclusion** These results indicated that Pim-2 kinase inhibits atherosclerotic inflammation by suppressing mTORC1 pathway.

[Key words] Pim-2 kinase;Atherosclerosis;mTORC1

Longitudinal myocardial strain changes and influencing factors in non-infarct yyocardium after primary PCI in acute ST-segment elevation yyocardial infarction patients

WU Han GONG Han XIA Xue SUN Huan YU Bo YANG Ping

China-Japan Union Hospital ofJilin University, Changchun 130033, China

[Abstract] Objective Myocardial injury after ST-segment elevation myocardial infarction (STEMI) can cause ventricular systolic dysfunction. A large number of previous studies have been conducted on the pathophysiology and functional protection of myocardial infarction area. However, the influencing factors and protective strategies of myocardial function in non-infarct myocardium(NIM) remain unclear. The present study evaluated the changes of left ventricular global longitudinal strain (GLS) and different segmental longitudinal strain (LS) after primary percutaneous coronary intervention (PCI) in STEMI patients. The segmental changes of non-infarct myocardium (NIM) and its influencing factors were further detected, providing new implications for NIM myocardial function protection. **Methods** 75 acute STEMI patients who underwent primary PCI in CHINA-JAPAN Union Hospital of Jilin University between January 2021 and June 2021 were included. Left ventricles were divided into infarct area, adjacent infarct area (ANM) and remote infarct area (RNM) according to the culprit artery. Clinical data, coronary angiography results, global longitudinal strain, regional strain, and left ventricular ejection fraction (LVEF) were collected within 1 week after PCI. Factors of NIM myocardial dysfunction and GLS. **Results** 38 anterior wall myocardial infarction patients and inferior wall myocardial infarction patients were included. The results showed that GLS was significantly negatively correlated with LVEF in STEMI patients ($P < 0.001$, $r=-0.802$). NIM dysfunction was found in 63 patients(84%) The LS of NIM was significantly correlated with

LVEF($P<0.001$).GLS was positively correlated with coronary artery stenosis score (Gensini score)($P<0.001$, $r=0.442$). The LS of NIM, including the ANM region and the RNM region, were significantly correlated with the coronary Gensini score ($P<0.001$, $r=0.412$;$P<0.05$, $r=0.355$;$P<0.05$, $r=0.317$).There was no significant correlation between LS of NIM and recanalization time ($P>0.05$). **Conclusion** NIM dysfunction exists widely in STEMI patients and correlates to global cardiac function in patients with myocardial infarction after primary PCI, which highlighted the NIM protection in STEMI patients. The function of NIM has no clear correlation with recanalization time, but it correlates with the severity of coronary lesion of patients. Therefore, methods on protecting NIM function warrant further investigation.

[Key words] STEMI;Longitudinal;PCI

Endothelial intracellular angiogenin protects against atherosclerosis by decreasing endoplasmic reticulum stress in a ST3GAL5–dependent manner

SU Enyong YU Peng ZHANG Baoli ZHANG Anjing XIE Shiyao ZHANG Chunyu ZOU Yunzeng LIU Ming JIANG Hong GE Junbo

Zhongshan Hospital, Fudan University, Shang hai 200032, China

[Abstract] Objective Angiogenin (ANG) is essential to promoting cellular adaptation to endoplasmic reticulum (ER) stress, a process closely associated with cardiovascular disease including atherosclerosis. This study aims to investigate the role of ANG in progression of atherosclerosis and elucidate its underlying molecular mechanisms. **Methods** Because ANG is a secreted protein, adeno–associated virus serotype 9 (AAV9) ANG–full length (ANG–FL) or ANG lacking the N–terminal signal peptide (ANG–ΔSP) overexpression vectors were established and injected into atherosclerosis–prone apolipoprotein E–deficient ($ApoE^{-/-}$) mice at $1\times1\ 012$ vg. Global or endothelial conditional knockout of ANG mice were bred with $ApoE^{-/-}$ mice to generate $ANG^{-/-}/ApoE^{-/-}$ mice, ANGfl/flTie2cre/+/$ApoE^{-/-}$ mice and their Cre–negative littermates (ANGfl/fl/$ApoE^{-/-}$) which were fed with a western diet for 13 weeks and administered with ER stress inhibitor 4–phenylbutyric acid (PBA) during the final 4 weeks. RNA sequencing was performed to detect differential gene expressions of $ApoE^{-/-}$ mice, $ANG^{-/-}/ApoE^{-/-}$ mice, ANGfl/flTie2cre/+/$ApoE^{-/-}$ mice and ANGfl/fl/$ApoE^{-/-}$ mice. In vitro, ANG knockdown and overexpression human umbilical vein endothelial cells (HUVECs) were constructed using CRISPR/Cas9 system or lentivirus transfection. HUVECs were transfected with small interfering RNA (siRNA;100 mmol/L) for 48 hours and exposed to oxidized low–density lipoprotein (ox–LDL,100 μg/mL) for 24 hours to study the mechanism of regulating ER stress by ANG. The levels of ER stress and inflammation were assessed by western blot and monocyte adhesion assay respectively. The histology analysis indicated atherosclerotic lesions. **Results** Reanalysis of expression profiling datasets found that ANG level reduced in patients' atherosclerotic lesions, which was further validated in aortas of $ApoE^{-/-}$ mice. Levels of ER stress markers and adhesion molecules, aortic roots lesions and macrophage deposition were markedly decreased in $ApoE^{-/-}$ mice injected recombinant AAV9 ANG–ΔSP overexpression vector compared with empty and ANG–FL overexpression vectors. Compared with ANGfl/fl/$ApoE^{-/-}$ mice, ANGfl/flTie2cre/+/$ApoE^{-/-}$ mice showed significantly elevated ER stress level, increased adhesion molecules expressions, atherosclerotic lesions and macrophage accumulation, which were significantly alleviated by ER stress inhibitor sodium 4–phenylbutyrate. Moreover, RNA sequencing results identified ANG–dependent down–regulation of ST3 Beta–Galactoside Alpha–2,3–Sialyltransferase 5 (ST3GAL5). In vitro, ANG–ΔSP overexpression significantly attenuated ox–LDL–induced ER stress and monocyte adhesion to endothelial cells, which were reversed by ST3GAL5 inhibition. **Conclusion** These results suggest that endothelial intracellular ANG provides a novel therapeutic strategy

against atherosclerosis and exerts atheroprotective effects via ST3GAL5–mediated ER stress suppression.

[Key words] Angiogenin;ST3GAL5–mediated; Atherosclerosis

Low - intensity pulsed ultrasound prevents angiotensin Ⅱ–induced aortic smooth muscle cell phenotypic switch via hampering miR–17–5p and enhancing PPAR–γ

ZHAO Kun ZHANG Dong KONG Xiangqing ZHOU Bin SUN Wei

The First Affiliated Hospital of Nanjing Medical University, Nanjing 225000, China

[Abstract] **Aim** Vascular events can trigger a pathological phenotypic switch in vascular smooth muscle cells (VSMCs), decreasing and disrupting the plasticity and diversity of vascular networks. The development of novel therapeutic approaches is necessary to prevent these changes. We aimed to investigate the effects and associated mechanisms of low–intensity pulsed ultrasound (LIPUS) irradiation on the angiotensin Ⅱ (Ang Ⅱ)–induced phenotypic switch in VSMCs. **Methods** In vivo, Ang Ⅱ was infused subcutaneously for 4 weeks to stimulate vascular remodeling of the whole wall artery in C57/Bl6 mice, and LIPUS irradiation (0.5 MHz, 77.20 mW/cm^2) was applied for 20 minutes every 2 days for 4 weeks. In vitro, cultured rat aortic VSMCs (RAVSMCs) were pretreated once with LIPUS irradiation for 20 minutes before 48 hours Ang Ⅱ stimulation. MiR–17–5p agomir and antagomir, and peroxisome proliferator–activated receptor gamma (PPAR–γ) activator (rosiglitazone) and inhibitor (GW9662) were used to treat the cells with or without LIPUS treatment. **Results** LIPUS irradiation prevents Ang Ⅱ–induced vascular remodeling of the whole wall artery without discriminating between adventitia and media in vivo and RAVSMC phenotypic switching in vitro. LIPUS irradiation downregulated miR–17–5p expression and upregulated PPAR–γ expression. The PPAR–γ activator rosiglitazone could mimic the favorable effects of LIPUS irradiation on Ang Ⅱ–treated RAVSMCs. In contrast, GW9662 and the miR–17–5p agomir could impede the LIPUS–mediated downregulation of RAVSMC proliferation and inflammation under Ang Ⅱ stimulation conditions, respectively. The inhibitory effects of GW9662 against the anti–remodeling effects of LIPUS irradiation in Ang Ⅱ–induced RAVSMCs could be blocked by pretreatment with the miR–17–5p antagomir. **Conclusion** LIPUS irradiation prevents Ang Ⅱ–induced RAVSMCs phenotypic switching through hampering miR–17–5p and enhancing PPAR–γ, suggesting a new approach for the treatment of vascular disorders.

[Key words] Ang Ⅱ;LIPUS;VSMCs

Low - intensity pulsed ultrasound ameliorates angiotension Ⅱ–induced cardiac fibrosis by alleviating inflammation via a caveolin–1–dependent pathway

ZHAO Kun ZHANG Dong KONG Xiangqing ZHOU Bin

The First Affiliated Hospital of Nanjing Medical University, Nanjing 225000, China

[Abstract] **Aim** Cardiac hypertrophy and fibrosis are major pathological manifestations observed in left ventricular remodeling induced by Angiotensin Ⅱ (Ang Ⅱ). Low - intensity pulsed ultrasound (LIPUS) has been reported to improve cardiac dysfunction and myocardial fibrosis in myocardial infarction (MI) through mechanotransduction

and its downstream pathways. Aimed to investigate whether LIPUS could exert a protective effect on ameliorating Ang II –induced cardiac hypertrophy and fibrosis and if so, to further elucidate the underlying molecular mechanisms. **Methods** Used Ang II to mimic the animal and cell culture models of cardiac hypertrophy and fibrosis, where LIPUS irradiation was applied for 20 minutes every 2 days from 1 week before surgery to 4 weeks after surgery in vivo, and every 6 hours for a total of 2 times in vitro. Following that, cardiac hypertrophy and fibrosis levels were evaluated by echocardiographic, histopathological, and molecular biological methods. Main results LIPUS could ameliorate left ventricular remodeling in vivo and cardiac fibrosis in vitro by reducing Ang II –induced release of inflammatory cytokines, while the protective effects were limited on cardiac hypertrophy in vitro. Given that LIPUS increased the expression of caveolin–1 related to mechanical stimulation, we inhibited caveolin–1 activity with pyrazolopyrimidine 2 (pp2) in vivo and in vitro, by which LIPUS–induced downregulation of inflammation was reversed and the anti–fibrosis effects of LIPUS were absent. **Conclusion** These results indicate that LIPUS could ameliorate Ang II –induced cardiac fibrosis by alleviating inflammation via a caveolin–1–dependent pathway, providing new insights for the development of novel therapeutic apparatus in clinical practice.

[Key words] Ang II ;Low - intensity pulsed ultrasound;LIPUS

The correlation between heart failure and gut microbiome metabolites

CHEN Lina LI Senhao AI Lanmu ZHOU Jun HUANG Junlin XU Feng
ZENG Xiangyuan HAN Jia
Shaoxing City Keqiao District Hospital of Traditional Chinese Medicine, Shaoxing 312000, China

[Abstract] Heart failure (HF) is a global public health problem, with morbidity and mortality increasing year by year. The gut microbiome actively affects the physiological and pathological activities of the human body in a variety of ways. More and more studies have suggested a strong correlation between HF and gut microbiome metabolites. This review summarizes the specific alteration of these metabolites and their connection to the progression of HF, aiming at considering new approaches toward regulating the gut microbiome and using its metabolic pathways to treat HF, potentially decreasing the morbidity and mortality of HF as well as improving prognosis.

[Key words] Heart failure; Gut microbiome;Metabolites

Differences of prevalent risk factors for patients of coronary artery disease in two hospitals in China and Germany

SHI Yuanhu TIAN Jing MA Ke SHEN Xiao ZHANG Xiaofeng
School of Medicine & Holistic Integrative Medicine, Nanjing University of Chinese Medicine, Nanjing 210003, China

[Abstract] **Background** Ethnic difference may affect associations between conventional risk factors for coronary artery disease (CAD) and the pathogenesis and severity of this disease. Furthermore, there is a lack of direct comparison based on angiographically approved CAD cohorts. In addition, there are many guidelines for cardiovascular diseases in the world. Although it is hoped that these clinical guidelines can assist in the treatment, differences between races

prompts for individualized treatment. That is different patients need different guidelines. **Methods** In this cross-sectional study of two study centers in China and Germany, the prevalence of conventional risk factors in angiographically evidenced CAD patients stratified by age from March 1, 2015 to August 31, 2016 were compared. Furthermore, a logistic regression analysis was performed to identify associations between the prevalence of these factors and the severity of coronary lesions. **Results** Overall, 613 patients were included. Among these patients, 274 patients were from Germany and 339 patients were from China. For patients < 60 years old, the proportion of male patients was significantly higher in the cohort in China ($P < 0.05$). However, differences in gender distribution disappeared in patients who were ⩾60 years old. For patients of ⩾60 years old, patients from China were more likely to be smokers ($P < 0.05$), while patients from Germany were more likely to have diabetes mellitus (DM) and dyslipidemia ($P < 0.05$). Comorbidities of hypertension and DM were independent predictors to the severity of coronary lesions in both cohorts, while the level of serum Cr remained as an independent predictor of severer coronary lesions in patients from Germany. **Conclusion** Differences may exist on the strength of the association between conventional CAD risk factors and the pathogenesis of CAD and its severity in these two cohorts of CAG-evidenced CAD patients from China and Germany.

[Key words] Coronary artery diseases;Risk factors;Chinese;Germany

Mechanical synchrony and myocardial work in heart failure patients with left bundle branch area pacing

LIU Wen HU Chunqiang WANG Yanan CHENG Yufei ZHAO Yingjie LIU Yang ZHENG Shaoxin CHEN Haiyan SHU Xianhong

Zhongshan Hospital, Fudan University, Shanghai 200032, China

[Abstract] Background Several clinical studies have demonstrated the feasibility of LBBAP in HF patients. However, the existing data are not sufficient and little is known about the efficacy of permanent left bundle branch area pacing (LBBAP)in delivering cardiac resynchronization therapy. This study aimed to evaluate the effect of LBBAP on mechanical synchronization and myocardial work in heart failure (HF) patients. **Methods** This is a multicenter, prospective cohort study. From February 2018 to January 2021, heart failure patients with reduced ejection fraction (LVEF⩽35%) and CLBBB who underwent LBBAP were enrolled in this study. Echocardiograms and electrocardiograms and were conducted before and 3-6 months after implantation. Intra- and interventricular synchronization were assessed using two-dimensional speckle tracking imaging (2D-STI). The left ventricular pressure-strain loop was obtained by combining left ventricular strain with noninvasive blood pressure to evaluate mechanical efficiency. **Results** Twenty-seven patients (mean age, 65.5 ± 8.8 years, 51.9% male) who received LBBAP were enrolled in this study. An echocardiographic response, defined as ⩾10% absolute improvement in LVEF compared with the baseline was observed in 24 of 27 patients (88.9%). Super-response (absolute increase⩾ 20% of LVEF or LVEF⩾50%) was identified in 12 of 27 patients (44.4%). LBBAP resulted in significant QRS narrowing [from (177.1 ± 16.7) ms to (113.0 ± 18.4) ms, $P < 0.001$] , improvement in LVEF [from (29.9 ± 4.8)% to (47.1 ± 8.3)%, $P < 0.001$],reduction in left ventricular end - systolic diameter and volume [LVESD: from (56.6 ± 7.8) mm to (45.0 ± 7.5) mm, $P < 0.001$; LVESV: from (141.4 ± 40.6) mL to (72.6 ± 31.5) mL, $P < 0.001$] . LBBAP significantly shortened the duration of interventricular mechanical delay (IVMD) [from (56.4 ± 28.5) ms to (28.9 ± 19.0) ms, $P < 0.001$] and (PSD) [from (143.4 ± 45.2) ms to (92.6 ± 35.1) ms, $P < 0.001$] during the follow-up, indicating its efficiency in improving mechanical synchronization. The global wasted work (GWW) [(410.3 ± 166.6) mmHg% vs (283.0 ± 129.6) mmHg%, $P < 0.05$] , global work efficiency (GWE) [(64.6 ± 7.8)% vs (80.5 ± 5.7)%, $P < 0.001$] , global constructive work (GCW) [(836.0 ± 198.4) mm Hg% vs (1321.6 ± 371.4) mmHg%, $P < 0.001$] and global work index(GWI)[(485.0 ± 200.7)

mmHg% vs (1093.3 ± 343.2) mmHg%, $P < 0.001$]were significantly improved. As with segmental myocardial work, segmental MWE was significantly improved in the septal [from (35.3 ± 17.8)% to (69.6 ± 19.0)%, $P < 0.05$], inferior [from (57.9 ± 21.7) % to (83.6 ± 13.7) %,$P < 0.05$], posterior [from (76.7 ± 13.0)% to (80.6 ± 17.1)%, $P < 0.05$], anterior[from (77.3 ± 13.7)% to (83.8 ± 10.7)%,$P < 0.05$],and anteroseptal [from (59.2 ± 22.8)% to (73.3 ± 15.3)%,$P < 0.05$] segments. There was a trend towards a reduction in mean segmental WW in every segment and it was significantly reduced in the septal[from (607.1 ± 276.5) mmHg% to (330.8 ± 254.3) mmHg%, $P < 0.001$], inferior[from (333.7 ± 199.8) mmHg% to (198.6 ± 169.8) mmHg%, $P < 0.05$] segments compared with the baseline. The MW differences between the lateral and septal segments were significantly reduced at the time of follow-up [from (1172.2 ± 563.5) mmHg% to (633.1 ± 596.6) mmHg%, $P < 0.05$], demonstrating the efficacy of LBBAP in improving mechanical efficiency. **Conclusion** LBBAP was effective in improving cardiac function, mechanical synchronization and mechanical efficiency and may be a promising alternative cardiac resynchronization therapy.

[Key words] Cardiac resynchronization therapy; Heart failure; Left bundle branch block; Myocardial work; Mechanical synchronization

The predictive role of lipoprotein(a) elevations in atherosclerosis progression of patients with relative low LDL-C level after coronary stent implantation: a case-control study

ZHU Lijun HUANG Jinyu

Hangzhou First People's Hospital, Hangzhou 310006, China

[Abstract] Background The incidence of major adverse cardiovascular events (MACE) is high in patients with acute coronary syndrome (ACS) and there are differences in the degree of risk faced by each individual. Therefore, accurate identification of the cardiovascular risk will benefit patients with guiding treatment and improving prognosis. lipoprotein(a) [Lp(a)] elevations (≥300 mg/L) is associated with MACE and atherosclerosis progression in patients with a high level of low-density lipoprotein cholesterol (LDL-C), while this association would no longer exist when LDL-C decreased. There is limited study concerning relative low LDL-C levels. This study aims to verify this correlation when LDL-C level=1.4-1.8 mmol/L. **Methods** This included a total of 782 patients who underwent angiography one year after stent implantation. According to the results of angiography, they were divided into the lesion progression group (n = 384) and the non-progression group (n=398). Risk factors of coronary artery lesion progression were investigated and multi-factor logistic regression analyses were performed. According to the LDL-C level after treatment, the patients were divided into three subgroups (LDL-C level < 1.4 mmol/L, n=316; LDL-C level=1.4-1.8 mmol/L, n=243; LDL-C level ⩾ 1.8 mmol/L, n = 223). The correlation between Lp(a) elevations and atherosclerosis progression in different sub-groups was compared. **Results** The level of Lp(a) in the lesion progression group was significantly higher than the non-progression group ($P < 0.05$). Multi-factor regression analysis showed that Lp(a) level was weakly correlated with lesion progression (OR = 1.018, 95%CI:1.011-1.026,$P < 0.05$). Nevertheless,there was a strong correlation between Lp(a) elevations and lesion progression (OR=2.196, 95%CI:1.557-3.099,$P < 0.05$) and this association was dependent on the LDL-C level.The higher LDL-C, the stronger correlation.When LDL-C=1.4-1.8 mmol/L, Lp(a) elevations still closely related to the progression of coronary atherosclerosis (OR =2.743,95%CI:1.499-5.020,$P < 0.05$). **Conclusion** Patients with LDL-C level⩾1.4 mmol/L and Lp(a) elevations shall be considered as very high-risk patients who may require further medication for the reduction of their LDL-C levels.

[Key words] Lipoprotein(a);Atherosclerosis ;Coronary stent implantation

Guanxin V protects against ventricular remodelling after acute myocardial infarction through the interaction of TGF–β 1 and vimentin

LIANG Bo GU Ning

Nanjing University of Chinese Medicine, Nanjing 210023, China

[Abstract] **Background** Though numerous studies indicated that traditional Chinese medicine has unique and irreplaceable advantages in the treatment of ventricular remodelling, the mechanistic contribution of traditional Chinese medicine in cardiac remodelling remains to be fully elucidated. This study aimed to investigate the anti–ventricular remodelling effect of Guanxin V (GXV) and provide scientific data for its clinical application. **Methods** A ventricular remodelling model after acute myocardial infarction was established by ligating the left anterior descending coronary artery of Syrian hamsters. Four groups, including the control, sham, model, and GXV treatment (6 g/kg/d), groups, were tested. The echocardiography and biochemical indexes of cardiac function and remodelling were determined, and the crucial protein involved in the signalling pathway were subsequently tested by qPCR and/or Western blotting. Moreover, we built remodelling model in cardiomyocytes and further explore the mechanism. Transmission electron microscopy was used to observe the ultrastructure of cardiomyocytes and co–immunoprecipitation was conducted the the interaction of transforming growth factor beta 1 (TGF–β 1) and vimentin. **Results** In hamster cardiac remodelling induced by acute myocardial infarction, GXV alleviated apoptosis, cardiac hypertrophy, cardiac remodelling, and even improved cardiac function. Mechanically, GXV inhibited the remodelling process by directly targeting TGF–β 1. Overexpression of TGF–β 1 exacerbated the ventricular remodelling, whereas GXV reversed this dysregulation. GXV also increased the down–regulated vimentin level in pathological ventricular remodelling. Moreover, the interaction of vimentin and TGF–β 1 was confirmed by co–immunoprecipitation, and GXV impeded this interaction. **Conclusion** The interaction of vimentin and TGF–β 1 may be a novel target for ventricular remodelling and GXV might be a new agent to fight against ventricular remodelling by targeting TGF–β 1 and impeding its interaction with vimentin.

[Key words] Acute myocardial;TGF–β 1;Guanxin V

Guanxin V protects cardiomyocytes against oxidative stress damage and apoptosis though TGF–β 1/smads pathway

LIANG Bo GU Ning

Nanjing University of Chinese Medicine, Nanjing 210023, China

[Abstract] **Background** Accumulating evidence indicates that oxidative stress plays a critical role in cardiovascular disease, which stands as a major cause of morbidity and mortality worldwide. Guanxin V, a traditional Chinese medicine, has a significant effect on cardiovascular disease. However, the deeper biological mechanisms remain unclear. Here, our study investigated the anti–apoptotic and anti–oxidative effects of Guanxin V on oxidative stress damage to cardio myocytes. **Methods** Cardiomyocytes were treated with hydrogen peroxide with or without the indicated concentration of Guanxin V. Cell apoptosis, reactive oxygen species–related markers were tested. Then used transmission electron microscopy to observe the ultrastructure of mitochondria. The levels of TGF–β 1, Collagen Type Ⅰ, and Collagen Type Ⅲ in supernatants were determined by enzyme–linked immunosorbent assay. Finally, the mRNA and protein levels

of collagen and TGF–β1/smads signaling were measured. **Results** Hydrogen peroxide could stimulate reactive oxygen species production in cardiomyocytes. Guanxin V significantly decreased hydrogen peroxide–induced cell damage, inhibited oxidative stress damage and apoptosis, and enhanced mitochondrial dynamic balance. Furthermore, Guanxin V attenuated oxidative stress damage induced TGF–β1/smads pathway activation. **Conclusion** This results demonstrated that Guanxin V effectively alleviated hydrogen peroxide–induced oxidative stress damage and apoptosis though down–regulating TGF–β1/smads signalling pathway, which increases our understanding of the molecular biological mechanism of Guanxin V in treating cardiovascular disease.

[Key words] Guanxin V; TGF–β1/smads;Cardiomyocytes

Inhibiting miR–22 alleviates cardiac dysfunction by regulating sirt1 in septic cardiomyopathy

ZHANG Mingming

Tangdu Hospital, The Fourth Military Medical University, Xi'an 710032, China

[Abstract] **Objective** Sepsis is a serious systemic inflammatory reaction with high mortality caused by bacterial infection. The main causes of sepsis include serious complication of severe infection, severe trauma, and major surgery. Further development of this condition can lead to septic shock, serious damage to many organs and finally death. Hence, sepsis is a serious disease that endangers human health. High morbidity and mortality are the most typical characteristics of septic cardiomyopathy. MicroRNAs are a class of small non–coding RNAs composed of 19–24 nucleotides that can combine with the 3' untranslated region (3'–UTR) of mRNA and cause mRNA degradation or inhibit mRNA translation. Numerous studies have reported that miRNAs play various roles in regulating inflammation, apoptosis, necrosis and autophagy in myocardial injury. microRNA–22 (miR–22) is reported to participate in some heart diseases. It has reported that miR–22 is the most abundant miRNA expressed in heart. It has been confirmed that upregulating miR–22 can result in myocardial ischemia–reperfusion (I/R) injury by targeting mitochondria.We aimed to reveal the role of miR–22 in septic cardiomyopathy and to explore the underlying mechanisms. **Methods** The cardiac–specific knockout mice were generated by crossing miR–22–flox mice with aMHC–Cre mice. For miR–22 overexpression mice, portion of miR–22HG sequence containing miR–22 coding region were inserted into Rosa26 locus via homologous recombination to generate the miR–22–KI–flox mice. MiR–22–KI–flox mice were then crossed with aMHC–Cre mice to generate the miR–22 cardiac specific overexpression (miR–22cOE) mice. All experimental mice were 6–8 weeks old male mice and have free access to food and water. The littermates wild–type (WT) were used as the control group. miR–22 cardiac–specific knockout (miR–22cKO) mice and miR–22 cardiac–specific transgenic (miR–22cOE) mice were subjected to a cecal ligation and puncture (CLP) operation, while a sham operation was used in the control group. Neonatal mice were used to isolate primary cardiomyocytes. And then transfected cardiomyocytes with miR–22 negative control (NC), mimic (final concentration 5 mM) or inhibitor (final concentration 50 mM) according to the manufacturer's instructions. Next, the cardiomyocytes were incubated with LPS for 12 h. The cardiac function, cardiomyocytes apoptosis, mitochondrial function and autophagic flux were detected. **Results** The echocardiogram results suggested that miR–22cKO CLP mice cardiac dysfunction was alleviated. The serum LDH and CK–MB were reduced in the miR–22cKO CLP mice. As expected, there was reduced apoptosis, increased autophagy and alleviated mitochondrial dysfunction in the miR–22cKO CLP mice, while it had contrary role in the miR–22cOE group. Inhibiting miR–22 promoted autophagy by increasing the LC3 II /GAPDH ratio and decreasing the p62 level. Additionally, culturing primary cardiomyocytes with lipopolysaccharide (LPS) simulated sepsis–induced cardiomyopathy in vitro. Inhibiting miR–22 promoted autophagic flux confirmed by an

increased LC3 II /GAPDH ratio and reduced p62 protein level under bafilomycin A1 conditions. This study confirmed that sirt1 is the target of miR–22 in septic cardiomyopathy by the luciferase reporter assay. **Conclusion** In conclusion, our results revealed that inhibiting miR–22 can improve cardiac function, reduce cardiomyocyte apoptosis and upregulate autophagy in CLP–induced cardiomyopathy. The protective effect of inhibiting miR–22 was confirmed by targeting sirt1 signaling. The present study provides a new direction for septic cardiomyopathy, which is vital for the treatment of septic cardiomyopathy.

[Key words] Cardiac dysfunction;Septic cardiomyopathy;MiR–22

MiR–22 inhibition alleviates cardiac dysfunction in doxorubicin–Induced cardiomyopathy by targeting the sirt1/PGC–1α pathway

ZHANG Mingming

Tangdu Hospital, The Fourth Military Medical University, Xi'an 710032, China

[Abstract] Objective Doxorubicin (DOX) has been a widely used chemotherapy drug since the 1960s, but its widespread use is limited given its dose–dependent cardiotoxicity. In a retrospective study, congestive heart failure (CHF) occurred in 5% of patients who received DOX treatment at a dose of 500–550 mg/m^2. The incidences of CHF in DOX–treated patients at doses of 551–600 and >601 mg/m^2 were 16% and 26%, respectively. DOX cardiotoxicity is a life–threatening side effect that leads to a poor prognosis in patients receiving chemotherapy. MicroRNAs (miRNAs) are a class of small single–stranded non–coding RNAs with a length of 19–24 nucleotides that bind to the 3′–untranslated region (3′–UTR) of mRNA, inhibit mRNA translation, and lead to mRNA degradation. It has been reported that miR–22 plays roles in heart diseases, such as diabetic cardiomyopathy, cardiac hypertrophy, and ischemia reperfusion injury. We investigated the role of miR–22 in doxorubicin–induced cardiomyopathy and the underlying mechanism in vivo and in vitro. **Methods** Specifically, we designed loss–of–function and gain–of–function experiments to identify the role of miR–22 in doxorubicin–induced cardiomyopathy. The cardiac–specific knockout mice were generated by crossing miR–22–flox mice with aMHC–Cre mice. For miR–22 overexpression mice, portion of miR–22HG sequence containing miR–22 coding region were inserted into Rosa26 locus via homologous recombination to generate the miR–22–KI–flox mice. MiR–22–KI–flox mice were then crossed with aMHC–Cre mice to generate the miR–22 cardiac specific overexpression (miR–22cOE) mice. Neonatal mice were used to isolate primary cardiomyocytes. And then transfected cardiomyocytes with miR–22 negative control (NC), mimic (final concentration 5 mM) or inhibitor (final concentration 50 mM) according to the manufacturer's instructions. The cardiac function, cardiac fibrosis ,cardiomyocytes apoptosis, mitochondrial function and mitophagy were detected. **Results** Our data suggested that inhibiting miR–22 alleviated cardiac fibrosis and cardiac dysfunction induced by doxorubicin. In addition, inhibiting miR–22 mitigated mitochondrial dysfunction through the sirt1/PGC–1α pathway. Knocking out miR–22 enhanced mitochondrial biogenesis, as evidenced by increased PGC–1α, TFAM, and NRF–1 expression in vivo. Furthermore, knocking out miR–22 rescued mitophagy, which was confirmed by increased expression of PINK1 and parkin and by the colocalization of LC3 and mitochondria. Overexpressing miR–22 aggravates cardiac dysfunction and mitochondrial dysfunction in DOXIC. Meanwhile, overexpressing miR–22 inhibits the level of mitophagy in DOXIC. **Conclusion** Then study revealed that miR–22 targets the sirt1/PGC–1a pathway to regulate mitochondrial biogenesis and mitophagy and then to alleviate mitochondrial dysfunction. miR–22 may represent a new target to alleviate cardiac dysfunction in doxorubicin–induced cardiomyopathy and improve prognosis in patients receiving chemotherapy.

[Key words] MiR−22;Doxorubicin;Cardiac dysfunction;Cardiomyopathy

Aspirin alone versus dual antiplatelet therapy after transcatheter aortic valve replacement: a systematic review and meta−analysis

LIN Xiaoxiao WANG Shuai HUANG Jinyu

Hangzhou First People's Hospital, Hangzhou 310006, China

[Abstract] **Background** The current American College of Cardiology and American Heart Association (ACC/AHA) guidelines recommend dual antiplatelet therapy with aspirin and clopidogrel for 6 months followed by lifelong aspirin after transcatheter aortic valve replacement (TAVR). However, studies that have DAPT to aspirin following TAVR have questioned this recommendation as DAPT has been associated with more bleeding events compared to aspirin. This study performed a systematic review and meta−analysis of all the RCTs comparing DAPT (aspirin plus clopidogrel) with aspirin alone as antithrombotic treatment following transcatheter aortic valve replacement. **Methods** The databases of the Embase, PubMed and Cochrane libraries were searched from inception to Oct 1, 2020, and randomized controlled trials (RCTs) reporting aspirin plus clopidogrel with aspirin alone as antithrombotic treatment after TAVI were included. Revman 5.3 was used to conduct the analysis. **Results** After screening 152 articles, 4 studies containing 1 086 patients (541 patients in the aspirin group and 545 patients in the DAPT group) were included. The results demonstrated that, at 30 days follow−up, compared with DAPT, aspirin was not associated with a statistically significant difference in the rate of bleeding events (*RR*=1.22, 95%*CI*:0.62 − 2.39, $P>0.05$), all−cause mortality (*RR*=1.21, 95%*CI*: 0.52 − 2.84, $P>0.05$), stroke (*RR*=0.81, 95%*CI*: 0.24 − 2.79, $P>0.05$) and MI (*RR*=4.00, 95%*CI*:0.45 − 35.22, $P>0.05$). But at the 6 to 12 months follow−up, DAPT appeared to increase the risk of bleeding events compared with aspirin alone (*RR*=1.67, 95%*CI*:1.24 − 2.24, $P<0.01$), and there was no significant difference in the rate of all−cause mortality (*RR*=0.89, 95%*CI*: 0.53 to 1.48, $P>0.05$), stroke (*RR*=1.04, 95%*CI*: 0.57 − 1.92, $P>0.05$) and MI (*RR*=1.65, 95%*CI*: 0.52 − 5.26, $P>0.05$) among two groups. **Conclusion** This study systematic review and meta−analysis suggested that aspirin alone could decrease the risk of bleeding, and was not associated with higher risk of mortality, stroke or myocardial infarction compared with DAPT.

[Key words] TAVR;Aspirin;Dual antiplatelet therapy;Meta−analysis

The association between T cell CD99 expression and coronary artery disease severity

LIN Xiaoxiao WANG Shuai HUANG Jinyu

Hangzhou First People's Hospital, Hangzhou 310006, China

[Abstract] Background: CD99 is a cell surface protein and plays an important role in diapedesis and inflammation. Coronary artery disease (CAD) is now considered an inflammatory disease and previous studies suggest a possible association between CD99 and atherosclerosis. In this study, we explored the relationship between T cell CD99 expression and CAD. **Methods** CD99 expression on T cells was measured in 524 consecutive patients who were presented to our center for coronary angiography. Atherosclerosis severity of CAD was assessed by the number of diseased vessels showing more than 50% diameter stenosis and quantified by Gensini score. The association between

the levels of CD99 expression on T cells and the severity of coronary artery disease was investigated. **Results** CD99 levels on T cells were significantly higher in the CAD group than those in the non-CAD group (63.43 ± 18.71 vs 51.88 ± 22.18, $P < 0.001$). The CD99 levels on T cells were significantly higher in the MVD group than those in the SVD group (67.01 ± 16.61 vs 53.67 ± 20.65, $P < 0.001$). After adjusting for sex, age, low-density lipoprotein cholesterol, total cholesterol, high-density lipoprotein cholesterol and triglyceride (TG), CD99 expression on T cells was strongly associated with Gensini score (β =0.262, t=3.022, 95%*CI*:0.091-0.432, $P < 0.05$) and MVD (*OR*=1.042,95%*CI*:1.025-1.059,$P < 0.01$). A combined model consisting of percentage of CD99 levels and traditional risk factors showed a 0.803 AUC (95%*CI*:0.746-0.860,$P < 0.01$) with a 58.7% sensitivity and 86.6% specificity. According to the likelihood ratio test, the combined model of CD99 expression and traditional risk factors was a better fit for predicting MVD, compared with the model consisting of traditional risk factors only (likelihood r=2.824, $P < 0.05$). **Conclusion** This study showed that there was a strong association between CD99 levels on T cells and CAD severity. CD99 is a potential biomarker to predict the risk and severity of CAD and a possible therapeutic target to prevent the development of CAD.

[Key words] Coronary heart disease;CD99; T cells;Multivessel disease;Atherosclerosis

Ticagrelor versus clopidogrel on coronary microvascular function in patients with st segment elevation myocardial infarction

LIN Xiaoxiao WANG Shuai HUANG Jinyu

Hangzhou First People's Hospital, Hangzhou 310006, China

[Abstract] Background Ticagrelor reduced the rate of major adverse cardiovascular events (MACE) compared with clopidogrel in patients with STEMI. However, little is understood about the efficacy of ticagrelor on coronary microvascular function in patients with STEMI compared with clopidogrel. We conducted this systematic and meta-analysis to evaluate the efficacy of ticagrelor versus clopidogrel on coronary microvascular function in patients with STEMI. **Methods** The databases of PubMed, Embase and Cochrane library were searched from inception to Jan 1, 2021, and randomized controlled trials (RCTs) reporting ticagrelor versus clopidogrel on coronary microvascular injury in patients with STEMI were included in our study. Revman 5.3 was used to conduct the analysis. **Results** After screening 60 articles, 4 studies including 779 patients (390 patients in the ticagrelor group and 389 patients in the clopidogrel group), published from 2014 to 2020 were included in our meta-analysis. Our results showed that there was no significant difference in the CTFC scores (95%*CI*:-4.71-2.86, $P > 0.05$), TIMI flow grade scores(95%*CI*:-0.03-0.08, $P > 0.05$)and MBG scores (95%*CI*:-0.03-0.44, $P > 0.05$) between ticagrelor and clopidogrel. **Conclusion** Based on current evidences, ticagrelor might not be more effective for the improvement of microvascular function in patients with STEMI compared with clopidogrel. More studies comparing ticagrelor and clopidogrel on coronary microvascular function in patients with STEMI were needed.

[Key words] Ticagrelor;Clopidogrel;Microvascular function;STEMI;Systematic review and meta-analysis

Gastrin/CCKBR axis mediates intestine glucose metabolism by targeting SGLT1/GLUT2 in type 1 and type2 diabetes

LIU Xue LIU Xing WU Xianxian SUN Shiyun LIU Xiaohui JIANG Xiaoliang YANG Zhiwei

Institute of Laboratory Animal Sciences, CAMS&PUMC), Beijing 100021, China

[Abstract] Intestine sodium/ glucose metabolism plays a crucial role in the progress of diabetes mellitus. astrin, binding to its receptor cholecystokinin B receptor (CCKBR), is involved in the blood glucose regulation through improving pancreatic β–cell function. However, whether Gastrin/CCKBR axis has an effect on intestine glucose metabolism is unknown. Adult intestine–specific Cckbr–knockout mice (Cckbrfl/fl villin–Cre) reveals prediabetes (pre–DM) states, which develops type 2 diabetes (T2DM) pathophysiological characteristics under high fat diet. Specific stimulation of intestine CCKBR by delivering Gastrin–SiO2 complex improve intestine glucose metabolism via sodium–glucose cotransporter 1/ glucose transporter 2 (SGLT1/GLUT2) and hormones–mediated anti–diabetic feature both in type 1 diabetic (NOD mice) and type 2 diabetic mice (high fat diet induced mice). In Vitro study elucidated that gastrin directly decrease SGLT1 expression via PKC/NF–KB pathway in human intestine epithelial cells (HIEC), but not directly regulate endocrine function in enteroendocrine cells (NCL–H716). Human intestine samples Ex Vivo study also demonstrated that gastrin directly attenuates glucose absorption in brush border membrane vesicles (BBMV). Diabetic patients showed lower CCKBR expression localized to the BBMV than normoglycemic individuals. Our study concluded the crucial role of Gastrin/ CCKBR axis in the regulation of blood glucose homeostasis. Gastrin–SiO2 complex can be considered as a promising drug candidate to prevent type 1 and type 2 diabetes mellitus.

[Key words] Diabetes;Glucose metabolism;CCKBR

Predictive value of inflammation–based GPS, PLR, and GRACE score for major cardiovascular and cerebrovascular events during hospitalization in patients with acute myocardial infarction

ZHU Houyong XU Xiaoqun CHEN Tielong HUANG Jinyu

The Affiliated Hangzhou First People's Hospital, Zhejiang University School of Medicine, Hangzhou 310013, China

[Abstract] Backgroud Acute myocardial infarction (AMI) is one of the leading causes of mortality worldwide, and the major adverse cardiovascular and cerebrovascular events (MACEs) resulting from it are not only the direct cause of death, but also a huge economic burden on the health care system. The efficient prediction and prevention of MACEs are considered effective measures to avoid death outcomes. The Global Registry of Acute Coronary Events (GRACE) score is considered to have a certain predictive ability for hospitalization and provides a 5–year mortality risk for patients with acute coronary syndrome (ACS), but its composition lacks the part of inflammation assessment. In addition, some studies have reported that inflammation–based Glasgow Prognostic Score (GPS) and platelet–to–lymphocyte ratio (PLR) also have a good predictive value for the occurrence of MACEs in patients with ACS. It is interesting what score can effectively predict the occurrence of MACEs during hospitalization in patients with AMI. The goal of this study was to evaluate the

predictive ability of the GPS, PLR, GRACE score and combined diagnostic models for the MACEs in patients with AMI. **Methods** In this retrospective cohort study, eligible patients were required to meet the third global definition of myocardial infarction. The primary outcome of this study was the occurrence of MACEs during hospitalization. The area under the curve (AUC) was calculated by receiver operating characteristic (ROC) curve analysis to assess the predictive ability of the GPS, PLR, GRACE scores, and joint diagnostic models for primary outcomes; univariate and multivariate logistic regression analyses were performed. Subgroup analysis were completed according to the type of percutaneous coronary intervention (PCI), the type of AMI, and the presence or absence of acute infection.GPS was defined as follows: patients with an elevated hypersensitive C–reactive protein (H–CRP) level (> 10 mg/L) and a low albumin level (< 35 g/L) were designated as a GPS of 2. The presence of one abnormality associated with either the H–CRP level or albumin level was designated as a GPS of 1. If both metrics were normal, its value was designated as 0 point. The redefined GPS (RGPS) was based on high–sensitivity H–CRP and albumin data from the previous study and redefined by optimal thresholds: patients with an elevated H–CRP level (> 12.57 mg/L) and a low albumin level (< 35.95 g/L) were designated as a GPS of 2. The presence of one abnormality associated with either the H–CRP level or albumin level was designated as a GPS of 1. If both metrics were normal, its value was designated as 0 point. The definition of the PLR score (PLRS) was based on the quartile range of the PLR in the previous study, as follows: patients with an elevated PLR (> 211.25) were designated as a PLRS of 2, but if patients with a decreased PLR (< 105.71) were designated as a PLRS of 0, its value was designated as 1 point (i.e., between the two). **Results** A total of 175 patients were included in this study. The average age was 65 (54–80) years, 73.1% of patients were male, 60.6% of patients had a history of hypertension, 37.7% of patients had a history of diabetes mellitus, and 34.3% had acute infection. Of these patients, 40 (22.9%) had MACEs. The baseline characteristics of patients were categorized according to the GPSs. Compared with the low–score group, the high–score group had older patients ($P < 0.001$), a higher prevalence of diabetes ($P < 0.05$), a higher acute infection rate ($P < 0.001$), a higher prevalence of severe kidney disease ($P < 0.015$), lower hemoglobin levels ($P < 0.001$), higher Killip classes ($P < 0.001$), lower blood lymphocyte levels ($P < 0.001$), higher D–dimer levels ($P < 0.001$), higher creatinine levels ($P < 0.001$) and higher type B natriuretic peptide (BNP) levels ($P < 0.001$). There were missing values for low density lipoproteincreatinine (LDL), BNP, and D–dimers, with missing rates of 1.7%, 3.4, and 1.7, respectively, that were completed through the expectation maximization method.The results of unit ROC curve analysis for the MACEs showed that the AUCs were 0.780 (95%*CI*:0.696–0.864) for the GPS, 0.766 (95%*CI*:0.682–0.850) for RGPS, 0.561 (95%*CI*:0.458–0.664) for PLRS, and 0.793 (95%*CI*:0.706–0.880) for GRACE. The GPS, RGPS and GRACE had higher AUC values than the PLRS ($P < 0.001$, $P < 0.001$, and $P < 0.001$, respectively). Multivariate ROC curve analysis revealed that this AUC value was 0.809 (95%*CI*:0.726–0.893) for the GPS combined with GRACE, 0.783 (95%*CI*:0.701–0.864) for the GPS combined with the PLRS, 0.794 (95%*CI*:0.707–0.880) for GRACE combined with the PLRS, and 0.841 (95%*CI*:0.761–0.921) for the GPS combined with GRACE and the PLRS. The combined diagnostic model of the GPS plus GRACE and the PLRS had a higher AUC value than the combination of the GPS, RGPS and GRACE ($P < 0.05$, $P < 0.05$, and $P < 0.05$, respectively) .Univariate logistic regression analysis revealed that the OR for in–hospital MACEs was 3.053 (95%*CI*:0.997–9.349) for the GPS (1 vs 0) (Table 3), 18.133 (95%*CI*:0.997–9.349) for the GPS (2 vs 0), 1.029 (95%*CI*:1.018–1.039) for the GRACE score, 1.052 (95%*CI*:1.024–1.081) for age, 5.517 (95%*CI*:2.588–11.762) for acute infection, 7.389 (95%*CI*:1.301–41.965) for severe renal damage, 0.515 (95%*CI*:0.282–0.941) for PCI type, 1.027 (95%*CI*:1.005–1.049) for heart rate, 2.850 (95%*CI* 1.964–4.136) for Killip classification, 0.963 (95%*CI*:0.945–0.982) for hemoglobin, 0.411 (95%*CI*:0.207–0.817) for lymphocyte count, 1.604 (95%*CI*:1.214–2.121) for D–dimer, 0.676 (95%*CI*: 0.592–0.771) for albumin, 1.011 (95%*CI*:1.002–1.019) for H–CRP, 1.012 (95%*CI*:1.003–1.022) for creatinine and 1.001 (95%*CI*:1.001–1.002) for BNP. The multivariate logistic regression model goodness–of–fit test was completed using the Hosmer–Lemeshow method, which showed that the model had sufficient calibration ($P > 0.05$). The results showed that the OR for hospitalized MACEs was 5.573 (95%*CI*:1.588–19.554) for GPS (2 vs 0),and the OR for MACEs was 1.023 (95%*CI*:1.009–1.036) for GRACE score. In the ST–elevation myocardial infarction (STEMI) group, the AUC for in–hospital MACEs was 0.737 (95%*CI*:0.647–0.814)

for the GPS, 0.732 (95%*CI*:0.643–0.810) for the RGPS, 0.586 (95%*CI*: 0.491–0.676) for the PLRS, and 0.788 (95%*CI*: 0.703–0.858) for GRACE. The AUC was 0.807 (95%*CI*:0.724–0.874) for the GPS combined with GRACE, 0.738 (95%*CI*: 0.649–0.815) for the GPS combined with the PLRS, 0.791 (95%*CI*: 0.706–0.860) for GRACE combined with the PLRS, and 0.816 (95%*CI*:0.734–0.882) for the GPS combined with GRACE and the PLRS. The combined diagnostic model of the GPS plus GRACE and the PLRS had a higher AUC value than the GPS and RGPS ($P < 0.05$ and $P < 0.05$, respectively). In the non–ST–elevation myocardial infarction (NSTEMI) group, the AUCs were 0.864 (95%*CI*:0.749–0.940) for the GPS, 0.830 (95%*CI*:0.708–0.916) for the RGPS, 0.511 (95%*CI*:0.376–0.644) for the PLRS, and 0.877 (95%*CI*: 0.764–0.948) for GRACE. The AUC was 0.913 (95%*CI*:0.809–0.971) for the GPS combined with GRACE, 0.869 (95%*CI*:0.755–0.943) for the GPS combined with the PLRS, 0.877 (95%*CI*: 0.764–0.948) for GRACE combined with the PLRS, and 0.912 (95%*CI*:0.808–0.971) for the GPS combined with GRACE and the PLRS. The combined diagnostic model of the GPS plus GRACE seemed to have a higher AUC value than each single score, but there was no significant difference. The combined diagnostic model of the GPS plus GRACE and the PLRS had a higher AUC value than the RGPS ($P < 0.05$).In the PCI group, the AUC for in–hospital MACEs was 0.738 (95%*CI*: 0.654–0.811) for the GPS, 0.731 (95%*CI*:0.647–0.805) for the RGPS, 0.522 (95%*CI*:0.433–0.610) for the PLRS, and 0.704 (95%*CI*:0.618–0.781) for GRACE. The AUC was 0.760 (95%*CI*:0.677–0.830) for the GPS combined with GRACE, 0.763 (95%*CI*:0.681–0.833) for the GPS combined with the PLRS, 0.718 (95%*CI*:0.633–0.793) for GRACE combined with the PLRS, and 0.776 (95%*CI*:0.695–0.844) for the GPS combined with GRACE and the PLRS. The combined diagnostic model of the GPS plus GRACE and the PLRS seemed to have a higher AUC value than each single score, but there was not statistically significantly different. In the non–PCI group, the AUCs were 0.808 (95%*CI*:0.662–0.911) for the GPS, 0.788 (95%*CI*:0.638–0.896) for the RGPS, 0.642 (95%*CI*:0.483–0.780) for the PLRS, and 0.828 (95%*CI*:0.684–0.925) for GRACE. This AUC was 0.856 (95%*CI*: 0.718–0.944) for the GPS combined with GRACE, 0.826 (95%*CI*:0.682–0.924) for the GPS combined with the PLRS, 0.834 (95%*CI*:0.692–0.929) for GRACE combined with the PLRS, and 0.862 (95%*CI*:0.725–0.948) for the GPS combined with GRACE and the PLRS. The combined diagnostic model of the GPS plus GRACE and the PLRS had a higher AUC value than the RGPS alone ($P < 0.05$).In the acute infection group, the AUC for in–hospital MACEs was 0.693 (95%*CI*: 0.560–0.806) for the GPS, 0.664 (95%*CI*: 0.530–0.781) for the RGPS, 0.551 (95%*CI*:0.417–0.680) for the PLRS, and 0.700 (95%*CI*:0.568–0.812) for GRACE. This AUC was 0.762 (95%*CI*: 0.635–0.863) for the GPS combined with GRACE, 0.701 (95%*CI*:0.569–0.813) for the GPS combined with the PLRS, 0.705 (95%*CI*:0.571–0.816) for GRACE combined with the PLRS, and 0.761 (95%*CI*:0.634–0.862) for the GPS combined with GRACE and the PLRS. Compared with the RGPS alone, the combined diagnostic model of the GPS plus GRACE and the PLRS and the combined diagnostic model of the GPS plus GRACE had a higher AUC value ($P < 0.05$ and $P < 0.05$, respectively). In the nonacute infection group, the AUCs were 0.731 (95%*CI*:0.640–0.809) for the GPS, 0.726 (95%*CI*: 0.635–0.805) for the RGPS, 0.510 (95%*CI*:0.415–0.604) for the PLRS, and 0.786 (95%*CI*: 0.700–0.857) for GRACE. This AUC was 0.802 (95%*CI*: 0.717–0.870) for the GPS combined with GRACE, 0.760 (95%*CI*:0.672–0.835) for the GPS combined with the PLRS, 0.811 (95%*CI*:0.728–0.878) for GRACE combined with the PLRS, and 0.832 (95%*CI*:0.751–0.895) for the GPS combined with GRACE and the PLRS. The combined diagnostic model of the GPS plus GRACE and the PLRS seemed to have a higher AUC value than each single score, but there was not statistically significantly different. **Conclusion** This study showed that the combined diagnostic model including the GPS plus GRACE and the PLRS had better predictive ability for MACEs during hospitalization compared with that of each individual score. Thus, the use of a combined model with the GPS plus GRACE and the PLRS will be of clinical benefit in a broad group of individuals with AMI. However, large, multicenter, and prospective studies still need to be performed to clarify the predictive power of the combined diagnostic model for patients with AMI during hospitalization and follow–up and to further optimize this model.

[Key words] Acute myocardial infarction;GPS;GRACE

Hyperuricemia is associated with an increased prevalence of ventricular tachycardia and fibrillation in patients with ST–elevation myocardial infarction after primary percutaneous coronary intervention

HU Xianqing

Jinhua Municipal Central Hospital, Jinhua 321000, China

[Abstract] **Background** There is an independent association between hyperuricemia and atrial fibrillation, but little is known about the relationship between hyperuricemia and ventricular tachycardia and fibrillation (VT/VF) in patients with ST–segment elevation myocardial infarction (STEMI). **Objective** To investigate the relationship between hyperuricemia and VT/VF in STEMI patients undergoing primary percutaneous coronary intervention (PPCI). **Methods** The data from a cohort of STEMI patients undergoing PPCI at Jinhua Municipal Central Hospital from 2013 to 2018 were analyzed. Hyperuricemia was defined as a serum uric acid level > 7 mg/dL for men and > 6 mg/dL for women. The endpoint of the study was the occurrence of VT/VF, including 1) non–sustained ventricular tachycardia (nsVT) on Holter monitoring,2) sustained ventricular tachycardia (SVT)/VF on cardiac monitoring. **Results** Of 634 patients included in the study, 147 (23.2%) of them had hyperuricemia. The occurrence of VT/VF after PPCI was significantly higher in patients with hyperuricemia (19.0% vs 9.4%, $P < 0.05$) compared with those with normal serum uric acid levels. Hyperuricemia was associated with a significantly higher risk of VF/VT (*OR*=2.11,95%*CI*:1.11–4.03,$P < 0.05$). The strength of this association remained statistically after adjustments for age, sex, history of hypertension, estimated glomerular filtration rate (eGFR), hypersensitive C reactive protein (hsCRP), plasma natrium, peak troponin I, fasting glucose, B–type natriuretic peptides and no reflow in PPCI (*OR*=2.73,95%*CI*:1.19–6.27, $P < 0.05$). **Conclusion** There is a significant association between hyperuricemia and increased prevalence of VT/VF in STEMI patients after PPCI, independently of multiple risk factors and potential confounders.

[Key words] STEMI;Hyperuricemiav;Increased prevalence

Stumpless lesion improves the value of J–CTO score in predicting the antegrade procedure outcome of CTO intervention in patients with ST–elevation myocardial infarction after primary percutaneous coronary intervention

HU Xianqing

Jinhua Municipal Central Hospital, Jinhua 321000, China

[Abstract] **Background** Percutaneous coronary intervention (PCI) of coronary chronic total occlusion (CTO) is one of the most challenging procedures of interventional cardiology. Debate continues with regard to the predictors that influence the antegrade procedure success. **Methods** The CTO PCIs were prospectively registered from May 1, 2012 to August 22, 2017 in a single center. Variables of patients' characteristics, CTO morphology, PCI strategy, procedure materials and outcomes were recorded. Multivariable logistic regression model was adopted to identify predictors of procedure outcome. **Results** A total of 193 CTO PCIs were consecutively included, and 187 antegrade

PCIs were finally analyzed. The antegrade technical and procedure success rates were both 67.91%. Multivariable logistic regression indicated that the stumpless CTO (*OR*=2.813,95%*CI*: 1.120–7.062,*P* < 0.05) and long lesion with occlusion length ⩾ 20 mm (*OR*=2.196,95%*CI*: 1.087–4.437,*P* < 0.05) independently predicted the procedure outcome. The area under the receiver–operator characteristic (ROC) curve for discriminating failed CTO PCI was 0.621 (95%*CI*:0.534–0.708,*P* < 0.05) for Japanese multicenter CTO registry (J–CTO) score, which significantly increased to 0.673 (95%*CI*:0.592–0.755,*P* < 0.05) after scoring 2 points to the stumpless CTO. **Conclusion** The stumpless CTO and occlusion length ⩾20 mm independently predict the antegrade procedure failure. Scoring 2 points to the stumpless CTO improves the value of J–CTO score in predicting the procedure outcome.

[Key words] CTO;PCI;ST–elevation myocardial

MicroRNA–29b suppresses TGF–β–induced epithelial–mesenchymal transition in renal interstitium of spontaneously hypertensive rats

YANG Deye WU Yihao

The Affiliated Hospital of Hangzhou Normal University, Hangzhou 310015, China

[Abstract] Objective MicroRNA–29b (miR–29b) has been recently reported to regulate fibrosis in renal diseases. However, very little is known about its functional role in hypertensive nephropathy. Here we studied whether alterations in miR–29b expression affect hypertension–induced renal dysfunction and renal fibrosis. **Methods** We assessed renal dysfunction and fibrosis before and after administering lentiviral vectors encoding miR–29b mimics or inhibitors. Renal function was assessed by measuring serum creatinine (SCr), blood urea nitrogen (BUN) and urinary protein (UP) levels. Renal fibrosis was assessed with Sirius Red immunostaining, and by quantifying collagen Ⅰ, α–smooth muscle actin (α–SMA) and transforming growth factor–β (TGF–β)gene expression and protein levels by PCR and Western blot analysis, respectively. The spatial distribution of collagen Ⅰ, α–SMA and TGF–β was assessed by immunostaining. **Results** MiR–29b overexpression and inhibition significantly decreased and increased, respectively, serum creatinine (*P* < 0.05), urea nitrogen (*P* < 0.05) and urinary protein levels (*P* < 0.05) in SHRs. Importantly, miR–29b overexpression in SHRs lowered urinary protein content by 6.75% compared with normotensive controls. The interstitial deposition of collagen Ⅰ, α–SMA and TGF–β was dramatically decreased with miR–29b overexpression. In contrast, knockdown of miR–29b promoted TGF–β induced expression of collagen Ⅰ and α–SMA both on a gene and on a protein level. We confirmed that miR–29b negatively regulates the expression of TGF–β during hypertensive nephropathy. **Conclusion** MiR–29b may serve as an anti–fibrotic target in the pathophysiology of hypertension–related renal fibrosis by down–regulating TGF–β. Administering an agent that increases miR–29b function prevents renal fibrosis and ameliorates renal injury in hypertensive nephropathy.

[Key words] MiR–29b;Pathophysiology of hypertension–related;TGF–β

The association of the Syntax score with the levels of lipoprotein(a) in patients with stable coronary artery disease

XU Weifeng

Ningbo Medical Center Lihuili Hospital, Ningbo 315040, China

[Abstract] Lipoprotein(a) [Lp(a)] is associated with the severity of coronary lesions evaluated using the Syntax score in patients with stable coronary artery disease (CAD). The amount of low-density lipoprotein cholesterol (LDL-C) contained in Lp(a) is calculated. However, the effect of LDL-C levels on the association of Lp(a) levels with the Syntax score in patients with stable CAD remains unclear. Six hundred forty-six patients with stable CAD confirmed with selective coronary angiography between February 2017 and July 2018 were enrolled in the present study. Patients were divided into 2 groups according to Lp(a) or LDL-C levels. Lp(a) levels were measured with an AU5800 Chemistry Analyzer. The Syntax score was calculated by two advanced interventional cardiologists. SPSS 22.0 (SPSS Inc, Chicago, IL, USA) was used for statistical analyses. The concentration of Lp(a) ranged from 1 to 192 mg/dL (median 14 mg/dL, interquartile range 7 to 25 mg/dL). The Lp(a) > 30 mg/dL group had a higher Syntax score, higher levels of total cholesterol (TC) and LDL-C and an increased prevalence of hypertension (HTN). Pearson's correlation analysis showed a positive correlation between the Syntax score and the levels of Lp(a) (r=0.108, P < 0.05). The LDL-C ≥ 100 mg/dL group presented with a significantly higher Lp(a) level, 16 (9-29) vs 13 (7-24). The multivariate logistic regression analysis revealed a positive predictive value of an LDL-C level ≥ 100 mg/dL for an Lp(a) level > 30 mg/dL. Pearson's correlation analysis identified a correlation between Lp(a) levels and the LDL-C levels (r=0.258, P < 0.001) and the Syntax score (r=0.249, P < 0.001) in the LDL-C ≥ 100 mg/dL group, but not with LDL-C levels (r=0.089, P > 0.05) or the Syntax score (r=-0.020, P > 0.05) in the LDL-C < 100 mg/dL group. The multivariate logistic regression analysis revealed the positive predictive value of an Lp(a) level > 30 mg/dL for a Syntax score ≥ 23 only in the LDL-C ≥ 100 mg/dL group after adjustment for confounding factors, (OR=2.895, 95%CI:1.286-6.518, P < 0.010). A receiver operating characteristic (ROC) curve analysis confirmed the predictive value of Lp(a) levels for a Syntax score ≥ 23 in the LDL-C ≥ 100 mg/dL group with a cutoff value for Lp(a) > 30 mg/dL. Interestingly, the association between Lp(a) levels and the Syntax score was only maintained in the LDL-C ≥ 100 mg/dL group. An Lp(a) level > 30 mg/dL was only an independent predictor of a Syntax score ≥ 23 in the LDL-C ≥ 100 mg/dL group. The value of Lp(a) levels in predicting severity of diseased coronary vessels and the effect of LDL-C levels on the association of Lp(a) levels with the Syntax score require further investigations.

[Key words] Lp(a);LDL-C;Stable coronary artery disease

Effect of profilin-1 on the asymmetric dimethylarginine induced vascular lesion associated hypertension

NI Guohua

Sichuan Academy of Medical Sciences & Sichuan Provincial People's Hospital (Chengdu Jinjiang Sohome Comprehensive Outpatient Clinic), Chengdu 610020, China

[Abstract] Objective Previous studies have demonstrated that the levels of asymmetric dimethylarginine (ADMA), an endogenous inhibitor of nitric oxide (NO) synthesis, are strongly associated with hypertension, diabetes, and cardiovascular diseases. Profilin-1, an actin-binding protein, has been documented to be involved in endothelial injury and proliferation of vascular smooth muscle cells (VSMCs) in hypertension. However, the role of profilin-1 in ADMA-

induced vascular injury in hypertension remains largely unknown. **Methods** 40 healthy subjects and 42 matched patients with essential hypertension were enrolled, and the related indexes of vascular injury in plasma were detected. Rat aortic smooth muscle cells (RASMCs) were treated with different concentrations of ADMA for different periods of time and transfected with profilin-1 shRNA to interrupt the expression of profilin-1. To determine the role of the Janus kinase 2/signal transducer and activator of transcription 3 (JAK2/STAT3) pathway, RASMCs were pretreated with AG490 or rapamycin. The expression of profilin-1 was tested using real-time PCR and western blot analysis. Cell proliferation was measured by flow cytometry and MTT assays. **Results** Compared with healthy subjects, the levels of ADMA andprofilin-1 were markedly elevated, the levels of NO were significantly decreased in hypertensive individuals ($P < 0.05$). In vitro, ADMA induced the expression of profilin-1 in a concentration- and time-dependent manner in cultured RASMCs ($P < 0.05$), concomitantly with promoting the proliferation of RASMCs. Furthermore, ADMA-mediated proliferation of RASMCs and upregulated expression of profilin-1 were inhibited by blockade of the JAK2/STAT3 pathway or knockdown of profilin-1 by shRNA. **Conclusion** Profilin-1 may be involved in the ADMA-mediated vascular lesions in hypertension.

[Key words] Asymmetric dimethylarginine; Hypertension; JAK2/STAT3 pathway;Profilin-1; Proliferation

ST2L expression on monocyte subsets is associated with the severity of acute coronary syndrome and plaque vulnerability

ZHUANG Jianhui JU Peinan XU Yawei

Shanghai Tenth People's Hospital, Shanghai 200072, China

[Abstract] Background Pro-inflammatory monocyte infiltration and conversion to macrophages is an established risk factor for acute coronary syndrome (ACS) and plaque instability visualized by optical coherence tomography (OCT). While increased serum levels of soluble ST2 isoform (sST2) predict poor outcomes in patients with ACS and heart failure, whether the transmembrane ST2 isoform (ST2L) could early assess the severity of ACS and the vulnerability of plaques remains elusive. **Methods and Results** Using flow cytometry, we observed that the proportion and absolute number of ST2L on monocyte subsets 1 (Mon1) and Mon2 significantly declined, accompanied with increased serum sST2, in ACS patients as compared to controls. However, only the proportion of ST2L+/Mon2 remained closely associated with the severity of ACS characterized by the burden and length of atherosclerotic plaque and the number of stenotic vessels. With regard to the plaque instability, patients with thin cap fibrous atheroma (TCFA) calculated by optical coherence tomography (OCT) had lower absolute number [Non-TCFA $(1.26 \times 104) \pm (0.63 \times 104)$/mL vs TCFA $(0.92 \times 104) \pm (0.37 \times 104)$/mL,$P < 0.05$] and lower percentage (Non-TCFA 17.65% ± 3.10% vs TCFA 13.17% ± 2.29%, $P < 0.01$) of ST2L+/Mon2 than those without TCFA. Receiver- operating characteristics curves revealed that the discrimination power of the proportion of ST2L+/Mon2 against TCFA was higher than that of absolute ST2L+/Mon2 number. In multivariate analysis, the proportion of ST2L+/Mon2 remained an independent determinant for TCFA. **Conclusion** Compared to circulating sST2, the proportion of ST2L expressing on Mon2 subsets is more strongly associated with the severity of ACS and plaque vulnerability.

[Key words] Monocyte subsets;Acute coronary syndrome;ST2L

Secondary prevention of coronary heart disease appears better in older compared to younger adults from 20 years survey in united states: results from the nhanes 1999 – 2018

LIU Xiaowei　Nathan D Wong　CHEN Xiaofeng　DU Changqing　TANG Lijiang
Zhejiang Hospital, Hangzhou 310013, China

[Abstract] **Background** Little is known about the use of secondary prevention strategy in older subjects, especially in the older person who with multiple co–morbidities. We aimed to assess health outcomes and the extent of their adherence to guideline–based secondary prevention targets in older (aged 65–80 years) as compared to younger (aged 18–64 years) patients. **Methods** This examined data from US adults aged 18 years and older with a self–reported history of coronary heart disease (CHD) from the US National Health and Nutrition Examination Survey (NHANES) from 1999 to 2018. We estimated the proportions of those who reported recommended taking medications or had risk factors controlled and lifestyle modifications among US adults with CHD at or above age 80 versus below as well as those with other co–morbidities. **Results** The older persons (n=1 524) were more likely than younger (n=2 336) to take β blockers ($P < 0.0001$), angiotensin converting enzyme inhibitors/angiotensin receptor blockers (ACEIs/ARBs) ($P < 0.0001$), statins ($P < 0.0001$), an–tiplatelet drugs ($P < 0.05$). Nonsmoking status, low–density lipoprotein cholesterol (LDL–C) , and glycated hemoglobin controlled were better in older persons ($P < 0.0001$, $P < 0.0001$, $P < 0.05$, respectively). The rates of lifestyle modification except alcohol consumption were low in both older and younger, these conditions also existed in those with other co–morbidities. **Conclusion** Although secondary prevention of CHD appeared better in older compared to younger adults, a large gap still exist between the secondary prevention guidelines and their adherence. In order to achieve 'Healthy Aging', a systematic approach for prevention of CHD is urgently needed.

[Key words] Older compared;Younger adults;Coronary heart disease

Cancer in patients with newly diagnosed coronary artery disease

LIU Xiaowei　TANG Lijiang　CHEN Xiaofeng
Zhejiang Hospital, Hangzhou 310013, China

[Abstract] **Objective** Coronary artery disease (CAD) and cancer are the leading causes of death worldwide and share some risk factors, such as aging and smoking. Concurrence of the two types of diseases makes the management more challenging. Especially in patients who need stent implantation followed by dual antiplatelet therapy, fateful perioperative complications such as bleeding and stent thrombosis may occur during the later surgery for cancer. There is a lack of data regarding prevalence of cancer in patients with CAD and the predictor for cancer in this population. In this study we investigated the prevalence of cancer in patients with newly diagnosed CAD and the related risk factors. **Methods and Results** From January 2009 to March 2015, 3 555 consecutive patients with newly angiographically documented CAD were prospectively enrolled. CAD was defined as > 50% stenosis in any major coronary vessel. Serum levels of tumor markers including carcinoembryonic antigen (CEA), alpha fetoprotein (AFP), carbohydrate antigen125 (CA125), carbohydrate antigen 153 (CA153), carbohydrate antigen199 (CA199), squamous cell cancer antigen (SCC–Ag) and prostate–specific antigen (PSA) were measured. Diagnosis of cancer was confirmed by

pathologic examination, abdominal ultrasound, emission computed tomography bone scan, computed tomography (CT) or magnetic resonance imaging. The prevalence of cancer in patients with CAD was 0.73% (19 out of 3 555) including nasopharynx cancer (*n*=2), esophagus cancer (*n*=3), colon cancer (*n*=1), liver cancer (*n*=2), pancreatic cancer (*n*=1), colorectal cancer (*n*=1), lung cancer (*n*=2), non-Hodgkin's lymphoma (*n*=1), leukemia (*n*=1), and prostate cancer (*n*=5). Seventeen cancer patients received stent implantation, including 7 AMI patients undergoing emergency PCI. Using multivariate analysis, older age and metabolic syndrome were independently associated with present of cancer in CAD patients ($P < 0.01$). **Conclusion** The prevalence of cancer in patients with CAD was 0.73%. The older age and metabolic syndrome were independently associated with present of cancer in CAD patients. But, the specific interaction mechanisms between CAD and cancer remains unclear.

[Key words] Coronary artery disease;Cancer;The older age;Metabolic syndrome

Analysis of clinical features and coronary angiography in 10 patients with de winter syndrome

NI Guohua

Sichuan Academy of Medical Sciences & Sichuan Provincial People's Hospital (Chengdu Jinjiang Sohome Comprehensive Outpatient Clinic), Chengdu 610020, China

[Abstract] Objective To investigate the clinical characteristics and electrocardiogram (ECG) changes of patients with de winter syndrome, so as to increase the awareness of de Winter ECG pattern and conducting early emergency interventional therapy for the patients. **Methods** The clinical data of 10 cases of patients with de winter syndrome admitted to the First Affiliated Hospital of Xinjiang Medical University from January 2015 to May 2019 were retrospectively analyzed, to summarize the clinical characteristics, de Winter ECG pattern, the timing of emergency interventional therapy, prognosis, and other factors. **Results** Among the 10 patients with de winter syndrome, 9 males and 1 female, 3 cases of acute extensive anterior wall myocardial infarction (MI), 3 cases of non-ST -segment elevation MI (NSTEMI), 2 cases of acute anterior wall MI, and 2 cases of acute anterior septal MI. All the cases were in line with de winter ECG pattern, and they all had dynamic evolution characteristics. Of these, 7 patients developed ST-segment elevation MI (STEMI) and 3 patients developed NSTEMI. All cases were performed coronary angiography (CAG) and 9 patients were performed percutaneous coronary intervention(PCI). CAG showed that there were 6 cases of multi-vessel coronary disease, 4 cases of proximal occlusion of the left anterior descending artery, 2 cases of subtotal occlusion, 1 case of 95% stenosis in the proximal middle segment of the stent. There was 1 case of middle occlusion of the anterior descending branch and 1 case of subtotal occlusion, all the above 9 cases were performed PCI. One case had 95% stenosis in the middle segment of anterior descending branch, and no interventional therapy was performed due to hematuria. **Conclusion** de winter ECG pattern should be regarded as a STEMI equivalent, prompt recognition of the de winter ECG pattern and a timely diagnosis is of the utmost importance, to perform early emergency medical and interventional therapy. This study will enable cardiovascular clinicians to increase the awareness of de Winter ECG pattern and conducting early emergency interventional therapy for the patients, to improve the outcome and prognosis of the de winter syndrome.

[Key words] STEMI; De winter; ECG

Pharmaceutical care strategy of antiviral drugs for COVID-19 patients with cardiovascular disease

NI Guohua

Sichuan Academy of Medical Sciences & Sichuan Provincial People's Hospital (Chengdu Jinjiang Sohome Comprehensive Outpatient Clinic), Chengdu 610020, China

[Abstract] The novel coronavirus disease 2019 (COVID-19), caused by severe acute respiratory syndrome coronavirus 2 (SARS-CoV-2), has spread worldwide. SARS-CoV-2 has rapidly grown into a pandemic and affected multiple organs, particularly the cardiovascular system. A large number of COVID-19 patients have potential cardiovascular disease (CVD) and/or cardiac risk factors.There is increasing evidence that COVID-19 is associated with increased morbidity and mortality from cardiovascular diseases. Moreover, COVID-19 aggravates the development of cardiovascular disorders, such as myocardial injury, acute coronary syndrome (ACS), arrhythmias, cardiomyopathy, and venous thromboembolism. Many adverse effects and potential drug interactions have been identified, and cardiovascular are exposed to more side effects than other organs. A wide range of cardiotoxicity of IFN-a has been reported,and the most common cardiovascular complications are cardiac arrhythmia, ACS, dilated cardiomyopathy, atrial extrasystole, transient hypotension, pericarditis, and sudden death.some side effects can be life-threatening, especially in patients with cardiovascular diseases (such as hypertension, arrhythmia, ischemic heart disease), and they usually occur in high-risk cardiac patients and result in sudden death, even after the end of therapy, these side effects are unpredictable. Rigorous cardiological attention and monitoring of all patients undergoing interferon therapy are warranted. All patients receiving treatment with interferon should be monitored during and after the end of treatment.

[Key words] Pharmaceutical care strategy;COVID-19;ACS

An assessment of dose-area product and effective dose based on angiographic records comparing between coronary angiography and coronary angiography with intervention: a monocenter retrospective study

CEN Zemin LI Hao QIAN Hai LIN Yuping CHEN Shiyong LUO Kenan

Ningbo Medical Center Lihuili Hospital

[Abstract] **Objective** The purpose of this study was to evaluate dose-area product and effective dose in coronary angiography (CA) with or without percutaneous coronary intervention (PCI), and to get information about to what extent CA+PCI had more radiation dose than CA only. **Methods** In 2017-2018, a total of 980 patients' data undergoing CA with or without PCI in Ningbo Medical Center Lihuili Hospital were collected retrospectively, including 777 cases of CA and 203 cases of CA+PCI. Dose-area product (DAP), cumulative air kerma (Ka,r), fluoroscopic time (FT) were collected and converted into effective dose (ED). **Results** The median value of estimated effective dose for CA was 1.27 mSv; for CA+PCI, the median value was 5.36 mSv. CA+PCI's value was about 4.2 times of CA's. Correlation analysis showed positive correlation between ED and the following: FT, Ka,r, number of runs acquired and BMI. **Conclusion** The results conformed to intuition , and showed that CA+PCI had more radiation doses than CA. operators should stick to ALARA principle and assess intervention indications carefully.

[Key words] Coronary angiography;Angiographic records comparing;PCI

Combinational therapy with aspirin and ticagrelor alleviates vascular inflammation and angiotensin Ⅱ–driven abdominal aortic aneurysm formation in mice

LIU Xiaowei WENG Yingzheng LUO Jiangjie CHEN Xiaofeng TANG Lijiang
Zhejiang Hospital, Hangzhou 310013, China

[Abstract] **Background** Abdominal aortic aneurysm (AAA) is a severe form of blood vessel–related disease. Medial degeneration and inflammation are typical characteristic of AAA. Activated platelets release many pro–inflammatory cytokines and participate in the initial inflammatory response to various vascular diseases. Although there are some studies on the effects of APAs on AAA, it is yet unknown whether the new P2Y12 receptor inhibitor ticagrelor (T) can inhibit AAA. Herein, we explored the consequences of ticagrelor exposure on AAA progression and determined whether a combinational therapy, involving T and aspirin (A), exerts a stronger inhibitory effect in vivo. **Methods** AAA was established in apolipoprotein E–deficient ($ApoE^{-/-}$) mice via a 28–day administration of angiotensin Ⅱ (Ang Ⅱ). Next, the mice were arbitrarily separated into 5 groups: saline infusion alone (sham), Ang Ⅱ infusion alone, Ang Ⅱ infusion plus oral A (10 $mg\cdot kg^{-1}\cdot d^{-1}$), Ang Ⅱ infusion plus oral T (120 $mg\cdot kg^{-1}\cdot d^{-1}$), Ang Ⅱ infusion plus combinational therapy with A (10 $mg\cdot kg^{-1}\cdot d^{-1}$) and T (120 $mg\cdot kg^{-1}\cdot d^{-1}$). **Results** The combined treatment markedly suppressed the Ang Ⅱ –driven elevation of maximal aortic diameter, aneurysm formation (26.7% decrease, $P<0.05$), alterations in aortic expansion, elastic lamina destruction, platelet deposition, and inflammatory cytokine accumulation. In addition, it also diminished matrix metalloproteinase (MMP)–2 and MMP–9 production. **Conclusion** A combinational therapy of A and T, but not individual drugs, inhibits Ang Ⅱ –driven AAA generation in mice in vivo, and this process may be regulated by a suppressed inflammatory response.

[Key words] Aspirin;Ticagrelor;Abdominal aortic aneurysm;Ang Ⅱ

Anomalous origin of the left anterior descending artery from the right sinus of Valsalva with an interarterial course

QIAN Hai XU Weifeng WANG Ying LOU Ke'nan ZHANG Luxing
Ningbo Medical Center Lihuili Hospital, Ningbo University, Ningbo 315040, China

[Abstract] Anomalous origin of coronary arteries from the opposite sinus of valsalva is a rare congenital malformation considered ''malignant'' when it has an interarterial course. Modern imaging techniques are used for effective identification of anatomical features of anomalous coronary arteries and helps to further classify them as benign or malignant anomalies. This study presents a case of a 59–year–old presenting with anomalous origin of the left anterior descending artery from the right sinus of Valsalva with an interarterial course between the aorta root and right ventricular outflow tract.

[Key words] Coronary arteries;The aorta root;Right ventricular outflow tract

LCZ696 attenuates ROS/NLRP3 mediated pyroptosis in trastuzumab-induced H9C2 cell model via ameliorating Sirt3 expression

ZANG Yanxiang BAI Nan LOU Qi LIU Guangzhong WANG Hong DUAN Yuchen LI Jianqiang LI Weimin

The First Affiliated Hospital of Harbin Medical University, Harbin 150000, China

[Abstract] **Objective** Trastuzumab-induced cardiomyopathy have been a kind of clinical crucial problems in the field of cardio-oncology. LCZ696, clinically named sacubitril/valsartan, was administered to treat the patients with heart failure, so that it may be a substantial prevention to attenuate chemotherapy-induced cardiotoxicity. **Methods** This firstly confirmed that LCZ696 and trastuzumab can affect the content of Sirt3 and NLRP3 in H9C2 cell, which confirmed the concentration of LCZ696 (10 μM) and trastuzumab (100 nM). Then H9C2 cells were allocated into 3 groups: Con group; TRA group; TRA+LCZ696 group.Then investigated the change of mRNA expression and protein synthesis of cultured H9c2 cardiocardiomyocytes on exposure to trastuzumab alone or plus LCZ696. **Results** Meanwhile, it turns out that LCZ696 can ameliorate the mRNA expression and content of Sirt3, inhibit the level of ROS, NLRP3, ACS, Caspase-1 and IL-1β in trastuzumab-induced H9C2 cell model. **Conclusion** In summary, LCZ696 reduces the oxidative stress caused by ROS and NLRP3-mediated pyroptosis by protecting the activity of Sirt3 in H9C2 cells.

[Key words] LCZ696;H9C2 cells;Sirt3

A cohort study on the correlation between low-density lipoprotein cholesterol and all-cause mortality in coronary intensive care unit patients

WENG Yingbei WANG Jie XUE Yangjing JI Kangting

The Second Affiliated Hospital and Yuying Children's Hospital, Wenzhou Medical University, Wenzhou 325000, China

[Abstract] **Objective** The aims of this study were to investigate the relationship between LDL-C levels and all-cause mortality in CCU patients, adjusting for a wide range of potential confounding factors, to examine the potential of LDL-C in predicting the prognostic value of CCU patients. **Methods** Clinical data were extracted from Medical Information Mart for Intensive Care-Ⅲ database (MIMIC-Ⅲ database version 1.4). Baseline data were collected within 24 hours after the patient was first admitted to the hospital. Our study endpoints are 30-day, 90-day, and one-year mortality. Cox proportional hazard regression and propensity score-matched (PSM) analysis were used to analyze the association between LDL-C levels and prognostic value of CCU patients. **Results** It included a total of 1 476 patients with an average age of 66.7±14.1 years (66% were male). For 30-day all-cause mortality, the hazard ratios (95% confidence interval) of high LDL-C level group (≥55 mg/dL) was 0.42 (0.29, 0.62), which was compared with low LDL-C level group (<55 mg/dL) in unadjusted model. This association remained similar in multivariate models. Similar correlations were observed for 90-day and one-year all-cause mortality. The relationship between all-cause mortality and LDL-C levels in CCU patients was further verified by propensity score-matched (PSM) analysis. **Conclusion** This data suggest that LDL-C is associated with a reduced risk of 30-day, 90-day, and one-year mortality of patients in the

CCU. And this result is still stable in the PSM model. LDL–C may be an easily available and cost–effective strategy for predicting the prognostic value of CCU patients. The results need to be verified in prospective trials.

[Key words] LDL–C;CCU;PSM model

Association between the percentage of platelets and lymphocytes and 30–day mortality in CCU patients

XUE Yangjing WENG Yingbei WANG Lei JI Kangting WANG Jie

The Second Affiliated Hospital and Yuying Children's Hospital, Wenzhou Medical University, Wenzhou 325000, China

[Abstract] Background Platelet–to–lymphocyte percentage ratio (PLR), a novel inflammation marker, has been proved to be associated with mortality in cardiovascular critical illnesses. The purpose of this study was to explore whether PLR can be a marker in predicting mortality among CCU patients. Methods A retrospective analysis of data from the Multiparameter Intelligent Monitoring in Intensive Care Ⅲ database (MIMIC– Ⅲ v1.4) was conducted. The primary outcome was 30–day mortality and the two secondary outcomes were 90–day and one–year mortality. The association between PLR and mortality was evaluated using the Cox proportional hazards models. Then we collected data from CCU patients in the Second Affiliated Hospital of Wenzhou Medical University, and performed Pearson correlation analysis on their C reactive protein (CRP)and PLR. Results A total of 3 423 patients were eligible. For 30–day mortality, after adjusted for age, gender and ethnicity, a trend suggested that a higher PLR was associated with an increased risk of mortality (PLR > 28.90; *HR*=2.20). After adjusting for more confounders, it indicated that a relatively low PLR (< 13.72) had a low mortality risk. Same tendencies were observed for 90–day and one–year mortality. Pearson correlation analysis for CRP and PLR showed that the R value was 0.320 ($P < 0.05$). Conclusion Patients with elevated PLR at CCU admission were associated with higher mortality risk. Pearson correlation analysis showed that there was a correlation between CRP and PLR.

[Key words] PLR;CRP;CCU

Resuscitation of patient with massive right coronary air embolism with implementation of electric defibrillation during coronary intervention

NIE Qian DONG Mei XIE Wen CHENG Wenqiang

Hospital of Chengdu University of Traditional Chinese Medicine, Chengdu 610072, China

[Abstract] Coronary air embolism, is one of the inadvertent and old complications of coronary angiography which persistently happened during the procedure over years. It report a case of complicating massive air embolism in the right coronary artery(RCA) during PCI, then coronary slow flow(CSF), bradycardia and hypotension occured consequently. After emergency catecholamines being given to the patient, the cardiac arrest happened. The patient was resuscitated successfully by electric defibrillation and recovered with TIMI 3 coronary flow at last. This figure that by making myocardium strongly contract through electrical stimulation by cardioverter Defibrillator might be a method to tackle massive coronary air embolism.

[Key words] Resuscitation;Coronary air embolism;Electric defibrillation

Stress cardiomyopathy caused by subarachnoid hemorrhage

LYU Feng TAO Yuan

Shengzhou People's Hospital, Shengzhou 312400, China

[Abstract] Stress cardiomyopathy(SCM) is a syndrome of transient left ventricular dysfunction with electrocardiographic changes and elevated myocardial enzymes, but without coronary artery disease. The disease is usually associated with severe physical or emotional stress, acute illness, etc. In recent years, it has been found in some neurological emergencies, especially in patients with subarachnoid hemorrhage (SAH) . SAH is likely to result in death and severe disability, whereas patients who develop SCM after SAH usually have a higher mortality and a worse prognosis.

[Key words] SCM;SAH;Left ventricular dysfunction

Plasma ATP can be a marker for human hypertension

CHEN Yiwen SHEN Xiao ZHANG Huafang XIA Shudong

The Fourth Affiliated Hospital of Zhejiang University School of Medicine, Yiwu 322000, China

[Abstract] Adenosine 5′ – triphosphate (ATP), as danger/damage related molecules (DAMPs), activate abnormal immune driving development and progression of hypertension. It was reported that ATP was significantly elevated in hypertensive mice and maintained a significant rise in 2 weeks after the onset of hypertension.However, there are few studies on the concentration of ATP in human with hypertension. Thus, we conducted this study to investigate the correlation between plasma ATP level and the hypertension in a Chinese population. This study enrolled 867 patients with hypertension (HTN, *n*=609)and normotensive controls (NTN, *n*=258). **Results** The ATP levels were significantly higher in theHTNthan in the NTN group (median ATP, 1.199 μM versus 0.905 μM, $P < 0.01$) and were reduced in the controlled groupwho were taking anti–hypertensive medications and had both average SBP below 140 mmHg and average DBP below 90 mmHg(C– HTN) (median ATP, 1.079 μM versus 1.199 μM, $P < 0.01$). As a risk factor, ATP is closely related to the prevalence of hypertension and the degree of blood pressure control.

[Key words] Hypertension; ATP; Marker

Diagnostic performance of CFD–based computed FFR derived from coronary CT angiography for assessment of functional severity of coronary artery stenosis

LI Changling JIANG Jun TANG LiJiang DU Changqing HU Yumeng LENG Xiaochang HE Jingsong FENG Li DONG Liang SUN Yong XIANG Jianping WANG Jian'an

The Second Affiliated Hospital Zhejiang University School of Medicine, Hangzhou 310009, China

[Abstract] **Objective** The objective of this study was to evaluate the feasibility and diagnostic accuracy of a novel computational fluid dynamics (CFD)–based technology for the diagnosis of functionally significant coronary artery disease (CAD) from coronary computed tomographic angiography (CCTA), using wire–based FFR as a reference standard. Fractional Flow Reserve (FFR) is the gatekeeper for lesion–specific revascularization decision–making in patients with stable CAD. The potential of a novel computed tomography (CT) FFR technology AccuFFRct to identify ischemia–causing lesions noninvasively has not been sufficiently assessed. **Methods** This retrospective multicenter study included 151 patients who underwent routine invasive FFR for suspected CAD. CCTA was performed less than 2 months before ICA. AccuFFRct was computed and interpreted in a blinded fashion by professionals. The 3D patient–specific anatomic model, including the coronary artery tree, the aorta and the heart was semi–automatically reconstructed from CCTA data. During the model reconstruction, a deep–learning segmentation method was used to extract the left ventricle. Coronary artery segmentation was performed using colliding fronts method, while aorta images were segmented with a fast marching algorithm. Then, the level–set algorithm was used to optimize the borders of coronary arteries. The final anatomic model was reconstructed by a marching cubes algorithm. The 3D segmented geometric model was first pre–processed before meshing. A volume mesh model was then generated for the computation AccuFFRct using CFD simulation with the finite volume method. For boundary conditions, the total coronary flow was calculated by the mass of the left ventricle myocardium, which could be easily obtained from CCTA–extracted myocardial volume. To estimate hyperemia, the mean blood flow rate was quadrupled and aortic pressure was reduced to 0.8 times the baseline value at rest condition. As for the outlets, blood flow distribution was determined by Murry's law using the lumen diameters of each outlet vessel. The arterial wall was assumed to be rigid with no–slip boundary conditions. Blood was modelled as an incompressible viscous Newtonian fluid (density ρ = 1 056 kg/m^3, viscosity = 0.0035 Pa·s) in the CFD simulation.By solving the Navier–Stokes equations on a standard desktop workstation, numerical results of the flow field and pressure field of coronary arteries can be acquired and visualized on the 3D anatomic model. The AccuFFRct values were computed as the pressure ratio of the distal pressure located at the measuring point of FFR to the aortic pressure.Compared to invasive FFR, a threshold of $\leqslant$ 0.80 was used to indicate the hemodynamically relevant stenosis. **Results** On a per–patient basis, the overall accuracy, sensitivity, specificity, positive predictive value (PPV), and negative predictive value (NPV) of AccuFFRct for detecting ischemia were 89.0%, 84.6%, 91.5%, 84.6% and 91.5%, respectively. The AccuFFRct and FFR was well correlated with Pearson's correlation coefficient r= 0.677 (P < 0.001). The AUC of AccuFFRct determination was 0.899. **Conclusion** AccuFFRct measured from the CCTA provides accurate detection of the functional significance of coronary stenosis within 35 minutes, which may eventually become a safe and effective gatekeeper to ICA, thereby leading to improved patient outcomes.

[Key words] CDA;FFR;Coronary artery stenosis

Serum uric acid is associated with the progression of left ventricular diastolic dysfunction in apparently healthy subjects

YANG Chendie WANG Xiaoqun

Ruijin Hospital, Shanghai Jiao-Tong University School of Medicine, Shanghai 200025, China

[Abstract] **Background** Left ventricular (LV) diastolic dysfunction (LVDD) is the defining feature of heart failure with preserved ejection fraction (HFpEF), and predicts subsequent incident heart failure (HF) and all–cause mortality. Mounting evidence reveals that cardiometabolic risk factors play critical roles in the development of LVDD. In this study, we sought to investigate the relation between serum uric acid (SUA) level and the progression of LVDD in apparently healthy

patients. **Methods** A total of 1 082 apparently healthy subjects without diagnosed cardiovascular disease and with relative normal LVDD (grade 0–1) were consecutively enrolled. SUA levels were measured and repeat echocardiography and tissue Doppler imaging (TDI) were performed at baseline and during 1–year follow–up. **Results** By dividing the study population based on quartiles of SUA, we found subjects in higher quartiles had greater increases in TDI–derived early diastolic velocity (e′) and E (peak LV filling velocity) /e′ ratios during 1–year follow–up. After multivariate adjustment, high SUA persisted to be an independent predictor for the subsequent worsening of LVDD (*OR*=1.351 ,95%*CI*:1.125–1.625, per 100 μmol/L SUA). Subgroup analysis suggested that the association between SUA and LVDD development was more pronounced in subjects without other cardiometabolic risk factors involved. Factor analysis demonstrated that high SUA was the major cardiometabolic attribute in patients with LVDD progression. **Conclusion** This study findings suggest that high SUA is an independent cardiometabolic risk factor for the progression of LVDD in apparently healthy subjects.

[Key words] LVDD;SUA;Healthy subjects

The impact of HbA_{1C} level on heart failure with recovered ejection fraction in patients with type 2 diabetes

YANG Chendie WANG Xiaoqun

Ruijin Hospital, Shanghai Jiao-Tong University School of Medicine, Shanghai 200025, China

[Abstract] Background Heart failure (HF) with improved or recovered ejection fraction (EF, HFrecEF) has been recognized as a new type of HF with different underlying clinical phenotype, pathophysiology and prognosis. However, few studies have analyzed the relationship between type 2 diabetes and HFrecEF, and the impact of glycemic level on myocardial function recovery. Purpose In the present study, this sought to investigate the relation between HbA_{1C} level and HFrecEF in patients with type 2 diabetes. **Methods** A total of 796 HF patients with reduced left–ventricular ejection fraction (LVEF, < 40%) and type 2 diabetes were consecutively enrolled from August 2012 to July 2020. During follow–up for up to 24 months, patients were classified into HFrecEF for whom developed recovered LVEF (≥40% and absolute increase ≥5%) and HFrEF for whose LVEF was persistently reduced (< 40%). The relation between HbA_{1C} and the recovery of LV function was analyzed. **Results** HF patients with type 2 diabetes had significantly lower rates of LVEF recovery when having higher versus lower HbA_{1C} levels in the baseline (the lowest tertile: 62.4%, intermediate tertile: 50.4%, the highest tertile, 46.8%, $P < 0.01$). There were stepwise decreases in changes of LVEF ($P < 0.01$) and increases in changes of LV end–systolic diameter (LVESd, $P > 0.05$) with increasing tertiles of LVEF during follow–up. In the subgroup analysis, the impact of HbA_{1C} on LVEF recovery was more prominent in patients with ischemic heart disease ($P < 0.001$) than those with dilated cardiomyopathy ($P > 0.05$). A significant interaction term was present between HbA_{1C} and etiology of heart failure with regard to LVEF recovery ($P < 0.05$). After multivariate adjustment of conventional confounding factors, high HbA_{1C} level remained to be an independent risk factor lower incidence of HFrecEF in patients type 2 diabetes. **Conclusion** This study suggests that optimal glycemic control is an independent predictor for incidence of HFrecEF in patients with type 2 diabetes.

[Key words] HFrecEF;Type 2 diabetes; Glycemic control

Basic biological characteristics of lncRNA B230352I09 and its role in the process of myocardial injury

CHEN Yumei XU Feixiang XUE Mingming WANG Sheng DU Shilin TONG Chaoyang
Department of Emergency Medicine, Zhongshan Hospital, Fudan University, Shanghai 200032, China

[Abstract] **Objective** To explore the basic biological characteristics of lncRNA B230352I09 and its role in the process of myocardial injury. **Methods** This analyzed the biological characteristics of lncRNA B230352I09 on the UCSC website and predicted the possible binding protein of lncRNA B230352I09 by the catRAPID. Real-time fluorescence quantitative (RT) PCR method was applied to detect the expression of lncRNA B230352I09 in heart tissues at different time points (0, 1, 3, 7d) within 7 days after birth, the organs distribution and expression of lncRNA B230352I09 in neonatal mouse and the expression pattern of lncRNA B230352I09 in the heart of mice with myocardial injury. In addition, we constructed hypoxia model by culturing primary cardiomyocytes to detect the effect of lncRNA 230352I09 overexpression on hypoxic cardiomyocyte apoptosis by Hoechst staining kit, the effect of lncRNA B230352I09 overexpression on ROS content of hypoxic cardiomyocyte by DCFDA probe and changes inmitochondrial membrane potential of hypoxic cardiomyocytes by JC-1 Fluorescent probes. **Results** Full-length of mouse B230352I09 was 663bp, located in the chr7:123031415-123066439 forward strand. RBBP6 gene was adjacent to B230352I09, which may be the target of lncRNA B230352I09 by catrapid prediction analysis. With the development of the heart, the expression level of lncRNA B230352I09 showed a gradual downward trend. The main expression organs of lncRNA B230352I09 in 1-day-old mice were heart, brain, kidney and liver. In heart tissue, lncRNA B230352I09 was mainly expressed in cardiomyocytes. After myocardial injury, the expression level of lncRNA B230352I09 showed an increasing trend compared with the normal developing mice, but there was no statistical significance. Hoechst staining showed that lncRNA B230352I09 could significantly inhibit the apoptosis of hypoxic cardiomyocytes. LncRNA B230352I09 significantly reduced ROS production in hypoxic cardiomyocytes by DCFDA probe assay. JC-1 fluorescent probe was used to detect the mitochondrial membrane potential, and the results showed that the mitochondrial membrane potential of cardiomyocytes in the lncRNA B230352I09 overexpression group was significantly higher than that in the control group. **Conclusion** In heart tissue, lncRNA B230352I09 was mainly expressed in cardiomyocytes. LncRNA B230352I09 has a protective effect in the process of myocardial injury in mice, mainly by inhibiting apoptosis of cardiomyocytes, reducing ROS production, and protecting mitochondrial membrane potential of cardiomyocytes.

[Key words] Heart tissue; LncRNA B230352I09;ROS

Intracardiac echocardiography-guided optimization of procedural workflow in patients undergoing left atrial appendage closure

DU Xianfeng ZHUO Weidong HE Bin CHU Huimin
Ningbo First Hospital, Ningbo 315010, China

[Abstract] **Background** The reduction of fluoroscopic exposure under the application of intracardiac echocardiography (ICE) in the left atrial appendage closure (LAAC) procedure has been well proved. **Objective** The

aim of this study is to establish pilot experience of the LAAC workflow optimization under the ICE guidance on the basis of conventional fluoroscopy–only minimalistic approach. **Methods** A total of 89 patients with nonvalvular atrial fibrillation [female 32.6%, aged (71.8 ± 9.1) years, mean CHA_2DS_2–VASc score (4.5 ± 1.5); mean HAS–BLED score (2.9 ± 0.7)] were enrolled into the optimized group. The ICE catheter was introduced into the left atrium to evaluate the LAA size and its closure results from three orthogonal anatomic landmarking positions (Axis–X: from left pulmonary veins LPVs to LAA; Axis–Y: from right PV ostium to LAA; Axis–Z: from mitral annulus ostium to LAA). Intraprocedural and follow–up outcomes were compared to those from 179 patients who underwent the LAAC procedures following the minimalistic approach. **Results** There was no difference between groups on the baseline characteristics except for more pacifier devices were applied in the optimized group (50.6% vs 19.6%, $P < 001$). Significant reduction of fluoroscopy time [(5.6 ± 2.9) vs (7.0 ± 3.2)min, $P < 001$], fluoroscopy exposure [(103.1 ± 61.7) vs (139.4 ± 102.3) mGy,$P < 0.05$] and contrast volume [(73.8 ± 58.7) vs (103.5 ± 44.7) mL,$P < 001$] were observed in the optimized group without prolonging the procedure duration. More patients achieved low–fluoroscopic procedures (< 50 mGy) in the optimized group (23.6% vs 7.8%, $P < 001$). Fourteen (15.7%) contrast–free cases were recorded in the optimized group. No difference of peri–procedural safety endpoints was recorded. However, the incidence of device–related thrombus (DRT) during follow–up was higher (5.6% vs 0.6%, $P < 0.05$) in the optimized group. **Conclusion** LAAC procedure workflow could be optimized following the orthogonal triaxial assessment using ICE to reduce the fluoroscopy and contrast consumption. Pacifier devices favors the ICE–guided procedures for better imaging manifestation, however, the DRT incidence might be higher as well.

[Key words] Atrial fibrillation; Left atrial appendage closure; Intracardiac echocardiography;Fluoroscopy exposure

Validation of a novel catheter–based renal denervation system of cryoablation: a preclinical study and case series

Ji Meng CHEN Han SHEN Li YAO Zhifeng WU Yizhe GE Junbo

Department of Cardiology, Zhongshan Hospital, Fudan University, Shanghai 200032, China

[Abstract] Background Renal denervation has been one of the most rapidly developing and promising therapeutic methods in the treatment of hypertension in recent years. It conducted a preclinical experiment in swine and an early clinical study in humans to confirm the safety and efficacy of cryoablation renal denervation (cryo–RDN) with a CryoFocus balloon catheter in resistant hypertension patients. **Methods** A novel cryoablation balloon catheter was used for cryo–RDN in both swine and patients (n=29 and 6, respectively). In swine, cryo–RDN was conducted in both renal arteries. A reduction in renal and serum norepinephrine (NE) concentration and safety were the primary endpoints. In the clinical cases, cryo–RDN was performed after anatomical confirmation by renal angiography. The change in the 24–h systolic blood pressure (SBP) and the occurrence of device–related adverse events after 6 months were set as the primary efficacy and safety endpoints, respectively. **Results** In the preclinical study, both the renal and serum NE concentrations decreased significantly compared with baseline ($P < 0.05$). Renal function was unchanged without stenosis of the renal artery or other abnormalities. Data from the case series showed no evidence of vascular complications or biochemical disruption. The baseline mean office blood pressure (OBP) of the 6 participants was 158.17/93.00 mmHg, and their mean 24–h average blood pressure (ABPM) was 145.83/89.67 mmHg. At the end of the follow–up period, the 24–h SBP and 24–h DBP were significantly decreased with an average reduction of –12.16 mmHg ($P < 0.05$) and –8.50 mmHg ($P < 0.05$). Similarly, the office SBP and DBP decreased by –21.7 mmHg ($P < 0.05$) and –11.5 mmHg ($P > 0.05$) after 6 months. **Conclusion** Cryo–RDN with this dedicated cryoablation balloon catheter was safe and feasible for

reducing blood pressure in the preclinical and case series. Further clinical evaluation of its safety and efficacy at a larger scale is needed.

[Key words] Renal denervation system;Cryoablation;Novel catheter

Impact of mean platelet volume on long-term clinical outcomes in Chinese patients with type 2 diabetes mellitus undergoing percutaneous coronary intervention: a propensity-matched analysis

JIANG Chunying LING Zhi LU Wen XU Yawei HAN Bing

Xuzhou Central Hospital, Xuzhou 221009, China

[Abstract] **Background** Mean platelet volume (MPV), a biological marker of platelet function, links to thrombosis and atherosclerosis in the cardiovascular system. However, little is known about the impact of MPV on long-term clinical outcomes in diabetic patients undergoing percutaneous coronary intervention (PCI). **Methods** This study retrospectively analyzed data from participants of 2 groups (Group A and Group B) on a 1:1 basis by identical propensity scores. Baseline characteristics and PCI parameters were compared. Composite end points were analyzed for clinical independent predictors. **Results** Diabetic patients with higher MPV [(8.52 ± 1.66) vs. (8.02 ± 0.71) fL, $P < 0.01$] presented more multi-vessel disease (62.05% vs. 43.08%, $P < 0.001$) and implanted minor diameter stents [(3.02 ± 0.42) vs. (3.12 ± 0.44) mm, $P < 0.05$] as compared with non-diabetes patients. MPV was positively correlated with fasting plasma glucose and glycosylated hemoglobin A (HbA_{1C}) levels in the whole propensity-matched patients (r=0.402, $P < 0.01$; r=0.163, $P < 0.05$). After a 72-months follow-up period, higher incidences of cardiac mortality and coronary events were observed in the patients of Group A as compared with Group B (*HR*=2.34 , $P < 0.05$; *HR*=1.57, $P < 0.05$). Adjusted multivariable logistic regression analysis showed that HbA1C (*HR* =1.914, 95%*CI*: 1.306-2.807, $P < 0.05$) and MPV (*HR*=4.850, 95%*CI*: 2.016-11.664, $P < 0.01$) were independently related to major adverse cardiac events (MACEs). **Conclusion** Patients with higher MPV and HbA_{1C} are at higher risk of developing MACEs when compared to patients without diabetes after PCI. Thus, measuring MPV could be a beneficial tool for evaluating cardiovascular risk in diabetic patients after PCI treatment for coronary artery disease.

[Key words] MPV;HbA_{1C};PCI;Coronary artery disease

The relationship between adverse outcomes and a full spectrum of ejection fraction in patients without acute myocardial infarction undergoing percutaneous coronary intervention

LIU Yupeng SONG Jingjing TAng Yida

Fuwai Hospital, Beijing 100037, China

[Abstract] **Background** There is insufficient study evaluating how the risk of adverse cardiovascular outcomes varies across the full range of LVEF in patients undergoing percutaneous coronary intervention (PCI). A more comprehensive evaluation could provide further understanding of prognosis and support the management of these

patients. Purpose The present study aimed to assess the association between left ventricular ejection fraction (LVEF) and major adverse cardiovascular events (MACE) in patients with coronary artery diseases undergoing PCI. Methods A consecutive series of 9 475 patients without acute myocardial infarction (AMI) undergoing PCI were enrolled into the study and followed up for a median 2.4 years. Patients were stratified into 8 groups by 5% intervals: under 40%, 40%–45%, 45%–50%, 50%–55%, 55%–60%, 60%–65%, 65%–70%, and over 70%. MACE, consisting of cardiac death, myocardial infarction, stent thrombosis, and revascularization, was evaluated as the outcome. Results MACE occurred in 594 (6.3%) patients. The MACE rates decreased before LVEF under 65% while increased after LVEF over 70%, showing a U–shaped pattern. The 65%–70% group showed the lowest rate of MACE (4.5%). Consistently, in the Cox regression, the association between LVEF and MACE presented as a U–shaped pattern regardless of different age and sex groups, and after adjusted for clinical and procedural covariables. The LVEF categories lower than 65% or higher than 70% were independent predictors of MACE, compared with 65%–70% group (Hazard ratios 1.311 to 2.657, all $P>0.05$). Similar trend was also observed in restricted mean survival time analysis. Conclusion LVEF and MACE displayed a U–shaped association and patients with LVEF of 65%–70% showed the lowest risk of MACE. The present study provided an insight into how the MACE risk changed in a wide spectrum of LVEF in patients without AMI undergoing PCI, which might improve preprocedural evaluation.

[Key words] LVEF; MACE;PCI

Predictors of in–hospital mortality in drug–induced thrombotic microangiopathy

WANG Xiaoya

The Second Affiliated Hospital of Zhejiang University, Hangzhou 310009, China

[Abstract] Background Although drug–induced thrombotic microangiopathy(DITMA) has been reported and studied for several decades, there is no data on predictors of mortality in this specific population. Methods We searched EMBASE and PUBMED databases to identify reports of DITMA. Multiple logistic regression analysis was used to determine independent predictors of in–hospital mortality in DITMA patients. Results Among 394 patients(mean age 50.57 years, 57.36% women) with DITMA, in–hospital mortality was 12.94%. Independent predictors of increased in–hospital mortality in DITMA patients were malignancy (*OR*=2.53, 95%*CI*:1.26–5.07, $P<0.01$), severe thrombocytopenia (*OR*=2.15, 95%*CI*:1.12–4.12, $P<0.05$) and platelet transfusion (*OR*=2.64, 95%*CI*:1.07–6.52, $P<0.05$). Independent predictors of increased in–hospital mortality in DITMA patients with severe thrombocytopenia were malignancy (*OR*=7.31, 95%*CI*:2.39–22.36, $P<0.01$) and cardiac involvement (*OR*=4.33, 95%*CI*:1.19–15.70, $P<0.05$). Independent predictors of increased in–hospital mortality in DITMA patients without severe thrombocytopenia was platelet transfusion(*OR*=4.28, 95%*CI*:1.26–14.59, $P<0.05$). Conclusion In this retrospective study of DITMA, in–hospital mortality was 12.94%. Malignancy, low platelet level and platelet transfusion were identified as independent predictors of increased in–hospital mortality. Moreover, plasma exchange therapy may not improve the survival rate of DITMA.

[Key words] Drug–induced thrombotic microangiopathy; Predictor; In–hospital mortality

Single cell transcriptomics sequencing reveals the molecular pathologic mechanism of plaque erosion immune network

QIAN Jun　CHEN Fei　LIU Xuebo

Shanghai Tongji Hospital, Shanghai 200065, China

[Abstract] **Objective** Plaque rupture(PR) followed by thrombosis is considered the main mechanism of acute coronary syndromes(ACS), accounting for approximately two-thirds of acute myocardial infarction. In recent years, the proportion of plaque erosion(PE) increased with the intensity of lipid-lower therapy, and the pathological difference with PR is unclear. Here, we used single cell RNA sequencing to identify subsets of immune cells and genes mediating inflammation and to dissect the immunological network of ACS. **Methods** Transcriptomic profiles of peripheral blood mononuclear cells were analysed in 5 patients diagnosed with PR and 5 patients with PE by single cell RNA sequencing. By focusing our analysis on immune cells, we obtained a higher resolution identification of the monocyte and T cell subsets in patients experiencing with PR and PE. **Results** Compared with patients with PE, the classical monocytes of PR showed an significantly increased expression of leukocyte-endothelial cell adhesion genes as ICAM1, ITGAL, RUNX3 and pro-inflammatory genes as CCL5, TLR7, and CX3CR1 with similar cell numbers. Non-classical monocytes were predominated in patients with PR, and its gene ontology(GO) term were mainly enriched in cellular response to lipopolysaccharide, positive regulation of NF-kB transcription factor activity and cellular response to interferon-gamma. Among the upregulated genes in PR with non-classical monocytes were CCL5, TLR7, and CX3CR1, which augments inflammatory response. While up-regulated genes in PE mainly induced a neutrophil degranulation and regulation of neutrophil apoptotic process. Conversely, the number of intermediate monocytes in patients with PE was significantly increased, and plays an important role in activating neutrophils and leading to neutrophils degranulation. T cells were observed at the highest percentage of all immune cells. The GO analysis of regulatory T cells(Tregs) in patients with PE was mainly enriched in autophagy, process utilizing autophagic mechanism and macroautophagy, with NAMPT was significantly associated with these biological process. Moreover, the NAMPT expression level was significantly increased in PE. $CD4^+$ effector T cells, in which the expression of CCL5, CXCR3 and NKG7 were upregulated in PR, mainly enriched in the cell activation, chemokine and cytokine production. While $CD8^+$ effector T cells expressed more effector molecule in patients with PE as GZMB, GNLY and PRF1, which may promote the apoptosis and shedding of endothelial cells. **Conclusion** This study demonstrates that circulating monocytes of patients with PR exhibit a highly pro-inflammatory characteristic compared to PE, while $CD8^+$ effector T cells releasing a series of effector molecules caused endothelial cell death, which may contribute to the progress of PE.

[Key words] Plaque rupture; Acute coronary syndromes; Plaque erosio

Prosthetic valve endocarditis and re-intervention after transcatheter aortic valve implantation

ZHU Qifeng　LI Bohui　LIU Xianbao　WANG Jian'an

The Second Affiliated Hospital of Zhejiang University, Hangzhou 310009, China

[Abstract] Transcatheter aortic valve implantation(TAVI) has been widely accepted and recognized as mainstream treatment for a large portion of patients with aortic stenosis(AS), while prosthetic valve durability remains as one of major concerns for TAVI indication expansion. Prosthetic valve endocarditis significantly impaires device durability, leading to

bioprosthetic valve dysfunction and poor prognosis in most cases. Here we present a series of multi-modality images on a patient suffered from prosthetic valve endocarditis and re-intervention.

[Key words] Transcatheter aortic valve implantation; Aortic stenosis

Diagnostic value of trimethylamine N-oxide in aortic stenosis

GUO Yuchao

The Second Affiliated Hospital of Zhejiang University, Hangzhou 310009, China

[Abstract] **Background** To evaluate the diagnostic value of trimethylamine N-oxide in aortic stenosis. **Methods** Three hundred and nine consecutive patients with severe aortic stenosis were included in this study from 2013 to 2018 (AS group). Seven hundred and eleven patients with normal coronary angiogram were included as control (control group). One hundred and seventeen pairs patients were assembled by Propensity Score Matching. Trimethylamine N-oxide levels in plasma were determined using stable isotope dilution high-performance liquid chromatography with on line electrospray ionization tandem mass spectrometry (LC/MS/MS) using d9-(trimethyl)-labelled internal standard. **Results** Compared with patients with normal coronary angiogram, patients with severe aortic stenosis had higher TMAO value (5.66 ± 10.26 μmol/L vs 3.04 ± 2.98 μmol/L, $P < 0.01$). Univariant logistic regression revealed that aortic stenosis was associated with higher TMAO level, male, smoking history, hyperlipidemia, diabetes mellitus, COPD, low BMI, low LVEF, low eGFR. Multivariant logistic regression revealed significant relation ship between AS and TMAO level (*OR*=1.075, 95%*CI*:1.014-1.14, $P < 0.01$). The AUC of ROC of TMAO was 0.693(95%*CI*:0.655-0.731). **Conclusion** The TMAO level was higher in aortic stenosis patients. Prospective assessment of outcomes after TAVR using trimethylamine N-oxide is needed in patients with aortic stenosis.

[Key words] Diagnostic value; Trimethylamine N-oxide; Aortic stenosis

Functional assessment of coronary artery stenosis from coronary angiographic and CTA images: angio-FFR versus CT-FFR

JIANG Jun LI Changling TANG Lijiang LENG Xiaochang DU Changqing HU Yumeng HE Jingsong FENG Li DONG Liang SUN Yong HU Xinyang XIANG Jianping WANG Jian'an

The Second Affiliated Hospital of Zhejiang University, Hangzhou 310009, China

[Abstract] **Objective** CT-FFR and angio-FFR based on coronary images were developed in order to make a functional evaluation of coronary artery disease. This study was designed to compare the diagnostic performances of angio-FFR and CT-FFR for hemodynamically significant coronary stenosis when FFR≤0.80. **Methods** One hundred and ten patients with 139 vessels were retrospectively enrolled in this study to compute angio-FFR and CT-FFR values for each lesion with the wire-measured invasive FFR value as a reference. Angio-FFR was calculated using dedicated software(AccuFFRangio, version 1.0, ArteryFlow, Hangzhou, China) by technicians who were blinded to FFR. AccuFFRangio is software intended for performing calculations with X-ray angiographic images of the coronary arteries. These calculations are based on contours, which are automatically detected in two angiographic views of

the same vessel. AccuFFRangio enables interventional cardiologists and researchers to obtain accurate anatomical quantifications of one or more lesions in the analyzed coronary segment to determine the functional significance of the individual and consecutive multiple lesions.Angio–FFR was computed using dedicated software (AccuFFRangio, version 1.0, ArteryFlow, Hangzhou, China) by technicians who were blinded to FFR. Two angiographic images with the angle of projections > 25° apart at the end–diastolic frame were selected and 3D reconstruction for the segmented vessels was conducted. Percentage area stenosis(AS%) and diameter stenosis (DS%) were calculated from the 3D–QCA model. Then the contrast frame count was performed to calculate the flow velocity. Based on the segmented vessel, calculated velocity and input aortic pressure, AccuFFRangio distribution could be calculated through the pressure drop equations. As for CT–FFR, Three dimensional (3D) computer model of coronary arteries and the left ventricular myocardium were reconstructed in surface–triangulation format and isolation of the region of interest was carried out. Then 3D segmented geometries were cleared through the Geomagic tool (Geomagic Inc, Morrisville, North Carolina). The blood flow and pressure of the coronary artery tree were simulated by using CFD analysis and the resting flow was estimated from the myocardium mass. Hyperemia condition was applied during the CT–FFR calculation to each branch of the coronary artery tree. **Results** Diagnostic accuracy, sensitivity, specificity, PPV, and NPV for angio–FFR were 92.7%, 85.7%, 96%, 90.9%, 93.5% for per–patient basis and 92.8%, 85.7%, 95.7%, 85.7%, 95.2% for per–vessel basis, respectively, and those of CT–FFR were 89.1%, 82.9%, 92%, 82.9%, 92% for per–patient and 89.2%, 82.9%, 91.3%, 76.3%, 94.1% for per–vessel, respectively. The correlation coefficient value of angio–FFR and FFR(r=0.75 per–patient, r=0.74 per–vessel) was higher than that of CT–FFR and FFR(r=0.66 per–patient; r=0.61 per–vessel), and the Bland–Altman chart showed that angio–FFR had a larger average difference and a smaller root mean squared deviation value than that of CT–FFR compared with FFR (FFR–angio–FFR, −0.016 ± 0.057, FFR–CT–FFR, 0.003 ± 0.074 for per–patient). Also, Angio–FFR had a slightly higher AUC value than that of CT–FFR (angio–FFR:0.924, 95%*CI* 0.857 to 0.966, CT–FFR:0.897, 95%*CI* 0.825 to 0.947 for per–patient), but the difference was negligible for per–patient or per–vessel bias. **Conclusion** Taking invasive FFR≤0.80 as a reference, angio–FFR and CT–FFR calculated based on the two types of images accurately diagnose functional ischemia of coronary stenosis, while angio–FFR is superior in accuracy. At the same time, they have a specific correlation with FFR, but some results still deviate considerably. The application scenarios of the two methods are different, that angio–FFR prefers to evaluate the need for PCI treatment in the catheterization room. In contrast, CT–FFR prefers to screen coronary function before any invasive treatment.

[Key words] CT–FFR; Angio–FFR; Invasive treatment

Piezo1 channel regulates the electrical remodeling after myocardial infarction through Ca^{2+} handling

SU Sheng'an ZHANG Yuhao XI Yutao XIE Yao MA Hong XIANG Meixiang

The Second Affiliated Hospital of Zhejiang University, Hangzhou 310009, China

[Abstract] **Background** Myocardial infarction(MI) is one of the leading causes of death worldwide. The progression after MI is associated with an aggressive activation of mechanical stress, which leads to deleteriously structural and electrical cardiac remodeling, eventually causing cardiac sudden death and progressive heart failure. The alteration of cardiac mechanics after MI mediates the mechano–sensitive ion channel remodeling, which is closely related to the incidence of arrhythmia. Piezo1 is a newly recognized mechano–sensitive cation channel while its role in MI is unclear. **Objective** This study evaluated the role of Piezo1 after MI. **Methods and Results** Piezo1 was up–regulated in the myocardium of patients with advanced heart failure and mainly located at the intercalated disc of cardiomyocyte in

mouse. Cardiomyocyte–conditional Piezo1 knockout mice(Piezo1Cko) exhibited increased survival rate and preserved cardiac function after MI. Piezo1Cko mice also displayed a dramatically decreased mortality in response to the programmed electrical stimulation after MI with significantly reduced incidence of ventricular tachycardia. In contrast, activation of Piezo1 in mouse myocardium increased the electrical instability reflecting by alterations in electrocardiogram. Mechanistically, Piezo1 regulated Ca^{2+} transient and affected SERCA2 and phosphorylated–RyR2 expressions, leading to mishandling of Ca^{2+} homeostasis. Furthermore, in human induced–pluripotent stem cell derived cardiomyocytes (hiPSC–CMs), Piezo1 activation remarkably triggered cellular arrhythmogenic remodeling through significantly shortening the duration of action potential and inducing early afterdepolarizations and triggered activity. **Conclusion** This study uncovered a previously unrecognized proarrhythmic role of Piezo1 in cardiac remodeling, which is achieved through regulating Ca^{2+} handling, implying a promising therapeutic target in sudden cardiac death and heart failure.

[Key words] Piezo1 channel; Electrical remodelin; Myocardial infarction

A mouse model of recurrent myocardial ischemia induces trained immunity in macrophages and cardiac inflammation

ZHU Jinyun

The Second Affiliated Hospital of Zhejiang University, Hangzhou 310009, China

[Abstract] Background Recent studies have shown that innate response can exert adaptive features building immunological memory. This process has been termed 'trained immunity'. Recurrent myocardial ischemia is common in patients with coronary artery disease, which predicts adverse outcome and high mortality in patients with unstable angina. Our study aims to elucidate the effect and mechanism of recurrent transient myocardial ischemia on macrophages and cardiac inflammation. **Methods** We developed a surgical mouse model of recurrent transient myocardial ischemia, which was induced by ligating the left anterior descending coronary artery for 5 min followed by resting 1 week. Mice were divided in trained and sham groups. The trained mice were subjected to the first, second and third insult of transient ischemia. Before and after the first, second and third ischemia insult, heart function was examined by echocardiography. Heart tissues from all groups were investigated for cardiac fibrosis, inflammation, and oxidative stress markers. Cardiac immune cell filtration and inflammation were examined by flow cytometry, quantitative real–time polymerase chain reaction, and immunohistochemistry. For an in vitro assay, monocytes were isolated and placed in normoxia (21%O_2) and hypoxia (2%O_2) for 24h followed by a resting period of 3 days after the training, both groups were replaced in normoxia for the last 24h. Several cytokines were then quantified by ELISA. Blood leukocyte count and IL–6 were retrospectively analyzed from patients with stable angina and unstable angina. **Results** Recurrent ischemia(third ischemia) triggers significant cardiac fibrosis and aggravated cardiac dysfunction in mice as compared to sham, first and second ischemia insults. There are more macrophages ($CD11b^+Ly–6G^-F4/80^+$) in the recurrent ischemia myocardium, whereas no difference of neutrophils ($CD11b^+Ly–6G^+$). Intriguingly, cardiac macrophages are basically $CCR2^+$(C–C chemokine receptor 2) cells, suggesting that vast majority of them are derived from bone marrow. In vitro assay, hypoxia training results in significantly increased mRNA level and production of proinflammatory cytokines, such as IL–6, IL–8, TNF–α, and IL–1β, compared with normoxia and only once hypoxia insult. The underlying mechanisms is that hypoxia training in macrophages leads to activate mTOR–HIF1α pathway and increased ROS and lactate production. There are no differences in peripheral blood leukocytes in stable angina, except for patients with recurrent angina who had increased number of white blood count compared with their first episode of chest pain. A positive correlation between peripheral leukocyte count and recurrent angina was discovered. **Conclusion** The data suggested that monocyte–derived

macrophages can be trained and ignited by preceding recurrent ischemia/hypoxia insult, cause cardiac inflammation, and predict outcome of ischemia in angina.

[Key words] Myocardial ischemia; Trained immunity; Macrophages; Cardiac inflammation

Serum free fatty acids independently predict adverse outcomes in acute heart failure patients

JIN Chunna YU Yi

The Second Affiliated Hospital of Zhejiang University, Hangzhou 310009, China

[Abstract] **Background** Serum circulating free fatty acid(FFA) is elevated in patients with heart failure(HF) compared to healthy control populations. It still remains unclear whether FFAs influence clinical outcomes in acute heart failure(AHF) patients. The present study aims to investigate the prognostic role of FFAs among patients with AHF. **Methods** This single–center, observational prospective cohort study enrolled 183 AHF patients admitted for AHF in the second affiliated hospital Zhejiang university school of medicine. The study endpoint was the composite of all–cause mortality and HF hospitalization within 1 year after discharge. FFA were modeled as quartiles as well as a continuous variable(per SD of FFA). The restricted cubic splines and cox proportional hazards models were applied to evaluate the association between the circulating FFAs level and all–cause mortality and/or HF hospitalization. **Results** A total of 183 patients with AHF(de novo and decompensated chronic HF) were evaluated[*n*=183, 73.0(63.0, 79.0) years, 66.0% men] in our study. During a flow up of 1 year, the composite endpoint occurred to 75 patients(40.98%). The result of cubic splines supported a linear relationship between FFAs level and the incidence of death and/or HF hospitalization. There was a positive association between FFAs level and the risk of death and/or HF hospitalization. Multivariable adjusted hazard ratios(95%*CI*) for death and/or HF hospitalization were 2.341(1.114–4.920), 1.414(0.660–3.026), 3.374(1.586–7.177), from the lowest to the highest quartile of FFAs, respectively, while the hazard ratio(95%*CI*) for death and/or HF hospitalization was 1.429 (1.091, 1.873) per SD(303.08 μmol/L) increase in FFA concentration. **Conclusion** Among patients hospitalized with AHF, higher circulating FFA level was associated with increased risk of adverse outcomes.

[Key words] Serum circulating free fatty acid; Heart failure

The effect of adaptive left ventricular pacing in the CRT treatment of patients with chronic heart failure

YAN Xigui ZHENG Yong FU Xinyan YANG Xuemei CHEN Yuwen LIU Wenmin

The Affiliated Hospital of Hangzhou Normal University, Hangzhou 310015, China

[Abstract] **Objective** To evaluate the effect of adaptive cardiac resynchronization therapy(ACRT) and rate–adaptive atrioventricular delay(RAAVD) in the treatment of chronic heart failure(CHF). **Methods** A total of 54 CHF patients, treated with CRT in our hospital from May 2018 to June 2020, were divided into three groups according to the treatment methods, with 14 patients in the ACRT group, 20 patients in the RAAVD group, and 20 patients in the biventricular pacing (BVP) group. The relative indices of the New York Heart Association Functional Classification (NYHA–FC), prior to the aortic blood flow velocity–time integral(AVI), interventricular mechanical delay(IVMD) time, left ventricular end diastolic diameter(LVEDd), left ventricular ejection fraction(LVEF) and mitral regurgitation area(MRA), of the 3 groups

before and 1 month, 3 months, and 6 months after implantation were compared. **Results** Compared with preoperative indices, the NYHA–FC, QRS wave duration, septal to posterior wall motion delay(SPWMD), IVMD, MRA and LVEDd indices were significantly improved in all 3 groups after 6 months of implantation($P < 0.05$), and the LVEF and AVI were increased($P < 0.05$). Compared with the BVP group, the QRS wave duration was significantly shorter in the ACRT group at 6 months after surgery (133.6 ± 9.3 vs. 142.5 ± 8.5 ms, $P < 0.01$), AVI increased (21.7 ± 1.6 vs. 20.3 ± 2.0 cm, $P < 0.05$), MRA is smaller (2.7 ± 1.0 vs. 3.7 ± 1.2 cm², $P < 0.01$), and IVMD is smaller (38.9 ± 7.3 vs. 44.5 ± 8.1 ms, $P < 0.05$). The other indicators were not statistically significantly different between these two groups ($P > 0.05$). Compared with the BVP group, the QRS wave duration of the RAAVD group was significantly shorter (135.5 ± 8.9 vs. 142.5 ± 8.5 ms, $P < 0.05$) at 6 months after surgery, AVI increased (21.6 ± 2.0 vs. 20.3 ± 2.0 cm, $P < 0.05$), MRA decreased(3.0 ± 0.8 vs. 3.7 ± 1.2 cm², $P < 0.05$) , and the other indicators were not statistically significantly different between these two groups($P > 0.05$). Various indicators were not significantly different between the BVP group and RAAVD group. **Conclusion** ACRT, RAAVD and BVP can effectively improve the prognosis of CHF patients. Both RAAVD and BVP have advantages over BVP in shortening the QRS wave duration, reducing the MRA and increasing the AVI. Besides these advantages, ACRT can also reduce the IVMD.

[Key words] Rate–adaptive atrioventricular delay; Chronic heart failure; Adaptive cardiac resynchronization therapy

Comparison of efficacy and safety of WATCHMAN and ACP in clinical application running head

FU Xinyan ZHENG Yong ZHANG Na PENG Huaiming LIU Wenmin YAN Xigui YANG Dong CHEN Yuwen ZHANG Xingwei

The Affiliated Hospital of Hangzhou Normal University, Hangzhou 310015, China

[Abstract] **Background** There is controversy of WATCHMAN and AMPLATZER cardiac plug (ACP) for left atrial appendage closure(LAAC). **Objective** To disclosure which occluder is better. **Methods** This study retrospectively analyzed 53 non–valvular atrial fibrillation (NVAF) patients who underwent LAAC between May 2015 and January 2018 at the Affiliated Hospital of Hangzhou Normal University. Twenty–seven patients were implanted with the WATCHMAN, and 26 were implanted with the ACP. A retrospective analysis was performed for the surgical procedures and intraoperative data. Patients were follow–up to detection for leakages around the occluder. **Results** Twenty–six(96.30%) and twenty–five(96.15%) patients were successfully implanted with the WATCHMAN and ACP device, respectively. WATCHMAN had a significantly shorter fluoroscopy time than ACP(41.85 ± 16.78 vs. 51.80 ± 28.85 min, $P < 0.05$), but there were no significant differences in contrast agent dosage and total operation time. One patient in either group suffered from loss of the sealing device, and needed surgical intervention. During the follow–up, no significant differences of peripheral leakage were observed between these two groups. **Conclusion** Compared with the ACP, the WATCHMAN has a shorter fluoroscopy time, but there is no significant difference in the amount of contrast agent used and both have comparable effectiveness and safety in LAAC.

[Key words] Left atrial appendage closure;WATCHMAN;AMPLATZER cardiac plug

Effect of quercetin on the pharmacokinetics of selexipag and its active metabolite in beagles

MEI Yibin

The People's Hospital of Lishui, Lishui 323000, China

[Abstract] **Objective** Quercetin is a naturally occurring flavonoid, and its glycosides can be consumed at least 100 mg per day in food. Quercetin can inhibit cytochrome P450 (CYP) enzymes, especially CYP2C8. It's still unknown whether quercetin and selexipag interact. The study investigated the effect of quercetin on the pharmacokinetics of selexipag and its active metabolite (ACT-333679) in beagles. **Methods** UPLC-MS/MS was used to investigate the pharmacokinetics of orally administered selexipag (2 mg/kg) with and without quercetin pre-treatment [2 mg/(kg·day) for 7 days] in beagles. The effect of quercetin on the pharmacokinetics of selexipag and ACT-333679 and its potential mechanism was studied through the pharmacokinetic parameters processed by DAS software. **Results** The assay method was validated for selexipag and ACT-333679, and the lower limit of quantification was 1 ng/mL for both analytes. The recoveries of them were 84.55%~91.58% and 81.21%~93.90%, respectively. The intra- and inter-day of accuracy and precision, the matrix effect and the stability of the two analytes under different conditions had met the requirements of the bioanalytical method. Treatment with quercetin led to an increased in Cmax and AUC_{0-t} of selexipag about 43.08% and 26.92%, respectively. While the Cmax and AUC_{0-t} of ACT-333679 also increased about 11.11% and 18.87%, respectively. **Conclusion** The study indicated that quercetin could inhibit the metabolism of selexipag and ACT-333679 when co-administration. Meanwhile, the pharmacokinetics of them were affected significantly. Therefore, the clinical dose of selexipag should be used with caution when co-administered with foods high in quercetin.

[Key words] Cytochrome P450; Active metabolite; Beagles

Substance P ameliorates BAPN-induced thoracic aortic dissection through modulation of M2 monocyte-skewed monocytopoiesis

PIAO Jiyuan

The Second Affiliated Hospitalof Zhejiang University, Hangzhou 310009, China

[Abstract] **Objective** Thoracic aortic dissection(TAD) is one of lethal cardiovascular diseases with few treatments in clinic. Although many clinical trials have been used to treat TAD, they have not resolved the fundamental problems. Substance P(SP) is well-known to provide anti-inflammatory effects and promote restoration of damaged endothelium, leading to vasculature protection and the facilitation of tissue repair. Thus, in this study, we explored the protective effects of SP on development of TAD. **Methods** To create an aortic dissection preclinical disease model, the lysyl oxidase inhibitor—BAPN was administered to SD rats orally for 4 weeks and SP was injected intravenously, concurrently with BAPN treatment, twice a week for 4 weeks. And the survival rate, aorta histology, the local and circulating immune-cell profiles, and molecular changes in the aorta were analyzed in vitro and in vivo. **Results** BAPN treatment caused the dilation of aorta with infiltration of monocyte and elevation of pro-inflammatory cytokine within 1 week and aortic dissection within 4 weeks-post treatment. However, SP clearly attenuated BAPN-induced inflammation, smooth muscle cell(SMC) phenotype switching and SMC apoptosis, leading to inhibition of development of TAD. After analyzing the early

stage of disease progression, we found that SP treatment mitigated BAPN highly activated inflammatory responses via accelerating M2–biased monocytopoiesis in the spleen thereby supplying M2–monocytes and anti–inflammatory cytokine enriched environment in the circulation within 24 hours. Although SP did not ameliorate BAPN–promoted monocyte chemoattractant protein–1 level in the blood, SP–induced vast quantity of M2–monocyte and its secretomes were sufficient to suppress inflammatory conditions. Furthermore, SP injection also blocked the inflammation evoked–VCAM–1 expression to protect endothelium and this function might contribute to the decline in infiltration of monocytes and immune suppression from the early stage of TAD. **Conclusion** This study supports that SP blocks TAD development by modulating endothelial dysfunction and immune response, simultaneously.

[Key words] Thoracic aortic dissection; M2 monocyte–skewed monocytopoiesis

Evaluation of left ventricular systolic function in patients with coronary microvascular dysfunction by three–dimensional speckle–tracking imaging

YU Ziheng CHENG Zhenfeng LU Kongjie

Huzhou Central Hospital, Huzhou 313000, China

[Abstract] **Objective** The objective of this study is to evaluate the left ventricular systolic function of patients with coronary microvascular dysfunction (CMD) using the three–dimensional speckle–tracking imaging (3D–STI) technique. **Methods** From June 2018 to June 2019, 72 subjects from Huzhou Central Hospital were enrolled, including 42 CMD in–patients with typical chest pain or chest tightness and positive treadmill exercise stress test, but without coronary stenosis on coronary angiography (the CMD group) and another 30 healthy individuals who were undergoing physical examinations in an outpatient clinic (the control group). Using 3D–STI technique, the global longitudinal strain (GLS), global radial strain (GRS), global circumferential strain (GCS), global area strain (GAS), and left ventricle were measured. **Results** Compared with the control group, GLS and GAS were significantly reduced in the CMD group ($P < 0.05$), while GRS and GCSwere similar in both groups($P > 0.05$). Univariate logistic regression analysis showed that GLS and GAS were the influencing factors of CMD. For the diagnosis of CMD, the area under the ROC curve of GLS was 0.883, and the area under the ROC curve of GAS was 0.875. GAS of –29.3% (log–rank test chi–square=34.245, $P < 0.01$) was a strong predictor of major adverse cardiac events. **Conclusion** 3D–STI technique has obvious advantages in the evaluation of the left ventricular systolic function for CMD patients. Moreover, 3D–STI parameters, especially GLS and GAS, can detect the early abnormal changes in the ischaemic myocardium. Being timelier and more sensitive than echocardiography, 3D–STI should be recommended for clinical application.

[Key words] Coronary microvascular dysfunction; Three–dimensional speckle–tracking imaging; Left ventricular systolic function

Diallyl trisulfide suppresses angiotensin Ⅱ–induced vascular remodeling via inhibition of mitochondrial fission

LU Zhaoyang　YANG Bin　LI Bao

The Second Hospital of Shanxi Medical University, Xi'an 300010, China

[Abstract] **Objective** To investigate whether DATS mitigates Ang Ⅱ–induced vascular smooth muscle cells (VSMCs) phenotypic switch and vascular remodeling, and if so, to determine the underlying molecular events. **Methods** Male C57BL/6 mice were used to establish vascular remodeling model by continuous 2–week Ang Ⅱ infusion using a subcutaneous osmotic pump. Animals were intraperitoneally injected with DATS or vehicle. Physiological parameters, vascular morphology and molecular markers were assessed. For in vitro studies, VSMCs were pretreated with or without DATS for 1 h, then were stimulated with Ang Ⅱ, Mitochondrial morphology, phenotypic switching of VSMCs were also measured. **Results** In primary mouse VSMCs, we found that Drp1–dependent mitochondrial fission regulated mitochondrial reactive oxygen species (mtROS) generation, which eventually promoted Ang Ⅱ–induced VSMC proliferation, migration, and phenotypic switching. Moreover, Ang Ⅱ was found to up–regulate the Rho–associated coiled coil–containing protein kinase 1(ROCK1), which regulated mitochondrial fission and VSMC phenotypic switching by phosphorylating Drp1. However, the biological effect of Ang Ⅱ was able to abrogated by DATS. Consistent with the effects in VSMCs, we found that DATS markedly alleviated mitochondrial fission, VSMC differentiation, and vessel wall thickening in an animal model of Ang Ⅱ–induced vascular remodeling, which were regulated by ROCK1/Drp1 signal. **Conclusion** Our findings showed that DATS mitigated Ang Ⅱ–induced vascular remodeling by suppressing Drp1–mediated mitochondrial fission in an ROCK1–dependent manner.

[Key words] Vascular smooth muscle cells; Molecular events

Long–term stroke rates after catheter ablation or antiarrhythmic drug therapy for atrial fibrillation: a meta–analysis of randomized controlled trials with trial sequential analysis

SONG Jikai

Zhejiang Provincial People's Hospital, Hangzhou 310000, China

[Abstract] **Objective** The prevailing view is that ablation does not reduce the incidence of stroke in atrial fibrillation (AF), and guidelines suggest that long–term anticoagulation is required after ablation, regardless of the success of the procedure. We performed a meta–analysis of recent randomized, controlled trials (RCTs) to verify whether ablation compared with drugs reduced the incidence of stroke and whether long–term anticoagulation after ablation was necessary. **Methods** We systematically searched the PubMed, Embase, and Cochrane Central Register of Controlled Trials databases for RCTs of AF catheter ablation (CA) compared to medical therapy (MT). The risk ratio (RR) and weighted mean difference (WMD) with 95%*CI*s were calculated using a random–effects model. A trial sequential analysis (TSA) was used to further validate the reliability of the primary outcomes. **Results** Seventeen RCTs were included, comprising 5,258 patients (CA, n=2 760, MT, n=2 498). Compared with medical therapy, CA was associated with a reduction in stroke/transient ischaemic attacks (TIAs)(RR=0.61, 95%*CI*:0.386–0.965, I^2=0.0%, $P<0.05$) and deaths (RR=0.7, 95%*CI*:0.55–0.89, I^2=0.0%, $P<0.05$). CA was associated with improvement in left ventricular ejection fraction

(LVEF) (WMD=5.39, 95%*CI*:2.45–8.32, I^2=84.4%, $P<0.05$) and the rate of maintenance of sinus rhythm (SR) (*RR*=3.55, 95%*CI*:2.34–5.40, I^2=76.7%, $P<0.05$). **Conclusion** CA for AF had more favourable outcomes in terms of stroke/TIAs, deaths, change in LVEF, and the maintenance of SR at the end of follow–up compared to MT. In addition, long–term anticoagulation was not necessary after ablation.

[Key words] Atrial fibrillation; Meta–analysis

Study on the influence of sandstorm weather on the incidence of coronary heart disease in Gansu Hexi corridor

LI Xinghui

Gansu Provincial Hospital, Lanzhou 730000, China

[Abstract] **Objective** To observe and analyze the influence of sandstorm weather on the incidence of coronary heart disease in Gansu Hexi corridor. **Methods** The sandstorm weather data in Hexi corridor of Gansu Province from January 1, 2016 to December 31, 2020 were obtained from Gansu Meteorological Bureau. A total of 1500 residents from five cities which 300 residents in each city were selected as the exposure group.The same number of residents in the less sandstorm area of Southeast Gansu Province were selected as the control group, and the meteorological data of the same period were obtained. The relevant factors of the control group and the exposure group were matched.The subjects were followed up and examined regularly, including outpatient, emergency and inpatient case registration, inflammatory factors testing included C–reactive protein (CRP), Interleukin–1 (IL–1), Interleukin–6 (IL–6), tumor necrosis factor–α(TNF–α) and macrophage inflammatory protein–2 (MIP–2), and routine ECG and echocardiography examination. **Results** The frequency of sandstorm in Hexi corridor was higher than that in southeast of Gansu province ($P<0.05$).The number of patients with coronary heart disease, outpatients, inpatients and unstable angina pectoris in the exposure group were higher than those in the control group ($P<0.05$). CRP, IL–1, TNF–α and MIP–2 in exposure group were higher than that in the control group ($P<0.05$). The proportion of ECG with myocardial ischemia or infarction and arrhythmia in exposure group was higher than that of control group ($P<0.05$), and the proportion of echocardiography with cardiac cavity enlargement and LVEF<50% in exposure group was higher than that of control group ($P<0.05$). **Conclusion** Sandstorm weather can induce the incidence and progress of coronary heart disease in Hexi corridor, Gansu Province. Local people need to minimize personal exposure and strengthen sandstorm control.

[Key words] Influence; Coronary heart disease; Sandstorm weather

Tanshinone Ⅱa protects cardiomyocytes against radiation injury by inhibiting the p38 MAPK signaling pathway

WANG Gang XIE Ping

Gansu Provincial Hospital, Lanzhou 730000, China

[Abstract] **Objective** Radiation therapy is one of the main strategies for tumor treatment, but causes damage to relevant tissue organs inevitably during the treatment process. Cardiovascular adverse effects caused by thoracic radiation therapy are collectively referred to as radiation–induced heart disease(RIHD). Currently, there is no uniform standard for the treatment of RIHD. In this study, we investigated the effects of tanshinone ⅡA on cardiomyocytes by establishing a

model of radiation injury to cardiomyocytes. **Methods** The cardiomyocyte model of radiation injury was established by H9C2 cardiomyocytes, and the expression of proteins related to p38 mitogen activated protein kinase (MAPK) signaling pathway was detected by western blot analysis. Then, the apoptosis related proteins Bax, Bcl–2, Caspase–3 were detected by western blot analysis, and the apoptosis experiments were performed using flow cytometry to clarify the effects of radiation injury and tanshinone Ⅱ A, p38 MAPK on cardiomyocytes. Finally, radiation–induced myocardial injury was clarified by clonogenic assay and detection of the level of lactate dehydrogenase (LDH) in the culture medium. **Results** After radiation, H9C2 cells showed increased levels of p38 MAPK and its phosphorylation, increased levels of Bax, and decreased values of Bcl–2 / Bax, and in cell apoptosis assay and clonogenic assay, cell growth was inhibited and apoptosis rate was increased, indicating that p38 MAPK signaling pathway was activated and radiation increased H9C2 cell apoptosis.The expression of p38 MAPK and its phosphorylation levels were significantly decreased, while Bcl–2 and the Bcl–2/Bax ratio were both increased, the apoptosis rate was decreased, and the clonogenic rate was increased after tanshinone Ⅱ A treatment was administered. It indicated that tanshinone Ⅱ A had an inhibitory effect on the p38 MAPK signaling pathway and exhibited a certain protective effect on cardiomyocytes. **Conclusion** Tanshinone Ⅱ A reduced apoptosis by inhibiting p38 MAPK signaling pathway caused by radiation injury, thereby protecting cardiomyocytes.

[Key words] Radiation–induced heart disease; Radiation therapy; Tanshinone Ⅱ A

Canagliflozin impairs injured skeletal muscle regeneration by downregulating leucyl–tRNA synthetase 2 expression

LIN Yinuo

The First Affiliated Hospital of Wenzhou Medical University, Wenzhou 325800, China

[Abstract] Objective Gliflozins are a new class of oral antidiabetic drugs that decrease urinary glucose reabsorption by inhibiting sodium–glucose cotransporter 2 in proximal tubules. However, canagliflozin was recently reported to increase the risk of lower extremity amputation while the underlying mechanism remains largely unexplored. **Methods** Diabetic and non–diabetic mice were treated with gliflozins and subjected to femoral artery ligation. In situ muscle contractile recovery, fatigue properties, as well as morphological and histological regeneration after hindlimb ischemia were evaluated. The effects of gliflozins on myoblast differentiation and cellular mitochondrial activities were assessed in vitro. Ischemic tibialis anterior (TA) muscles 3 days post injury were analysed using single–cell RNA sequencing. The sequencing results were further confirmed by PCR and WB. The effects of canagliflozin on Leucyl–tRNA Synthetase 2 (LARS2), and the effects of LARS2 on myoblasts differentiation were confirmed by siRNA knock–down and plasmid/AAV–based gene delivery methods both in vivo and in vitro. **Results** Both in vivo and in vitro data indicate that canagliflozin (CANA), rather than dapagliflozin (DAPA) or empagliflozin (EMPA), impairs intrinsic myogenic regeneration and differentiation, thus hindering ischemic limb muscle contractile properties, fatigue resistance recovery and tissue regeneration. Mitochondrial structure and activity are both disrupted by canagliflozin in myoblasts. Single–cell RNA sequencing of ischemic tibialis anterior muscle reveals a decrease in LARS2 in muscle stem cells (MuSCs) attributable to canagliflozin. Further investigation explicates the noncanonical function of LARS2, which plays pivotal roles in regulating myoblast differentiation and muscle regeneration by affecting mitochondrial structure and activity. Enhanced expression of LARS2 directly stimulates myoblasts to form large multinucleated syncytial myotubes, restores the differentiation of canagliflozin–treated myoblasts, and accelerates ischemic skeletal muscle regeneration in canagliflozin–treated mice. **Conclusion** CANA treatment, instead of DAPA or EMPA, delays ischemic limb function

recovery and tissue regeneration. Such impairment is due to the downregulation of LARS2 in MuSCs, which attenuates intrinsic myogenic regeneration and differentiation. Further investigation revealed that LARS2, as an essential factor for mitochondrial maintenance, plays pivotal roles in myoblast differentiation regulation.

[Key words] Leucyl–tRNA synthetase 2; Skeletal muscle regeneration

Blood urea nitrogen and in–hospital mortality in critically ill patients with cardiogenic shock: analysis of the MIMIC–III database

ZENG Chunlai

Lishui Central Hospital, Lishui 323000, China

[Abstract] **Objective** The association of blood urea nitrogen(BUN) and prognosis has been the focus of research recently. Therefore, the objective of this research was to investigate the association between BUN and hospital mortality in critically ill patients with cardiogenic shock (CS).Design A retrospective cohort study. Setting and participants Data were obtained from the MIMIC–III V1.4 database. Data on 697 patients with CS were analyzed. **Methods** Logistic regression and subgroup analyses were used to assess the association between BUN and hospital mortality in patients with CS. **Results** The average age of 697 participants was 71.14 years, and about 42.18% were male. In the multivariate logistic regression model, after adjusting for age, sex, diabetes, cardiac arrhythmias, hypertension, urine output, SAPS II, SOFA, creatinine, anion gap, and heart rate, high BUN showed strong associations to an increase in–hospital mortality (per SD increase: *OR*=1.47, 95%*CI*:1.13–1.92). A similar result was observed in groups of BUN tertile (BUN 23–37 mg/dL versus 6–22 mg/dL, *OR*=1.42, 95%*CI*:0.86–2.34), BUN 38–165 mg/dL versus 6–22 mg/dL, *OR*=1.99, 95%*CI*:1.10–3.62, $P < 0.05$). Subgroup analysis did not reveal any significant interactions in various subgroups. **Conclusion** Higher BUN was associated with adverse clinical outcomes in critically ill patients with cardiogenic shock.

[Key words] Blood urea nitrogen; MIMIC–III database

Association between triglyceride–glucose index and type 2 diabetes mellitus in the Japanese population: a secondary analysis of a retrospective cohort study

ZENG Chunlai

Lishui Central Hospital, Lishui 323000, China

[Abstract] Triglyceride–glucose index (TyG index) is associated with type 2 diabetes mellitus (T2DM) but research on this relationship is limited in Japan. The purpose of this study was to evaluate the correlation between TyG index and the risk of T2DM in the Japanese population. Here, 12 732 participants were selected from the NAGALA study (NAfld in the Gifu area, longitudinal analysis) conducted between 2004 and 2015 for a retrospective cohort analysis. The association between TyG index and T2DM was assessed using the Cox proportional–hazard model. Subgroup analyses were conducted according to age, sex, smoking status, alcohol consumption, waist circumference, BMI, and follow–up duration. The formula for TyG index was expressed as ln [fasting triglyceride level(mg/dL) × fasting plasma glucose

level (mg/dL)/2]. After follow–up, 150(1.18%) patients developed T2DM. After adjusting for potential confounders, a linear relationship was observed between TyG and the risk of T2DM. After adjusting for age, sex, BMI, waist circumference, HDL–cholesterol, total cholesterol, systolic blood pressure, regular exercise, smoking status, and alcohol consumption, TyG index, as a continuous variable, was associated with an increased risk of T2DM (*HR*=1.79, 95%*CI*:1.25–2.57). Compared with the first quartile of TyG index, subjects in the fourth quartile were 2.33–fold more likely to develop T2DM (*HR*=2.33, 95%*CI*:1.09–4.96, $P < 0.05$). Subgroup analyses showed that the association between TyG index and incident T2DM stably existed in different subgroups according to the variables tested. Therefore, TyG index was linearly related to the risk of incident T2DM in the Japanese population and may be used as a monitoring tool.

[Key words] Triglyceride–glucose index; Type 2 diabetes mellitus; Japanese

Using the COXBOOST machine learning model to predict the prognosis of patients with cardiogenic shock

RONG Fangning WANG Jie CHEN Zhi QIAN Lala LIU Shuai QIAN Lu XUE Yangjing JI Kangting

The Second Affiliated Hospital and Yuying Children's Hospital, Wenzhou Medical University, Wenzhou 325000, China

[Abstract] **Objective** To develop a model based on CoxBoost machine learning method to predict the hospital mortality of MIMIC–III cardiogenic shock patients and evaluate the performance of this model. **Methods** Cardiogenic shock patients were selected from MIMIC–III V1.4. CoxBoost prediction model, traditional Cox regression model and SAPS–II scoring model were constructed and evaluated. **Results** A total of 1 142 patients were included in this study, of which 678 patients died during hospitalization. The C index of Cox boost model [0.73(0.71, 0.76)] was higher than that of traditional Cox regression model[0.66(0.63,0.69)] and SAPS–II score model [0.69(0.67, 0.72)], there was significant difference($P < 0.05$). Compared with the traditional Cox regression model, the NRI and IDI of Cox boost model are 0.16 and 0.07, respectively. Compared with the SAPS–II scoring model, the NRI and IDI of Cox boost model are 0.19 and 0.07. The model is shown in the form of nomogram. **Conclusion** The Cox Boost machine learning model is superior to Cox regression model and SAPS–II score model in predicting the mortality of CS patients.

[Key words] Cardiogenic shock; Prognosis

Short term outcomes of early initiation of impella on survival in acute myocardial infarction complicated by cardiogenic shock: a meta–analysis

ZHONG Ming

Jinhua Municipal Central Hospital, Jinhua 321000, China

[Abstract] **Objective** Mortality in patients with acute myocardial infarction(AMI)complicated by cardiogenic shock(CS) remains high despite the use of early revascularization therapy. Early initiation of Impella support with regard to the emergent revascularization procedure is not well defined. **Methods and Results** The meta–analysis was performed

to compare the clinical outcomes of the Impella pre percutaneous coronary intervention(PCI) strategy and Impella post PCI strategy for AMI complicated by CS. Eight studies were included, and a total of 896 patients were involved in the meta-analysis. The primary outcome was in-hospital or 30 days mortality. The secondary end points were bleeding, limb ischaemia, reinfarction and stroke. Compared with the Impella post PCI strategy, the Impella pre PCI strategy was associated with a significant reduction in-hospital or 30 day mortality(*OR*=0.44, 95%*CI*:0.32-0.60, $P<0.05$). There were no significant differences in rates of bleeding(*OR*=0.61, 95%*CI*:0.34-1.07, $P>0.05$), limb ischaemia(*OR*=0.62, 95%*CI*:0.28-1.37, $P>0.05$), reinfarction(*OR*=0.42, 95%*CI*:0.04-4.11,$P>0.05$), or stroke(*OR*=0.67, 95%*CI*:0.10-4.48, $P>0.05$). **Conclusion** Our data suggest that the early initiation of Impella was associated with a short term survival benefifit in patients presenting with AMI complicated with CS.

[Key words] Acute myocardial infarction; Cardiogenic shock; Meta-analysis

PFO closure with only intracardiac echocardiography guidance: single center experience

MA Shenghui

The Second Affiliate Hospital of Zhejiang University, Hangzhou 310009, China

[Abstract] Objective Transcatheter closure of patent foramen ovale(PFO) guided by intracardiac echocardiography(ICE) is superior to conventional ultrasound or fluoroscopy guidance. We evaluated the safety, feasibility and effectiveness of PFO closure guided by intracardiac echocardiography without the use. **Methods** From November 2019 and March 2020, 20 consecutive patients with PFO and recurrent cryptogenic cerebral ischemic stroke were enrolled to perform PFO closure under the guidance of ICE in the Second Affiliated Hospital of Zhejiang University. The PFO risk score was moderate to high risk, which were considered as PFO related stroke. ICE catheter was advanced to the right atrium under near-field ultrasound guidance through right femoral vein access. Using Carto 3 system, the PFO and left atrial(LA) geometries were created without fluoroscopy. Under the ICE guidance, the guide wire was inserted into the left atrium with the support of SL-1 sheath. After catheter exchanging, the device was delivered and the occlude was positioned. The operation related complications were recorded during the operation, and tee or right heart contrast echocardiography were reviewed 3 months later. **Results** Among 20 PFOs, 17 were mainly in the anterosuperior region of the fossa ovale while 3 were in the posterosuperior region. The average height was 0.21 ± 0.10 mm. Nineteen patients were performed the 24 mm PFO occluder while one was performed a 28 mm PFO occluder. The average procedural time was 41.5 ± 8.4 min. Absence of right to left shunt was confirmed in all 20 patients after correct placement the device. No residual shunt were seen in all patients at 3 months after procedure, neither the device erosion, migration thrombosis or atrial fibrillation. **Conclusion** Transcatheter PFO closure with only intracardiac echocardiography guidance is feasible, safe and effective. No obvious complications were found in the short-term follow-up.

[Key words] Patent foramen ovale; Intracardiac echocardiography

Diagnostic performance of AccuFFRangio in functional assessment of coronary stenosis compared to pressure wired–derived FFR

DONG Liang JIANG Jun TANG Lijiang DU Changqing LENG Xiaochang
HE Jingsong HU Yumeng SUN Yong LI Changling XIANG Jianping WANG Jian'an
The Second Affiliate Hospital of Zhejiang University, Hangzhou 310009, China

[Abstract] **Objective** Noninvasive fractional flow reserve (FFR) has been increasingly used in the clinical workflow to assist clinical decision–making for PCI intervention. This clinical study aims at evaluating the diagnostic accuracy of the coronary stenosis assessed by a non–invasive fractional flow reserve analysis method (termed as AccuFFRangio) based on invasive coronary angiography(ICA), which is a blinded, self–control, retrospective, and dual–center clinical investigation study. **Methods** Coronary angiography and related information for 298 patients with 298 vessels are collected, and AccuFFRangio is used to assess the FFR for these patients. The average age of the patients was 65 ± 10 years, 99 (33.2%) were women. Among 298 interrogated vessels, AccuFFRangio is successfully assessed in 298 vessels (100%), whereas FFR measurement was obtained in 298 vessels (100%). The interrogated vessels had an average FFR of 0.83 ± 0.10. FFR≤0.80 was noted in 81 vessels (27.2%). AccuFFRangio was computed with the AccuFFRangio V1.0 software (ArteryFlow Technology, Hangzhou, China) by participating physicians and technicians blinded to FFR. Two angiographic images with projections > 25° apart at the end–diastolic frame were selected for three–dimensional (3D) reconstruction of the segmented vessel. Then the TIMI frame count was performed in an angiographic run to calculate the flow velocity. Based on the segmented vessel, calculated velocity and input aortic pressure, AccuFFRangio distribution can be calculated through the pressure drop equation. Compared with the wire–measured FFR values, we evaluated AccuFFRangio performance by its accuracy, sensitivity, specificity, positive predictive value (PPV) and negative predictive value (NPV). **Results** Good correlations were observed with a correlation coefficient of r=0.812 (P < 0.01). Bland–Altman plot showed that there were good agreements between AccuFFRangio and FFR with a mean difference value of 0.001(–0.128, 0.131) for per–vessel. The number of patients with the absolute difference between AccuFFRangio and FFR falling out of the 95%*CI* –0.128 to 0.131 was 11(3.7%). The accuracy of AccuFFRangio was 93.3% in this clinical investigation. Overall sensitivity, specificity, PPV and NPV for per–vessel basis were 92.6%, 93.5%, 84.3% and 97.1%, respectively. The AUC for AccuFFRangio was 0.96(95%*CI*: 0.93–0.98). Moreover, the mean time for AccuFFRangio assessment (including 3D angiographic reconstruction and frame count analysis) was 4.10 ± 2.17 min. **Conclusion** In this study, clinical research aims to evaluate the diagnostic accuracy of the coronary stenosis assessed by AccuFFRangio, which is blinded, self–control, retrospective, and dual–center clinical investigation. Comparing the investigational results with the gold standard invasive FFR, the accuracy, sensitivity, and specificity of AccuFFRangio in identifying hemodynamically significant coronary stenosis are 93.3%, 92.6%, and 93.5%, respectively. This clinical study demonstrates that AccuFFRangio is clinically feasible and the performance is superior to angiographic assessment by 2D–QCA for evaluation of coronary artery stenosis.

[Key words] Noninvasive fractional flow reserve; Invasive coronary angiography

Long non-coding RNA MALAT1 regulates sca1-positive vascular adventitial progenitor cells differentiate into smooth muscle cells through EPAC/Rap1 signaling pathway in vascular repair

LYU Lingxia

The First Affiliated Hospital, School of Medicine, Zhejiang University, Hangzhou 310006, China

[Abstract] **Objective** Atherosclerosis can lead to a series of severe vascular diseases such as coronary heart disease, stroke and peripheral vascular diseases as well as vascular restenosis during subsequent treatment. It's widely acknowledged that promoting the repair of vascular injury has been an extremely important treatment method for preventing and treating such diseases. Metastasis-associated lung adenocarcinoma transcript 1 (MALAT1) is an abundantly expressed and exceptionally conserved nuclear long non-coding RNA. Accumulating work has proved that lncRNA-MALAT1 participates in the pathogenesis of various vascular diseases, to which sca-1+ adventitial progenitor cells within the vessel wall may contribute. We sought to elucidate the role of lncRNA-MALAT1 on sca-1+ progenitor cells to differentiate into SMCs and to understand the underlying mechanisms. **Methods** We conducted single cell RNA sequencing of mice injured femoral artery and found that lncRNA-MALAT1 was significantly down-regulated after injury compared to the control group. In the meantime, sca1+ adventitial progenitor cells (APCs) were found to be involved in vascular repair and angiogenesis. sca1+ APCs were isolated and cultured in vitro. Given that sca1+ APCs can differentiate into different vascular cells during vascular injury and repair, TGF-β was used to induce them specifically differentiate into smooth muscle cells (SMCs) and mimic an injury status. We found that under the induction of TGF-β1, the cell morphology changed from short ellipse to myocyte-like spindle, and the expression of VSMCs-specific markers SMαA, SM22α, and SMMHC gradually increased, which was consistent with the results of previous studies. In this process, a dramatic down-regulation of lncRNA-MALAT1 were also observed. We designed a siRNA to knock down lncRNA-MALAT1 in sca1+ APCs and treated cells with TGF-β afterwards. qPCR and western blotting were conducted to measure the level of smooth muscle cell markers including smooth muscle alpha-actin (SMA), SM22alpha, and smooth muscle myosin heavy chain (SMMHC). Immunofluorescence staining consistent results. **Results** showed that knocking down MALAT1 promoted sca1+ APCs differentiate into SMCs. To yield insights into the mechanism by which lncRNA-MALAT1 suppresses sca1+ APCs to differentiate into VSMCs, we performed protein microarray experiment and KEGG analysis. According to the results, the Rap1 signaling pathway is most likely to be involved in this process. Numerous studies illuminated that the EPAC1/Rap1 pathway regulates endothelial barrier and angiogenesis. Protein microarray revealed that knocking down lncRNA-MALAT1 activated EPAC/Rap1 signal pathway. Either suppressing or activating this pathway could promote or inhibit TGF-β induced differentiation from sca1+ APCs to SMCs. **Conclusion** Sca1-positive adventitial progenitor cells can differentiate into vascular smooth cells. Under the induction of TGF-β, the cell morphology changed from short ellipse to myocyte-like spindle, and the expression of VSMCs-specific markers SMαA, SM22α, and SMMHC gradually increased. Down-regulation of long non-coding RNA lncRNA-MALAT1 in sca1+ APCs promoted TGF-β induced differentiation into SMC through activating EPAC/Rap1 signaling pathway, which may influence vascular repair and remodeling. This experiment provided novel target for regulating vascular stem cells in vessel damage and repair.

[Key words] Long non-coding RNA; Adventitia; MALAT1; Mice; Vascular stem cell

Admission lactate levels combined with lactate clearance for predicting acute kidney injury in ST–segment elevation myocardial infarction patients: a retrospective observational study

LIANG Dongjie

The First Affiliated Hospital of Wenzhou Medical University, Wenzhou 325000, China

[Abstract] **Objective** Acute kidney injury (AKI) is common in the hospitalization of patients with ST–segment elevation acute myocardial infarction (STEMI) and is associated with significant morbidity and mortality risks. The aim of this study was to evaluate the predictive value of the admission lactate combined with lactate clearance for AKI in STEMI patients. Materials and **Methods** This was a retrospective, observational study that included STEMI patients who were admitted to the coronary care unit (CCU) of the First Affiliated Hospital of Wenzhou Medical University between January 2014 and August 2018. Lactate clearance was calculated as (initial lactate – 12–h lactate/initial lactate) × 100. Patients were classified into four groups according to admission lactate levels and lactate clearance at 12–h: group 1, Lactate ≤ 2.2 mmol/L and Lactate clearance > 0%, group 2, Lactate > 2.2 mmol/L and Lactate clearance > 0%, group 3, Lactate ≤ 2.2 mmol/L and Lactate clearance ≤ 0%, group 4, Lactate > 2.2 mmol/L and Lactate clearance ≤ 0%. The study endpoint was AKI occurrence during the hospitalization which was defined according to the kidney disease: improving global outcomes(KDIGO) guidelines. **Results** A total of 1 790 STEMI patients were included: 280 in group 1 670 in group 2 601 in group 3, and 239 in group 4. The mean age of patients was 64.3 ± 13.2 years and 353 (19.7%) patients developed AKI. The incidence of AKI was 10.7%, 17.6%, 21.0% and 33.1% in groups 1, 2, 3, and 4, respectively. After multivariate analysis, group 4 was associated with the highest risk of AKI (*OR*=3.78, 95%*CI*: 2.29–6.24, $P < 0.01$) followed by group 3(*OR*=2.67, 95%*CI*:1.70–4.19, $P < 0.05$) and group 2(*OR*=1.61, 95%*CI*:1.02–2.54, $P < 0.05$), when compared to group 1. **Conclusion** The combination of admission lactate and lactate clearance at 12–h can better identify STEMI patients at high risk of AKI.

[Key words] Acute kidney injury; ST–segment elevation acute myocardial infarction

Investigation and analysis of sudden cardiac death in 96 patients with coronary heart disease after percutaneous coronary intervention

LI Xinghui

Gansu Provincial People's Hospital, Lanzhou 730000, China

[Abstract] **Objective** To investigate the incidence of sudden cardiac death (SCD) after percutaneous coronary intervention (PCI) in patients with coronary heart disease (CHD) in some areas of Gansu Province, and to analyze its high–risk factors. **Methods** The patients who had successfully performed PCI in Gansu Provincial People's Hospital from January 1, 2012 to December 31, 2018 were selected as the subjects. The number of SCD cases was obtained by follow–up, and the incidence of SCD after PCI was determined. The demographic data, cause of death, type of CHD, season and time period of SCD were analyzed. The risk factors of SCD were analyzed by logistic regression analysis, including gender, age, place of residence, traditional risk factors and type of CHD, number of coronary artery lesions, results of

echocardiography and secondary preventive drug use. **Results** The incidence of SCD after PCI was 1.7%. The age group of 70–79 years old is the most, male is more than female, rural is more than urban, mostly in winter (December to February), time period (06:00–11:59). Fatigue and emotional excitement are the most common inducements. Acute and chronic myocardial infarction are the main causes of primary CHD. Age, gender, rural area, family history of CHD, history of diabetes mellitus, first onset of ACS, coronary lesions > 3 or combined with left main , left ventricular ejection fraction (LVEF) < 40%, combined with ventricular aneurysm and irregular medication are risk factors for SCD. **Conclusion** The incidence of SCD in patients with CHD after PCI is relatively high in this area. For the high–risk populations, the medical staff, patients and their families, and government departments should work together to strengthen prevention and control measures.

[Key words] Sudden cardiac death; Percutaneous coronary intervention; Coronary heart disease

Using deep learning method to identify left ventricular hypertrophy on echocardiography

YU Xiang YAO Xinxia WU Bifeng ZHOU Hong XIA Shudong

The Fourth Affiliated Hospital, School of Medicine, Zhejiang University, Yiwu 322000, China

[Abstract] **Objective** Left ventricular hypertrophy (LVH) is an independent prognostic factor for cardiovascular events and it can be detected by echocardiography in the early stage. In this study, we aim to develop a semi–automatic diagnostic network based on deep learning algorithms to detect LVH. **Methods** We retrospectively collected 1 478 transthoracic echocardiograms, included 655 patients, 186 hypertensive heart disease (HHD), 206 hypertrophic cardiomyopathy (HCM), and 56 cardiac amyloidosis (CA), along with 207 controls). The diagnosis of LVH was defined by an experienced echocardiographer and reviewed by a cardiologist. For the deep learning architecture, we introduced ResNet and U–net++ to complete classification and segmentation tasks respectively. The models were trained and validated independently. Then, we connected the best–performing models to form the final framework and tested its capabilities. **Results** In terms of individual networks, the view classification model produced AUC=1.0. The AUC of the LVH detection model was 0.97 (95%*CI*:0.93–0.99), with corresponding sensitivity and specificity of 97.6% (95%*CI*:87.1%–99.9%) and 86.8% (95%*CI*: 78.8%–92.6%) respectively. For etiology identification, the independent model yielded good results with AUC=0.91 (95%*CI*: 0.84–0.96) for HCM, AUC=0.94 (95%*CI*: 0.87–0.98) for CA, and AUC=0.88 (95%*CI*: 0.81–0.94) for HHD. Finally, our final integrated framework automatically classified four conditions (Normal, HCM, CA, and HHD), which achieved an average of AUC=0.91, with an average sensitivity and specificity of 86.2% and 88.7%. **Conclusion** Deep learning architecture has the ability to detect LVH and even distinguish the latent etiology of LVH.

[Key words] Left ventricular hypertrophy; Hypertensive heart disease; Echocardiography

SPION induced cell damage and m1 like polarization in macrophages could be reduced by MTP–131

LU Qizheng ZHENG Hao YAO Xiaobo ZHANG Youming WANG Chailin

OU Jinbo SHEN Yunli

Shanghai East Hospital, Tongji University School of Medicine, Shanghai 200120, China

[Abstract] **Objective** Superparamagnetic iron oxide nanoparticles (SPION) is recognized as being a novel

MRI contrast agent and targeted carrier, which has attracted much attention over the last two decades. However, the cytotoxicity of SPION limits its clinical transformation in cardiovascular field. Macrophages are the main inflammatory cells, which play an important role in the repair process after acute myocardial infarction. The aim of this study was to explore the effects of SPION on the function and polarization of macrophages, and whether mitochondria targeted antioxidant peptides MTP-131 modification could improve the macrophage toxicity of SPION. **Methods** All the RAW 264.7 mouse macrophages are incubated with SPION and new type SPION loaded with MTP-131 (arginyl-2,'6'-dimethyltyrosyl-lysyl-phenylalaninamide) at the concentration of 50 μg Fe/mL for 24 h. Scanning electron microscope (SEM) was used to observe morphological change and phagocytosis of macrophages, and transmission electron microscope (TEM) was employed to observe mitochondria damage and flow cytometry was applied to detect cell apoptosis and the markers of macrophage polarization. The inflammation related factors of cell culture supernatant are tested by enzyme linked immunosorbent assay (ELISA). The molecular events were analyzed by real-time quantitative polymerase chain reaction (RT-PCR) and fluorescence imaging. Macrophages migratory ability was evaluated by transwell using transwell assay and crystal violet staining. All the experiments were repeated three times. **Results** Compared with the control group, SPION significantly induced cell damage, evidenced by the reduction of cell viability and the increase of early cells apoptosis and the reactive oxygen species (ROS), whereas these features occur less in SPION loaded with MTP-131 groups (all $P < 0.05$). Moreover, macrophages migratory ability was inhibited by SPION, while loading MTP-131 could reduce this effect. After 24h incubation, the pro-inflammatory factor TNF α was significantly upregulated in the SPION group compared to the SPION loaded with MTP-131 group ($P < 0.05$). Correspondingly, the median fluorescence intensity of CD86 and CD80, two classic pro-inflammatory (M1 Like) subtypes maker of macrophage, were expressed higher in the SPION group than those in the SPION loaded with MTP-131 group ($P < 0.05$). Surprisingly, higher levels of anti-inflammatory factors IL-10 and TGF- β were tested in SPION loaded with MTP-131 groups compared with the SPION group ($P < 0.05$). Notably, mitochondrial morphology serious disruption was observed by TEM in the SPION group, but less in the SPION loaded with MTP-131 group. Taken together, SPION can induce macrophage injury and apoptosis by inducing oxidative stress. More than that, SPION can promote macrophages to polarize into M1 like macrophages which secrete pro-inflammatory factors. Mitochondria may be the main target organelle of SPION. However, co-loading mitochondria targeted antioxidant peptides MTP-131 can significantly mitigate the SPION induced macrophage toxicity in vitro study. **Conclusion** Macrophages cell damage and migratory ability lost could mediate by SPION though disrupt mitochondria. SPION has a potential to induce macrophage pro-inflammatory effect, evidenced by promoting macrophages to polarize into M1 like cells secreting more pro-inflammatory factors, whereas co-loading mitochondria targeted antioxidant peptides MTP-131 could significantly mitigate the cell injure and pro-inflammatory effects of SPION in vitro study.

[Key words] Superparamagnetic iron oxide nanoparticles; Mitochondria targeted antioxidant peptides; Polarization; Macrophage

Percentage of neutrophils to plasma albumin ratio as a new predictor of all-cause mortality in patients with heart failure

HU Zesong WANG Jie XUE Yangjing JI Kangting

The Second Affiliated Hospital of Wenzhou Medical University, Wenzhou 325000, China

[Abstract] **Objective** Neutrophils and plasma albumin have been shown to be independent predictors of mortality from many diseases. The purpose of this study is to explore the effect of neutrophil percentage to plasma albumin ratio

(NPAR) as an independent predictor on all-cause mortality in patients with heart failure. **Methods** Extract clinical data from Medical Information Mart for Intensive Care-III database(MIMIC III v1.4). The population was divided equally by NPAR. The main result of the study was the 30-day mortality, and the secondary results were in-hospital mortality, 90-day mortality and 365-day mortality. The Cox proportional hazards regression model was used to estimate HR with 95%*CI* for the association between NPAR and outcomes. ROC curve analysis was used to analyze and evaluate the predictive value of NPAR. We also collected patients data from the Second Affiliated Hospital of Wenzhou Medical University, and used person correlation analysis to determine the relationship between NPAR and length of stay in hospital and cardiac troponin I (cTnI) and N-terminal pro brain natriuretic peptide (NT-proBNP). **Results** In MIMIC-III database, a total of 2 942 patients were selected. For 30-day mortality, compared with the reference (NPAR < 22.56), the *HR* (95%*CI*) values of the mid-tertile (NPAR 22.56-27.64) and the upper tertile (NPAR > 27.64) were 1.27 (1.01-1.59) and 2.29 (1.87-2.81), respectively. After adjusted for age, gender and ethnicity in adjust I, the upper tertile (NPAR > 27.64) was also observed an increasing trend of 2.18 (1.78-2.67). After further adjusted for potential confounders in adjust II, the upward trend remained statistically significant in the upper tertile: 1.52 (1.22-1.90). A similar trend was also observed in the analysis results of 90-day mortality and 365-day mortality. Among the results of all-cause in-hospital mortality, only the upper tertile (NPAR > 27.64) was observed to increase in the non-adjusted and adjust I, which were 1.37 (1.10-1.72) and 1.31 (1.04-1.64), respectively. In the subgroup analysis, we did not observe significant interactions. Data from the Second Affiliated Hospital of Wenzhou Medical University showed that the correlation coefficient between length of stay in hospital and NPAR was 0.305, which was better than the correlation coefficient of neutrophil percentage or plasma albumin alone. The same results were obtained in cTnI and NT-proBNP. **Conclusion** In patients with heart failure, NPAR was independently associated with all-cause mortality. NPAR was positively correlated with length of stay in hospital and cTnI and NT-proBNP. Our results still need to be verified by more prospective case-control studies.

[Key words] Plasma albumin ratio; Heart failure; Neutrophil percentage

Non-alcoholic fatty liver disease and the risk of myocardial infarction: a meta-analysis

NI Jie WEN Wen ZHOU Mengyun WANG Chunyi JIANG Jingjie FU Xinyan CHEN Juan REN Kaihan GE Zhongjun CHENG Yongran ZHANG Xingwei WANG Mingwei

The Affiliated Hospital of Hangzhou Normal University, Hangzhou 310000, China

[Abstract] Objective Many studies have assessed the association between non-alcoholic fatty liver disease(NAFLD) and the risk of coronary artery disease(CVD), but the necessary correlation has not been established. Whether NAFLD by itself is associated with an increased risk of CVD events and death remains an issue of debate due to incomplete data. Considering that CVD includes a heterogeneous spectrum of clinical conditions, this study used myocardial infarction (MI) as a single primary endpoint. Therefore, the purpose of this study is to evaluate the association between NAFLD and the risk of MI. **Methods** We searched PubMed, Embase, and the Cochrane Library for case control studies that were published prior to April 20, 2021, and that contained data on MI in patients with NAFLD. A random effects model was used with the odds ratio as the effect size. The frequency of MI was compared between patients with and without NAFLD. We also determined the pooled prevalence of MI in patients with NAFLD. Publication bias and heterogeneity were considered using funnel plots, meta-regression, and the trim and fill method. **Results** A total of 19 168 798 patients with NAFLD was included in the 10 articles we obtained. A total of 26 649 cases (0.96%) of patients with NAFLD had MI complications, and 28 136 cases (0.40%) of patients with non-NAFLD had MI complications.

Meta–analysis of the data showed that MI was significantly associated with patients with NAFLD, with a pooled OR of 1.76, 95%*CI*:1.33–2.33, $P < 0.01$, I^2=95%. There was no significant difference in the incidence of death between patients with NAFLD and non–NAFLD patients. Sensitivity analyses did not modify these findings, and funnel plots did not reveal significant publication bias. **Conclusion** This study showed that the incidence of MI was higher in participants with NAFLD compared to those without NAFLD. Patients with NAFLD exhibited a higher risk of MI complications, which further showed that NAFLD may be an independent risk factor for the development of MI. These data indicate that NAFLD can be used as a new type of CVD risk factor that indicates greater likelihood of the development of MI than traditional risk factors. More importantly, this meta–analysis provides reliable evidence that early detection of cardiovascular disease in patients with NAFLD is beneficial because it can prevent disease development and advancement. Detection of fatty liver by abdominal sonographic examination may provide valuable information for CVD risk assessment.

[Key words] Non–alcoholic fatty liver disease; Coronary artery disease

Efficacy and safety of ticagrelor 60 mg in patients with coronary artery disease requiring dual antiplatelet therapy: a PRISMA–compliant meta–analysis

XU Wencheng ZHANG Haifu ZHOU Mengyun WEN Wen WANG Chunyi NI Jie JIANG Jingjie FU Xinyan GE Zhongjun REN Kaihan CHENG Yongran WANG Mingwei ZHANG Xingwei MAO Qin

The Affiliated Hospital of Hangzhou Normal University, Hangzhou 310000, China

[Abstract] Objective Patients with coronary artery disease require antiplatelet therapy with P2Y12 receptor antagonists. This study aimed to analyze the antiplatelet effect of ticagrelor 60 mg in patients with coronary artery disease after 1–month follow–up and the clinical outcome after 1–year follow–up. **Methods** Electronic databases PubMed, OVID, Cochrane Library, and Web of Science using "Ticagrelor" "brilique" "AZD6140" "lowdose" "60 mg" and "coronary artery disease" were searched up to November 1, 2020, for studies on ticagrelor use in in patients with coronary artery disease requiring dual antiplatelet therapy. The short–term clinical outcome was the antiplatelet effect of ticagrelor 60 mg versus ticagrelor 90 mg and clopidogrel. The long–term outcome was the occurrence of clinical adverse events of ticagrelor 60 mg versus ticagrelor 90 mg. **Results** A total of 7 clinical studies involving 14 767 participants were included. At 1–month follow–up, the measurement of P2Y12 reaction unit, ticagrelor 60 mg bid, although higher than ticagrelor 90 mg bid, was significantly lower than clopidogrel (75 mg qd). The incidence of high platelet reactivity was not significantly different between the ticagrelor 60 mg and 90 mg groups ($P < 0.05$). At 1–year follow–up, no significant difference in myocardial infarction or stroke was found in the ticagrelor 60–mg group compared with the ticagrelor 90–mg group, but the ticagrelor 60–mg group was superior in reducing minor bleeding. **Conclusion** Ticagrelor 60 mg possessed a stronger platelet–inhibitory effect compared with clopidogrel and provided prophylaxis of embolic events similar to that of standard ticagrelor at a much lower dose, with a lower risk of minor bleeding.

[Key words] Coronary artery disease; Meta–analysis; Ticagrelor

Effect of air pollution on metabolism–associated fatty liver disease: a hospital–based study

WANG Mingwei WEN Wen ZHOU Mengyun WANG Nan Wang Chunyi NI Jie
JIANG Jingjie GE Zhongjun ZHANG Xingwei FENG Zhanhui CHENG Yongran
The Affiliated Hospital of Hangzhou Normal University, Hangzhou 310000, China

[Abstract] Background Many studies have shown that the fine particulate matter in air is related to the incidence rate of chronic diseases. However, research on air pollution and metabolism–associated fatty liver disease (MAFLD) is limited. Objective The purpose of this study was to explore the relationship between the incidence rate of MAFLD and air pollutants. Methods Using a quasi–poisson regression generalized additive model. Stratified analyses by season and age were also performed. Results A 10 μg/m^3 increase of PM10, PM2.5, and NO_2 concentrations corresponded to 0.82(95%*CI*:0.49–1.15), 0.57(95%*CI*:0.18–0.98), and 0.86(95%*CI*:0.59–1.13) elevation in MAFLD. NO_2 has the highest effect in the transition season, while PM10 has the highest effect in the cool and hot seasons. In the two age groups with 45 years as the dividing line, PM2.5 has the highest impact estimate: 2.69(95%*CI*:0.77–5.61) and 2.88 (95%*CI*:0.37–6.40). The impact values of PM2.5 in male and Female were 3.60(95%*CI*:0.63–6.57) and 1.65(95%*CI*:1.05–2.25), respectively. The most important link is in different lag models, there is a significant correlation. Conclusion The effects of different air pollutants on MAFLD incidence rate were different in different seasons, ages, and gender.

[Key words] Air pollution; Metabolism–associated fatty liver disease

Association of neutrophil with altered modular segregation of brain networks in coronary heart disease

WEN Wen Wang Chunyi ZHOU Mengyun NI Jie JIANG Jingjie CHENG Yongran
GE Zhongjun CHEN Juan ZHANG Xingwei WANG Mingwei WANG Chunjie
The Affiliated Hospital of Hangzhou Normal University, Hangzhou 310000, China

[Abstract] Background Previous studies have shown that coronary heart disease (CHD) could cause increases in neutrophils, impairments in cognitive function and changes in brain activities. However, little is known about the brain network organizations in subjects with CHD and the relationship of this network organization with neutrophils and cognitive functions. Objective The present study aimed to address these issues with graph theory. Methods According to the clinical guidelines, 15 patients with CHD and 13 healthy controls were selected. Resting State Functional Magnetic Resonance Imaging (RS–fMRI) data were collected to explore the functional brain network organization of the subjects. Mean participation coefficient (PC) of different brain network modules was calculated and compared between CHD patients and healthy controls to examine group differences in modular segregation. Based on the results, further group comparison analyses were performed to explain the PC changes and to explore the relationship between PCs and neutrophils and cognitive functions. Results Compared with healthy controls, patients with CHD exhibited significantly higher neutrophils and leukocytes. In addition, patients with CHD showed significantly decreased PC in the cingulo–opercular network (CON), which was mainly driven by decreased connections between the CON and other brain modules. Moreover, our study found that, in the CHD group, lower PC of the CON was associated with more neutrophils and leukocytes, as well as higher NLR ratio. Although the two groups showed no group differences in the frontal–parietal

network (FPN), our study showed that lower PC of the FPN was associated with better cognitive performance in the control group, but not in the CHD group. **Conclusion** Neutrophils are closely related to the pathogenesis of coronary heart disease and play an important role in the separation of brain network modules in patients with coronary heart disease. In addition, FPN is closely related to cognitive function. Subsequent enrolment should be expanded to demonstrate the correlation between CHD and cognition. These findings extend our understanding of the neural mechanism of CHD and have important implications for developing effective interventions to treat CHD subjects.

[Key words] Coronary heart disease; Neutrophil; Brain networks

The visceral adiposity index as a predictor for adverse cardiovascular outcomes in patients with non–ST–segment elevation acute coronary syndrome undergoing percutaneous coronary intervention

ZHAO Qi ZHAO Ziwei CHENG Yujing XU Yingkai SUN Tienan ZHOU Yujie

Beijing Anzhen Hospital, Beijing 100029, China

[Abstract] **Objective** The visceral adiposity index (VAI) is proposed as a surrogate marker of insulin resistance (IR) and, when increased, is related to elevated cardiovascular risks. However, the prognostic value of VAI in patients diagnosed with non–ST–segment elevation acute coronary syndrome (NSTE–ACS) undergoing elective percutaneous coronary intervention (PCI) remains unclear. **Methods** The current study ultimately enrolled 2308 subjects diagnosed with NSTE–ACS who received elective PCI. All participants received a routine follow–up after discharge. The VAI was obtained from the equation described by former studies. Adverse cardiovascular events included all–cause death, nonfatal myocardial infarction(MI), nonfatal ischemic stroke, and ischemia–driven revascularization, composite of which was defined as the primary endpoint. **Results** Overall, 547(23.7%) primary endpoints were documented during a 48–month follow–up. Despite adjusting for confounding variates, the VAI remains to be a significant risk predictor for the primary endpoint, with a *HR*(95%*CI*) of 2.257(1.765–2.843) ($P < 0.01$). A significant incremental effect on the predictive performance for the primary endpoint was found when adding the VAI into a baseline model including traditional cardiovascular risk factors [area under the receiver–operating characteristic curve (AUC) 0.828 for baseline model vs. 0.851 for baseline model+VAI, $P < 0.01$, net reclassification improvement (NRI) 0.185, $P < 0.01$, integrated discrimination improvement (IDI) 0.026, $P < 0.01$]. **Conclusion** The VAI is an independent risk predictor for adverse cardiovascular events in subjects diagnosed with NSTE–ACS undergoing elective PCI. Further prospective studies are needed to verify the present results.

[Key words] Visceral adiposity index; Non–ST–segment elevation acute coronary syndrome

Association of serum chromogranin B with left ventricular function in patients with stable angina undergoing successful recanalization for chronic total occlusion:relation to collateral conditions

WANG Xiaoqun　SHEN Weifeng

Ruijin Hospital, Shanghai Jiaotong University School of Medicine, Shanghai 200020, China

[Abstract] **Objective** Coronary collaterals provide salvaging effect on the ischemic myocardium subtended by occluded coronary artery. We investigated the relation of chromogranin B (CgB) and collateral conditions to left ventricular (LV) functional improvement after successful recanalization of chronic total occlusion (CTO). **Methods** Serum level of CgB was assayed in 237 patients with stable angina and CTO of at least one major coronary artery. The degree of coronary collaterals supplying the distal aspect of a total occlusion was graded according to Rentrop classification. Two-dimensional echocardiography was performed before and 12 months after successful recanalization of CTO. **Results** Serum levels of CgB were comparable between patients with poor and good collaterals [934(IQR:315-2 422) pg/mL vs. 1 124(IQR:436-2 674) pg/mL, $P>0.05$]. CgB correlated positively with NT-proBNP level ($r=0.42$, $P<0.01$) both in patients with poor and good collaterals, and was inversely related to LV ejection fraction ($r=-0.23$, $P<0.01$) only in good collateral condition. At 12 months, the increase in LV ejection fraction was reduced stepwise across tertiles of serum CgB in patients with poor collaterals($P<0.05$) but not in those with good collaterals ($P>0.05$). After multivariate adjustment, elevated serum CgB remained an independent determinant of impaired LV functional improvement after recanalization of CTO lesions with low collateralization. **Conclusion** LV function and its recovery potential in CTO patients are associated with CgB level and collateral conditions. Elevated circulating CgB level may serve as a surrogate biomarker of impaired LV functional improvement after successful CTO recanalization in patients with poor coronary collaterals.

[Key words] Stable angina; Chromogranin B; Left ventricular function

The interaction between hyperuricemia and admission lactate increases the risk of acute kidney injury in ST-segment elevation myocardial infarction patients

LIANG Dongjie　HE Yanlei

The First Affiliated Hospital of Wenzhou Medical University, Wenzhou 325000, China

[Abstract] **Objective** Recently hyperuricemia has been recognized as a risk factor for acute kidney injury, but little is known on whether the association between hyperuricemia and acute kidney injury(AKI) in ST-segment elevation myocardial infarction (STEMI) is modified by lactate. This study aimed to investigate the effect of the interaction between hyperuricemia and lactate on the risk of acute kidney injury(AKI). **Methods** This was a retrospective, observational study that included STEMI patients who were admitted to the coronary care unit (CCU) of the First Affiliated Hospital of Wenzhou Medical University between January 2014 and August 2018. Hyperuricemia was defined as a serum uric acid (SUA) level > 7 mg/dL for males and > 6 mg/dl for females. AKI was defined and staged according to the Kidney Disease Improving Global Outcomes (KDIGO) guidelines. Logistic regression models were used to determine the association

between hyperuricemia and AKI in the overall population and subgroups stratified based on admission lactate levels (≤ 2.2 mmol/L or > 2.2 mmol/L). **Results** A total of 1 718 STEMI patients were included. Multivariate analysis indicated that hyperuricemia was associated with AKI (*OR*=1.37, 95%*CI*:1.03–1.83, *P* < 0.05). However, the prognostic effect of hyperuricemia was only observed in patients with lactate level > 2.2 mmol/L (*OR*=2.10, 95%*CI*:1.37–3.22, *P* < 0.01, but not in those with lactate level≤ 2.2 mmol/L (*OR*=0.85, 95%*CI*:0.54–1.32, *P* > 0.05). The interaction between hyperuricemia and lactate levels had a significant effect on AKI (*P* < 0.01). **Conclusion** Hyperuricemia was associated with acute kidney injury in STEMI patients with lactate level > 2.2 mmol/L, but not in those with lactate level ≤ 2.2 mmol/L.

[Key words] ST–segment elevation myocardial infarction; Lactate; Hyperuricemia

Mechanisms by which long non–coding RNA–HRAT modulates ischemia/reperfusion induced myocardial injury

YIN Deling XIN Bin

The Second Affiliated Hospital of Zhejiang University, Hangzhou 310009, China

[Abstract] Objective Increasing evidence suggests that long noncoding RNAs (lncRNAs) contribute to myocardial ischemia/reperfusion(I/R) injury. However, the mechanisms by which lncRNAs modulate myocardial I/R injury remain to be investigated. Our studies was aimed to identify new lncRNAs that are abnormally expressed in cardiomyocytes with hypoxia/reoxygenation (H/R) process by RNA sequencing, and explore its role and mechanisms in myocardial I/R injury. Our studies provide a new insight for novel therapeutic targets for the prevention and treatment of myocardial injury induced by I/R. **Methods** New lncRNAs with abnormal expression in cardiomyocytes after H/R treatment were screened by RNA sequencing and verified by qRT–PCR. The characteristics of lncRNA–HRAT were identified by the Coding Potential Calculator Online, RNA fluorescence in situ hybridization (FISH) and qRT–PCR analysis of nuclear/cytoplasmic RNA. After overexpression of lncRNA–HRAT with lentivirus, the effect of lncRNA–HRAT on H/R–induced cardiomyocyte apoptosis was verified by Western Blot and flow cytometry. A mouse myocardial I/R model was utilized, and the expression of lncRNA–HRAT in mouse heart was detected by qRT–PCR. The cardiomyocyte–specific lncRNA–HRAT knockout (HRAT–CKO) mice were constructed, the effects of cardiomyocyte–specific deficiency of lncRNA–HRAT on myocardial I/R injury were assessed by serum biochemical kit, 2, 3, 5–triphenyltetrazole chloride (TTC) staining and echocardiography.The potential interacting miRNAs of lncRNA–HRAT was analyzed by using online softwares, and their expression was verified by qRT–PCR. The luciferase reporter assay, RNA immunoprecipitation Assay and qRT–PCR were perfomed to verify the regulation between lncRNA–HRAT and its potential target miR–370–3p. The expression of miR–370–3p after H/R and I/R treatment was detected by qRT–PCR. After overexpression of miR–370–3p with miRNA mimic, the effect of miR–370–3p on H/R–induced cardiomyocyte apoptosis was verified by Western Blot and flow cytometry. The downstream target genes of miR–370–3p were predicted using online softwares. The luciferase reporter assay, qRT–PCR and Western blot were perfomed to verify the regulation between miR–370–3p and its potential target RNF41. The regulatory relationship between lncRNA–HRAT and RNF41 was verified by Western Blot. **Results** Compared with the control group, 222 lncRNAs were upregulated and 807 lncRNAs were downregulated after H/R treatment. Among them, the expression of lncRNA TCONS_00029632 was significantly up–regulated and consistent with the sequencing results. Based on its potential functions, we termed it hypoxia/reoxygenation associated transcript (lncRNA–HRAT) and selected for further studies. LncRNA–HRAT was located on chromosome 13 and had no coding potential and was distributed in both the cytoplasm and nucleus. It can affect the expression of neighboring gene Adora1 in cis. The expression of lncRNA–HRAT was significantly increased in the mouse hearts following I/R and H/R–treated cardiomyocytes, and the

upregulated lncRNA–HART could promote apoptosis in cardiomyocytes. Cardiomyocyte–specific deficiency of lncRNA–HRAT significantly diminished the content of CK in serum after I/R, decreased myocardial infarct area and improved cardiac dysfunction. LncRNA–HRAT directly binds and negatively regulates miR–370–3p. MiR–370–3p was significantly downregulated in the mouse hearts following I/R and H/R–treated cardiomyocytes, and overexpression of miR–370–3p inhibited H/R–induced cardiomyocytes apoptosis. RNF41 is a downstream target of miR–370–3p. LncRNA–HRAT acted as a ceRNA of miR–370–3p to promote the expression of RNF41. **Conclusion** Overexpression of lncRNA–HRAT promotes cardiomyocytes apoptosis induced by H/R. Cardiomyocyte–specific knockout of lncRNA–HRAT can alleviate myocardial injury induced by I/R. LncRNA–HRAT promotes H/R–induced cardiomyocyte apoptosis through miR–370–3p/RNF41 signaling pathway.

[Key words] LncRNA–HRAT; Ischemia/reperfusion; Doxorubicin; Myocardial injury

Nonalcoholic fatty liver disease and the risk of incident hypertension: a meta–analysis

JIANG Jingjie NI Jie ZHOU Mengyun WEN Wen Wang Chunyi CHENG Yongran GE Zhongjun CHEN Juan WANG Mingwei ZHANG Xingwei MAO Qin

The Affiliated Hospital of Hangzhou Normal University, Hangzhou 310000, China

[Abstract] Objective Revious epidemiologic studies have shown the clinical association between non–alcoholic fatty liver disease(NAFLD) and cardiovascular disease(CVD). However, there is only limited information about the effect of NAFLD on hypertension. Accordingly, the aim of this study is to assess the association between NAFLD and the risk of hypertension(HT). **Methods** We searched PubMed, Embase, and the Cochrane Library for studies that were published prior to May 13, 2021.And that contained data on HT in patients with NAFLD. A random effects model was used with the odds ratio as the effect size. The frequency of HT was compared between patients with and without NAFLD. Publication bias and heterogeneity were considered using funnel plots, meta–regression, and the trim and fill method. **Results** A total of 12 960 patients with NAFLD was included in the 5 articles we obtained. A total of 4 371 cases (33.7%) of patients with NAFLD had HT, and 7 520 cases(23.5%) of patients with non–NAFLD had HT. Meta–analysis of the data showed that HT was significantly associated with patients with NAFLD, with a pooled *OR* of 1.99(95%*CI*:1.63–2.43), $P<0.01$, I^2=91%. **Conclusion** This study showed that the incidence of HT was higher in participants with NAFLD compared to those without NAFLD. NAFLD was a factor for hypertension.

[Key words] Non–alcoholic fatty liver disease; Cardiovascular disease; Hypertension

LCZ696 treatment rudeces inflammation and improves lvef via inhibiting pDrp1/Drp1 in murine model of viral myocarditis

XU Jing

The Second Affiliated Hospital of Wenzhou Medical College, Wenzhou 325000, China

[Abstract] Objective Viral myocarditis (VMC) is the pathogeny of heart failure with few specific treatments. The improvement of left ventricular ejection fraction (LVEF) is a critical predictor for the prognosis of VMC and heart failure. LCZ696 is a novel drug used in heart failure to improve the LVEF, but there is no research in VMC. Therefore, we

evaluated the effects and mechanism of LCZ696 to improve LVEF in VMC. **Methods and Results** Four-week-old male BALB/c mice were randomly divided into 4 groups: negative control (NC) group, LCZ696 group [60(mg·kg/d), 7 days, ip.], VMC group (10^5TCID50 Coxsackievirus B3(CVB3), 0.1 mL ip.), VMC+LCZ696 group (n=10 in each group). The LVEF was evaluated by echocardiographic and it was significantly improved in the VMC+LCZ696 group compared with the VMC group. In addition, histological analysis and western blot results showed that LCZ696 attenuated inflammation and cardiomyocyte apoptosis. The expression of inflammatory factors (IL-6 and cleaved IL-1β) and apoptosis factor(cleaved caspase-3) were decreased in VMC+LCZ696 compared with the VMC group. Moreover, Increased mitochondrial fission, mitochondrial fission protein dynamin-related protein 1 (Drp1) expression and phosphorylation were observed in the VMC group which was suppressed after LCZ696 treatment. Then, adeno-associated virus 9 (AAV9) which main affinity tissue is heart tissue was injected to produce Drp1-expression inhibit mice. 2-week-old male BALB/c mice were randomized to AAV9, VMC, VMC+AAV99 or no treatment (n=10 in each group), AAV9 inoculated at 2 weeks of age and CVB3 at 4 weeks of age. Compared with VMC group, VMC+AAV99 group showed an increase in LVEF, survival rate, and the lower level of Drp1 expression, mitochondrial fission as well as attenuating of inflammatory and apoptosis. Similarly, reduced inflammation and apoptosis were also found after inhibition of Drp1 with Mdivi-1 in HL-1 infected CVB3. **Conclusion** The LCZ696 shows a protective effect in VMC by improving the LVEF, attenuating cardiac inflammation and cardiomyocyte apoptosis which may due to the inhibition of mitochondrial fission.

[Key words] LCZ696; VMC; LVEF; Drp1; Mitochondrial fission; Apoptosis;CVB3

Lactate dehydrogenase is associated with flow-mediated dilation in hypertensive patients

CAI Xiaoqi WANG Tingjun XIE Liangdi

The First Affiliated Hospital of Fujian Medical University, Fuzhou 350005, China

[Abstract] Objective The level of lactate dehydrogenase(LDH) has been proved to gradually increase during the course of atherosclerosis, in hypertension(HTN). In this cross-sectional study, the relationship between LDH and endothelial function evaluated by flow-mediated dilation(FMD) was investigated in hypertensives. **Methods** The present study was conducted in subjects from the database of the research: Target organ damage and related risk factors in hypertensives (registered number:ChiCTR2000039448,URL:http://www.chictr.org.cn/index.aspx). One thousand five hundred and seven Chinese subjects(aged 61.2 ± 12.5 years, 53.8% male) from our hospital were enrolled in the present study. According to the level of LDH, hypertensive patients (n=1216) were subdivided into 3 groups: LDH1(lowest tertile of LDH, n=399), LDH2(mediate tertile of LDH, n=409) and LDH3(highest tertile of LDH, n=408). Meanwhile, 291 age and gender-matched normotensives served as controls. FMD of right anterior tibial artery was assessed by high-resolution color Doppler ultrasound, and FMD < 8% was used as the cut point for endothelial dysfunction. **Results** The level of LDH in hypertensives was significantly higher than normotensives (P < 0.01). Whereas, FMD was obviously more blunted in hypertensives, compared with normotensives (P < 0.01). There was an increasing trend of endothelial dysfunction (FMD < 8%) from control,LDH1,LDH2 to LDH3 group (36.8% vs. 49.4% vs. 55.0% vs. 59.8%, P < 0.01). Stepwise multiple liner regression analysis demonstrated an independent correlation between LDH and FMD in hypertensives (β =-0.145, P < 0.05), while this association did not exist in normotensives. After stratified analysis in hypertensives, the relevance persisted in the male (β =-0.280, P < 0.01), young and middle-aged (age < 65 years, β =-0.237, P < 0.01), hypertensives with grade 2 HTN (β =-0.293, P < 0.05), duration of HTN < 3 years (β =-0.326, P < 0.05), metabolic syndrome (β =-0.232, P < 0.05) and those without statin therapy (β =-0.216, P < 0.05). **Conclusion** The level

of LDH was inversely correlated with FMD among hypertensive patients, independent of age, gender, blood pressure and multiple risk factors. LDH may serve as a potential marker for early atherosclerosis in hypertensives.

[Key words] Lactate dehydrogenase; Flow-mediated dilation; Endothelial dysfunction; Hypertension; Atherosclerosis

Impact of pre-revascularization and post-revascularization cardiac arrest on survival prognosis in patients with acute myocardial infarction and following emergency percutaneous coronary intervention

ZHOU Changzuan LIN Qingcheng XIANG Guangze CHEN Mengmeng CAI Mengxing ZHU Qianli ZHOU Rui HUANG Weijian SHAN Peiren

The First Affiliated Hospital of Wenzhou Medical University, Wenzhou 325000, China

[Abstract] **Objective** To evaluate the effects of the occurrence and timing of sudden cardiac arrest (SCA) on survival of acute myocardial infarction (AMI) patients who underwent emergency percutaneous coronary intervention (PCI). **Methods** We analyzed 1 956 consecutive AMI patients with emergency PCI from 2014 to 2018. Patients with cardiac arrest events were identified and their medical records were reviewed. **Results** Patients were divided into non-cardiac arrest group (NCA group, n=1 724), pre-revascularization cardiac arrest (PRCA group, n=175) and post-revascularization SCA (POCA group, n=57) according to SCA timing. Compared to NCA group, PRCA group and POCA group presented with higher brain natriuretic polypeptide (BNP), more often Killip class 3/4, atrial fibrillation and less often completed recovery of coronary artery perfusion (all $P<0.05$). Both PRCA and POCA patients showed increased 30-day all-cause mortality compared to NCA patients (8.0% and 70.2% vs. 2.9%, both $P<0.01$). However, as compared to NCA, PRCA did not lead to higher mortality during long-term follow-up (median time 917 days)(16.3% vs. 18.6%, $P>0.05$), whereas POCA were associated with increased all-cause mortality (36.3% vs. 18.6%, $P<0.01$). Multivariate analysis identified Killip class 3/4, atrial fibrillation, high maxium MB isoenzyme of creatinine kinase and high creatinine as predictive factors for POCA. In Cox regression analysis, POCA was found as a strong mortality-increase predictor (HR=8.87, 95%CI:2.26-34.72, $P<0.05$) for long-term all-cause death. **Conclusion** POCA appeared to be a strong life-threatening factor for 30-day and long-term all-cause mortality among AMI patients who admitted alive and underwent emergency PCI. However, PRCA experience did not lead to a poorer long-term survival in 30-day survivors.

[Key words] Cardiac arrest; Resuscitation; Acute myocardial infarction; Survival; Percutaneous coronary intervention

Analysis of the incidence and influencing factors associated with binary restenosis of target lesions after drug coated balloon angioplasty for patients with in-stent restenosis

XUE Weihao　WU Lianpin

The Second Affiliated Hospital and Yuying Children's Hospital of Wenzhou Medical University, Wenzhou 325000, China

[Abstract] **Objective** The goal of this study was to investigate the incidence and influencing factors associated with target lesion re-restenosis after drug coated balloon(DCB) angioplasty in patients with in-stent restenosis (ISR). Drug coated balloon angioplasty is a novel and effective therapeutic strategy for patients with coronary artery disease requiring revascularization especially in in-stent restenosis. However, there are still some patients who develop binary restenosis after drug coated balloon therapy while the incidece ande possible influencing factors have not yet been adequately assessed. **Methods** This was a prospective, randomized, multicenter trial. A total of 211 patients with in-stent restenosis who underwent percutaneous coronary intervention (PCI) with drug coated balloon were enrolled at 13 centers from August 2017 to October 2018. After 9 months angiographic follow-up, patients were divided into restenosis group and non-restenosis group according to whether the target lesions show restenosis again. The primary endpoint was the rate of binary restenosis, demographic data, clinical features, and laboratory tests were retrospectively reviewed, and logistic regression analyses were used to identify possible influencing factors. **Results** All patients in this study had successfully underwent drug coated balloon angioplasty, and there were 166 patients with 185 lesions who took part in angiography follow-up after 9 months, of which 41 patients with 43 target lesions had developed restenosis and the rest had no restenosis, the rate of binary restenosis was 23.2%. Univariate analysis showed that there were significant differences on the average length of target lesions and the diameter of pre-dilation balloon between ISR group and no-ISR patients ($P<0.05$). Demographic data (BMI, gender, age, the history of smoking, diabetes, hypertension, hyperlipidemia, myocardial infarction, heart failure, myocardial ischemia), left ventricular ejection fractions, blood routine test (white blood cell, neutrophils, red blood cell, hemoglobin and platelet), biochemical test (alanine aminotransferase, aspartate aminotransaminase, alkaline phosphatase, total bilirubin, direct bilirubin, triglycerides, high-density lipoprotein, low-density lipoprotein, creatinine and fasting plasma glucose), other lesions and surgical instrument features (diameter stenosis before procedure, reference vessel diameter, the number of calcified lesions, location of target lesions, length and maximal inflation pressure of both pre-dilation balloon and treating balloon and so on) showed no difference in two groups of patients. Logistic regression analyses showed that pre-dilation balloon diameter (*OR*=0.948, 95%*CI*:0.906-0.993, $P<0.05$) and length of lesion (*OR*=1.887, 95%*CI*:1.095-3.251, $P<0.05$) may be possible influencing factors when patients occurred binary restenosis after treating with DCB. **Conclusion** In this study, we found that the incidence of binary restenosis after DCB treatment remained relatively high level, the average length of lesions and the diameter of pre-dilation DCB may be possible influencing factors in patients treated with DCB, and studies with larger sample size and more complete follow-up data on this issue are needed in the future.

[Key words] Coronary artery disease; Drug-coated balloon; In-stent restenosis; Influencing factors

Assessment high–power catheter ablation in patients with atrial fibrillation: a meta–analysis

CHEN Yihe　XIAO Fangyi

The First Affiliated Hospital of Wenzhou Medical University, Wenzhou 325000, China

[Abstract] **Objective** High–power radiofrequency (RF) catheter ablation was considered as a promising alternative strategy to conventional–power ablation in the treatment of patients with atrial fibrillation (AF). This study sought to compare the efficacy and safety of high–power energy delivery to that of conventional–power setting in AF catheter ablation. **Methods** We performed a systematic review of relevant literature in Pubmed, Embase, Cochrane library, and Google Scholar database. Sixteen eligible studies totaling 3 307 patients (1,929 for high–power ablation; 1,378 for conventional–power ablation) met inclusion criteria. **Results** During a median 12 months follow–up, high–power ablation showed a significantly higher AF/atrial tachycardia free survival rate in comparison with conventional–power ablation (*RR*=1.09, 95%*CI* 1.02 to 1.15, $P<0.05$). Notably, high–power strategy convincingly decreased the procedure time (WMD=–46.11 min, 95%*CI* 59.15 to 33.07, $P<0.01$) and RF ablation time (WMD=–19.19 min, 95%*CI* –24.47 to –13.90, $P<0.01$), along with reduced fluoroscopy time (WMD=–7.82 min, 95%*CI* –15.13 to –0.68, $P<0.05$). In addition, there was no perceptible difference in the potential risk of procedure–related complications between these two approaches (*RR*=0.81, 95%*CI* 0.48 to 1.37, $P>0.05$). **Conclusion** High–power RF catheter ablation was associated with an improvement in long–term sinus rhythm maintenance for treatment of AF, without exacerbating the risk of adverse events during the procedure. Impressively, high–power pulmonary vein isolation had the potential to shorten application duration and minimize fluoroscopic exposure.

[Key words] Radiofrequency; Atrial fibrillation; Meta–analysis

Association between plasma inflammatory growth factors and delayed device endothelialization after left atrial appendage closure

XU Jing

Shanghai East Hospital, Tongji University School of Medicine, Shanghai 200120, China

[Abstract] **Objective** To investigate whether inflammatory and growth factors (IGFs) were associated with incomplete device endothelialization (IDE) at 6 months after left atrial appendage closure (LAAC). **Methods** The enrolled patients were divided into complete device endothelialization(CDE) and IDE group by cardiac computerized tomography(CCT). Ten IGFs were determined using ELISA kits in initial enrolled 25 patients. IGFs with statistical differences between the two groups were further verified in the cohort. **Results** IDE and CDE were detected in 65 and 36 patients, respectively. Among the ten IGFs, plasma bFGF and MMP–9 were significantly lower in patients with IDE compared to those with CDE ($P<0.05$, respectively).Further verification test showed bFGF was significantly different between the two groups ($P<0.05$).Multivariate regression analysis showed bFGF was an independent factor for IDE (*OR*=8.353, 95%*CI*: 2.089–33.403, $P<0.05$). C–statistics of bFGF for discriminating patients with IDE from those with CDE was 0.788 (95%*CI*:0.695–0.882, $P<0.05$), with a cut–off value of 284.8 pg/mL (sensitivity 71.9%, specificity 73.7%). **Conclusion** Reduced plasma bFGF level confers an increased risk for IDE after LAAC.

[Key words] Inflammatory;Growth factors;Left atrial appendage closure

Risk of new-onset atrial fibrillation post-cavotricuspid isthmus ablation in typical atrial flutter without history of atrial fibrillation

LI Jiahui XIE Haiyang CHEN Yanqiao CAO Zhongjing TANG Qinghui GUO Xiaogang SUN Qi MA Jian

Fuwai Hospital, National Center for Cardiovascular Diseases, Chinese Academy of Medical Sciences and Peking Union Medical College, Beijing 100037, China

[Abstract] **Objective** To describe the incidence of atrial fibrillation (AF) after cavotricuspid isthmus (CTI) ablation in typical atrial flutter (AFL) patients without history of AF and to identify risk factors for new-onset AF after the procedure. **Methods** A total of 191 patients with typical AFL undergoing successful CTI ablation were enrolled. Patients with history of AF, structural heart disease, cardiac surgery or ablation, or were in usage of anti-arrhythmia drug after the ablation were excluded. Clinical and electrophysiologic data were collected. **Results** There were 47 patients (24.6%) developing new AF during a follow-up of(3.3 ± 1.9)years after CTI ablation. Multivariate Cox regression analysis revealed that sleep apnea (*HR*=4.305, 95%*CI*:1.753-10.573, $P < 0.05$), advanced interatrial block (aIAB) (*HR*=2.035, 95%*CI*:1.027-4.032, $P < 0.05$), and left atrial diameter (LAD) > 42 mm (*HR*=2.595, 95%*CI*:1.428-4.715, $P < 0.05$) were independent risk factors of new-onset AF. A combination of aIAB and LAD > 42 mm (χ^2=30.658) was better than aIAB alone (χ^2=19.288) or LAD > 42 mm (χ^2=15.360) alone in predicting AF occurrence after CTI ablation ($P < 0.05$). **Conclusion** Sleep apnea, aIAB and LAD > 42 mm are risk factors of new-onset AF after CTI ablation in AFL patients without history of AF. A combination of aIAB and LAD > 42 mm are more reliable in predicting new-onset AF occurrence.

[Key words] Atrial fibrillation;Atrial flutter;Risk

Lopinavir used in COVID-19 inhibits cardiac hERG potassium channel current, but facilitates protein trafficking

ZHENG Zequn

Lihuili Hospital Affiliated to Ningbo University, Ningbo 315041, China

[Abstract] **Objective** Based on the concern of prolongation of QT interval, we investigated the effect of lopinavir on the hERG channel. Considering the two most critical mechanisms for the blocking of the hERG channel: direct channel blocking and the inhibition of channel protein trafficking, this study hypothesize that the decrease in channel current induced by lopinavir used in novel coronavirus disease of 2019 (COVID-19) is mainly due to the defective trafficking for the hERG protein. **Methods** HEK-293 cells stably expressing hERG protein were used to evaluate the blocking effect before and after drug treatment. HEK-293 cell line stably expressing hERG was created using plasmid transfection followed by Puromycin (2 μg/mL) selection. Following 24 hours of drug incubation, Western blotting was used to detect different mature forms of hERG proteins (immature 135 kDa and mature 155 kDa) before and after the application of lopinavir with concentration gradient (0~20 μmol). 10 μmol drug-treated cells were resuspended into single cells and I_{kr} current generated by hERG channel was detected using whole-cell patch clamp. I_{kr} was elicited by 3 s depolarizing steps from a holding potential of -80 mV to potentials ranging from -60 to +50 mV in 10 mV increments.

This was followed by a 3 s repolarization phase to −40 mV to elicit tail currents. **Results** Molecular experimental data showed that after the application of the corresponding concentration, hERG protein not only showed no inhibitory effect, but increased in a concentration−dependent manner. However, consistent with the previous results shown by electrophysiological analysis, whole−cell patch clamp showed that 10 μmol lopinavir reduced the tail current density of the hERG channel. **Conclusion** Lopinavir, an antiretroviral drug used in the COVID−19, inhibits the cardiac hERG potassium channel and reduces the I_{kr} currents it produces , but promotes the maturation of hERG channel proteins. This study results indicates that the decrease of I_{Kr} current induced by lopinavir is not due to the decrease of hERG protein on the cell membrane, but most likely due to the direct channel blocking effect of the drug after entering the cell.

[Key words] Lopinavir; hERG; Novel coronavirus disease of 2019

The effect of SGLT2 inhibitor on the metabolism of water and sodium

TANG Jun

Zhejiang Provincial People's Hospital, Hangzhou 310014, China

[Abstract] SGLT2 inhibitors exert hypoglycemic and diuretic effects by inhibiting the absorption of sodium and glucose from the proximal tubule. Available data indicate that SGLT2 inhibitors transiently enhanced urinary sodium excretion and urinary volume. When combined with loop diuretics, SGLT2 inhibitors exerted a meaningful synergistic natriuretic effect. The favorable diuretic profile of SGLT2 inhibitors may offer significant advantage in the management of volume status in patients with heart failure but probably not a dominant mechanism to the superior long−term heart failure outcomes observed with these agents. This first part of this 3−part review explores the causes of transient natriuresis and diuretic mechanisms of SGLT2 inhibitors. The second part provides an overview of the synergistic effect of SGLT2 inhibitors. And the third part summarizes the mechanisms of cardiovascular protection associated with diuretic effects of SGLT2 inhibitors.

[Key words] SGLT2 inhibitor; Metabolism; Effect

Evaluation of optimal dual antiplatelet therapy duration for high−risk patients with diabetes following PCI

WANG Haoyu

Fuwai Hospital, National Center for Cardiovascular Diseases, Chinese Academy of Medical Sciences and Peking Union Medical College, Beijing 100037, China

[Abstract] **Objective** Diabetes mellitus (DM) is frequently encountered in patients who underwent PCI and contributes to a prothrombotic state and residual cardiovascular risk, posing unique challenges in the antiplatelet management of such patients due to a higher risk for ischemic events and mortality than patients without DM. Diabetic patients often have many other concomitant co−morbidities that predispose them at high ischemic risk, which suggests that this high−risk population may derive particular benefit from prolonged use of DAPT. The efficacy and safety of prolonged (> 1−year) dual antiplatelet therapy (DAPT) duration in high−risk patients with DM undergoing PCI remain unknown. **Methods** All patients undergoing PCI at our hospital between January 2013 and December 2013 were

prospectively enrolled into our hospital PCI registry. 3 696 high-risk diabetics patients with at least one additional atherothrombotic risk factor (age≥ 65 years, current smoking, chronic renal dysfunction with estimated glomerular filtration rate < 60 mL/min, heart failure, peripheral artery disease, history of ischemic stroke, history of myocardial infarction, multivessel coronary artery disease) were screened for inclusion. The enrichment criteria of high-risk features were captured based on PEGASUS-TIMI 54 and COMPASS trials. The decision to discontinue or remain on DAPT after 1 year was made at the discretion of the patient's physician (and possibly influenced by the patient), wherein the individualized risks of ischemic versus bleeding events are carefully considered for each patient. The primary efficacy end point was major adverse cardiac and cerebrovascular events (MACCE) during follow-up, defined as a composite of all-cause death, MI, or stroke. The primary safety end point was clinically relevant bleeding, which was determined as the Bleeding Academic Research Consortium type 2, 3, or 5 bleeding. **Results** Of 3 696 high-risk patients with DM who were event-free at 12 months after index procedure, 2 580 (69.8%) patients received DAPT > 1-year, with the mean duration of DAPT was 672 days (*SE*: 3.31), whereas 1 116 (30.2%) patients received DAPT≤1-year, of whom the mean duration of DAPT was 349 days (*SE*: 1.84). The most prevalent enrichment criterion in high-risk patients with DM was multivessel CAD (81.5%), 58.1% had current smoking, 32.1% had age > 65 years, 21.9% had previous MI. After a median follow-up of 29.2 months (*IQR*: 26.7- 31.1 months), a total of 91 MACCEs, including 36 all-cause death, 45 stroke, and 21 MIs, were recorded. Based on multivariate Cox regression model and inverse probability of treatment weighting (IPTW) analysis, long-term (> 1-year) DAPT reduced the risk of primary efficacy outcome (1.7% vs. 4.1%, adjusted hazard ratio(adjHR): 0.382, 95%*CI*: 0.252-0.577, IPTW-*HR*: 0.362(0.241-0.542), as well as cardiovascular death and definite/probable stent thrombosis, compared with short-course (≤1-year) DAPT. Risk of the safety endpoint of clinically relevant bleeding [adj*HR*: 0.920(0.467-1.816), IPTW-*HR*: 0.969(0.486-1.932)] was comparable between longer DAPT and shorter DAPT. A lower number of net clinical benefit adverse outcomes was observed with > 1-year DAPT versus ≤1-year DAPT[adj*HR*: 0.471(0.331-0.671),IPTW-*HR*: 0.462 (0.327-0.652)]. The beneficial effect of extended DAPT on primary efficacy end point was consistent across the number of enrichment high-risk criteria fulfilled without any significant interaction, with absolute risk reductions that appeared larger in DM patients with accumulated ≥3 additional high-risk characteristics. **Conclusion** In the large, prospective observational study of DES-treated high-risk DM patients with additional atherothrombotic risk factors, physicians are more likely to recommend remaining on DAPT after 1 year in high-risk DM patients, likely reflecting concerns surrounding cessation of DAPT in the setting of a prothrombotic state. Continuation of DAPT beyond 1 year had lower risks of atherothrombotic events versus short-term (≤1-year) DAPT with similar risks of bleeding events, thereby maximizing a significant net clinical benefit. These observations suggest that extended DAPT might be a viable treatment option in high-risk DM patients with acceptable bleeding risk.

[Key words] PCI; Diabetes mellitus; Antiplatelet therapy duration

MOTS-c attenuates oxidative stress injury and inflammatory response of H9c2 cells through Nrf2/ARE and NF-κB pathway

SHEN Caijie

Ningbo First Hospital, Ningbo 315000, China

[Abstract] Objective To investigate whether MOTS-c could alleviate H_2O_2-induced oxidative stress and inflammatory status in H9c2 cells through activation of Nrf2/ARE and inhibition of NF-κB pathway. **Methods** Rat H9c2 cardiomyocytes was obtained and 10, 20 or 50 μM MOTS-c were pre-treated for 24 h before treatment of H_2O_2. Then, 100 μM H_2O_2 were treated for 1 h for inducing oxidative stress. Inhibition model of sh-Nrf2 was constructed via lentivirus

expressing system, and activation model of NF-κB were achieved using phorbol 12-myristate 13-acetate (PMA). Cell viability were determined using CCK8 assay. Western blotting and RT-qPCR were employed for measurement of relative protein and mRNA expression, relatively. Intracellular ROS level was detected using dichloro-dihydro-fluorescein diacetate (DCFH-DA) and MDA and SOD levels was determined via commercial kit. Immunofluorescence analysis was utilized for the visualization of protein expression and distribution in cells. ELISA was used to detect the levels of inflammatory cytokines including TNF-α, IL-6 and IL-1β. **Results** We found that H_2O_2 treatment could significantly decrease cell viability, increase the level of ROS and MDA and decrease the level of SOD, and upregulate the expression of inflammatory cytokines including TNF-α, IL-6 and IL-1β in H9c2 cells. The expression of Nrf2, HO-1 and NQO-1 was significantly downregulated in H_2O_2 group, while the phosphorylation of NF-κBp65 was promoted by H_2O_2. However, pre-treatment of MOTS-c could significantly reversed H_2O_2-induced damage in H9c2 cells. Moreover, both inhibition of Nrf2/ARE pathway and activation of NF-κB pathway would significantly decrease the effects of MOTS-c, suggesting that MOTS-c might play its role in alleviating oxidative damage via Nrf2/ARE and NF-κB pathway. **Conclusion** Our investigation indicated that MOTS-c could protect against H_2O_2-induced inflammation and oxidative stress in H9c2 cells through inhibiting NF-κB and activating Nrf2/ARE pathways.

[Key words] MOTS-c;H_2O_2; Oxidative stress;Inflammatory status;Nrf2/ARE;NF-κB

Plasma CA125 and BNP, which predict acute heart failure better in patients with acute myocardial infarction?

HU Xiaokang

Jinhua Municipal Central Hospital, Jinhua 321000, China

[Abstract] Objective Evaluate the relationship between CA125 and acute heart failure in AMI patients, and also compared plasma CA125 with brain natriuretic peptide (BNP). **Methods** This cohort study enrolled 2 025 patients in the Coronary Care Unit of the First Affiliated Hospital of Wenzhou Medical University, between January 2016 and October 2019. The diagnosis of acute MI is a clinical diagnosis based on patient symptoms, ECG changes, and highly sensitive biochemical markers, as well as coronary angiography results. We used the ROC curve to evaluate the predictive ability of CA125 and BNP for AHF, and multivariate regression analysis was also used to determine its predictive ability. At the same time, to balance the baseline characteristics associated, a propensity score–matched cohort design was used, yielding 864 patients.The study excluded patients with malignant tumors, active infections, and severe liver and kidney disease. The study conformed to the guidelines set forth in the Helsinki declaration, and the protocol was approved by the Medical Ethics Committee of the First Affiliated Hospital of Wenzhou Medical University. **Results** Among 2025 patients hospitalized for AMI, acute heart failure was found in 30.02%. The results of the ROC analysis revealed that BNP, CA125 and BNP+CA125 significantly predicted the development of AHF (AUC: BNP 0.762, CA125 0.660, and BNP+CA125 0.760, all $P<0.01$). But multivariate regression analysis showed that CA125 was not a good predictor of acute heart failure in the overall cohort ($P>0.05$), while BNP were still powerful predictors ($P<0.01$). After propensity score matching, 864 patients were included. The ability to predict AHF were also shown with AUC values of 0.621 for BNP, 0.564 for CA125, and 0.619 for BNP+CA125 (all $P<0.01$). In the matched cohort (n=432 in each group), the results of multivariate analysis still showed that BNP were still powerful predictors ($P<0.01$), and CA125 also has no predictive power($P>0.05$). **Conclusion** BNP levels have a good predictive value for the occurrence of AHF in patients with AMI. However, the prediction of AHF by CA125 levels were limited by factors such as age, heart rate, blood pressure, previous-stroke history and CKD history.

[Key words] Plasma CA125; BNP;Acute myocardial infarction;Acute heart failure

CD34$^+$ cell–derived fibroblasts are crucial for fibrosis during the heart failure

DU Luping XU Qingbo

The First Affiliated Hospital of Zhejiang University School of Medicine , Hangzhou 310003, China

[Abstract] **Objective** CD34$^+$ stem cells have been used to treat the patients with heart failure, but the outcome is variable. It is of great significance to scrutinize the fate and the mechanism of CD34$^+$ stem cell differentiation in vivo during heart failure and explore its intervention strategy. **Methods** Performed single cell RNA sequencing (scRNA–seq) of the total non–cardiomyocytes and enriched CD34–tdTomato$^+$ lineage cells in the murine pressure overload models (transverse aortic constriction, TAC), and total non–cardiomyocytes from human adult hearts. By analyzing the transcriptomes of 59 505 single cells from the mouse hearts and 22 537 single cells from the human hearts, we illustrated the dynamics of cell landscape during the progression of heart hypertrophy (or heart failure), including CD34$^+$ stem cells, fibroblasts, endothelial cells and immune cells. By combining mouse genetic lineage tracing and bone marrow transplantation models, we demonstrated that non–bone marrow derived CD34$^+$ cells give rise to fibroblasts and endothelial cells, while bone marrow derived CD34$^+$ cell turned into immune cells only in response to pressure overload. **Results** Partial depletion of CD34$^+$ stem cells alleviated the severity of myocardial fibrosis with a significant improvement of cardiac function in CD34–CreERT2,Rosa26–eGFP–DTA models. Similar changes of non–cardiomyocyte composition and cellular heterogeneity were also observed in patients with heart failure. Moreover, immunostaining showed a double labelling of CD34 and fibroblast markers in human heart tissues. Mechanistically, our single cell pseudotime analysis of scRNA–seq data and in vitro cell culture study revealed that Wnt– β –catenin and TGF β 1/Smad pathways are critical in regulating CD34$^+$ cell differentiation towards fibroblasts. **Conclusion** This study provides a cellular landscape of CD34$^+$ cell–derived cells in the hypertrophy heart of human and animal models, indicating that non–bone marrow derived CD34$^+$ cells differentiate into fibroblasts is largely accounts for cardiac fibrosis. These findings may provide novel insights for the pathogenesis of cardiac fibrosis and have further potential therapeutic implications for the heart failure.

[Key words] CD34$^+$ stem cells; Single–cell RNA sequencing; Lineage tracing; Myocardial fibrosis; Heart failure

Non–bone marrow CD34$^+$ progenitor cells are crucial for endothelial repair of injured arteries

JIANG Liujun CHEN Ting XU Qingbo

The First Affiliated Hospital of Zhejiang University School of Medicine, Hangzhou 310003, China

[Abstract] **Objective** To investigate the exact identity and the role of CD34$^+$ cells in vascular regeneration. **Methods** Compared with healthy arteries, CD34 expression percentage was significantly increased in diseased femoral arteries from patients. Using a guide–wire induced endothelial denudation model, reported the transcriptional profiling of over 30 000 cells by single–cell RNA sequencing analysis and provided a cell atlas of normal and lesioned arteries in mouse, in which a heterogeneous population of CD34$^+$ cells were revealed. **Results** Combining the inducible lineage tracing CD34–

CreER^{T2},R26–tdTomato mouse model and bone marrow transplantation experiments, showed that non–bone marrow CD34$^+$ mesenchymal cells acquired endothelial cell fate in the injured femoral artery rather than pre–exiting ECs, while bone marrow–derived CD34$^+$ cells differentiated into immune cells locally after vessel injury. Depletion of non–bone marrow CD34$^+$ cells using a diphtheria toxin induced cell ablation model, exacerbate neointimal lesions of the injured vessel. Furthermore, isolated vascular adventitia CD34$^+$ cells displayed endothelial differentiation, in which microRNA–21–Smad7–pSmad2/3 pathway regulated endothelial gene expression and function during differentiation. **Conclusion** This study provides a transcriptional and cellular landscape of vessels after endothelial denudation. This study findings suggest heterogeneous CD34$^+$ cells serve as a contributor not only to endothelial regeneration but also an inflammatory response that may provide therapeutic insights into vascular diseases.

[Key words] CD34$^+$; Endothelial repair; Injured arteries

Clinical characteristics and follow–up data of acute coronary syndrome caused by coronary spasm after percutaneous coronary intervention

ZHAO Zhihong

Shanghai Pudong New Area Zhoupu Hospital, Shanghai University of Medicine & Health Sciences, Shanghai 201318, China

[Abstract] Objective To analysis the percutaneous coronary intervention (PCI) patients whom acute coronary syndrome (ACS) caused by coronary artery spasm (CAS), the clinical features, diagnosis and treatment process and long–term cardiovascular events. **Methods** Retrospectively analyzed clinical features, diagnosis and treatment experience and occurrence of cardiovascular events of the PCI patients admitted to our hospital for ACS, from June 2016 to June 2020, and followed–up (27 ± 12) months. **Results** 8 PCI patients whom re–hospitalization diagnosised ACS, CAS was identified by coronary angiography, including 3 (37.5%) left coronary artery PCI patients whom acute inferior myocardial infarction caused by right coronary artery CAS. 1 (12.5%) left circumflex branch PCI patient whom acute anterior wall myocardial infarction caused by left anterior descending branch CAS. 4 (50.0%)PCI patients whom ACS caused by CAS occurred before and after stents, of whom 2 patients acute myocardial infarction caused by right coronary artery and left anterior descending branch CAS respectively, 1 patient right coronary CAS occurred during the implantation of right coronary PCI stent, 1 patient with right coronary artery CAS during left anterior descending branch PCI. All patients with CAS disappeared after intraoperative administration of nitroglycerin in the coronary artery. Atypical angina episodes were still observed during hospitalization and after long–term oral treatment with nitrates, calcium antagonist diltiazem, and statins, but no serious cardiovascular events occurred. **Conclusion** The PCI patients whom ACS induced by CAS, calcium antagonist diltiazem combined with nitrate drugs is the essential for alleviating CAS and improving the symptoms, and has a good prognosis.

[Key words] Percutaneous coronary intervention; Acute coronary syndrome; Coronary artery spasm

Notoginsenoside R1 protects against myocardial ischemia/reperfusion injury via TAK1–JNK/p38 signaling in mice

ZENG Jingjing SHI Hanqing REN Fangfang ZHAO Xiaoshan LI Lei

The Second Affiliated Hospital and Yuying Children's Hospital of Wenzhou Medical University, Wenzhou 325000, China

[Abstract] **Objective** Assessed the cardioprotective effects of NG–R1 in MI/R injury and obtained insights into its cardioprotective mechanisms. **Methods** MI/R injury was induced in mice by occluding the left anterior descending coronary artery for 30 min followed by 4 h of reperfusion. Mice treated with NG–R1 (25 mg/kg) 30 min prior to ischemic surgery and then were subjected to MI/R. Murine neonatal cardiomyocytes were subjected to hypoxia/reoxygenation (H/R) insult in vitro. Transforming growth factor β–activated protein kinase 1 (TAK1) was silencing by siRNA in vitro or AAV9 vector in vivo to examine NG–R1 molecular mechanism. Cardiac function was measured using echocardiographic and hemodynamic. Cardial damage was analysed using triphenyltetrazolium chloride staining. Apoptosis was measured by flow cytometry and TUNEL staining. **Results** Echocardiography showed that, compared with those in the MI/R group, the left ventricular ejection fraction (LVEF) and left ventricular shortening (LVFS) of the MI/R+NG–R1 group were significantly increased. Compared with MI/R group, NG–R1 pretreatment decreased the myocardial infarction area, reduced the number of TUNEL–positive cardiomyocytes, suppressed caspase–3 activity, inhibited the Bcl–2/Bax ratio and decreased the level of cTnI and CK–MB in the plasm following MI/R injury. Pretreatment with NG–R1 increased the viability, ameliorated LDH release, reduced the expression of cleaved caspase3 and the Bcl–2/Bax ratio under H/R injury. Western blot analysis further showed that p38 mitogen–activated protein kinase (p38 MAPK), c–Jun N–terminal kinase (JNK) and extracellular signal–regulated kinase (ERK) were activated by MI/R and H/R stimulation, but only the activation of JNK and p38 was inhibited by NG–R1. In addition, TAK1 was activited after MI/R injury, while NG–R1 inhibited the activation of TAK1. Notably, overexpression of TAK1 with adenovirus vectors in cells aggravated H/R injury and partially reversed the cardioprotective effects of NG–R1, which was manifested as increased apoptosis and increased expression of cleaved caspase 3. In addition, the protective effects of NG–R1 were abolished in TAK1–silenced cells subjected to H/R injury. And compared with the MI/R+Sh–TAK1 group, the NG–R1 plus MI/R+Sh–TAK1 group did not provide additional protection to reduce the infarct area. NG–R1 did not provide additional protection in attenuating cardiomyocyte apoptosis after MI/R injury in TAK1–silenced mice. **Conclusion** This study observed that NG–R1 alleviates myocardial injury and improved cardiac function after MI/R. Mechanistically, NG–R1 mitigated TAK1–JNK/p38 signaling mediated apoptosis, thus reducing MI/R injury both in vitro and in vivo. In addition, overexpression of TAK1 aggravated H/R injury and partially reversed the cardioprotective effects of NG–R1 in vitro. And NG–R1 did not provide additional protection to TAK1–silenced cardiomyocytes subjected to MI/R injury both in vitro and in vivo. In summary, this study presents the first direct evidence that NG–R1 alleviates MI/R injury by suppressing the activity of TAK1, subsequently inhibiting JNK/p38 signaling and attenuating apoptotic stress.

[Key words] Notoginsenoside R1; Myocardial ischemia/reperfusion; TAK1; JNK; p38; Apoptosis

Cardiotoxicity of epidermal growth factor receptor 2 targeted drugs for breast cancer

WANG Wei

Zhejiang Provincial People's Hospital, People's Hospital of Hangzhou Medical College, Hangzhou 310014, China

[Abstract] Breast cancer is the most common tumor in women, and its number is increasing year over year. Human epidermal growth factor receptor 2 (HER2 or ErbB2) overexpression is responsible for 20% to 25% of invasive breast cancers and is associated with poor prognosis. HER2 therapy has significantly improved overall survival in patients with HER2(+) breast cancer. However, despite its therapeutic benefits, its cardiotoxicity is a major concern, especially when used in conjunction with anthracyclines. The main anti-ErbB2-targeting drugs with cardiotoxicity are the mechanism of cardiotoxicity induced by drugs is not fully understood. Currently, NGR1 / HER-2 inhibiting HER dimer formation causes increasing ROS in mitochondria, and inhibition of PI3K/Akt and Ras/MAPK pathways directly leads to cell apoptosis. MMP2 are newly discovered pathways. In addition, although ACEIs /ARBs/ β -blockers and other drugs have an inhibitory effect on heart dysfunction caused by ErbB2-targeted drugs. NT-proBNP does well in monitored TIC during target drugs treatment and a predictive effect on disease prognosis. It is non-invasive, inexpensive, reproducible, and worthy of the attention of clinicians. NT-proBNP may serve as a biological marker for clinical prediction of the occurrence of cardiotoxicity.

[Key words] Epidermal growth factor receptor 2; Targeted drugs; Breast cancer

Aptamer generated by cell-selex for specific targeting of rat cardiomyocytes

XIE Zuoyi

The Second Affiliated Hospital and Yuying Children's Hospital of Wenzhou Medicial University, Wenzhou 325000, China

[Abstract] Objective To generate an aptamer that can target rat cardiomyocytes. Methods Performed a cell-SELEX procedure to generate aptamers for specific binding to rat cardiomyocytes. The basic principle of the cell-SELEX method includes positive selection, target sequence recovery, and negative selection and PCR amplification, During the positive screening process, the random library of single-stranded DNA (ssDNA) is incubated with the target (H9c2) cells. After that, the cell-binding oligonucleotides are subjected to negative selection, using nontarget cells (HUVEC cells) to remove nonspecific binding oligonucleotides. The supernatant containing the unbound ssDNA is harvested and used for PCR amplification. After about ten cycles of the screening procedure, the final library reaches a certain level of significant affinity and is then sequenced. During the cell-SELEX procedure, used flow cytometric analysis to motor the progress of selection. Results Selected the top ten most frequent sequences from the sequencing results as candidate sequences, then we performed binding affinity analysis to identify the most optimal aptamer. Based on the NUPACK software, predicted the aptamer's secondary structure and truncated unnecessary nucleotides for optimization. Finally, a optimal aptamer termed H5-1c was obtained. To determine if a temperature shift would change the affinity , under the conditions of 4 and 37 ℃, respectively, measured the dissociation constants of aptamer-cell interaction ,and

they were both measured in the low nanomolar range. And the binding capacity of aptamers to living cells was visualized using confocal fluorescence microscopy. Both the results indicate that temperature shift does not affect aptamer–cell interaction. To investigate the specific recognition of H5–1c for other cell lines(HL77O2,BEAS–2B etc), subjected several different cell lines to flow cytometry analysis. The result suggested aptamer H5–1c has excellent selectivity. Furthermore, the aptamer is more stable after chemical modification in the fetal bovine serum sample. In vivo fluorescence imaging study indicated the aptamer H5–1c possesses in vivo heart targeting ability. **Conclusion** This study shows the aptamer H5–1c has diagnostic and therapeutic potential to specifically deliver imaging or therapeutic agents to heart.

[Key words] H9c2; Cell–SELEX; Aptamer; Cell imaging; In vivo imaging

Exosomes derived from hypoxic cardiomyocytes alleviate cardiomyocyte oxidative stress injury by inducing alternatively activated macrophages

TANG Junnan ZHANG Zenglei XU Yanyan CAO Chang WANG Bo GUO Jiacheng QIN Zhen LU Yongzheng ZHANG Jianchao ZHANG Li WANG Wei ZHANG Jinying

The First Affiliated Hospital of Zhengzhou University, Zhengzhou 450000, China

[Abstract] Objective To evaluate the ability of hypoxic cardiomyocyte–derived exosomes (Hypo–Exo) to activate alternatively activated macrophages (M2 macrophages), and the effect of activated M2 macrophages on damaged cardiomyocytes. **Methods** The ability of cardiomyocytes–derived exosomes to modulate the naïve macrophage activation was evaluated. To further confirm the results, the exosomes obtained from human blood samples were used to induce macrophage polarization. In return, M2 macrophages whether alleviate oxidative stress injury of H9c2 cells was further studied. Quantitative real–time PCR, Western blotting, TUNEL assay, and immunohistochemistry were used to examine the mechanism in this study. **Results** This study results revealed that hypoxia facilitated the production of transforming growth factor–beta (TGF–β) in H9c2 cell–derived exosomes. Moreover, exosomes derived from normal cardiomyocytes (Nor–Exo) and Hypo–Exo induced RAW264.7 cells into classically activated macrophages (M1) and M2 macrophages, respectively. The effect of cardiomyocyte–derived exosomes on macrophage activation was abolished by Dynasore. Likewise, macrophage activation was induced by circulating exosomes isolated from human normal controls (hNor–Exo) or patients with acute myocardial infarction (hAMI–Exo). Activated M2 macrophages played a role in alleviating oxidative stress injury of H9c2 cells. **Conclusion** This study results demonstrated that the interaction between cardiomyocytes and macrophages is indispensable for maintaining heart homeostasis via inducing the polarization of macrophages through cardiomyocyte–derived exosomes, and the macrophage polarization serves to regulate cardiomyocytes apoptosis.

[Key words] Hypoxic cardiomyocytes; Macrophages; Cardiomyocyte

MicroRNA–21 mediates a positive feedback on angiotensin II–induced myofibroblast transformation

YOU Jiayin　LI Dongjiu　WANG Changqian

Shanghai Ninth People's Hospital, Shanghai 200030, China

[Abstract] **Objective** To explore the role of microRNA–21(miR–21) in post–myocardial infarction(MI) cardiac fibrosis. **Methods** MI was established in wild–type (WT) and miR–21 knockout (KO) mice. Primary mice cardiac fibroblasts (CFs) were isolated from WT and miR–21 KO mice and were treated with angiotensin II (Ang II) or Sprouty1 (Spry1) siRNA. Histological analysis and echocardiography were used to determine the extent of fibrosis and cardiac function. **Results** Compared with WT mice, miR–21 KO mice displayed smaller fibrotic areas and decreased expression of fibrotic markers and inflammatory cytokines. In parallel, Ang II–induced myofibroblasts transformation was partially inhibited upon miR–21 KO in primary CFs. Mechanistically, found that the expression of Spry1, a previously reported target of miR–21, was markedly increased in miR–21 KO mice post MI, further inhibiting ERK1/2 activation. In vitro studies showed that Ang II activated ERK1/2/TGF–β/Smad2/3 pathway. Phosphorylated Smad2/3 further enhanced the expression of α–SMA and FAP and may promote the maturation of miR–21, thereby downregulating Spry1. Additionally, these effects of miR–21 KO on fibrosis were reversed by siRNA mediated knockdown of Spry1. **Conclusion** This study findings suggest that miR–21 promotes post–MI fibrosis by targeting Spry1. Furthermore, it mediates a positive feedback on Ang II, thereby inducing the ERK/TGF–β/Smad pathway. Therefore, targeting the miR–21–Spry1 axis may be a promising therapeutic option for ameliorating post–MI cardiac fibrosis.

[Key words] Myocardial infarction; MicroRNA–21; Angiotensin II

Long–term recording of cardiac arrhythmias in non–infected population with cardiac implantable device during the COVID–19 pandemic: a cohort study

WANG Yaoji　JIN Qiqi　ZHENG Cheng　LIN Jiaxuan　LIN Yifan　XU Que　LI Jin　LIN Jiafeng

The Second Affiliated Hospital and Yuying Children's Hospital of Wenzhou Medical University, Wenzhou 325000, China

[Abstract] **Objective** To elucidated arrhythmias burden in cardiac implantable device non–infected population during coronavirus disease 2019 (COVID–19) pandemic. **Methods** In this 366–days observational cohort study, Described of sustained ventricular tachycardia(SVT), non–sustained ventricular tachycardia(NSVT), atrial fibrillation(AF) and atrial tachycardia (AT) burden during COVID–19 epidemic(high–risk period, low–risk period and whole epidemic period) by intracardiac electrocardiogram.Multivariate regressions were performed to evaluate association between the COVID–19 pandemic and arrhythmia , and each arrhythmia potential risk factors. **Results** There was a bigger proportion of patients with AF during the COVID–19 pandemic(38.36% vs. 26.03%, $P<0.05$). Although no evidence of increased per patient daily arrhythmia burden in COVID–19 period, but during high–risk period, the daily NSVT($P<0.05$), AT($P<0.05$), AF($P<0.05$) occurrences and NSVT($P<0.05$) duration were increased compared with pre–COVID–19 period. After constructed log–binomial regression models and GEE models, found the impact of COVID–19 pandemic

could promote the onset of AF(95%*CI*:1.324 −4.553, $P<0.05$) in non−infected population although arrhythmias are likely the consequence of systemic illness. Controlling heart rhythm by RFCA could reduce the AF incidence(21.43% vs 55.00% ,$P<0.05$) and daily occurrences (0.0000, 0.0027 vs. 0.0000, 241.7978, U=80.5, $P<0.05$) during COVID−19 pandemic. **Conclusion** During COVID−19 pandemic, some arrhythmia incidence and daily burden were increased. The impact of pandemic could promote the onset of AF in non−infected population although arrhythmias are likely the consequence of systemic illness, and controlling heart rhythm by RFCA may help reduce the incidence and daily AF occurrences during COVID−19 pandemic.

[Key words] Coronavirus disease 2019; Cardiac arrhythmias; Non−infected population

The red blood cell distribution width/albumin ratio: a promising predictor of mortality in intensive care unit heart failure patients: a cohort study

NI Qingwei WANG Xue CHEN Peng

The Second Affiliated Hospital and Yuying Children's Hospital of Wenzhou Medical University, Wenzhou 325000, China

[Abstract] **Objective** This article explains the association between the red blood cell distribution width/albumin ratio (RAR) and outcomes in intensive care unit (ICU)patients with heart failure. **Methods** Clinical data was extracted from the Multiparameter Intelligent Monitoring in Intensive Care III (MIMIC−III) database version 1.4. And a part of data was extracted from the second affiliated hospital and Yuying children's hospital of Wenzhou medical university. The primary outcome was 30−day mortality and the secondary outcomes were 90−day and one−year mortality. Cox proportional hazard models were used to reveal the associations between RAR and outcomes. Multivariate analyses were used to control for confounders. **Results** This study enrolled 2 841 ICU heart failure patients. For 30−day mortality, the hazard ratio (*HR*) for the second ($4.33<RAR<5.44$) and the third ($RAR>5.44$) tertiles were 1.89(1.41, 2.54) and 3.48(2.65,4.56), respectively, compared to the first tertile ($RAR<4.33$). As the RAR increases, the mortality rate gradually raises. In the model adjusted for multiple con−founders, the fifth quintile ($RAR\geqslant6.25$) showed a significant mortality risk (*HR*=1.44,95%*CI*: 1.07−1.94) compared to the fourth (RAR 5.20−6.24) (*HR*=1.80, 95%*CI*: 1.16−2.80). A similar trend was observed for 90− day and one−year mortality. For heart failure patients, the third ($RAR>5.44$) tertile found that high RAR significantly increased the risk of sepsis and requiring renal replacement therapy. In addition, the data, from our hospital heart failure patients in normal ward, suggested that there is a positive correlation between RAR and CRP. **Conclusion** The RAR was an independent predictor of 30−day, 90−day, and one−year mortality for ICU patients with heart failure. The RAR was a promising clinical biomarker as a convenience, readily available predictor of the mortality of heart failure patients.

[Key words] Intensive care unit;Heart failure; Mortality;Red blood cell distribution width/albumin ratio;Prognosis

Association between the neutrophil percentage–to–albumin ratio and outcomes in cardiac intensive care unit patients

WANG Xue　WANG Jie　WU Shujie　NI Qingwei　CHEN Peng

The Second Affiliated Hospital and Yuying Children's Hospital of Wenzhou Medical University, Wenzhou 325000, China

[Abstract] **Objective** The neutrophil percentage–to–albumin ratio (NPAR) is a systemic inflammation–based predictor associated with many diseases' outcomes. Nevertheless, there are few studies on the relationship between NPAR and inflammatory markers, and more importantly, the prognostic value of NPAR in critically ill patients with cardiovascular disease (CVD) remains unknown. **Methods** The data of this retrospective cohort study was from the Medical Information Mart data for Intensive Care III database (MIMIC–III) and the Second Affiliated Hospital of Wenzhou Medical University. Linear regression, logistic regression model, and Cox regression model were used to assess the associations between NPAR levels and length of stay, renal replacement therapy (RRT) use, and 30–day, 90–day and one–year mortality, respectively. The Pearson correlation coefficient was used to present the correlation between NPAR and C–reactive protein (CRP). **Results** This study included 1 599 patients in MIMIC–III and 143 patients in the Second Affiliated Hospital of Wenzhou Medical University. The elevated NPAR was independently associated with increased of 30–day, 90–day, and one–year all–cause mortality (*HR*=1.51, 1.61, 1.53, 95%*CI*:1.02–2.24,1.14–2.28,1.15–2.03, all $P<0.05$), it was also associated with increase the length of stay in hospital and ICU (β =2.76, 1.54,95%*CI*: 1.26– 4.27,0.62–2.47, all $P<0.01$). This study found that patients with higher NPAR were more likely to receive RRT (*OR*=2.50, 95%*CI*: 1.28–4.89, $P<0.05$). Moreover, this study confirmed that NPAR was statistically positively correlated with CRP (r=0.406, $P<0.01$). **Conclusion** Elevated NPAR on admission was independently associated with increased of all–cause mortality and length of stay among CICU patients. The results showed that CICU patients with higher NPAR were more likely to receive RRT. Besides, this study also provided the evidence that there was a positive correlation between NPAR and inflammatory indicators (ie. CRP).

[Key words] Neutrophil percentage–to–albumin ratio; Intensive care unit; Patients

A promising prognostic marker systemic inflammation response index (siri) in elderly heart failure patients: a retrospective cohort study

WANG Xue　NI Qingwei　CHEN Peng

The Second Affiliated Hospital and Yuying Children's Hospital of Wenzhou Medical University, Wenzhou 325000, China

[Abstract] **Objective** Heart failure (HF) is a clinical syndrome with significantly higher prevalence in the elderly or patients older than 60 years old. It is also the leading cause of mortality in the elderly. Within this study, we attempt to apply the systemic inflammation response index (SIRI) to express a correlation between prognosis of elderly HF patients, a novel biomarker based on the counts of peripheral venous blood neutrophil (N), monocyte (M), and lymphocyte (L) within the patient. This study hypothesize that this novel biomarker could be utilized as a better auxiliary predictive tool for risk of HF. **Methods** This retrospective cohort study was conducted using the Medical Information Mart data

for Intensive Care III database (MIMIC–III) and the Second Affiliated Hospital of Wenzhou Medical University. Linear regression, logistic regression, and cox proportional hazards regression models were used to assess the association between the SIRI levels and the length of stay in hospital and ICU, renal replacement therapy (RRT) use, HF–associated infection, and all–cause mortality, respectively. Moreover, the Pearson correlation coefficient was used to verify the correlation between SIRI and C–reactive protein (CRP). **Results** Within this study, the eligible elderly HF patients with included 3,964 patients from MIMIC–III and 261 patients from the Second Affiliated Hospital of Wenzhou Medical University. SIRI was an independent predictor of 30–day, 90–day, and one–year all–cause mortality in critically ill elderly patients with HF[tertile 3 versus tertile 1: adjusted *HR*, 95%*CI*: 1.42 (1.13, 1.78), 1.41 (1.18, 1.68),1.19 (1.03, 1.37), respectively]. The tendency ($P < 0.05$) of 90–day mortality was more significant than that for 30–day and one–year mortality (both $P < 0.05$). Elevated SIRI was associated with increased the length of stay in hospital and ICU after adjusting for multiple confounders[tertile 3 versus tertile 1: β, 95%*CI*: 0.85 (0.16, 1.54), 0.62 (0.18, 1.06), both $P < 0.05$, respectively] . Furthermore, this study found that patients with higher SIRI levels were more likely to receive renal replacement therapy (RRT) and more susceptible to infect and develop to sepsis [tertile 3 versus tertile 1: *OR*, 95%*CI*: 1.55 (1.06, 2.28), 2.11 (1.66, 2.68), both $P < 0.05$, respectively]. On the other hand, this study confirmed that SIRI was statistically positively correlated with CRP ($r = 0.343$, $P < 0.01$). **Conclusion** Our results suggest SIRI may be an easily accessible, reproducible, and low–cost biomarker for predicting all–cause mortality in elderly patients who have suffered from a HF. In addition, elevated SIRI was significantly related to an increased risk of the length of stay in hospital and ICU and HF–associated infection, and the patients with higher SIRI were more likely to receive RRT. Moreover, this study also verified that there was a statistically significant positive correlation between SIRI and inflammatory marker (ie. CRP). To validate our conclusions, more prospective cohort studies are required.

[Key words] Heart failure; Systemic inflammation response index; Elderly

PD–1/PD–L1 inhibitor–induced immune–related myocarditis

WENG Yingbei JI Kangting

The Second Affiliated Hospital and Yuying Children's Hospital of Wenzhou Medical University, Wenzhou 325000, China

[Abstract] In recent years, tumor immunotherapy has achieved a series of breakthroughs, and immune checkpoint inhibitors (ICI) have achieved significant results in the treatment of advanced malignancy. Among them, PD–1/PD–L1 inhibitor treatment is more effective in the treatment of various malignant tumors such as melanoma and lung cancer. But at the same time, suppressing important regulatory sites of the body's immune system will trigger a series of inflammatory responses in many normal organs and tissues. Immune–related myocarditis is more common in the cardiovascular system toxicity caused by PD–1/PD–L1 inhibitors. This article is a review of the epidemiology, pathological manifestations, clinical manifestations, auxiliary examinations, diagnosis, treatment and prognosis of immune–related myocarditis caused by PD–1/PD–L1 inhibitors.

[Key words] PD–1/PD–L1 inhibitors; Myocarditis;Immune–related

Effect of chronic kidney disease on prognosis in patients with ischemic heart failure

WU Zejia　LI Liwen

Dongguan People's Hospital, Dongguan 523000, China

[Abstract] **Objective** To investigate the effect of chronic kidney disease (CKD) on the prognosis in patients with ischemic heart failure (IHF). **Methods** This is a prospective cohort study and participants with IHF were consecutively enrolled from the Department of Cardiology, Guangdong Provincial People's Hospital from December of 2015 to June of 2019. Participants were followed through October 15th, 2020 using phone call interview. Participants were followed until the occurrence of clinical endpoint, which was defined as all-cause mortality. Length of follow-up was calculated using the date of the last follow-up or the date of death minus the date of discharge from index hospitalization. **Results** 1 568 patients with IHF were included from December 2015 to June 2019. Patients were divided into the CKD (n = 434) and non-CKD (n = 1134) groups based on the estimated glomerular filtration rate of 60 mL/(min • 1.73 m^2). The incidence rate of all-cause mortality in CKD and non-CKD patients was 13.7 per 100 person-years and 6.1 per 100 person-years, respectively, with an incidence rate ratio of 2.44 (95%*CI*: 1.89-3.15,P < 0.01). After a median follow-up of 2.1 years, the cumulative incidence rate of all-cause mortality in CKD and non-CKD patients was 40.7% and 19.4% (P > 0.05). Adjusted for multiple covariates, CKD were still associated with all-cause mortality (*HR*=1.35, 95%*CI*:1.03-1.76, P < 0.05). in patients with IHF, all-cause mortality was consistently increased with CKD as compared with non-CKD in 8 subgroups. With the decrease of eGFR, the risk of all-cause mortality in patients with IHF gradually increased. **Conclusion** CKD is an important risk factor for poor prognosis in patients with IHF. Management of CKD is essential to reduce all-cause mortality in IHF patients.

[Key words] Chronic kidney disease; Ischemic heart failure; Prognosis

Sex differences in pancoronary plaque characteristics in stemi patients: a 3-vessel OCT study

ZHAO Linlin　GUO Xiaogang　YU Bo

The First Hospital of Zhejiang Province, Hangzhou 310000, China

[Abstract] **Objective** To investigate: (1) nonculprit plaque characteristics in patients with ST-segment elevation myocardial infarction (STEMI) in males versus females, focusing on pancoronary vulnerability. (2) clinical and morphological predictors of pancoronary vulnerability in males versus females. **Methods** Between July 2016 and June 2018, 583 patients (134 females) treated by 3-vessel optical coherence tomography (OCT) at the time of primary percutaneous intervention were included with 103 patients excluded from final analysis. In patients with multiple lesions by OCT imaging, especially within the culprit vessel, the lesion with the most severe stenosis or with evidence of recent plaque disruption, including significant thrombus, was determined as the culprit lesion. Patients with in-stent restenosis (n=16), imaging of the culprit vessel after pre-dilation (n=4), poor image quality (n=29), or incomplete imaging (n=54) were excluded. Plaque features of both culprit and nonculprit lesions (in both culprit and nonculprit arteries) were compared according to sex. **Results** A total of 583 culprit lesions and 1 419 nonculprit plaques were analyzed. Both patient-based (16.7% vs. 7.5%, P < 0.05) and plaque-based (8.1% vs. 3.2%, P < 0.05) analyses showed that nonculprit plaque rupture (NC-PR)

was more prevalent in males versus females. The total length of analyzed OCT pullbacks was (203.3 ± 32.7) mm: (82.5 ± 21.1) mm in the RCA, (68.5 ± 18.5) mm in the LAD, and (47.9 ± 13.5) mm in the LCX. There was no difference in the length of the analyzed segments between males versus females[(206.3 ± 32.4) mm vs.(194.5 ± 32.7) mm, $P < 0.05$]. Patient–level multivariate analysis showed that male sex and culprit PR were independently predictors of NC–PR (*OR*=2.39, 95%*CI*: 1.18–4.81, $P < 0.05$, *OR*=1.96, 95%*CI*: 1.16–3.30, $P < 0.05$). Culprit PR and age were independently associated with pancoronary vulnerability no matter in males or females, yet HDL–C and TC/HDL–C ratio were independently associated with pancoronary vulnerability in males. Nonculprit plaques in males had a higher prevalence of NC–PR, larger minimal lumen area (MLA) and a wider maximum lipid arc, yet lower prevalence of MLA < 3.5 mm^2 than those in females. Other nonculprit plaque characteristics were not different between the two groups. In males, nonculprits located in untreated arteries contained more lipid, a thinner fibrous cap, and more microchannels and calcifications than nonculprits located in the treated artery. However, in females, nonculprits located in untreated arteries contained less lipid rich plaque (LRP) and fewer thin–cap fibroatheromas (TCFAs) compared with nonculprits located in the treated artery. **Conclusion** In patients with STEMI, compared to females, males had a higher rate of pancoronary vulnerability, and sex–specific role of risk factors in pancoronary vulnerability should be considered. These findings suggest that sex, as a traditional readily available clinical risk factor, cannot be ignored in predicting the pancoronary vulnerability, and it will be more effective to adjust strategies of lipid–lowering therapy according to sex.

[Key words] Sex; Plaque vulnerability; Optical coherence tomography; ST–segment elevation myocardial infarction

The molecular mechanism of UT–B knockout enhances cardiac hypertrophy

LYU Xuejiao DU Yanwei TAN Wenxi DAI Yinchong FU Shuang YU Lanying
LIU Tiantian WANG Xue ZHANG Wenfeng MENG Yan
Jilin University, Changchun 130117, China

[Abstract] Objective To investigate the role and mechanism of action of UT–B in cardiac hypertrophy induced by pressure overload. **Methods** A cardiac hypertrophy model was established by abdominal aorta banding. Echocardiography, histology, hematoxylin and eosin staining, and western blotting were conducted to evaluate cardiac function, morphology, nitric oxide (NO) synthesis, and oxidative stress. Proteasome activities were also examined using a fluorescent peptide substrate. **Results** Systolic functional parameters (EF, FS) and diastolic functional parameters (E/A) did not change significantly in UT–B knockout mice compared with those in wild–type mice, but they were decreased significantly after abdominal aorta banding in UT–B knockout mice. Moreover, UT–B knockout mice showed increased heart volume and atrial natriuretic peptide (ANP) expression after abdominal aortic banding. Moreover, reactive oxygen species (ROS) and malondialdehyde levels were upregulated in UT–B knockout mice and were further increased after abdominal aorta banding, whereas the antioxidant enzyme activity was downregulated. In addition, nitric oxide (NO) levels and endothelial nitric oxide synthase (eNOS) expression were downregulated in UT–B knockout mice and were further decreased after abdominal aorta banding. **Conclusion** UT–B knockout enhances cardiac hypertrophy induced by abdominal aorta banding via upregulation of ROS levels and downregulation of NO levels in the heart tissue, suggesting that UT–B plays an important role in the maintenance of cardiac function.

[Key words] Urea transporter–B;Cardiac hypertrophy;Nitric oxide; Reactive oxygen species

Enhanced platelet inhibition with alleviated gastric injury by adding panax quinquefolius saponin to dual antiplatelet therapy via regulating eicosanoids metabolism: a lipidomic research

WANG Wenting YANG Lin SONG Lei LI Changkun YANG Bin WANG Mingming KOU Na MA Yan XUE Mei SHI Dazhuo

National Clinical Research Center for Chinese Medicine Cardiology; Cardiovascular Center, Xiyuan Hospital, China Academy of Chinese Medical Sciences, Beijing 100091, China

[Abstract] **Objective** To investigate the integrated efficacy of PQS+DAPT on platelet aggregation, myocardial infarction (MI) expansion and gastric injury in a rat model of acute MI (AMI) and to explore the mechanism regarding eicosanoids metabolic regulation using an AA–targeted lipidomic approach. **Methods** Male Wistar rats were subjected to permanent left coronary artery occlusion to induce AMI. Sham rats underwent the same surgery except for ligation. Rats were randomized and treated with saline (for sham and AMI group), PQS, DAPT or PQS+DAPT for 4 weeks (n=12 per group). At day 29 after surgery, platelet aggregation induced by adenosine diphosphate (ADP) was measured by light transmission aggregometry. MI expansion, myocardial pathology was evaluated by triphenyltetrazolium chloride staining and hematoxylin–eosin staining, respectively. Severity of gastric mucosal injury was examined by scanning electron microscope (SEM). A comprehensive characterization of eicosanoids profile in rat serum and gastric mucosa was performed with liquid chromatography–mass spectrometer–based lipidomic analysis. **Results** Maximum platelet aggregation rate induced by ADP ($MPAR_{ADP}$) increased markedly post MI compared with sham rats, indicating enhanced platelet reactivity. Rat treated with PQS alone and in combination with DAPT showed significantly decreased $MPAR_{ADP}$ compared with those in AMI group. Furthermore, PQS +DAPT further decreased $MPAR_{ADP}$ compared with DAPT, suggesting a reinforced anti–aggregatory effect of the combined therapy. Since platelet hyperreactivity is associated with atherothrombosis, infarct size and myocardial pathology were also evaluated. Accordingly, PQS monotherapy and PQS+DAPT suppressed MI expansion post MI, with a significantly reduced infarct size in response to PQS+DAPT compared with DAPT. Additionally, pathological analysis revealed attenuation of myocardial injury by adding PQS to DAPT, characterized by mitigated inflammatory infiltration, myocardial necrosis, and fibrosis. Eicosanoids metabolism is highly sensitive to pathophysiological alterations such as drug intervention. As locally functioning molecules, they can also be secreted by tissues and stable metabolites may accumulate in circulation. AA– targeted lipidomic analysis revealed markedly enhanced serum level of 6–keto–prostaglandin (PG)F1a and 6,15–diketo–13,14–dihydro–PGF1a, downstream metabolites of PGI_2, and markedly decreased serum level of TAB_2, a stable metabolite of TXA_2, in PQS+DAPT group compared with DAPT group. TXA_2, released mainly by platelets upon activation, acts as a potent agonist for platelet aggregation and is known to involve in the initiation and progression of atherothrombosis. PGI_2 in circulation is largely produced by vascular endothelial cells, which down–regulates the reactivity of platelets nearby via counteracting platelet–derived TXA_2. Interestingly, several epoxyeicosatrienoic acids (EETs) (5,6–EET, 8,9–EET, 11,12–EET, 14–15–EET) and downstream dihydroxyeicosatrienoic acids (DHETs) (8,9–DHET, 11–12DHET) were strikingly increased by adding PQS to DAPT. EETs, potent vasodilators produced by endothelial cells, also has been shown to hyperpolarize platelets and inactivate them by inhibiting platelet adhesion to endothelial cells. These observations may account for the anti–adhesion effect of PQS+DAPT in our previous study. Collectively, adding PQS to DAPT achieved reinforced platelet inhibition and suppressed MI expansion by maintaining antithrombotic miliue via promoting AA/PGI_2 and AA/EET synthesis while suppressing AA/TXA_2 metabolism. DAPT induced a vast ablation of the gastric epithelium, leading to the exposure of denuded lamina propria. By contrast, gastric mucosa in PQS+DAPT–treated rats showed a few apical erosions while the severity of surface desquamation was diminished, indicating alleviation of gastric injury by adding PQS

to DAPT. DAPT–induced GI injury is associated with suppressed generation of mucosal prostaglandins (PGs), which are among the potent mediators in gastric mucosal defense. Intriguingly, lipidomic analysis revealed markedly enhanced gastric level of PGE_2, PGD_2 and PG downstream metabolites (11b–PGF2a, 13,14–dihydro–15–keto–PGE_2, 6–keto–PGF1a). Therefore, gastroprotective effect of PQS on DAPT–induced gastric injury is associated with up–regulation of gastric AA/PG production, which partly counteracts the pharmacological action of DAPT. **Conclusion** Combining PQS with DAPT achieved greater platelet inhibition and diminished MI expansion by preserving an antithrombogenic condition attributed to up–regulated AA/PGI_2, AA/EET and down–regulated AA/TXA_2 metabolism. PQS mitigated DAPT–induced gastric mucosa injury via promoting local PG production. PQS may provide increased benefits as a complementary agent to DAPT.

[Key words] Acute myocardial infarction; Platelet aggregation; Gastric injury

A new risk factor associated with cardiovascular disease: clonal hematopoiesis of indeterminate potential

YU Xiongkai QIAN Ningjing WANG Yaping

The Fourth Affiliated Hospital Zhejiang University School of Medicine,Yiwu 322000, China

[Abstract] Clonal haematopoiesis is a prevalent disease associated with all–cause death. Not only because it can be a precancerous lesion of blood system diseases, but also because it has a strong association with cardiovascular disease. Recent studies have shown that clonal hematopoiesis of indeterminate potential (CHIP), as defined by clonal haematopoiesis in absence of hematologic malignancies, is associated with adverse heart failure progression in patients with ischemic and non–ischemic heart diseases,particularly in patients with ten–eleven translocation 2 (TET2) mutations or DNA methyltransferase 3 alpha (DNMT3A) mutations. With advances in sequencing technology, preliminary data has shown a good association between the size of these mutations and the risk of death below the 2% variant allele frequency (VAF) threshold for defining CHIP. CHIP may already exist as an independent new risk factor for cardiovascular disease, and the intervention of CHIP will be an important topic. And more research needs to be done in the association of new VAF thresholds and other types of mutations with cardiovascular disease. This review summarizes the latest research on CHIP, discusses in detail the important association between clonal hematopoiesis and accelerated cardiovascular disease, and rationalizes the intervention of CHIP in combination with existing evidence, which may be beneficial for future treatment.

[Key words] Clonal hematopoiesis;CHIP;Cardiovascular disease;TET2;DNMT3A–AK2;Risk factor

Research progress of machine learning and deep learning in intelligent diagnosis of the coronary atherosclerotic heart disease

LU Haoxuan HE Wenming YAO Yudong XIE Yanqing WANG Li TU Shuangshuang

The Affiliated Hospital of Medical School, Ningbo University, Ningbo 315020, China

[Abstract] The coronary atherosclerotic heart disease is a common cardiovascular disease with high morbidity, disability and societal burden. Early, precise and comprehensive diagnosis of the coronary atherosclerotic heart disease

is of great significance. The rise of artificial intelligence technologies, represented by machine learning and deep learning, provides new methods to address the above issues. In recent years, artificial intelligence has achieved an extraordinary progress in multiple aspects of coronary atherosclerotic heart disease diagnosis. Including the construction of intelligent diagnostic models based on artificial intelligence algorithms, applications of artificial intelligence algorithms in coronary angiography, coronary CT angiography, intravascular imaging, cardiac magnetic resonance, and functional parameters. This paper presents a comprehensive review of the technical background and current state of research on the application of artificial intelligence in the diagnosis of the coronary atherosclerotic heart disease and analyzes recent challenges and perspectives in this field.

[Key words] Artificial intelligence; Coronary atherosclerotic heart disease; Diagnosis

A randomized non–inferiority study of low–dose and standard–dose ticagrelor after intervention for acute coronary syndrome: study protocol for the tiger study

PANG Yanan MA Minglu WANG Dong WANG Hongyi HU Wei WANG Zhibing CHEN Yan WU Sicheng GE Junbo HOU Lei

Tongren Hospital Affiliated to Medical College of Shanghai Jiaotong University, Shanghai 200050, China

[Abstract] Current guidelines recommend that patients with acute coronary syndrome (ACS) who have successfully undergone percutaneous coronary intervention (PCI) should continue to use dual antiplatelet therapy (DAPT) for 12 months. The long–term use of standard–dose dual antiplatelet therapy will increase the risk of bleeding. An optimized antiplatelet strategy that can prevent ischemic events and reduce the risk of bleeding remains to be explored. The study is a prospective, multicenter, randomized, open–label, controlled study involving 2 120 patients from six clinical centers in China. Through the Interactive Web Response System (IWRS), ACS patients undergoing successful PCI will be randomly divided into the low–dose ticagrelor group or the normal–dose ticagrelor group, after taking 100 mg aspirin and 90 mg ticagrelor bid for 1 week. The primary endpoint is a composite of cardiovascular death, non–fatal myocardial infarction, stent thrombosis, repeat revascularization, stroke, and bleeding events of grade 2 or higher according to Bleeding Academic Research Consortium (BARC) criteria at one year. The secondary endpoints are bleeding events of grade 2 or higher according to BARC criteria at one year. Recent studies have confirmed that 90 mg ticagrelor alone can safely and effectively reduce bleeding without increasing ischemic events of patients with ACS after PCI. Compared with standard–dose DAPT, whether low–dose ticagrelor combined with aspirin can ensure the anti–ischemic effect while reducing the bleeding risk remains unclear in Chinese patients. The Tiger study will be the first large–scale, multicenter study to compare the efficacy and safety of low–dose and standard–dose ticagrelor combined with aspirin in ACS patients one week after successful PCI.

[Key words] Acute coronary syndrome; Percutaneous coronary intervention; Dual antiplatelet therapy

Study on the influence of self–management–oriented Pender's HPM nursing on quality of life and prognosis after PCI

LIU Wenqin

The Second Affiliated Hospital and Yuying Children's Hospital of Wenzhou Medical University, Wenzhou 325000, China

[Abstract] Introduction:In our country, the cardiovascular disease patients is about 300 million or so, each year about 3.5 million people die of cardiovascular disease, accounting for 41% of the total cause of death, among the top of the all diseases coronary atherosclerosis sex heart disease (CHD) is China's major cardiovascular disease in the population, its incidence is sharply rising trend in recent years, therefore, for coronary heart disease in people at high risk for early intervention in order to reduce the incidence of coronary heart disease has become a top priority.The key to the secondary prevention of CHD is to adopt appropriate secondary prevention mode, use measurable quality assessment criteria, strengthen treatment of sexual lifestyle changes, and improve the health level of the population by improving the quality of medical services.In recent years, the management of the self as a secondary prevention model, at home and abroad, its application in the prevention and control of chronic diseases and validation, proved its in correcting the bad behavior, the ability of disease management, improving treatment compliance, improve survival quality, and improve the marked effects of cost–benefit ratio and so on, is a kind of mode is worthy of reference for secondary prevention of coronary heart disease. Research question:Whether additional self–management can improve the quality of life of patients with coronary heart disease after PCI on the basis of following medical advice? Whether additional self–management can improve the prognosis of patients with coronary heart disease after PCI on the basis of following medical advice? Design:The control group received routine nursing care.That is to say, nurses give patients routine, coronary heart disease related knowledge education and nursing guidance, inform the management of complications,Emotional regulation, instruct patients to eat and drink reasonably and transport appropriately Exercise, regular rest and rest, and regular review, at the same time after the patient discharged from the hospital, regular follow–up, each Telephone follow–up once weekly and outpatient follow–up once a month were conducted to understand the patients. Situation and provide timely corrective action and guidance. On the basis of the control group, the observation group adopted the self–management–oriented PANDA health promotion nursing, and the corresponding nursing services were carried out according to the self–management–oriented health promotion nursing mode and process. Self–management behavior assessment: The scale has 27 items in seven dimensions, including three main dimensions, namely, daily life management, disease medical management, emotion management. Each item is scored by a five–point scale, the higher the score is, the better the patient's management behavior is.Numerous literature reviews, most of which use interviews, questionnaires and quasi–experimental research methods. Qualitative research methods are applied in a wide range. Participants:Convenience sampling was used to recruit the participants. Interventions:Nurse–led individualized self–management program (NISMP). The NISMP was developed on the basis on the UK Medical,In short,NISMP is a well–structured 12–month program that consists of six group education sessions of face–to–face individual counseling and 12 months of telephone follow–up.In patients undergoing PCI, including with AMI and PCI special healthy life and how to manage diet medication, symptoms, and stress, each groupbased interactive education meeting, including a brief introduction of the theme, group discussion, and transmit the personal experience of the patient actively communicate with the nurse, communication with peers to provide patients with paper heart patients education textbooks, strengthen diet daily exercise stress management, etc. The key learning points.

[Key words] PCI; Coronary atherosclerosis heart disease; Quality of life

Initial experience: effectiveness and safety of left atrial appendage closure in patients with hypertrophic cardiomyopathy with atrial fibrillation

LIN Yuannan XU Jing PAN Yang ZHENG Cheng XUE Yangjing LI Jin LIN Jiafeng LI Yuechun

The Second Affiliated Hospital and Yuying Children's Hospital of Wenzhou Medical University, Wenzhou 325000, China

[Abstract] **Objective** To investigate the effectiveness and safety of LAA occlusion in patients with HCM with AF in our center. **Methods and Results** Enrolled 16 consecutive patients with HCM with AF (seven men, median age 62.5 years, median CHA_2DS_2–VASc score 4.0, median HAS–BLED score 3.0) who underwent left atrial appendage closure (LAAC). The peri–procedure and post–procedure clinical outcomes were assessed. LAA occlusion was performed using three occluder devices (Watchman, in 11 patients. LAmbre, in 4 patients. ACP, in 1 patient). Successful device implantation was achieved in all patients without complications. After a median 12.5 months of follow–up (range: 6 to 24 months), all patients met the criteria for successful sealing and discontinued oral anticoagulant (OAC). One patient who developed pericardial effusion required percutaneous drainage unrelated to the device and/or procedure, and there were no cases of major bleeding or device–related thrombosis. During follow–up, no strokes were detected, resulting in an annualized stroke risk of 0% compared to an expected stroke rate of approximately 7% based on adjusted CHA_2DS_2–VASc in OAC–naïve patients. **Conclusion** LAAC appears to be effective and safe in patients with HCM with non–valvular AF associated with a high risk of stroke.

[Key words] Hypertrophic cardiomyopathy; Atrial fibrillation; Stroke prevention; Left atrial appendage; Left atrial appendage closure

Combined atrial fibrillation ablation and left atrial appendage closure: Watchman versus LAmbre devices

KE Jinyan

The Second Affiliated Hospital and Yuying Children's Hospital of Wenzhou Medical University, Wenzhou 325000, China

[Abstract] **Objective** Left atrial appendage (LAA) closure procedure (LAAC) combined with catheter ablation (CA) procedure is safe and feasible for non–valvular atrial fibrillation (NVAF). This study aimed to compare the efficacy and safety of Watchman versus LAmbre for NVAF patients who underwent a combined procedure. **Methods** 169 patients diagnosed AF, CHA_2DS_2–VASc scores $\geqslant 2$ and underwent combined procedure with Watchman (n=118) or LAmbre (n=51) device were enrolled in this study. Transthoracic echocardiography and transesophageal echocardiography were used to assess device stability, LAA sealing, and to rule out pericardial effusion and device surface thrombosis. AF recurrence was assessed by electrocardiogram or 24 hours dynamic electrocardiogram. The adverse events during periprocedural and post–procedural of the two groups were documented. **Results** The mean age, CHA_2DS_2–VASc score and HAS–BLED score of the Watchman and LAmbre were (67.4 ± 8.8) vs. (67.6 ± 8.1) years, (3.7 ± 1.5) vs. (3.7 ± 1.4), (2.5 ± 1.1) vs. (2.6 ± 1.0), respectively (all $P > 0.05$). The successful LAAC was achieved 100% in both groups.

Six (5.1%) and five (9.8%) patients were observed intraprocedural residual shunt (all < 3 mm) in Watchman and LAmbre group($P > 0.05$). At a mean follow-up (12.2 ± 6.5) vs. (11.6 ± 7.6) months, 35 and 13 patients were observed recurrence of AF in Watchman and LAmbre (29.7% vs. 25.5%, $P > 0.05$). One patient in each group observed peri-device leak ⩾ 3 mm (0.9% vs. 2.0%, $P > 0.05$). Except for 1 device-related thrombus and 1 transient ischemic attack in the Watchman group, no other major adverse events occurred in follow-up. **Conclusion** Watchman and Lambre were equal efficacy and safety in the combined procedure.

[Key words] Atrial fibrillation ablation; Left atrial appendage closure; Catheter ablation

Initial experience with rivaroxaban given twice daily after left atrial appendage closure with the Watchman device in patients with atrial fibrillation

JIN Lushen KE Jinyan LIN Yuannan XU Jing LIU Weike LI Yuechun

The Second Affiliated Hospital and Yuying Children's Hospital of Wenzhou Medical University, Wenzhou 325000, China

[Abstract] Objective Oral rivaroxaban is an emerging anticoagulant for post-implantation period after Watchman implantation. As per dosing regimen of rivaroxaban causes fluctuations in plasma concentration, we studied the feasibility and safety of giving rivaroxaban twice daily for patients with atrial fibrillation (AF) who underwent left atrial appendage closure (LAAC) with Watchman. **Methods** Enrolled consecutive patients with AF who underwent concomitant catheter ablation (CA) and LAAC or LAAC alone with Watchman device followed by twice-daily rivaroxaban. The peri-procedure and post-procedure clinical outcomes were assessed. **Results** 132 Patients received different doses of rivaroxaban, 96 in 10 mg twice-daily (standard-dose) group, 26 in 10 mg every morning and 5 mg every night (moderate-dose) group, and 10 in 5 mg twice-daily (low-dose) group. During a follow-up of (513 ± 186) days, no patient died and no stroke or thromboembolic event was observed. The rate of major bleeding was 0.8% (1/132), while minor bleeding occurred in 14 patients [4.2% (4/96) in standard-dose group, 23.1% (6/26) in moderate-dose group, 40.0% (4/10) in low-dose group]. The difference in the rate of bleeding events among three groups was significant ($P < 0.01$). The occurrence of device-related thrombus (DRT) was 1.5% (2/132), consistent with previous studies of novel oral anticoagulants after LAAC. **Conclusion** Twice-daily rivaroxaban is a feasible alternative regimen to prevent major bleeding events for patients after concomitant CA and LAAC or LAAC alone with the Watchman device, without increasing the risk of DRT.

[Key words] Rivaroxaban; Left atrial appendage occlusion; Atrial fibrillation; Catheter ablation

The potential role of RAAS-related hsa_circ_0122153 and hsa_circ_0025088 in essential hypertension

HE Wenming XIE Yanqing ZHANG Lina

The Affiliated Hospital of Medical School, Ningbo University, Ningbo 315020, China

[Abstract] Objective The dysregulation of renin-angiotensin-aldosterone system (RAAS) is closely related to the development of essential hypertension (EH). MicroRNAs (miRNAs) are an important regulator of RAAS. The sponge

effect of circular RNAs (circRNAs) on miRNAs makes the circRNA–miRNA–mRNA axis in EH possible, however, there is currently a lack of relevant evidence. **Methods** A circRNA–miRNA network was constructed based on the previous circRNAs microarray results. The expression of RAAS–related miRNAs and circRNAs were verified by qRT–PCR. Peripheral blood samples of 106 EH patients and 106 healthy volunteers were included in this study. GO and KEGG enrichment were performed to predict the role of candidate circRNAs in EH. **Results** In EH patients, RAAS–related hsa–miR–483–3p and hsa–miR–27a–3p were down–regulated, and hsa_circ_0122153 and hsa_circ_0025088 were up–regulated. The relative expression of RAAS–related circRNAs and target miRNAs showed a negative correlation (hsa_circ_0122153–hsa–miR–483–3p and hsa_circ_0025088–hsa–miR–27a–3p). Hsa_circ_0122153 or hsa_circ_0025088 combined with corresponding miRNAs and environmental factors may support the early diagnosis of EH. Hsa_circ_0122153 and hsa_circ_0025088 may participate in the regulation of aldosterone and the secretion of renin through the circRNA–miRNA–mRNA network, respectively. **Conclusion** Highly expressed hsa_circ_0122153 and hsa_circ_0025088 increase the risk of EH. The hsa_circ_0122153/hsa–miR–483–3p and hsa_circ_0025088/hsa–miR–27a–3p axis involving RAAS were potential EH pathways.

[Key words] Renin–angiotensin–aldosterone system; Essential hypertension; CircRNAs

Cardiac adipose tissue contributes to cardiac repair: a review

LIN Yan

Cardiovascular Key Laboratory of Zhejiang Province, The Second Affiliated Hospital, Zhejiang University School of Medicine, 88 Jiefang Road, Hangzhou 310009, China

[Abstract] Cardiac adipose tissue is a metabolically active adipose tissue in close proximity to heart. Recent studies emphasized the benefits of cardiac adipose tissue in heart remodeling, such as reducing infarction size, enhancing neovascularization and regulating immune response, through a series of cellular mechanisms. In the present manuscript, we provide a comprehensive review regarding the role of cardiac adipose tissue in cardiac repair. This review focus on different cardiac adipose tissues according to their distinguished anatomical structures. This review summarizes the latest evidence on the relationship between cardiac adipose tissue and cardiac repair.

[Key words] Cardiac adipose tissue; Heart; Cardiac repair

Circular RNA Fbxl5 regulates cardiomyocyte apoptosis during ischemia reperfusion injury via sponging microRNA–146a

YOU Jiayin LI Dongjiu MAO Chengyu WANG Changqian

Shanghai Ninth People's Hospital Affiliated to Shanghai JiaoTong University School of Medicine, Shanghai 200030, China

[Abstract] **Background** Cardiomyocyte apoptosis critically contribute to ischemia reperfusion injury (IRI), which lacks effective therapeutic options. Circular RNAs (circRNAs) serve as novel diagnostic and therapeutic targets in various cardiovascular diseases. CircRNA Fbxl5 is one of the abundantly expressed circRNAs in the heart and its role in myocardial IRI remains unknown. **Methods and Results** Wild type (WT) mice and neonatal mice ventricular myocytes (NMVMs) were used and subjected to myocardial IRI and anoxia reoxygenation (AR), respectively. The study found

that circRNA Fbxl5 was significantly upregulated in the ischemic myocardium as well as in NMVMs subjected to AR. Knockdown of circRNA Fbxl5 ameliorated cardiomyocyte apoptosis, thereby decreasing infarct size and preserving cardiac function. Additionally, in vitro knockdown of circRNA Fbxl5 in NMVMs subjecting to AR recapitulated the in vivo findings. Mechanistically, identified that circRNA Fbxl5 directly sponged and suppressed the endogenous microRNA–146a (miR–146a), thereby weakening its inhibitory effect on MED1, which could further promoted the apoptotic death of cardiomyocytes. **Conclusion** Our findings revealed a critical role for circRNA Fbxl5 in regulating cardiomyocyte apoptosis during IRI. The underlying miR–146a–MED1 signaling serves as an important cascade in regulating the apoptotic death of cardiomyocytes.

[Key words] Cardiomyocyte apoptosis;CircRNAs; Effective therapeutic options

Adipose–derived stem cells differentiate into smooth muscle cells via Clec11a^{+} subpopulation

XIE Yao JI Yongli LU Yunrui MA Yuankun NI Hui SHEN Jian MA Hong
JIN Chunna CHEN Yuwen LIN Yan XIANG Meixiang
The Second Affiliated Hospital, Zhejiang University School of Medicine, Hangzhou 310003, China

[Abstract] Adipose derived stem cells (ADSCs) can differentiate into vascular lineages and participate in vascular remodeling. Perivascular ADSCs (PV–ADSCs) draw attention due to their unique location. The heterogeneity of subcutaneous (SUB–) and abdominal ADSCs were well addressed, but PV–ADSCs' heterogeneity hasn't been investigated. In the present study, applied single–cell analysis to compare SUB–ADSCs and PV–ADSCs respectively regarding their subpopulations, functions, and cell fates. The present study uncovered 4 subpopulations of PV–ADSCs including Dpp4^{+}, Col4a^{2+}/Icam1^{+}, Clec11a^{+}/Cpe^{+} and Sult1e1^{+} cells, among which Clec11a^{+} subpopulation closely participated in and regulated the PV–ADSCs differentiation towards smooth muscle cells (SMCs). The present study revealed the relationship between PV–ADSCs and SMCs.

[Key words] Adipose derived stem cells; Vascular lineages; Participate

Piezo1–mediated mechanotransduction promotes cardiac hypertrophy by impairing calcium homeostasis to activate calpain/calcineurin signaling

ZHANG Yuhao
The Second Affiliated Hospital, Zhejiang University School of Medicine, Hangzhou 310003, China

[Abstract] Mechanotransduction has been lately recognized as a major regulator of organ homeostasis under a myriad of pathological conditions. However, the identification and molecular features of mechanotransducer on cardiomyocytes are largely sparse. This study, identified Piezo1 as a novel mechanosensor mediating pressure–overload induced hypertrophy. This study observed Piezo1 was upregulated during pathological hypertrophy, which mostly located in T–tubule and intercalated disc area, and was responsible for the elevation of [Ca^{2+}]i with hypertrophic stumili. Piezo1 knockout attenuated pressure–overload induced cardiac hypertrophy and adverse remodeling. And also demonstrated that Piezo1 was responsible for Yoda1– and stretch–induced cardiomyocyte hypertrophy in vitro, which was due to

the enhancing activity of calcineurin and calpain. This study result may decipher the role of Piezo1 under pathological condition, implying a promising therapeutic target for cardiac dysfunction.

[Key words] Mechanotransduction; Piezo1; Cardiac dysfunction

MMP9 negatively controls sepsis–induced heart failure by regulating the function of dendritic cells

DENG Jiewen

The Second Affiliated Hospital, Zhejiang University School of Medicine, Hangzhou 310003, China

[Abstract] Myocardial dysfunction caused by sepsis is usually considered to be the result of the interaction of complex factors such as genetic, metabolic, molecular and structural changes. Here we found that the inhibitor of MMP9 suppresses anti–infection immunity in mice. This study showed that MMP9–deficient mice had a significantly higher survival rate than wild–type control mice in response to Intraperitoneal injection of lipopolysaccharide (LPS). Notably, MMP9 inhibitors exerted the potent anti–infective therapeutic effects in mouse. Compared to the control group, the survival time of C57 mice injected intraperitoneally with MMP9 inhibitor prolonged, and the secretion of the inflammatory factors IL–6, TNF–α and IL–17a in the serum reduced after 8 hours infection. Cardiac ultrasound showed that the reduction of cardiac ejection fraction was smaller than that in the control group, and the infiltration of CD45 positive immune cells in the heart alleviated, including dendritic cells, gama delta T cells and neutrophils. These results were basically consistent with the experimental results of MMP9 knockout mice. The role of MMP9 in macrophages, neutrophils and T cells has been reported, but the role of MMP9 in dendritic cells is rarely reported. Whether and how dendritic cells play a role in heart failure caused by LPS infection, which related to the expression of MMP9. This study found that the results of Dog mice transfused with BMDC from mmp9 knockout mice were consistent with the previous results. And the results in vitro showed that MMP9 affected the function of BMDC through NF–κB signaling pathway, reducing the secretion of IL–6 and NO to protect cardiomyocytes H9c2. These results provide a new perspective for the study of the mechanism of the occurrence and development of septic cardiac insufficiency.

[Key words] Myocardial dysfunction; MMP9; Dendritic cells

Predictive value of type d personality for cardiac events in Chinese patients with acute myocardial infarction

LI Jiahui WU Wenjing LI Nan WANG Jian ZU Liyuan YE Xiaojun

China-Japan Friendship Hospital, Beijing 100029, China

[Abstract] **Objective** To investigate the association between type D personality and adverse cardiac events in chinese patients after acute myocardial infarction (AMI). **Methods** Patients with AMI admitted to cardiac care unit (CCU) of China–Japan Friendship Hospital, Beijing, China between January 2016 and December 2017 were enrolled. At baseline, 257 patients provided written informed consent and completed psychological questionnaires at enrollment by theirselves or with the nurses' help. Type D personality was assessed at baseline with 14–item Type D Scale–14 (DS14). Anxiety and depression were quantified using Hospital Anxiety and Depression Scale (HADS). In–hospital cardiac events were a composite of major adverse cardiac events (MACEs) including ventricular tachycardia/fibrillation,

acute recurrent myocardial ischemia, reinfarction, cardiogenic shock, acute pulmonary edema and cardiac death. Post–discharge endpoints were defined as a composite of unstable angina, reinfarction, cardiac revascularization(PCI/CABG) and cardiac death. Multivariable logistic regression analysis was used to calculate odds ratios (*OR*) and determine the independent predictors of in–hospital MACEs, while cox regression analysis was used to evaluate post–discharge endpoints. **Results** 54 patients (21%) were classified as Type D personality defined by the combination of a negative affectivity (NA) score≥10 and a social inhibition (SI) score≥10 on the DS14. All other patients were classified as non–Type D with 30 (12%) NA only, 45 (17.5%) SI only, and 83 (79%) having low scores on both traits. Type D personality was not significantly related to age, sex, BMI, PCI, hypertension, diabetes and smoking. Patients with Type D personality displayed significantly higher scores of anxiety ($P<0.01$) and depression ($P<0.01$) than non–Type D patients did. AMI patients with Type D personality had higher prevalence rates of anxiety ($P<0.05$) and depression ($P<0.01$). Type D group also displayed significantly higher level of blood lipoprotein(a) ($P<0.05$). There was no difference in length of stay during hospitalization between Type D and non–Type D patients ($P>0.05$). The incidence of in–hospital MACEs was higher in type D than in non–Type D patients ($P<0.05$). Multivariate logistic regression showed three significant independent predictors of in–hospital MACEs: age ($P<0.01$), type–D personality($P<0.05$) and killip classification($P<0.05$). The average follow–up time was 31 (23–37.5) months after discharge. 5 patients were lost to follow–up with 3 patients in non–type D and 2 in type–D group. 3 patients died all in non–type D group. One died of severe pneumonia and heart failure. The other two died of Non–ST elevation AMI and cardiogenic shock. There were 35 post–discharge events in total patients, of which 12 events in type–D group and 23 in non–type D group. Type D patients had higher incidences of post–discharge events($P<0.05$). In the analysis of post–discharge events by Cox regression, χ^2 of the Cox regression equation was 10.029 ($P<0.05$). Smoking ($P<0.05$) and type–D personality ($P<0.05$) were independent predictors of long–term cardiac events. Kaplan–Meier curves showed significant difference in event–free survival between type D and non–type D group ($P<0.05$). **Conclusion** Type D personality is an independent predictor of in–hospital and post–discharge cardiac events after AMI in Chinese patients.

[Key words] Predictive value; Type d personality for cardiac events; Acute myocardial infarction

Prognosis and simple nomogram of post–PCI acute heart failure in patients with non–ST–segment elevation myocardial infarction: a 13 120 Chinese cohort study

GUO Zhaodong YING Ming WANG Bo LIU Yong DONG Shaohong

Shenzhen People's Hospital, Shenzhen 518002, China

[Abstract] Objective To evaluate the association of post–PCI AHF and long–term cardiovascular (CV) death and establish a simple nomogram model for predicting post–PCI AHF in this patient group. **Methods** In this prospective observational study, 13 120 NSTEMI patients undergoing coronary angiography (CAG) were included in the final analysis. Patients were assigned into the non post–PCI AHF group (n=12 350) or the post–PCI AHF group (n=770). **Results** The overall incidence of post–PCI AHF was 770/13 120 (5.9%). The incidence of long–term CV death was significantly higher in the post–PCI AHF group than in the non post–PCI AHF group (50.6% vs. 17.0%, $P<0.01$). After adjusting for female, LVEF, eGFR, anemia, hypertension, diabetes mellitus, and PCI, post–PCI AHF was the strongest predictor of long–term CV death (*HR*= 3.11, 95%*CI*: 1.83 – 5.30, $P<0.01$). A simple nomogram developed based on the four variables was with the AUC 0.83 on internal validation. Decision curve analysis (DCA) indicated that our model was clinically useful. **Conclusion** In patients with NSTEMI undergoing CAG, post–PCI AHF is the strongest predictor of long–term CV

death. The simple nomogram showed an effective value of predicting post-PCI AHF using pre-PCI predictions.

[Key words] Prognosis and simple nomogram; Post-PCI acute heart failure; Non-ST-segment elevation myocardial infarction

Association of high-sensitivity C-reactive protein and long-term cardiovascular death may differ from lipoprotein(a) levels among patients undergoing coronary angiography: a 24 220 Chinese cohort study

GUO Zhaodong YING Ming WANG Bo LIU Yong DONG Shaohong

Shenzhen People's Hospital, Shenzhen 518002, China

[Abstract] Objective To investigate whether the association of high-sensitivity C-reactive protein (hs-CRP) with long-term cardiovascular (CV) death differs from another inflammation biomarker, lipoprotein(a), in patients undergoing coronary angiography (CAG). Methods A total of 24,220 patients undergoing CAG were included in the final analysis from a prospective, observational study. We divided them into 4 groups according to hs-CRP level (high ⩾4.8 mg/L, low <4.8 mg/L) and lipoprotein(a) level (high ⩾50 mg/dL, low <50 mg/dL). Results The overall incidence of long-term CV death was 1 332/24 220 (5.5%). In the high lipoprotein(a) group, after adjusting for LDL-cholesterol concentration (LDL-C), age, sex, smoking status, diabetes mellitus, and estimated glomerular filtration rate (eGFR), a high hs-CRP level was an independent predictor of long-term CV death ($P<0.05$). In the low lipoprotein(a) group, a similar result was not found ($P>0.05$). Conclusion The data suggested that the association of hs-CRP with long-term CV death may differ from lipoprotein(a) levels among patients undergoing CAG. In those patients with high hs-CRP levels, a high lipoprotein(a) level might be a simultaneous intervention target for improving long-term CV prognosis in the future.

[Key words] High-sensitivity C-reactive protein; Long-term cardiovascular death;Coronary angiography

TEAD1 exerts critical roles in cardiac remodeling through wnt signaling pathway

SONG Shuai SUN Aijun GE Junbo

Zhongshan Hospital, Gudan University, Shanghai 200082, China

[Abstract] Objective Pathological cardiac fibrosis and hypertrophy, the common features of left ventricular remodeling, often progress towards heart failure (HF). However, the mechanisms underlying pathological cardiac remodeling remain largely unknown. TEA domain transcription factor-1 (TEAD-1) is essential for proper heart development and is implicated in cardiac specific gene expression. The role of TEAD1 in pressure overload and Angiotensin II (Ang-II)-induced cardiac remodeling and HF remain to be investigated. Methods TEAD1 was continuous up-regulated in TAC (transverse aortic constriction)-induced remodeling heart samples compared with sham samples by mass spectrometry analysis. We analyzed TEAD1 expression in patients with atrial fibrillation (AF), hypertrophic cardiomyopathy (HCM) and dilated cardiomyopathy (DCM) and mice subjected to TAC, myocardial infarction (MI) and Ang-II infusion by Western blot and RT-qPCR. Conditional deletion of TEAD1 was achieved by crossing the

floxed TEAD1 mouse model with fibroblasts and myofibroblasts–specific Cre transgenic mice. TAC and Ang–II infusion were performed on fibroblasts and myofibroblasts–specific TEAD1 knockout mice to assess the role of TEAD1 in cardiac remodeling. WT male mice were treated twice a day with TEAD1 inhibitor INA (50 mg/kg) for a month. Heart function was examined by echocardiography and related cellular and molecular markers were examined. Primary ventricular fibroblasts were used to dissect molecular mechanisms. Mass spectrometry and coimmunoprecipitation assays were conducted to identify the proteins that interacted with TEAD1. RNA–seq analysis, ChIP and luciferase reporter gene assay were used to explore the mechanisms by which TEAD1 regulates cardiac remodeling. **Results** The TEAD1 level was significantly increased in the remodeling hearts from patients with AF, DCM and HCM and mice subjected to TAC, MI and Ang–II infusion. The results of echocardiography and histology demonstrated that fibroblasts and myofibroblasts–specific TEAD1 knockout mice and TEAD1 inhibitor INA protected the heart from TAC and Ang–II–induced cardiac remodeling. RNA–seq identified wnt4 as a novel TEAD1 target. Wnt4 was identified to affect cardiac remodeling through wnt signal pathway. There was an interaction between TEAD1 and BRD4 protein through bromodomain domain. TEAD1 and BRD4 binds with the wnt4 promoter, resulting in wnt signal pathway–associated gene expression. Genetic wnt4 knockdown rescued the pro–transformation phenotype in TEAD1 overexpression fibroblasts. **Conclusion** This study findings suggest that TEAD1 plays a causative role in pathological cardiac remodeling, at least partially via the activation of wnt signaling in fibroblasts. Therapeutic strategies targeting the TEAD1–wnt axis may be effective for cardiac remodeling.

[Key words] TEAD1;Cardiac remodeling;Wnt signaling pathway

Mechanism study of COX6A2 gene knockout causing mitochondrial cardiomyopathy

JIANG Mengqi SONG Yuanxiu CUI Ming BAI Yun

School of Basic Medical Sciences, Peking University Health Science Center, Beijing 100191, China

[Abstract] **Objective** iPSC myocardial differentiation combined with CRISPR/Cas9 gene editing technology was used to establish a COX6A2 homozygous knockout human cardiomyocyte model, and to explore the mechanism of COX6A2 deletion–induced mitochondrial cardiomyopathy. **Methods** Combine CRISPR/Cas9 genome editing technology and human pluripotent stem cell cardiomyocyte differentiation technology to establish COX6A2$^{-/-}$ cell line and differentiate into cardiomyocytes. Immunofluorescence staining, electron microscopy and flow cytometry were used to observe the effect of COX6A2 knockout on the morphology of cardiomyocytes. Mitotracker and JC–1 fluorescent probe were used to observe the effect of COX6A2 on the number of myocardial mitochondria and membrane potential. The fluo–4/AM probe was used to explore the effect of COX6A2 on the calcium signal and contractility of cardiomyocytes. The Annexin V/APC fluorescent apoptosis detection was used to compare the differences in apoptosis between WT and KO hiPSC–CMs. Western blot and qPCR were used to detect differences in the expression of genes related to heart failure, fibrosis, ion channels and energy metabolism pathways in cardiomyocytes. **Results** Compared with WT hiPSC–CMs, the cell volume became larger, the number of mitochondria increased, and the cross–sectional area decreased ($P < 0.05$), indicating that the loss of COX6A2 did not affect the differentiation of hiPSCs into myocardium, but the cell morphology and number of mitochondria changed. COX6A2–/– (KO) hiPSC–CMs have decreased mitochondrial membrane potential and impaired mitochondrial function. QPCR results showed that the expression of KO hiPSC–CMs ion channel–related genes (SCN5A, KCNH2, KCNQ1) was significantly reduced, and the expression of energy metabolism–related genes (CPT1B, CD36, PPARGC1A, PPARGC1B, PDK4, GFPT1) was significantly reduced ($P < 0.05$). COX6A2 lacked Caused myocardial calcium activity disorder and weakened myocardial contractility ($P < 0.05$). Apoptosis detection results show

that the loss of COX6A2 promotes the apoptosis level of cardiomyocytes. **Conclusion** cytochrome c oxidase subunit 6A2 (COX6A2) is involved in maintaining the morphology and function of mitochondria, and plays an important role in maintaining the energy metabolism of cardiomyocytes. Loss of COX6A2 can lead to impaired mitochondrial function, unable to maintain the normal level of energy metabolism of cardiomyocytes, leading to premature aging and apoptosis of cardiomyocytes. This study helps to clarify the pathogenesis of mitochondrial cardiomyopathy, and provides new targets and directions for the prevention and treatment of mitochondrial cardiomyopathy.

[Key words] Mechanism study ; COX6A2 ; Mitochondrial cardiomyopathy

Expression of HIF-1a in circulation and its relationship with cardiac function in patients with heart failure

WANG Shaomei

Zhejiang Provincial People's Hospital, People's Hospital of Hangzhou Medical College, Hangzhou 310014, China

[Abstract] **Objective** For patients with heart failure(HF), whether HIF-1 α is expressed in vivo, whether the amount of its gene expression is parallel to the grading of cardiac function, and whether it can predict the prognosis of patients with heart failure has not been confirmed. HF is the end-stage manifestation of various cardiovascular diseases, especially in industrialized countries and aging societies. In patients with HF, tissue perfusion is insufficient due to congestion of pulmonary and systemic circulation and heart pump failure, which eventually leads to ischemia and hypoxia of multiple organs. The loss of cardiac function is characterized by decreased ejection fraction, increased LVED and clinical symptoms and signs of HF. At present, it is believed that the key to the transformation from oxidative metabolism to glycolysis metabolism is the intracellular adaptation to hypoxia mediated by HIF-1. In addition, HIF-1 also mediates the transformation of fatty acids to lipid synthesis by activating PPAR- γ transcription.In patients with HF, New York Heart Association (NYHA) functional Classification and circulating BNP levels are directly related to the severity of the disease.In this study, At present, BNP is increasingly used as a marker for the diagnosis and prognosis of HF.patients with HF were used to determine the expression of HIF-1 α and its relationship with levels of BNP,free fatty acids(FFA) and lactic acid(LA). **Methods** A total of 90 patients with HF were included in this study, We divided the patients according to the level of cardiac function(II-IV) and made statistical analysis. including 76 patients with acute left heart failure (84.4%), with an average age of (69.2 ± 12.8) years. This study used ELISA method to detect the levels of HIF-1 α, BNP, FFA and LA in the circulation of the patients. **Results** The average serum HIF-1α level in patients with heart failure was (2.47 ± 0.56)ng/mL. The level of serum HIF-1 α was (2.69 ± 0.43) ng/mL in cardiac function class Ⅲ group and (2.91 ± 0.58) ng/mL in cardiac function grade Ⅳ group, and there was significant difference between the two groups ($P < 0.05$). The level of serum HIF-1 α in patients with acute left HF was also significantly higher than that in patients with chronic HF ($P < 0.01$). The levers of HIF-1 α was significantly higher in HF patients with higher levels of FFA and LA than that patients with lower levels of FFA and LA. Meanwhile, there was a significant difference in the levels of FFA and LA between the two groups.Serum HIF-1 α was associated with level SpO_2, FFA ,LA ,cardiac function grade and acute left heart failure, but not with age, BNP and TNI. The level of serum HIF-1 α was closely related to cardiac function and aerobic metabolism in patients with HF. **Conclution** HIF-1 α was found in the peripheral blood circulation of patients with heart failure. In this study population, although the level of serum HIF-1 α was related to the cardiac function and energy metabolism of patients, but it could not independently predict the cardiac function of patients with heart failure.

[Key words] HIF-1α; Cardiac function; Heart failure

Development and validation of a nomogram for predicting radial artery spasm during coronary angiography

GUO Qixin

Hangzhou First People's Hospital, Hangzhou 310006, China

[Abstract] **Objective** To develop a user–friendly nomogram incorporating psychological factors to individually predict the risk of radial artery spasm. **Methods** Patients consecutively recruited in the stage between June 2020 through October 2020 constituted the development cohort for retrospective analysis to develop a prediction model. Least absolute shrinkage and selection operator (LASSO) regression and a logistic model combined with clinical significance were employed to screen out appropriate independent variables. The model's discrimination and calibration were subsequently evaluated and calibrated by using the C index, ROC curve and calibration plot. A decision curve analysis was also performed to evaluate the net benefit with the nomogram, and internal validation was assessed using the bootstrapping validation. **Results** Predictors contained in the risk nomogram included ''Age'' ''BMI'' ''Gender'' ''Hyperlipidemia'' ''Anxiety score'' ''Duration'' ''Latency time'' ''Vascular circuity'' ''Puncture number'' and ''UA''. The derived model showed good discrimination with an area under the receiver operating characteristic curve (AUC) of 0.894, a C–index of 0.899 and good calibration. A high C–index value of 0.866 could still be reached in the interval validation. The decision curve analysis of the nomogram provided better net benefit than the alternate options. **Conclusion** This study presents a nomogram that incorporates 10 clinical risk factors, which can be conveniently utilized to facilitate radial artery spasm risk prediction in patients undergoing coronary angiography.

[Key words] Nomogram;Predicting radial artery spasm; Coronary angiography

Antithrombotic therapy for patients after transcatheter aortic valve replacement: a systematic review and meta–analysis of randomized controlled trials

WANG Shuai LIN Xiaoxiao HUANG Jinyu

Hangzhou First People's Hospital, Hangzhou 310006, China

[Abstract] **Objective** Performed a systematic review and meta–analysis to evaluate the Antithrombotic therapy for patients after Transcatheter aortic valve replacement (TAVR). **Methods** The databases of Embase, PubMed, Cochrane library were searched from inception to May 1, 2021 were searched. and randomized controlled trials (RCTs) reporting Antithrombotic therapy for patients after TAVR were included. Revman 5.3 was used to conduct the analysis. **Results** From screening 102 articles, 4 studies containing 1 086 patients were included. After the follow up of 3 months, monotherapy appeared to increase the risk of bleeding events compare with dual therapy ($P < 0.01$) for patients with or without an indication for oral anticoagulation, and there was no significant difference in the rate of all–cause mortality ($P > 0.05$), stroke ($P > 0.05$) and MI ($P > 0.05$) among two groups. In patients without an established indication for oral anticoagulation after successful TAVR, a treatment strategy including rivaroxaban at a dose of 10 mg daily was associated with a higher risk of death or thromboembolic complications and a higher risk of bleeding than an antiplatelet–based strategy, although anticoagulation could prevent transcatheter heart valve dysfunction in short and long term. **Conclusion** Although the use of DAPT for 3 to 6 months after TAVR is the guideline–recommended regimen,

this practice is not well supported by current evidence. In patients with no indication for an OAC, SAPT may be safer rather than DAPT. Similarly, OAC monotherapy might be superior to an OAC plus SAPT in patients with an OAC indication. To date, no risk prediction models have been established to guide antithrombotic therapy. Ongoing investigations will provide better guidance for adjunctive antithrombotic regimens for patients after TAVR. The longer follow–up, loading dose and treatment duration should be considered in further studies compared aspirin with DAPT.

[Key words] Antithrombotic therapy;T ranscatheter aortic valve replacement; Monotherapy; Dual therapy; Systematic review and meta–analysis

Body mass index as independent predictor of 2–year follow–up malignant events in patients with slow coronary blood flow

GUO Qixin

Hangzhou First People's Hospital, Hangzhou 310006, China

[Abstract] **Objective** The phenomenon of slow coronary blood flow is common clinically and is related to the patient experiencing repeated chest distress. The mechanism of slow blood flow is still unclear, and the the factors affecting the long–term prognosis are unknown. Therefore, this study evaluated malignant events in this part of population through the results of a 2–year follow–up. **Methods** A total of 4 663 patients who underwent continuous coronary angiography were identified. Those patients with primary slow coronary flow were included in the study. CTFT is used to assess the severity of slow blood flow. The endpoint events were the occurrence of rehospitalization and out–of–hospital death within 2 years. The log–rank test, Kaplan–Meier method, and Cox regression were used to evaluate and analyze the final results. **Results** A total of 36 patients were readmitted to hospital, and 14 died suddenly outside the hospital during the follow–up period. In the stratified analysis. Adverse events were more frequently observed in the elderly people ($P < 0.01$). Compared with people with high levels of BMI, people with lower levels of BMI have a significant advantage trend ($P > 0.05$). In Cox regression analysis, high BMI (body mass index) was an independent predictor of adverse end events ($P < 0.05$). **Conclusion** BMI plays an important role in the influence of prognosis. Further research is needed to investigate this conclusion.

[Key words] Body mass index;Independent predictor; Slow coronary blood flow

Association between depression and clinical outcomes in patients with hypertrophic cardiomyopathy

HE Chaojie

The First Hospital of Jiaxing, Jiaxing 314000, China

[Abstract] **Objective** To examine the impact of depression on clinical outcomes in patients with Hypertrophic cardiomyopathy (HCM). **Methods** Between January 2014 and December 2017, 820 patients with HCM were recruited and followed for an average of 4.2 years. Endpoints were defined as sudden cardiac death (SCD) events and HCM–related heart failure events. A Chinese version of the Structured Clinical Interview followed the Diagnostic and Statistical Manual of Mental Disorders (DSM–5) and was used to diagnose depression. **Results** During the follow–up period, SCD events occurred in 75 individuals (21.8 per 1 000 person–years), and HCM–related heart failure events developed

in 149 individuals (43.3 per1 000 person–years). Kaplan–Meier cumulative incidence curves showed a significant association of depression disorders with SCD events ($P<0.01$) and HCM–related heart failure events ($P<0.01$). A multivariate Cox regression analysis indicated that depression was an independent predictor of SCD events and HCM–related heart failure events ($P<0.01$). **Conclusion** Depression is common among patients with HCM. The diagnosis of depression is significantly and independently associated with an increased risk of SCD events and heart failure events in patients with HCM.

[Key words] Association;Depression and clinical outcomes; Hypertrophic cardiomyopathy

Association between anxiety and clinical outcomes in Chinese patients with myocardial infarction in the absence of obstructive coronary artery disease

HE Chaojie

The First Hospital of Jiaxing, Jiaxing 314000, China

[Abstract] Objective Myocardial infarction in the absence of obstructive coronary artery disease (MINOCA) accounts for approximately 5%–6% of acute myocardial infarction (AMI) patients. Anxiety symptoms are common in patients with coronary artery disease (CAD), and are associated with a poor prognosis. However, the association between anxiety and MINOCA outcomes is less clear. Anxiety will be associated with clinical outcomes in patients with MINOCA. **Methods** Between November 2014 and December 2016, 620 hospitalized patients with MINOCA were recruited from a single center. Within 7 days of coronary angiography, anxiety was assessed using the Zung Self–Rating Anxiety Scale. The primary endpoint was all–cause mortality, secondary endpoint was any major adverse cardiovascular event (MACE). **Results** After three years, 87 deaths and 151 MACE had occurred. Kaplan–Meier curves indicated the unadjusted rates of all–cause mortality ($P<0.05$) and MACE ($P<0.05$) were significantly higher in the anxiety group compared with the control group of patients without anxiety. Multivariate Cox regression analysis showed that clinically significant anxiety was an independent prognostic factor for all–cause mortality as well as MACE ($P<0.05$). **Conclusion** Anxiety is significantly and independently associated with an increased risk of all–cause mortality and MACE in patients with MINOCA.

[Key words] Association;Myocardial infarction;Obstructive coronary artery disease

Association between obstructive sleep apnea–hypopnea syndrome and outcomes in patients with myocardial infarction in the absence of obstructive coronary artery disease

HE Chaojie

The First Hospital of Jiaxing, Jiaxing 314000, China

[Abstract] Objective To evaluate the association between Obstructive sleep apnea–hypopnea syndrome (OSAHS) and clinical outcomes in patients with Myocardial infarction in the absence of obstructive coronary artery disease (MINOCA). **Methods and Results** Between January 2015 and December 2016, we carried out a prospective and

consecutive cohort study of 583 patients with MINOCA and followed them up for three years. An apnea–hypopnea index of ⩾15 events per hour recorded by polysomnography was defined as the diagnostic criterion for OSAHS. The primary end point was all–cause mortality, and the second end point was major adverse cardiovascular or cerebrovascular events (MACCE), a composite of cardiac death, nonfatal myocardial infarction, heart failure, cardiovascular–related rehospitalization, and stroke. All–cause mortality happened in 69 patients and MACCE occurred in 113 patients during the three–year follow–up. Kaplan–Meier survival curves indicated the significant relationship of OSAHS with all–cause mortality ($P<0.05$) and MACCE ($P<0.05$). Multivariate Cox regression analysis indicated OSAHS as an independent predictor of all–cause mortality and MACCE ($P<0.05$), independent of age, sex, cardiovascular risk factors and discharge medications. **Conclusion** OSAHS is independently associated with increased risk of all–cause mortality and MACCE in patients with MINOCA. Intervention and treatment should be considered to alleviate OSAHS–associated risk.

[Key words] Obstructive sleep apnea–hypopnea syndrome; Myocardial infarction in the absence;Obstructive coronary artery disease

High mobility group box 1 promotes mitochondrial fusion through CXCR4/PSBM5 mediated Drp1 degradation in endothelial cells

ZHANG Shunrong XIE Xiaojie HUANG Jinyu

Affiliated Hangzhou First People's Hospital, Zhejiang University School of Medicine, Hangzhou 310006, China

[Abstract] Objective To clarify the effect of high mobility group box 1(HMGB1), a representative damage–associated molecular pattern (DAMPs) molecule, on mitochondrial dynamics in endothelial cells and the underlying mechanism. **Methods** Human endothelial cell line EA.hy926 was used, and cells were multiplied and divided into groups treated with different concentrations of recombinant HMGB1(rHMGB1).The morphology of mitochondria of EA.hy926 endothelial cells were observed with confocal microscope after staining with Mito–Tracker Green and transmission electron microscope (TEM). The expression changes of mitochondrial dynamics mediators dynamin–related protein 1 (Drp1), Mitofusin 1 (Mfn1), Mitofusin 2 (Mfn2), Optic atrophy 1(Opa1), and phosphatase and tensin homolog (PTEN)–induced kinase 1 (PINK1), were detected by Western blotting, the mRNA expression changes of Drp1 was detected with real time PCR. Meanwhile the expression changes of NLRP3, caspase 1 and cleaved caspase1 were also determined by Western blotting and the concentration of interleukin–1β (IL–1β) was detected by ELISA to observe the inflammatory phenotype changes in endothelial cells treated with rHMGB1.To explicit the mechanism of rHMGB1 induced change of mitochondrial dynamics, the expression levels of 20S proteasome subunit beta 5 (PSMB5) and the anti–oxidative response master regulator nuclear factor E2–related factor 2 (NRF2) were determined, specific inhibitors C29, TAK–242, FPS–ZM1, AMD3100 were used to block toll–like receptor 2 (TLR2), toll–like receptor 4(TLR4), receptor for advanced glycation end products (RAGE), and C–X–C–chemokine receptor 4 (CXCR4) respectively. In addition, PSMB5 was also inhibited with a specific inhibitor epoxomicin, and specific siRNAs were used to silence the expression of NRF2. **Results** Different concentrations of recombinant HMGB1 incubation for 24 hours promoted mitochondrial fusion in EA.hy926 endothelial cells, indicating as increased tubular or filamentous mitochondria and decreased granular mitochondria under confocal microscope, as well as an increase of mitochondrial area and decrease of mitochondrial number under TEM. No significant inflammatory phenotype changes were found in endothelial cells treated with rHMGB1. The expression level of Drp1, the essential mediator of mitochondrial fission, down–regulated

significantly, the expression levels of the two phosphorylated forms of p-Drp1-616 and p-Drp1-637, were also decreased proportionately, no significant expression changes of PINK1 and the fusion facilitator Mfn1, Mfn2, Opa1 were found. Inhibition TLR4, RAGE, and TLR2 receptors with TAK-242, FPS-ZM1, and C29 respectively had no significant influence on rHMGB1 induced mitochondrial fusion, only blocking CXCR4 with AMD3100 reversed rHMGB1 induced downregulation Drp1 and mitochondrial fusion. rHMGB1 increased the expression of NRF2 and PSMB5, and inhibition PSMB5 with epoxomicin abolished rHMGB1 induced Drp1 downregulation and mitochondrial fusion, whereas silencing NRF2 with specific siRNAs had no effect on rHMGB1 induced decrease of Drp1 and mitochondrial fusion. These results indicated that rHMGB1 promotes NRF2 independent mitochondrial fusion via CXCR4/PSMB5 pathway mediated DRP1 proteolysis. **Conclusion** HMGB1 can promote mitochondrial fusion but not inflammation through CXCR4/PSBM5 mediated Drp1 degradation in endothelial cells in a manner of NRF2 independent. HMGB1 may influence mitochondrial and cellular function of endothelial cells through this effect on mitochondrial dynamics.

[Key words] HMGB1; Mitochondrial dynamics; Inflammation; Endothelial cell; CXCR4; NRF2; PSMB5

SCN5A R225Q mutation induces aged-associated dilated cardiomyopathy via intracellular ph and the wnt/β-catenin pathway

HU Jingjing YANG Kun

Shanghai Institute of Cardiovascular Diseases, Zhongshan Hospital, Fudan University, Shanghai 200032, China

[Abstract] Objective Explored the mechanism of the R225Q mutation induced dilated cardiomyopathy (DCM) phenotype. **Methods** Prevalence of DI-S4 mutation was compared between idiopathic DCM patients and the Control subjects. R225Q knock-in and WT mice were subjected to doxorubicin (DOX), D-galactose(D-gal), or D-gal combined with DOX. **Results** Clinical data suggested that the DCM group had a higher DI-S4 mutation rate than the Control group. There was no difference in cardiac function between knock-in and Wild-type mice when injected with D-gal or DOX alone. Cardiomyocytes from these mice exhibited a hypertrophic phenotype with a weaker contraction/dilation function and an increased level of apoptosis. Mechanistically, this study found that R225Q could increase intracellular pH and further induce the activation of the WNT/β-catenin pathway as well as the overexpression of pro-hypertrophic (cyclin D1 and c-MYC) and pro-apoptotic (cleaved and total caspase-3) targets. WNT-C59 inhibitor improved cardiac function in the R225Q knock-in mice after D-gal and DOX injection. **Conclusion** This study results suggest that R225Q mutation is associated with increased susceptibility to DCM. Aging could enhance this process via activating WNT/β-catenin signaling in response to increased intracellular pH. Antagonizing the WNT/β-catenin pathway might be a potential therapeutic strategy for mitigating DCM pathogenesis.

[Key words] SCN5A; Wnt/β-catenin pathway; Cardiomyopathy

Efficacy and safety of long–term antithrombotic strategies in patients with chronic coronary syndrome: a network meta–analysis of randomized controlled trials

ZHU Houyong　HUANG Jinyu

Affiliated Hangzhou First People's Hospital, Zhejiang University School of Medicine, Hangzhou 310006, China

[Abstract] **Objective** To conduct a network meta–analysis to evaluate the efficacy and safety of long–term antithrombotic strategies in patients with chronic coronary syndrome (CCS). **Methods and Results** Four randomized studies were included (*n*=75 167, THEMIS, COMPASS, PEGASUS–TIMI 54, and DAPT). The odds ratios (*OR*) (95% confidence intervals) were calculated as the measure of effect size. The results of the network meta–analysis showed that, compared with aspirin monotherapy, the ORs for trial–defined MACEs were for ticagrelor plus aspirin for rivaroxaban monotherapy for rivaroxaban plus aspirin, and for thienopyridine plus aspirin. Compared with aspirin monotherapy, the ORs for trial–defined major bleeding were for ticagrelor plus aspirin, for rivaroxaban monotherapy, and for rivaroxaban plus aspirin. For death from any cause, the improvement effect of rivaroxaban plus aspirin was detected versus aspirin monotherapy, ticagrelor plus aspirin rivaroxaban monotherapy, and thienopyridine plus aspirin regimens. **Conclusion** All antithrombotic strategies combined with aspirin significantly reduced the incidence of MACEs and increased the risk of major bleeding compared with aspirin monotherapy. Considering the outcomes of all ischemic and bleeding events and all–cause mortality, rivaroxaban plus aspirin appears to be the preferred long–term antithrombotic regimen for patients with CCS and high–risk factors.

[Key words] Long–term antithrombotic strategies; Chronic coronary syndrome; Randomized controlled Trials

The m6A demethylase alkbh5 acts as a hypoxia–dependent cardiac fibroblast–to–myofibroblast transformation inducer to protect heart from cardiac rupture after myocardial infarction

YANG Kun　HU Jingjing　SUN Aijun　GE Junbo

Shanghai Institute of Cardiovascular Diseases, Zhongshan Hospital, Fudan University, Shanghai 310000, China

[Abstract] **Objective** Cardiac rupture accounts for a high proportion of sudden death in the early period after acute Myocardial Infarction (MI). However, the molecular mechanism underlying post–infarct cardiac rupture needs to be elucidated to develop strategies for its prevention. **Methods** A–ketoglutarate–dependent dioxygenase alkB homolog 5 (ALKBH5) gene editing mice and control C57Bl/6 wild–type (WT) mice were subjected to left coronary artery ligation. The level of N6–methyladenosine (m6A) modification was assessed by dot blot. This study evaluated the repair and cardiac function of ALKBH5–knockout and ALKBH5–knockin mice after MI compared with WT mice. The immunofluorescence staining and flow analysis were used to evaluate inflammatory cells after MI. And expression of ALKBH5 was modulated by adenovirus to study its function in regulating cardiac fibroblasts proliferation, migration and induction of fibroblast–to–myofibroblast transition. We performed m6A RNA immunoprecipitation sequencing to map transcriptome–wide m6A in WT and ALKBH5–knockout mice 5 days post–MI. Chromatin immunoprecipitation, RNA

immunoprecipitation and dual luciferase reporter assay were used to prove the binding relationship of HIF-1α, ALKBH5 and Sirtuin 2(SIRT2). **Results** The data indicate that ALKBH5 expression is significantly decreased while the level of m6A (N6-methyladenosine) modification is increased 3 days post-MI. And hypoxia stimulated cardiac fibroblasts shows remarkable up-regulation of ALKBH5 and down-regulation of m6A modification. The survival rate 28 days post-operation was significantly lower in ALKBH5 deficient mice than that in wild-type mice with evidence of cardiac rupture in all dead mice. And ALKBH5 deficient mice after MI also appeared wall thinning and deterioration of cardiac function. Then, we found it was fibroblast-to-myofibroblast transformation, not inflammatory cell infiltration, that was impaired in ALKBH5 deficient mice after MI, which was supposed to be the cause of the heart rupture. In addition, ALKBH5 overexpression improves the post-MI cardiac function. In vitro, our results indicate that hypoxia, but not TGF-β1 and Ang-II, up-regulates ALKBH5 expression in myofibroblasts in a HIF-1α-dependent transcriptional manner. Furthermore, we identified ALKBH5 as an important activator for fibroblasts proliferation, migration and fibroblast-to-myofibroblast transition. In mechanism, ALKBH5 decreased the stability of SIRT2 mRNA by m6A modification, thereby stimulating activation of fibroblasts. **Conclusion** Taken together, this study findings show that ALKBH5 acts as a hypoxia-dependent cardiac fibroblast-to-myofibroblast transformation inducer to protect heart from cardiac rupture after myocardial infarction in m6A modified manner. And reveal a novel molecular mechanism of HIF-1α/ALKBH5/SIRT2 in regulation of post-infarction cardiac remodeling.

[Key words] m6A; Hypoxia-dependent cardiac;Myocardial infarction

Rare variants in genes encoding PDZ-LIM proteins associated with idiopathic dilated cardiomyopathy: a single-center study

WANG Dongfei LYU Jialan GUO Xiaogang

The First Affiliated Hospital, Zhejiang University School of Medicine, Hangzhou 310003, China

[Abstract] **Objective** LDB3, PDLIM5, and PDLIM3 genes, which belong to PDZ-LIM family, have been linked to dilated cardiomyopathy (DCM). However, rare variants within these three genes associated with idiopathic DCM (IDCM) remain poorly understood. **Methods** This study employed sanger sequencing in 136 IDCM patients for rare variants in LDB3, PDLIM5, and PDLIM3 genes. 1 000 Genome Project and the Exome Aggregation Consortium database were used to filter rare variants. Bioinformatics analysis was applied to predict the effect of rare variants. And followed we conducted stratified analyses. **Results** This study identified 48 rare variants in 49 IDCM patients, including 30 novel variants, 4 missense variants, and 1 nonsense variant. Rare variants in the PDLIM5 gene were associated with decreased left ventricular ejection fraction and enlargement of left ventricular end systolic dimension, and early onset of IDCM. Carrying disease causing variants, coding variants, and multiple variants were risk factors for early emergence of IDCM. And disease causing variants were associated with higher serum potassium level, while missense variants were linked to lower systolic blood pressure. **Conclusion** This study conclude that IDCM patients, hosting rare variants within LDB3, PDLIM5, and PDLIM3 genes, are at higher risk for more severe clinical characteristics and early onset of IDCM.

[Key words] PDZ-LIM;Idiopathic dilated cardiomyopathy; Genes

Predictive value of three inflammation–based glasgow prognostic scores for major cardiovascular adverse events in patients with acute myocardial infarction during hospitalization: a retrospective study

ZHU Houyong　HUANG Jinyu

The Affiliated Hangzhou First People's Hospital, Zhejiang University School of Medicine, Hangzhou 310006, China

[Abstract] **Objective** To investigate whether three kinds of GPSs can effectively predict major cardiovascular adverse events (MACEs) in ST–elevation myocardial infarction (STEMI) or non–ST–segment elevation myocardial infarction (NSTEMI) patients undergoing primary percutaneous coronary intervention (PPCI), elective PCI (EPCI) or conservative drug therapy during hospitalization. **Methods** In this retrospective cohort study, patients with acute myocardial infarction (AMI) were divided into 0, 1 or 2 score according to the GPSs. Logistic regression and receiver operating characteristic (ROC) curve analysis were performed to assess the predictive value of GPSs for MACE and all–cause mortality during hospitalization. Three kinds of GPSs, Inflammation–based Glasgow Prognostic Score (GPS), modified GPS (MGPS) and high–sensitivity CRP–modified GPS (HS–MGPS), and Global Registry of Acute Coronary Events (GRACE) score were applied in this study. **Results** A total of 188 patients were enrolled. The ROC curve with MACE showed that the AUC of GPS ($P<0.01$) was larger than that of MGPS ($P<0.01$), HS–MGPS ($P<0.01$) and GRACE score ($P<0.01$). The ROC curve with all–cause mortality showed that the AUC of GPS ($P<0.01$) was similar to the HS–MGPS ($P<0.01$), and higher than the MGPS ($P<0.05$), but lower than the GRACE score ($P<0.01$). Multivariate logistic regression analysis showed that the GPS was an independent risk factor for the incidence of MACE during hospitalization. Compared with the odds ratio (OR) value for a GPS of 0, the OR for a GPS of 1 was 7.173 ($P<0.01$), and that for a GPS of 2 was 18.636 ($P<0.01$), but not an independent risk factor for all–cause mortality ($P>0.05$). GRACE score was an independent risk factor for MACE ($P<0.05$) and all–cause mortality ($P<0.01$). In the subgroups classified according to the type of AMI, the presence of disease interference GPSs and the type of PCI, the ability of GPS to predict the occurrence of MACE seemed to be greater than that of MGPS and HS–MGPS. **Conclusion** The GPS has a good predictive value for the occurrence of MACE during hospitalization in patients with AMI, regardless of STEMI or NSTEMI, the choice of PCI mode, and the presence or absence of diseases that interfere with GPS. However, GPS is less predictive of all–cause mortality during hospitalization than GRACE score, which may be due to the interference of patients with other diseases.

[Key words] Predictive value; Cardiovascular adverse events;Acute myocardial infarction

The undulating life of omega–3 fatty acids: what have we overlooked?

ZHU Houyong　XU Xiaoqun　HUANG Jinyu

The Affiliated Hangzhou First People's Hospital, Zhejiang University School of Medicine, Hangzhou 310006, China

[Abstract] Omega–3 fatty acid, a long–chain, polyunsaturated fatty acid, is found from plants and marine

organisms, and it may have a protective role against cardiovascular events in patients at high cardiovascular risk such as hyperlipidemia and diabetes, among others. Recent results from the Long–Term Outcomes Study to Assess Statin Residual Risk with Epanova in High Cardiovascular Risk Patients with Hypertriglyceridemia (STRENGTH), which enrolled 13 078 patients with high cardiovascular risk and high prevalence of diabetes, showed that 4g/d of omega–3 carboxylic acids (a final concentration of 75% of eicosapentaenoic acid (EPA) and docosahexaenoic acid) did not reduce cardiovascular events in high–risk patients. Interestingly, in subgroup analysis, Asian populations obtained cardiovascular benefit, but this result may not have been brought to the attention of the authors because of the not large number of included individuals. However, The results of the previous the Japan EPA Lipid Intervention Study (JELIS), which included 18 645 patients with hypercholesterolemia, revealed 1.8 g/d of EPA produced cardiovascular benefit. In addition, the results of the Reduction of Cardiovascular Events with Icosapent Ethyl – Intervention Trial (REDUCE–IT), which enrolled 8 179 patients with hypertriglyceridemia and high prevalence of diabetes, suggested after receiving a large dose of EPA of 4 g/d, there appeared to be more favorable benefits in subgroups of Western populations than in Asian. However, the randomized study of A Study of Cardiovascular Events in Diabetes (ASCEND), which included 15480 patients with diabetes receiving 1–g capsules containing either 840 mg of marine omega–3 fatty acids (460 mg of EPA and 380 mg of docosahexaenoic acid), showed no significant difference in the risk of serious vascular events compared with placebo. And most other clinical trials investigating the effect of low doses of EPA in Western populations failed to demonstrate cardiovascular benefit. A recently updated meta–analysis on the potential effect of omega–3 on cardiovascular outcomes suggested that it has a protective effect on cardiovascular and that this effect may present in a dose–dependent manner. However, this conclusion also does not seem to explain well the results of large–scale clinical studies. After all 1.8 g/d of EPA was given in the JELIS and 4 g/d of omega–3 carboxylic acids were given in the STRENGTH, and they included all patients with hyperlipidemia, but the results were not dose–dependent, or there might be a turning point in this protective effect.The importance of the omega–6 / omega–3 fatty acid ratio may not be paid attention to in the above studies. Omega–6 fatty acid, also a polyunsaturated fat essential for human health, must be consumed in appropriate foods for intake, such as vegetable oils, whole grains, nuts, seeds and so on. The potential cardiovascular effects of omega–6 fatty acids are also under long–standing debate and are thought to have dual cardiovascular effects, in particular its excessive intake could promote inflammation and thrombotic damage to the cardiovascular system.There is competition between EPA and omega–6 family, such as desaturase and cyclooxygenase. A study using UK populations as a sample showed that 3.6 g/d of EPA compared to 1.8 g/d increased bleeding time, which also implied that the amount of EPA that the UK population may need is closer to the high dose. The purified high–dose EPA can not only produce cardiovascular protection, but also reduce the inflammatory mediators and thrombosis from omega–6.In the current Western diet, the omega–6/omega–3 ratio has increased from 1∶1 in the late paleolithic period to 15–20∶1, which is much higher than that of the Japanese or some other Asian populations. Therefore, Western populations may need more purified EPA. However, a certain proportion of omega–6 / omega–3 may be more important than blindly increasing the amount of EPA. It may be somewhat strange but mechanistically plausible that excessive use of EPA in Asian populations will also lead to the pro–inflammatory effect of omega–3, partially offsetting its protective effect, although omega–3 produces a weaker proinflammatory effect than omega–6. The amount of EPA required in different populations may depend on the omega–6 / omega–3 ratio, but there may be a lack of balanced and dynamic monitoring of baseline data of omega–6 family and its metabolites, which leads to the controversy of the protective effect of omega–3 fatty acids on cardiovascular system.Therefore, in the future, focusing on omega–6 families and omega–6 / omega–3 ratios may help resolve controversies regarding the protection of omega–3 fatty acids in individuals at high risk for cardiovascular events such as hyperlipidemia and diabetes.

[Key words] Omega–3 fatty acid;Cardiovascular events;High cardiovascular risk

Shexiang tongxin dropping pill reduces coronary microembolization in rats via regulation of mitochondrial permeability transition pore opening and akt–gsk3β phosphorylation

DING Yu　ZHU Houyong　HUANG Jinyu

The Affiliated Hangzhou First People's Hospital, Zhejiang University School of Medicine, Hangzhou 310006, China

[Abstract] **Objective** To investigate the protective effects of Shexiang Tongxin Dropping Pill (STDP) following sodium laurate–induced coronary microembolization (CME) in rats. **Methods** Forty rats were divided into 4 groups: the control (sham) group, CME group, low–dose STDP pretreatment group (20 mg・kg^{-1}・d^{-1}), and high–dose STDP pretreatment group (40 mg・kg^{-1}・d^{-1}). The rats were intragastric administrated with STDP 2 weeks before operation. Moreover, the histopathological alterations were observed using optical microscopy and transmission electron microscopy. Antioxidant biomarkers were analyzed by enzyme–linked immunosorbent assay. Mitochondrial functions including the mitochondrial permeability transition pore (mPTP) mtDNA copy number were determined and proteins of AKT/GSK3β were analyzed by Western blot. **Results** The rats in the CME group showed a significant increase in the fibrinogen–like protein 2 expression level and mitochondrial dysfunction and a decrease in the expression level of antioxidant biomarkers (superoxide dismutase and catalase, $P<0.01$). In contrast, the rats in the low and high–dose STDP pretreatment groups showed a significant decrease in coronary microthrombi ($P<0.05$), moreover, STDP restored the antioxidant–related protein activities and mitochondrial function, inhibited mPTP opening, decreased AKT–Ser473 phosphorylation, and increased GSK3β–Ser9 phosphorylation ($P<0.05$). **Conclusion** STDP may be useful for treatment of CME, possibly via regulation of mPTP opening and AKT/GSK3β phosphorylation.

[Key words] Shexiang Tongxin Dropping Pill; Coronary microembolization; Rats

Loss of hepatic angiotensinogen attenuates sepsis–induced myocardial dysfunction

RONG Jiabing　TAO Ran　ZHANG Zhaocai　XU Yinchuan

The Second Affiliated Hospital, Zhejiang University School of Medicine, Hangzhou 310009, China

[Abstract] **Objective** To determine a role of AGT in SIMD and investigate the underlying mechanisms. **Methods and Results** Either intraperitoneal injection of lipopolysaccharide (LPS) or cecal ligation and puncture (CLP) significantly enhanced AGT abundances in liver, heart, and plasma. Deficiency of hepatocyte–derived AGT (hepAGT), rather than cardiomyocyte–derived AGT (carAGT), alleviated septic cardiac dysfunction in mice and prolonged survival time. Further investigations revealed that the effects of hepAGT on SIMD were partially associated with augmented angiotensin II (AngII) production in circulation. In addition, hepAGT was internalized by LDL receptor–related protein 1 (LRP1) in cardiac fibroblasts (CF), and subsequently activated NLRP3 inflammasome via an AngII–independent pathway, ultimately promoting SIMD by suppressing Sarco(endo)plasmic reticulum Ca^{2+}–ATPase 2a (SERCA2a) abundances in cardiomyocytes (CM). **Conclusion** HepAGT promoted SIMD via both AngII–dependent and AngII–independent pathways. We identified a liver–heart axis by which AGT regulated development of SIMD. This study may provide a

potential novel therapeutic target for SIMD.

[Key words] Lipopolysaccharide; Cecal ligation and puncture; HepAGT

Epidemiology of obesity and atrial fibrillation risk of metabolically healthy obesity in Chinese postmenopausal women

DU Zhi GUO Xiaogang

The First Affiliated Hospital, Zhejiang University School of Medicine, Hangzhou 310003, China

[Abstract] **Objective** To comprehensively assess obesity situation in postmenopausal women and explore the relationship between metabolically healthy obesity (MHO) and atrial fibrillation(AF). **Methods** The cross-sectional study was conducted from September 2017 to March 2019. A total of 22 900 permanent inhabitants aged ⩾40 years, except those with mental disorder or pregnancy, were invited to participate this investigation. Eventually, a total of 18 796 (85.4%) completed the investigation. In present analysis, being male (n=7 336), postmenopausal women without providing age of menopause and premenopausal women (n=2 343), and missing relevant covariates (n=22) were further excluded. Eventually, 9 095 postmenopausal women were remained analysis. General and central obesity were defined as body mass index ⩾ 28 kg/m^2 and waist circumference ⩾ 80 cm, respectively. MHO was considered as general obesity without metabolic disorders. The epidemiology of obesity including general obesity, central obesity and MHO was carefully identified in postmenopausal women. Logistic regression was used to evaluated the relationship between MHO and AF. **Results** The prevalence of general and central obesity in postmenopausal women were up to 18.2% and 64.1%, respectively. Almost all participants (97.7%) with general obesity suffered from central obesity. On the contrary, only 27.7% of participants with central obesity simultaneously suffered from general obesity, which means most of obese patients would be missed in postmenopausal women if waist circumference was not obtained. The proportion of comorbidities were high in postmenopausal women with obesity, including hypertension (67.1%), diabetes (23.6%) and dyslipidemia (45.9%), but awareness, treatment and control of them was unacceptable. Meanwhile, a significant proportion of postmenopausal women with general obesity was considered as MHO (21.3%). Compared with non-obesity participants, the risk of AF was not significant increasing in participants with MHO (P>0.05). However, obese postmenopausal women with metabolic disorders had increased risk of AF. **Conclusion** This study results suggested the huge burden of obesity in postmenopausal women. Meanwhile, considering high proportion and poor management of comorbidities, comprehensive management measures, including screening and control of comorbidities, should be applied for obese postmenopausal women to reduce the incidence of obesity-related cardiovascular disease. Meanwhile, in terms of the relationship between MHO and AF, controlling metabolic situation to prevent the emergence of AF might have meaningful clinical significance in obese participants.

[Key words] Obesity; Postmenopausal women; Metabolically healthy obesity; Atrial fibrillation; Epidemiology

Cardiac troponin I and risk of stroke: a mendelian randomization study

CHEN Heng　SUN Gang　ZHUO Chengui　ZHAO Jianqiang　ZU Aohan
WANG Qiqi　ZHENG Liangrong
The First Affiliated, Zhejiang University School of Medicine,Hangzhou 310003,China

[Abstract] **Objective** Cardiac troponin I (cTnI) is a well-established biomarker for stroke prediction, especially in patients with heart diseases. However, the causal effect of circulating cTnI on stroke remains unclear. **Methods and Results** This study employed mendelian randomization (MR) analysis to determine the associations between genetically predicted circulating cTnI levels and stroke and its subtypes. Summary-level data for exposure and outcomes were generated from different genome-wide association studies. Single-nucleotide polymorphisms (SNPs) associated with circulating cTnI at genome-wide significance level were employed as instrumental variables (IVs). This study used fixed-effect inverse-variance weighted (IVW) as the main method for pooling MR estimates. Sensitivity analyses and multivariable MR analyses were carried out to assess the robustness of the results . With fixed-effects IVW method, found genetically elevated plasma cTnI levels may have a causal effect on the risk of cardioembolic stroke (CES) ($P < 0.01$). However, after adjusting for atrial fibrillation and smoking in multivariable MR analysis, this causal association no longer existed. In addition, we found no causal effect of cTnI on the risk of stroke and its other subtypes, including any ischemic stroke, large artery stroke, cardioembolic stroke, small vessel stroke, and intracerebral hemorrhage. These results were consistent across sensitivity analyses. **Conclusion** Overall, this study provides little evidence that increased serum cTnI levels lead to a higher risk of stroke.

[Key words] Cardiac troponin I; Well-established biomarker; Heart diseases

TRPV1 channels regulate hypoxia-induced oxidative stress and cardiomyocyte apoptosis via the CaMKII/CREB/NGF axis in vitro

CHEN Qi　YE Lifang　WANG Shaomei　WANG Huan　WANG Lihong
Zhejiang Provincial People's Hospital, Hangzhou 310014, China

[Abstract] Transient receptor potential vanilloid 1 (TRPV1) is a ion channel which expressed in the cardiovascular system. In this study, the effects of TRPV1 on hypoxia-induced cardiomyocyte apoptosis and the mechanisms were analyzed. First, HL-1 cardiomyocytes were incubated in a hypoxic incubator, and TRPV1 expression was measured at different time points, the results showed that Hypoxia significantly increased TRPV1 expression in HL-1 cardiomyocytes. In addition, the TRPV1 channel, the CaMKII pathway, the CREB pathway and AP-1 protein expression were inhibited or down-regulated individually, we found that inhibition of TRPV1 and the CaMKII pathway reduced hypoxia-induced CaMKII phosphorylation and CREB activation. Decreased CREB pathway activation reduced Fos protein and c-Fos mRNA expression but had no effect on c-Jun mRNA levels in hypoxic HL-1 cardiomyocytes. siRNA targeting c-Fos and c-Jun down-regulated AP-1 and NGF expression. Then, anti-NGF neutralizing antibody (nAb) were used to observe the effects on oxidative stress, the results exhibited that treatment with anti-NGF nAbs further increased MDA levels, NADPH oxidase activity and Bax expression, while decreasing GSH levels and Bcl2 expression in hypoxic HL-1 cardiomyocytes.

Furthermore, the effects of the above treatments on cardiomyocyte viability and apoptosis were examined, hypoxia, TRPV1 channel antagonists, CaMKII pathway inhibitors, CREB pathway inhibitors, c–Fos and c–Jun siRNA, and anti–NGF nAb increased hypoxia–induced HL–1 cardiomyocyte apoptosis, while SOD treatment reversed these effects. This study results suggest that TRPV1 regulates the CaMKII/CREB/NGF axis, reduces oxidative stress and protects hypoxia–induced HL–1 cardiomyocytes in vitro. TRPV1 may be an important therapeutic target for the treatment of ischemic cardiomyopathy.

[Key words] Transient receptor potential vanilloid 1; Ion channel; Cardiovascular system

A randomized comparison of two paclitaxel–coated balloons for the treatment of in–stent restenosis: the LONGTY ISR China randomized trial

HU Po

The Second Affiliated Hospital, College of Medicine, Zhejiang University, Hangzhou 310000, China

[Abstract] **Objective** This study sought to evaluate the efficacy and clinical safety of the LONGTY drug–coated balloon (DCB) with that of SeQuent Please DCB in patients with in–stent restenosis (ISR). **Methods** This was a prospective, multicenter, randomized, noninferiority trial comparing LONGTY DCB with SeQuent Please DCB in patients with ISR. The primary endpoint was the target lesion late lumen loss at 9 months' follow–up. **Results** A total of 211 patients with ISR from 13 Chinese sites were included (105 were allocated to LONGTY DCB and 106 to SeQuent Please DCB). Device success was obtained in all patients.At nine–month angiographic follow–up, target lesion late lumen loss was (0.35 ± 0.42) mm with LONGTY versus (0.38 ± 0.45) mm with SeQuent Please ($P < 0.01$). Both groups had similar 1–year rates of target lesion revascularization (15.24% vs. 13.21%, $P > 0.05$). Over an extended follow–up of 2 years, the clinical endpoints, including cardiac death, myocardial infarction, and thrombus rate were very low and similar in both groups. **Conclusion** In this multicenter, head–to–head, randomized trial, the new–generation LONGTY DCB was noninferior to the SeQuent Please DCB for the primary endpoint of target lesion late lumen loss at 9 months.

[Key words] Efficacy; Clinical safety; LONGTY drug–coated balloon

The prognostic value of the age, bilirubin and albumin index in patients with heart failure

ZHONG Jiawei SUN Xingang CHEN Lu WANG Zhen HE Yuxian ZU Aohan CHEN Heng CHEN Miao JIANG Jiajia ZHENG Liangrong

The First Affiliated Hospital, Zhejiang University School of Medicine, Hangzhou 310000, China

[Abstract] **Objective** Liver dysfunction commonly occur in patient with heart failure (HF). The age, bilirubin, and albumin (ABA) index, a new noninvasive and easily calculated indicator for predicting liver fibrosis, was recently found to have higher efficiency than others, like fibrosis–4 (FIB–4) score. It is not clear that whether ABA index at admission can predict adverse outcome in patients with HF. **Methods** We retrospectively analyzed 245 consecutive patients with HF from December 2017 to December 2019 in a single center. The endpoint was a composite of all–cause death or rehospitalization for cardiovascular diseases within 2 years after admission. The prognostic predicting ability of ABA index

and FIB–4 score for adverse outcomes was evaluated. **Results** Univariate analysis showed that a higher ABA index ($P<0.01$), but not FIB–4 score ($P>0.05$), was associated with adverse outcomes within 2 years after admission. However, after adjusting for known prognostic factors, neither ABA index ($P>0.05$)nor FIB–4 score($P>0.05$) has independent predictive ability. **Conclusion** The ABA index is a promising predictor for prognosis in Chinese patients with HF. This discovery provides a new index to predict adverse outcomes for HF, however, needs to be confirmed in a large cohort urgently.

[Key words] Liver dysfunction; Heart failure; Albumin

Sanguinarine upregulated miR–210 expression level by stabilizing G–quadruplex to protect against myocardial ischemia/reperfusion injury

ZHANG Shiqin XU Ming

The Second Affiliated Hospital Zhejiang University School of Medicine, Hangzhou 310000, China

[Abstract] Objective To screen out one natural alkaloid which upregulated miR–210 expression by stabilizing the G–quadruplexes(G4) to protect against myocardial ischemia/reperfusion injury. **Methods** Bioinformatics analysis to analyze the potentiality of G–rich sequences located upstream of miR–210 gene to form specific nucleic acid secondary structure–G–quadruplex. Circular dichroism spectroscopy, ionization electrospray mass spectrometry, dimethyl sulfate foot printing experiments were performed to verify the formation of G–quadruplex upstream of miR–210 and to screen natural small molecule ligands based on the G–quadruplex. qPCR was used to detect the expression level of miR–210. Echocardiography was used to measure cardiac function. Evans Blue–TTC staining was used to evaluate myocardial infarct size, TUNEL staining to measure cardiomyocyte apoptosis. **Results** Here, this study found that there was a G–rich sequence located upstream of MIR–210, which was validated could form a non–canonical nucleic acid secondary structure, G4. Knockout or mutation of the G4 sequence significantly downregulated the expression level of miR–210. This study screened hundreds of traditional Chinese medicines, sanguinarine, a natural alkaloid with high affinity was selected as a ligand for binding and stabilizing the G–quadruplex. Sanguinarine protected cardiac function through significantly decreasing myocardial infarct size, cardiomyocyte apoptosis in the rat model of myocardial ischemia–reperfusion injury. **Conclusion** Sanguinarine up–regulated miR–210 expression level, decreased myocardial infarct size, cardiomyocytes apoptosis, which protected cardiac function.

[Key words] MicroRNA–210; Cardiovascular diseases; G–quadruplexes

The accuracy of left ventricular ejection fraction derived from deep neural network based coronary CT left ventricular segmentation:an observational clinical study

WANG Heyang XIANG Jianping LI Changling

The second Affiliated Hospital of Medical College of Zhejiang University, Hangzhou 310000, China

[Abstract] Objective To observe the accuracy of left ventricular ejection fraction derived from deep neural network

based coronary CT left ventricular segmentation, using a ultrasound ejection fraction value of 50% as the reference for diagnosing cardiac dysfunction. **Methods** This study was conducted at a single-center as a retrospective study in patients undergoing coronary CTA and classic cardiac ultrasound within 1 month. left ventricular ejection fraction analyses based on deep neural network were performed by Mailiu Biotechnology Co., Ltd. and were blinded for the personnel responsible for classic cardiac ultrasound data collection and downstream comparison. LVEFultra < 50% classified patients as having cardiac dysfunction. The primary endpoint was defined as the sensitivity of LVEFCT. **Results** The diagnostic performance of LVEFCT for identifying cardiac dysfunction were sensitivity of 91.4% , specificity of 92.7%, negative predictive value of 83.2%, positive predictive value of 96.5%, and accuracy of 91.8% , respectively. The Area under curve (AUC) was 0.977 when diagnostic value was investigated by ROC method ($P < 0.01$). **Conclusion** the overall diagnostic accuracy levels of deep neural network based coronary CT left ventricular segmentation were close with classic cardiac ultrasound in assessing cardiac dysfunction.

[Key words] Left ventricular ejection fraction;Cardiac dysfunction;CT

AGK acetylation contributes to PE-induced H9C2 cardiomyocyte hypertrophy and mitochondrial cristae dysfunction

YANG Yi

The Second Affiliated Hospital of Medical College of Zhejiang University, Hangzhou 310009, China

[Abstract] Objective To elucidate the role of acylglycerol kinase (AGK) in cardiac hypertrophy. **Methods** Cultured H9C2 cardiomyocytes were treated with phenylephrine (PE) and hypertrophy was confirmed by immunofluorescence of α-smooth muscle actin (α-SMA). Mitochondrial cristae structure was observed under transmission electron microscope. Cellular oxidative phosphorylation was assessed using OROBOROS Oxygraph-2k. Protein expression levels were determined using western blot and protein interactions were detected using co-immunoprecipitation. Protein silencing was achieve using transfection of shRNA and siRNA. Statistical analyses were conducted using Student's *t* test. **Results** We show that PE triggered hypertrophy and mitochondrial cristae dysfunction in cultured H9C2 cardiomyocytes and upregulated cellular AGK acetylation. AGK deacetylation in H9C2 cells was mediated by SIRT3, and enhancing of AGK acetylation by silencing SIRT3 worsened PE-induced hypertrophy and mitochondrial cristae dysfunction. Furthermore, Silencing of AGK induced mitochondrial cristae disorganization and OPA1 downregulation. **Conclusion** These results show that AGK acetylation contributes to PE-induced H9C2 cell hypertrophy. Mechanistically, AGK promotes OPA1 downregulation and mitochondrial cristae disorganization in H9C2 cardiomyocytes.

[Key words] Cardiac hypertrophy; Pathological pre-stage; Heart failure

Tetrandrine ameliorates myocardial ischaemia reperfusion injury through miR–202–5p/TRPV2

JIANG Wenbing

Wenzhou Central Hospital, Wenzhou 325000, China

[Abstract] **Objective** Aimed to investigate the therapeutic effects of Tetrandrine (Tet) on myocardial ischaemia reperfusion (I/R) injury and probe into underlying molecular mechanism. **Methods** H9C2 cells were divided into hypoxia/oxygenation (H/R) group, H/R + Tet group, H/R + Tet + negative control (NC) group, H/R + Tet + miR–202–5p inhibitor group. RT–qPCR was utilized to monitor miR–202–5p and TRPV2 expression, and TRPV2 protein expression was detected via western blot and immunohistochemistry in H9C2 cells. Cardiomyocyte apoptosis was evaluated through detection of apoptosis–related markers and flow cytometry. Furthermore, myocardial enzyme levels were detected by ELISA. Rats were randomly separated into sham operation group,I/R group,I/R + Tet group (50 mg/kg),I/R + Tet + NC group,I/R + Tet + miR–202–5p inhibitor group. miR–202–5p and TRPV2 mRNA expression was assessed by RT–qPCR. TRPV2 protein expression was detected through western blot and immunohistochemistry in myocardial tissues. Apoptotic levels were assessed via apoptosis–related proteins and TUNEL. Pathological changes were observed by H&E staining. Myocardial infarction size was examined by Evans blue–TCC staining. **Results** Abnormally expressed miR–202–5p as well as TRPV2 was found in H/R H9C2 cells and myocardial tissues of I/R rats, which was ameliorated following Tet treatment. Tet treatment significantly suppressed H/R– or I/R–induced cardiomyocyte apoptosis. ELISA results showed that CK–MB and LDH levels were lowered by Tet treatment in H/R H9C2 cells and serum of I/R rats. H&E staining indicated that Tet reduced myocardial injury in I/R rats. Also, myocardial infarction size was lowered by Tet treatment. The treatment effects of Tet were altered following co–treatment with miR–202–5p inhibitor. **Conclusion** The findings revealed that Tet may ameliorate myocardial I/R damage via targeting miR–202–5p/TRPV2 axis.

[Key words] Tetrandrine;Myocardial ischaemia reperfusion;MiR–202–5p;TRPV2

Tetrandrine attenuates left ventricular dysfunction in rats with myocardial infarction

JIANG Wenbing

Wenzhou Central Hospital, Wenzhou 325000, China

[Abstract] **Objective** To hypothesize that Tetrandrine attenuates left ventricular dysfunction and remodeling in rats with myocardial infarction. **Methods** Sprague–Dawley rats were randomly divided into 6 groups (n =5 each group) as follows: healthy control group, sham operation group, myocardial infarction model group, myocardial infarction + low–dose tetrandrine group (10 mg/ kg), myocardial infarction + high–dose tetrandrine group (50 mg/kg), myocardial infarction + high–dose tetrandrine group (80 mg/kg). The left ventricular end–diastolic and end–systolic diameters (LVIDd, LVIDs), ejection fraction (EF%) and left ventricular short–axis shortening rate (FS%) were measured using ultrasound. The pathological changes were observed by hematoxylin and eosin (H&E). The left ventricular tissue section TUNEL staining was presented. Furthermore, the triglyceride (TG), total cholesterol (TC), high density lipoprotein (HDL) and low density lipoprotein (LDL) in the arterial blood were examined. Intracellular Ca^{2+} homeostasis–related proteins including ryanodine receptor (RyR) calmodulin (CaM), CaM–dependent protein kinase II δ (CaMKII δ), protein kinase A (PKA), FK506 binding protein 12.6 (FKBP12.6) were measured using western blot. **Results** Ultrasound results showed

that in the myocardial infarction model rats, the levels of LVIDd and LVIDs were significantly higher, however, the levels of EF% and FS% were lower compared to sham operation group, which was alleviated by tetrandrine. H&E results showed that tetrandrine alleviated the pathological characteristics of myocardial infarction model rats. Furthermore, we found that tetrandrine significantly inhibited myocardial apoptosis in rats with myocardial infarction. Tetrandrine significantly inhibited the levels of TG, TC and LDL and increases the levels of HDL in the arterial blood of rats with myocardial infarction. Further analysis found that tetrandrine might alleviate myocardial infarction by regulating calcium homeostasis–related proteins. **Conclusion** Our findings revealed that tetrandrine attenuates left ventricular dysfunction in rats with myocardial infarction, which might be related with intracellular Ca^{2+} homeostasis.

[Key words] Myocardial infarction; Tetrandrine; Left ventricular remodeling; Apoptosis;Calcium homeostasis

Soluble receptor for advance glycation end–products inhibits ischemia/ reperfusion–induced myocardial autophagy via the STAT3 pathway

DANG Mengqiu

The Second Affiliated Hospital of Zhejiang University School of Medicine, Hangzhou 310009, China

[Abstract] The pathogenesis of myocardial ischemia/reperfusion (I/R) is poorly understood, but recent evidence suggests that autophagy plays crucial roles in I/R injuries. Soluble receptor for advanced glycation end–products (sRAGE) exerts protective effects during I/R by decreasing cardiac apoptosis, which is mediated via increasing the ubiquitin proteasome system (UPS) and signal transducer and activator of transcription 3 (STAT3). The present study examined the effects and mechanisms of sRAGE on I/R–triggered cardiac autophagy. I/R was performed in mice or primary neonatal cardiomyocytes with or without sRAGE administration or overexpression. Cardiac function and infarct size were detected in mouse hearts. Apoptosis, autophagy and autophagy–related signaling pathways were detected in mouse hearts and cardiomyocytes. The results demonstrated that sRAGE significantly improved cardiac function and reduced infarct size during I/R in mice. sRAGE inhibited I/R–induced apoptosis, which correlated with a reduction in autophagy–associated proteins, including ATG7, Beclin–1 and microtubuleassociated protein 1 light chain 3 (LC3). sRAGE reduced autophagosome formation during I/R in vivo and in vitro. sRAGE significantly activated STAT3, but not mammalian target of rapamycin (mTOR), during I/R in vivo and in vitro, and suppression of STAT3 abolished the sRAGE inhibition of autophagy during I/R in vitro. Activation of autophagy using ATG7 overexpression with an adenovirus significantly abolished the sRAGE–induced reduction of cardiac apoptosis during I/R. These results suggest that sRAGE inhibits I/R injuries in the heart via a decrease in autophagy, a process that is dependent on STAT3 activation.

[Key words] Ischemia; Reperfusion; STAT3

Risk factors for left atrial thrombi and spontaneous echo contrast in patients with atrial fibrillation and hypertension: a single–center retrospective study

ZHANG Xuan　YANG Jian

The First Affiliated Hospital of Zhejiang University School of Medicine, Hangzhou 310003, China

[Abstract] **Objective** Left atrial thrombi (LAT) is the main risk factor for stroke in patients with atrial fibrillation (AF). Spontaneous echo contrast (SEC) is known as a change in the early stage of LAT. On the other hand, hypertension is the most common cardiovascular complication of AF. Therefore, for AF patients with hypertension, more clinical evidence is needed to guide the prediction and management of LAT and SEC. **Methods** Retrospectively analyze AF patients with hypertension within 6 years (from January 2014 to December 2019) in a single center, and summarize their clinical information and transesophageal echocardiography (TEE) test results . The LAT or SEC reported by TEE are the main observation indicators. Use binary logistic regression analysis, propensity score matching (PSM) analysis, receiver operating characteristic analysis to find the risk factors of LAT. **Results** One thousand and eighty four people were included in the study, of which 439 received anticoagulant therapy, 21 found LAT, and 46 found SEC. After binary logistic regression analysis and PSM analysis, abnormal uric acid metabolism (abUA) is an independent risk factor for LAT in AF patients with hypertension. In addition, enlarged left atrium (LA) is an independent risk factor for SEC. **Conclusion** In patients with AF and hypertension, the risk factors of LAT and SEC are different. In this study, abUA is an independent risk factor for LAT, and the enlargement of LA is a risk factor for SEC.

[Key words] Left atrial thrombi;Atrial fibrillation;Spontaneous echo contrast

Genetic liability to blood pressure, antihypertensive drugs, and cardiovascular disease risk

LU Yunlong　YIN Xiang　ZHENG Liangrong

The First Affiliated Hospital, Zhejiang University School of Medicine, Hangzhou 310003, China

[Abstract] The study conducted mendelian randomization (MR) analyses to evaluate the association of blood pressure, antihypertensive drugs and risk of cardiovascular diseases (CVD). Genetic variants associated with systolic blood pressure, diastolic blood pressure, and antihypertensive drugs (including β–blockers and calcium channel blockers) were derived from a genome–wide association study of the International Consortium for Blood Pressure and UK Biobank. The associations with risk of CVD, including atrial fibrillation, coronary artery disease, myocardial infarction and heart failure, were combined by inverse–variance weighted method. Genetically determined higher systolic blood pressure (10 mmHg increase) and diastolic blood pressure (5 mmHg increase) were associated with increased risks of atrial fibrillation, coronary artery disease, myocardial infarction and heart failure. Both β–blockers and calcium channel blockers (10 mmHg decrement in SBP) significantly reduced risks of CVD. This study shows that genetic liability to higher blood pressure increases the risk of CVD, and supports the protective effect of antihypertensive drugs on CVD.

[Key words] Mendelian randomization; Cardiovascular diseases;Blood pressure

The interplay between mitochondria and store–operated Ca^{2+} entry: emerging insights into cardiac diseases

NAN Jinliang　LI Jiamin　LIN Yinuo　u-Hammad Saif Ur Rahman M　LI Zhengzheng　ZHU Lingjun

The Second Affiliated Hospital, Zhejiang University School of Medicine, Hangzhou 310009, China

[Abstract] Store–operated Ca^{2+} entry (SOCE) machinery, which includes Orai, TRPCs, and STIM1, is the key to cellular calcium homeostasis. The following characteristics of mitochondria are involved in the physiological and pathological regulation of cells: mitochondria mediate calcium uptake through calcium uniporter.Mitochondria are regulated by mitochondrial dynamic related proteins (OPA1, Mfn1/2, and Drp1) and form mitochondrial networks through continuous fission and fusion,mitochondria supply NADH to the electron transport chain through the Krebs cycle to produce ATP,under stress, mitochondria will produce excessive ROS to regulate mitochondria–ER interactions and related signaling pathways. It has been validated that both SOCE and mitochondria play critical roles in mediating cardiac hypertrophy, diabetic cardiomyopathy, and cardiac ischemia–reperfusion injury. All the mitochondrial characteristics mentioned above are determinants of SOCE activity and vice versa. The Ca^{2+} signaling dictates the reciprocal regulations between mitochondria and SOCE in accordance with specific pathological conditions of cardiomyocytes. The coupling of mitochondria and SOCE is essential for the pathological process of the heart. The study review the researches focusing on the reciprocal regulations between mitochondria and SOCE and provide potential interplay patterns of them in cardiac diseases.

[Key words] SOCE;Mitochondria;Review

Efficacy and safety of left atrial appendage closure with MemoLefort® in first 100 Chinese nonvalvular atrial fibrillation patients

CHANG Xiaoxin　XU Yawei　ZHANG Shu

Shanghai Tenth People's Hospital of Tongji University, Shanghai 200072, China

[Abstract] **Objective** This was a prospective, multicenter, single–arm trial to confirm the safety and efficacy of the MemoLefort® left atrial appendage closure (LAAC) device for ischemic stroke prevention in patients with nonvalvular atrial fibrillation (NVAF) in China. **Methods** One hundred patients over 18–years–old with non–valvular atrial fibrillation who had CHADS score 1were enrolled in this multi–center, single–arm trial. Ninety–nine patients in the sequence underwent percutaneous closure of the LAA. Follow–up visits were performed up to 1 year post–implant. **Results** The LAA closure rate for primary end point at 1 year follow–up was 97.4%, achieving the prespecified performance goal. The 2nd co–secondary endpoint was composite of all stroke,systemic embolism, hemorrhagic incidence,peri–procedure complications and cardiovascular/unexplained death. There was no hemorrhagic stroke or systemic embolism, and there were 5 cases of ischemic stroke classified as nondisabling based on the modified Rankin scale score. In the ITT cohort there was 4 cardiovascular death reported during the 1–year follow–up.The Clinical Events Committee adjudicated that one case may be related to the device, two cases have nothing to do with the device, and one case probably not be related to the device.One case of device associated embolism related to none of the ischemic stroke

incidence. **Conclusion** First result of the 100 patients trial demonstrated that the MemoLefort® LAAC device is an effective and safe nonphamarcological therapy for stroke prevention in Chinese novalvular atrial fibrillation patients.

[Key words] Left atrial appendage closure;Nonvalvular atrial fibrillation; Stroke

Nicotine induce mast cells degranulation to increase macrophage migration and promote foam cell formation

WANG Chen

The Second Affiliated Hospital, Zhejiang University School of Medicine, Hangzhou 310009, China

[Abstract] **Objective** To study whether mast cell act a key mediator in macrophage function and foam cell function in an in vitro model. **Methods** Primary cultured murine bone marrow–derived mast cells (BMCMCs) and murine abdominal perfusion–derived macrophages were used in this study. After 4 weeks'culturing in medium with recombinant murineIL–3, greater than 95% of the cell population was consisted of mast cells as proved by toluidine blue stain and immunostaining of mast cell specific chymase and tryptase. Mature mast cells were harvested and devided into 5 groups to be treated with PBS as a negative control, mast cell degranulation stimulator compound 48/80 as a positive control,100 μg/mL nicotine,100 μg/mL nicotine with 100 mmol/L mast cell stablizer disodium cromoglicate pretreatment and nicotine 100 μg/mL with nicotine receptor nAChR blocker 10 μg/mL mecamylamine pretreatment.At 0.5hr,1hr,2hrs after nicotine treatment,conditioned supernatants were harvested for β–hexosaminidase activity test to analyze the mast cell degranulation level,then the total supernatants were harvested and used to treat the murine peritoneal macrophages for 24 hrs.Migration ability of macrophages was tested by transwell assay, while foam cell foamation ability was tested by oil red O staining to show the OxLDL uptake. **Results** The study found that 100 μg/mL nicotine significantly induced mast cell degranulation, and this phenomenon has been suppressed when preteated by mast cell stablizer disodium cromoglicate or nAChR blocker mecamylamine pretreated mast cell. Foam cell formation ratio in the compound 48/80(71.0%±9.9%) and nicotine 100 μg/ml conditional treatment group(70.4%±14.7%) were significantly higher when comparing to the negative control(47.3%±4.2%)and mast cell stablizersodium cromoglicate pretreatment (44.6%±10.3%) andnAChR blocker mecamylamine pretreatment(50.1%±11.0%) inhibited the foam cell formation. Migration ability in the compound 48/80(104±23/field) and nicotine conditional treatment group(102±16/field) were also significantly higher comparing with the negative(33±14/field) and mast cell stablizersodium cromoglicate 100 mmol/L pretreatment(59±16/field) and nicotine 100μg/ml with nAChR blocker mecamylamine treatment conditional supernatant treatment group(32±11/field). **Conclusion** Nicotine might induce mast cell degranulation through nAChR and then activate mast cell to release a range of proinflammatory mediators to increase the migration ability of macrophages as well as the foam cell formation. Administration of mast cell stabilizer and nAChR blocker revealed the potential of applying mast cell stabilizer in preventing nicotine induced atherogenesis.

[Key words] Bone marrow–derived mast cells;Macrophage migration;Foam cell formation

Obstructive sleep apnea and atrial fibrillation: insights from a bidirectional Mendelian randomization study

SUN Xingang　CHEN Lu　HE Yuxian　LU Yunlong　ZHENG Liangrong

The First Affiliated Hospital of Zhejiang University School of Medicine, Hangzhou 310003, China

[Abstract] The study conducted a two-sample bidirectional Mendelian randomization (MR) study to clarify the causal inference between obstructive sleep apnea (OSA) and atrial fibrillation (AF). **Methods** The study obtained genetic instruments from genome-wide association studies (GWAS) for OSA (n=217 955) and AF (n=1 030 836), respectively. The fixed-effects inverse-variance-weighted (IVW) method was used as the main MR method, supplemented by several sensitivity analyses. For replication, another AF GWAS dataset was used to validate the causal effect of OSA on AF. Furthermore, multivariable MR analyses were performed to obtain direct MR estimates adjusting for potential confounders.Result Genetic liability to OSA was significantly associated with a higher AF risk in the fixed-effects IVW method (OR=1.210,95%CI:1.119-1.307,P<0.05).The causal estimates were consistent in MR sensitivity analyses as well as in replication analyses, and the significance remained after adjusting for potential confounders. In the reverse MR analyses, there was no evidence supporting the causal effect of AF on OSA. **Conclusion** The MR study strengthened the evidence of genetic liability to OSA with a higher AF risk. Whereas, genetic liability to AF was not causally associated with OSA.

[Key words] Mendelian randomization;Atrial fibrillation;Obstructive sleep apnea

Body mass index: an effective predictor of ejection fraction improvement in heart failure

YE Lifang　ZHENG Yaru　WANG Lihong

Zhejiang Provincial People's Hospital, Hangzhou 310014, China

[Abstract] **Objective** Heart failure patients with higher body mass index (BMI) exhibit better clinical outcomes. Therefore, we assessed whether the BMI can predict left ventricular ejection fraction (EF) improvement following heart failure. **Methods** The study included 184 patients newly diagnosed with dilated cardiomyopathy and reduced EF in our center and who underwent follow-up examination of EF via echocardiography after 6 months. The EF improved at 6 months in 88 participants, who were included in the heart failure with recovered EF (HFrecEF) subgroup. Patients in whom the EF remained reduced were included in the heart failure with persistently reduced EF (persistent HFrEF) subgroup. **Results** The analyses revealed that EF increase correlated with age (r =-0.254), left ventricular diastolic dimension (LVDD, r =-0.210), diabete, brain natriuretic peptide (r=-0.199) and BMI grade (all P<0.05). BMI grade was significantly associated with elevated EF after adjustment for other variables (P<0.05). On multivariable analysis, compared to patients with persistent HFrEF, those with HFrecEF had higher BMI (OR= 2.342 per one standard deviation increase,P<0.05) and lower LVDD (OR=0.466 per one standard deviation increase,P<0.05). ROC-curve analysis data showed that BMI>22.66 kg/m2 (sensitivity 0.841, specificity 0.594, AUC=0.745, P<0.05) indicate high probability of EF recovery in 6 months. **Conclusion** Our data suggest that higher BMI is strongly correlated with the recovered EF and that BMI is an effective predictor of EF improvement in patients with heart failure and reduced EF.

[Key words] Body mass index;Predictor;Ejection fraction;Heart failure

OPG/TRAIL ratio as a predictive biomarker of mortality in patients with type A acute aortic dissection

LU Jie LI Ping MA Ke LI Yang YUAN Hui ZHU Junming DUAN Weixun OU Jingsong HUANG Yonghong WU Long PAN Xueliang ZHANG Hui DU Jie LI Yulin

Beijing Anzhen Hospital affiliated to Capital Medical University, Beijing 100029, China

[Abstract] **Objective** Following hospital discharge, patients with type A acute aortic dissection (TA-AAD) may present an increase in mortality risk. However, little is known about specific biomarkers associated with post-discharge survival, and there is a paucity of prognostic markers associated with TA-AAD. **Methods** The study identify nine candidate proteins specific for patietns with TAAAD in a cross-sectional dataset by unbiased protein screening and in-depth bioinformatic analyses. In addition, the study explore their association with short-term and long-term mortality in a derivation cohort of patients with TA-AAD, including an internal (n=300) and external (n=236) dataset. An elevated osteoprotegerin (OPG)/tumour necrosis factor-related apoptosis-inducing ligand (TRAIL) ratio was the strongest predictor of overall, 30-day, post-30-day mortality in both datasets and was confirmed to be a strong predictor of mortality in an independent validation cohort (n=400). **Results** Based on OPG/TRAIL ratio-guided risk stratification, patients at high risk (> 33) had a higher 1-year mortality (55.6% vs. 4.3%,68.2% vs. 2.6%) than patients at low risk (< 4) in both cohorts. **Conclusion** The study show that an elevated OPG/TRAIL ratio is associated with a significant increase in short-term and long-term mortality in patients with TA-AAD.

[Key words] OPG;TRAIL;Type A acute aortic dissection

Elucidating the feasibility of using angiotensinogen and its redox status as predictors for sepsis

RONG Jiabing

The Second Affiliated Hospital of Zhejiang University School of Medicine, Hangzhou 310009, China

[Abstract] **Objective** To investigate whether the level of angiotensinogen (AGT) and its redox status can predict the occurrence of sepsis or not. **Methods** The study enrolled 79 consecutive patients admitted to the intensive care unit (ICU), dividing them into two groups: septic (n=45) and no septic (n=34). Clinical indicators were recorded: lactate, C-reactive protein (CRP), alanine transaminase (ALT), aspartate transaminase (AST), creatinine (Cr), and blood urea nitrogen (BUN). The total AGT levels were determined by ELISA.Oxidized AGT levels and Reduced AGT levels were determined by m-PEG Western blot. **Results** The ratio of Oxidized to Reduced AGT (Oxidized AGT/Reduced AGT), total AGT, lactate, CRP, AST, Cr, and BUN levels were higher in the sepsis group. In the sepsis group, correlation analysis found that total AGT level was positively correlated with lactate (r=0.313, P < 0.05) and BUN (r=0.369, P < 0.05). There was no correlation between total AGT and CRP, ALT, AST, and Cr (all P > 0.05). Oxidized AGT/Reduced AGT was positively correlated with lactate (r=0.312,P < 0.05) and CRP (r=0.360,P < 0.05).There was no correlation between Oxidized AGT/Reduced AGT and ALT, AST, Cr, and BUN (all P > 0.05).No correlation was found between total AGT or Oxidized AGT/Reduced AGT and various clinical indicators in the control group (all P > 0.05). The area under the curve (AUC) of lactate, total AGT, and Oxidized AGT/Reduced AGT were 0.7765, 0.6320, and 0.7170 respectively. By

evaluating net reclassification improvement (NRI) and integrated discrimination improvement (IDI) indicators, it was found that the combined model (lactate and Oxidized AGT/Reduced AGT) had improved ability in predicting the occurrence of sepsis compared to a single marker (IDI=4.72%, $P<0.05$). **Conclusion** The total AGT and Oxidized AGT/Reduced AGT were elevated in septic patients. The combined application of Oxidized AGT/Reduced AGT and lactate has important implication for predicting the occurrence of sepsis.

[Key words] Angiotensinogen;Sepsis;Feasibility

Association between optical coherence tomography and functionally severity assessed by quantitative flow ratio in coronary intermediate lesions

XUE Yuan MENG Haoyu WANG Liansheng

The First Affiliated Hospital of Nanjing Medical University, Nanjing 211103, China

[Abstract] Objective The study aimed at evaluating the diagnostic value exhibited by optical coherence tomography (OCT) parameters for identifying coronary stenosis with functional significance under the assessment of the quantitative flow ratio (QFR). **Methods** In 93 patients, 115 intermediate coronary lesions were assessed by OCT and QFR measurements, ICL was defined as a coronary lesion according to visual estimation with diameter stenosis between 50% and 90%. Functional relevance stenose was considered as severe when QFR≤0.80. **Results** Percentage area stenosis (AS) was (68.4%±8.8%) with minimal lumen area (MLA) (3.11±1.54) mm² by OCT. the average QFR was (0.82±0.10). OCT exhibited a moderate diagnostic value in general between QFR and OCT-measured MLA (AUC=0.83, 95%*CI*: 0.75-0.90) and AS (AUC=0.87, 95%*CI*:0.81-0.94). The optimal cut-off values exhibited by OCT-measured anatomic parameters for identifying stenosis that exhibited QFR ≤ 0.80 were 2.53 mm^2 (sensitivity 0.85, specificity 0.71) for MLA and 69% (sensitivity 0.84, specificity 0.78) for AS. AS were compared with independent t-test between OCT and QFR measurements, which shows no significant difference. **Conclusion** OCT-derived relevant intraluminal parameters have a good diagnostic value for predicting the functional ischemia evaluated by QFR. QFR may offer a rapid, simple method to evaluate area stenosis in coronary intermediate lesions.

[Key words] Optical coherence tomography;Quantitative flow ratio;Area stenosis

Exosomes secreted by Bone marrow-derived mesenchymal stem cells could inhibit valve interstitial cells calcification in vitro

HU Wangxing

The Second Hospital Affiliated to Zhejiang University School of Medicine, Hangzhou 310009, China

[Abstract] Objective Calcific aortic valve disease is an active process involving a wide range of pathologic changes,including lipid retention, inflammation, phosphate signalling and osteogenic transition. Valve interstitial cells(VICs) are the most prevalent cells in the heart valve and maintain normal valve structure and function. Bone marrow-derived mesenchymal stem cells are widely used for the treatment of diseases with its characters of antioxidant, anti-apoptosis, inhibition of inflammation, and regulation of immune responses ,among which exosomes derived from

MSCs appear to be great potential in therapy. The study hypothesized that exosomes, derived from mesenchymal stem cells, could inhibit the progression of CAVD in mice. **Methods** In order to determine whether exosomes could inhibit the transformation of VICs into osteoblasts, the study add the exosomes secreted by MSC in the calcification induction medium, and then detect the calcification markers, including Runx2, ALP, OC. The study also evaluated the expression of calcification markers by adding EXO to the inflammatory factor–induced calcification model in vitro. **Results** In this study we found that exosomes secreted by MSCs could inhibit the transformation of VIC into osteoblasts. Meanwhile in the inflammatory factor–induced model also appeared to be the same results. **Conclusion** The study found that exosomes secreted by MSCs could inhibit the phenotypic transformation of valve interstitial cells into osteoblasts in vitro.

[Key words] Valve interstitial cells;Calcific aortic valve disease;Phenotypic transformation

Prevalence, predictors, and impact of coronary artery ectasia in patients with atherosclerotic heart disease

XI Ziwei QIU Hong GUO Tingting WANG Yong LI Jianan LI Yang ZHENG Jianfeng

Fuwai Hospital, National Center for Cardiovascular Diseases, Chinese Academy of Medical Sciences and Peking Union Medical College, Beijiang 100037, China

[Abstract] **Objective** The clinical significance of coronary artery ectasia (CAE) was poorly understood. This study aimed to investigate the prevalence, potential predictors, and prognostic significance of CAE in patients with atherosclerotic coronary artery disease. **Methods** Consecutive patients undergoing PCI during January 2016 to December 2018 were included in our study and were followed up for at least 1 year. CAE was diagnosed when an abnormal dilation of > 1.5 folds the diameter of adjacent normal segments was found in angiography. **Results** A total of 590 patients with CAE were identified from 36 790 patients who underwent PCI according to coronary angiography and the overall rate of CAE among was 1.6% (95%*CI*:1.5%–1.7%). According to multivariable analysis, variables including BMI > 30 kg/m^2 (*RR*=2.413), ever–smoking (*RR*=1.669), hypertension (*RR*=1.221), acute myocardial infarction at admission (*RR*=1.343), no diabetes (*RR*=0.810), previous myocardial infarction (*RR*=1.545), no left main disease (*RR*=0.632) and multiple–vessel disease (*RR*=1.326), increased C–reactive protein (*RR*=1.006) were identified as predictors of CAE(all $P < 0.05$). Presence of CAE was not associated with the risk of adverse cardiovascular outcomes ($P < 0.05$). And the incidence of cardiovascular death or myocardial infarction also did not significantly differ between patients with or without CAE. **Conclusion** CAE occurs in 1.6% of patients undergoing PCI in this large cohort study. Higher BMI, ever–smoking, hypertension, acute myocardial infarction at admission, no diabetes, previous myocardial infarction, no left main disease, and multiple–vessel disease were predictors of CAE. And CAE has no significant impact on 1–year clinical outcomes after PCI.

[Key words] Coronary artery ectasia;Atherosclerotic heart disease;Prevalence

Comparison of silent stroke after transfemoral versus transapical aortic valve replacement in pure aortic regurgitation

DAI Hanyi　LIU Xianbao

The Second Hospital Affiliated to Zhejiang University School of Medicine, Hangzhou 310009, China

[Abstract] **Objective** To explore new cerebral ischemic lesions in pure native aortic valve regurgitation (pure AR) patients using diffusion-weighted magnetic resonance imaging (DW-MRI) and compare the difference between transfemoral (TF) and transapical (TA) TAVR. **Methods** The data of post-procedure silent stroke in patients with pure AR is still lacking.The prospective study enrolled consecutive patients with pure AR in our center from July 2018 to December 2020. Aortic stenosis defined as a peak aortic jet velocity of > 2.5 m/s on continuous-wave Doppler was excluded. The primary endpoint was to compare the ischemic lesions between TF and TA TAVR. **Results** There were 15 patients in TF TAVR group and 23 in TA TAVR group and the mean age was comparable between two groups[(71 ± 8) years vs. (70 ± 6) years,$P > 0.05$]. TF TAVR group had higher preoperative Society of Thoracic Surgeons scores [3.08(IQR:2.53~5.12) vs. 2.19(IQR:1.54 to 3.83),$P < 0.05$]. A higher numerically total ischemic lesions were observed in TA TAVR patients [4.0[2.0~11.0] vs 2.0[2.0~5.0],$P > 0.05$]. However, there was no significant differences between the two groups in the numbers, volume or distribution of ischemic lesions. **Conclusion** In the study existed silent stroke in pure AR TAVR patients with no difference between TF and TA TAVR groups. Multi-centers, prospective studies with more patients are warranted to confirm the present findings in the future.

[Key words] Pure native aortic valve regurgitation;Diffusion-weighted magnetic resonance imaging;Transfemora

CatLet score and Clinical CatLet score as predictors of long-term outcomes for patients with acute myocardial infarction undergoing delayed percutaneous coronary intervention

XU Jianping　SUN Beichen　HE Yongming

The First Affiliated Hospital of Soochow University, Soochow 215006, China

[Abstract] **Objective** Aimed at assessing whether the CatLet score (CS) and the Clinical CatLet score (CCS) predicted clinical outcomes for acute myocardial infarction (AMI) patients undergoing delayed percutaneous coronary intervention(PCI). **Methods** CS was calculated in 1 018 consecutively prospectively enrolled AMI patients. Primary endpoint was major adverse cardiac events (MACEs), a composite of myocardial infarction, cardiac death, and ischemia-driven revascularization. CCS was calculated using age, serum creatinine, and left ventricular ejection fraction. Tertile partitioning of CS and CCS were as follows: CS low≤12, CS mid 13~18, and CS top≥19,CCS low≤13, CCS mid 14~24, and CCS top≥25, respectively. **Results** Four-year hazard ratios (95%*CI*) for MACE were significantly higher with CS top compared with CS low, which was also the case for all-cause death, cardiac death, myocardial infarction, and revascularization. Stratifying outcomes across CCS tertiles resulted in similar results. Both scores were independent predictors of clinical outcomes after adjustment for a broad spectrum of risk factors. Areas-under-the-curve for CS and CCS for MACEs were 0.72(0.68-0.75) and 0.75(0.71-0.78), for all-cause death, 0.68(0.63-0.73) and 0.78(0.74-0.83),for cardiac death, 0.73(0.68-0.79) and 0.83(0.79-0.88), for myocardial infarction, 0.69(0.64-0.73) and 0.75(0.7-

0.79), and for revascularization, 0.66(0.61–0.7) and 0.63(0.58–0.68), respectively. Figure 1A–E showed Kaplan–Meier curves for MACEs, all–cause death, cardiac death, myocardial infarction, and revascularization at four years according to the CS tertiles. Figure 1F–J showed Receiver operating characteristic curves for these endpoints for CS and CCS. **Conclusion** CS and to a greater extent CCS were able to risk–stratify the long–term outcomes in AMI patients undergoing delayed PCI.

[Key words] CatLet;Clinical CatLet score;Percutaneous coronary intervention

Prognostic impact of periprocedural myocardial biomarker elevations and commonly used periprocedural myocardial infarction definitions after left main PCI

WANG Haoyu

Fuwai Hospital, Chinese Academy of Medical Sciences and Peking Union Medical College, Beijing 100037, China

[Abstract] Objective To assess the relationship of different thresholds of creatine kinase–myocardial band (CK–MB) and cardiac troponin (cTn) with subsequent mortality, and evaluate the prognostic significance of periprocedural myocardial infarction (PMI) according to various MI definitions in patients with left main (LM) disease. **Methods** The study enrolled 4 013 consecutive patients undergoing LM PCI at a single center from January 2004 to December 2016. CK–MB and cTnI were routinely collected at baseline and at frequent intervals between 8 and 48 hours after PCI, with additional draws required for elevated values or ongoing symptoms until declining values returned. PMI was also adjudicated by the Society for Cardiovascular Angiography and Interventions (SCAI), Academic Research Consortium–2 (ARC–2), and fourth Universal Definition of MI (UDMI) criteria. SCAI–defined PMI was adjudicated: (i) CK–MB $\geqslant 10\times$ URL (or cTn $\geqslant 70\times$ URL) or (ii) CK–MB $\geqslant 5\times$ URL (or cTn $\geqslant 35\times$ URL) plus one of the following: new pathological Q–waves in at least two contiguous leads or new persistent non–rate–related left bundle branch block. ARC–2–defined PMI was adjudicated for an absolute increment increase in cTn $\geqslant 35\times$ URL (or CK–MB $\geqslant 5\times$ URL) plus one of the following. **Results** Mean age was 60.1 years and 78.7% were men. Diabetes was present in 28.5% of patients and slightly more than half (51.8%) presented with unstable angina. Concomitant multivessel disease was present in 49.3% of patients, and the mean SYNTAX score was 22.7 ± 7.2. The distal LM was involved in 80.6% of cases. Distal LM bifurcation disease was treated with a provisional crossover technique in 72.6% of cases. 16.3% of patients had CK–MB $\geqslant 1\times$ URL and 67.6% had cTnI $\geqslant 1\times$ URL. PMI by the SCAI, ARC–2, and 4th UDMI definitions occurred in 53 (1.3%), 125 (3.1%), and 203 (5.1%) patients, respectively. A moderate correlation was present between the normalized peak cTnI and peak CK–MB values (r=0.62). The estimated geometric mean of the ratio of cTnI to CK–MB was 3.36 (95%*CI*: 3.13 to 3.62). The 3–year rate of CV mortality progressively increased with higher peak CK–MB values. **Conclusion** The insights from the present study may prove informative to standardize endpoints for future clinical trials. In this regard clinically relevant outcome measures should be included and actively surveilled, although equally important is not to overweight lesser measures of myonecrosis that are more frequently detectable but less strongly prognostic.

[Key words] Periprocedural myocardial infarction;Cardiac troponin;Creatine kinase–myocardial band

Impact of coronary lesion complexity in percutaneous coronary intervention: long-term outcomes from the large, Fuwai PCI registry

WANG Haoyu

Fuwai Hospital, Chinese Academy of Medical Sciences and Peking Union Medical College, Beijing 100037, China

[Abstract] **Objective** The present study sought to examine the prevalence, clinical characteristics and long-term outcomes of patients undergoing percutaneous coronary intervention (PCI) to complex lesions (3 vessels treated, ⩾3 stents implanted, ⩾3 lesions treated, bifurcation with 2 stents implanted, total stent length > 60 mm, treatment of chronic total occlusion, unprotected left main PCI, in-stent restenosis target lesion, and severely calcified lesion) in a prospective registry. **Methods** 10 167 consecutive patients undergoing PCI were prospectively enrolled in Fuwai PCI Registry. Clinical outcomes were stratified by procedure complexity, and further by number and type of complex features. The primary ischemic endpoint was 30-month major adverse cardiovascular events (MACE) (composite of cardiac death, myocardial infarction, definite/ probable stent thrombosis, and target lesion revascularization), and primary bleeding endpoint was 30-month Bleeding Academic Research Consortium (BARC) type 2, 3, or 5 bleeding. **Results** Of 10 167 patients with available angiographic characteristics, 3 651 (35.9%) underwent complex PCI. Patients who underwent complex PCI were more likely to be elderly and male with a high prevalence of diabetes mellitus and hypertension. Subjects with complex PCI were more likely to display involvement of thrombotic lesion, type B2/C lesion, and higher SYNTAX scores. In adjusted Cox regression analysis, patients having complex PCI procedures experienced higher risks of MACE (*HR*=1.63, 95%*CI*: 1.38 – 1.92), MI (*HR*=2.16,95%*CI*:1.62 – 2.87), definite/probable ST (*HR*=2.71,95%*CI*: 1.66 – 4.41), and TLR (*HR*=1.59,95%*CI*: 1.29 – 1.95), compared with noncomplex PCI(all $P < 0.05$). In contrast, the risk of clinically relevant bleeding was statistically similar between the 2 groups (*HR*=0.86,95%*CI*: 0.66 – 1.11,$P > 0.05$). By including complex PCI as a continuous variable within the same multivariable models, the risk of MACE tended to be greater as the number of high-risk procedural characteristics increased. Individual high-risk features, such as ⩾3 stents implanted, bifurcation with 2 stents, > 60 mm total stent length, in-stent restenosis target lesion, and severely calcified lesion, are independent predictors for MACE but not for clinically relevant bleeding. **Conclusion** Compared with noncomplex PCI, PCI complexity was associated with a considerably higher risk of adverse ischemic events. The findings provide operators with novel insights regarding clinical outcomes of individual complex features and emphasize that the number and types of complex features both have an impact on procedural outcomes.

[Key words] Percutaneous coronary intervention;Major adverse cardiovascular events;Long-term outcome

Usefulness of cardiometabolic index for the estimation of diabetes risk among general population in rural China: a community–based study

WANG Haoyu

Fuwai Hospital, Chinese Academy of Medical Sciences and Peking Union Medical College, Beijing 100037, China

[Abstract] **Objective** Aimed to validate CMI's utility of discriminating diabetes and compares it with other indexes among general Chinese population. **Methods** Analyses were based on a cross–sectional study of 11 478 participants that underwent assessment of metabolic and anthropometric parameters in rural areas of northeastern China in 2013. CMI was calculated by TG/HDL–C × WHtR. Multivariate logistic regressions were performed to clarify CMI's association with diabetes, ROC analyses were engaged to investigate CMI's discriminating ability for diabetes. **Results** The prevalence of diabetes was 9.93% in males while 10.76% in females, and increased with CMI's increment. Multivariate logistic regression analyses were carried out to further evaluate the association between CMI and diabetes, and the results were showed in Table 2. CMI had a strong association with diabetes, the odds ratios (ORs) for 1 SD increase of CMI were 1.645 (1.533 – 1.766) and 1.462 (1.355 – 1.579) for females and males respectively in crude model. After adjustment of age, race, education levels, income levels and physical activity, the degree of this association changed but still strong, each SD increment of CMI would enhance the risk of DM by 56.8% and 48.7% for females and males respectively. Further adjustment of hypertension, family history of DM, medication usage, CVD history, vegetable intake, meat intake and fatty food intake attenuated the association but not too much, there were still 1.47 and 1.42 times of risk for diabetes in females and males respectively, when CMI had one SD increment. After dividing CMI into quartiles, the risk of prevent diabetes increased robustly with higher CMI quartiles. When comparing top quartiles with bottom categories, risk of prevalent diabetes got 3.74 times increase in females and 3.70 times augmentation in males. P values for linear trend were less than 0.05 in both sexes, indicating the linear trends from lowest to the highest quartiles were significant. The ROC results showed an excellent discriminating power of CMI (AUC: 0.702 for females, 0.664 for males). **Conclusion** An increasing CMI was correlated with higher odds of diabetes, supporting CMI as a useful and economic measure to screen and quantify diabetes in general Chinese population. Monitoring and promoting achievement of dyslipidemia and abdominal obesity based on CMI may improve subclinical and cardiovascular outcomes.

[Key words] Usefulness;Cardiometabolic index;Diabetes risk

Four–tiered classification of left ventricular hypertrophy based on ventricular concentricity and dilatation identifies ischemic stroke in the general population

WANG Haoyu

Fuwai Hospital, Chinese Academy of Medical Sciences and Peking Union Medical College, Beijing 100037, China

[Abstract] **Objective** Left ventricular hypertrophy (LVH) is traditionally classified as concentric or eccentric based on LV relative wall thickness. We evaluated the prediction of ischemic stroke in a new 4–group LVH classification

based on LV concentricity (mass/end-diastolic volume0.67) and indexed LV end-diastolic volume (EDV) in the general Chinese population. **Methods** The cross-sectional study consisted of 11 037 general Chinese population (mean age 54 years; 54% women) from Northeast China Rural Cardiovascular Health (NCRCH) study who underwent echocardiography measurement. A 4-tiered classification of LVH was proposed where eccentric LVH is subdivided into ''indeterminate hypertrophy (*n*=484)'' and ''dilated hypertrophy (*n*=386)'' and concentric LVH into ''thick hypertrophy (*n*=246)'' and ''both thick and dilated hypertrophy (*n*=138)'' based on the presence of increased LV end-diastolic volume. **Results** Compared with normal LV geometry (2.6%), indeterminate (7.4%) and thick hypertrophy (10.2%) showed a higher prevalence of ischemic stroke ($P < 0.05$). Ischemic stroke was significantly greater in participants with indeterminate (*OR*=1.635, 95%*CI*: 1.115 - 2.398) and thick [2.143(1.329 - 3.456)] hypertrophy but not significantly in those with dilated [1.251(0.803 - 1.950)] and both thick and dilated hypertrophy [0.926(0.435 - 1.971)] compared with normal geometry in multivariable analysis. Additionally, the continuous parameters of LV concentricity 0.67 (*OR*=1.067,95%*CI*:1.024 - 1.113) was independently associated with the presence of ischemic stroke in multivariable analysis adjusted for age, sex, race, physical activity, current smoking and drinking status, BMI, TC, hypertension and diabetes, while LVEDV/BSA was not (*OR*=0.957,95%*CI*:0.859 - 1.065). **Conclusion** In a large-scale Asian population, we identified that thick hypertrophy carried the greatest odd for ischemic stroke, independently of traditional risk factors, followed by indeterminate hypertrophy. The new 4-tiered categorization of LVH can permit a better understanding of which subjects are at high enough risk for ischemic stroke to warrant early targeted therapy.

[Key words] Left ventricular hypertrophy;Northeast China Rural Cardiovascular Health;End-diastolic volume

Washing the seeds food, eliminating the contaminants, promoting the food safety and public health

XU Hanyou

International Liasom Hospital in Anji, Huzhou 313399, China

[Abstract] **Objective** It is imperative to eliminate the contaminants in the seeds food for promoting people' health around the world before the contaminants are eaten and harmed the human-being. **Methods** Because the author is a doctor and coming from countryside where produce the seeds food in China. So the author has experienced the bad situation of the contaminants in the seeds food and how the countryside local peasants to eliminate the contaminants in the seeds food. The old process was by using the water wetted white cloth of cotton to soak repeatedly under the contaminated seeds food and then washing the contaminants(which coming from the seeds food) out on the white cloth of cotton. When the process went on and on. The contaminants in the seeds food must be fainter and fainter until the washed water is clear. The food processing was finished. The fact has told us that every work for the clearing the contaminated seeds food. The clear washing water was changed into dirty muddy water. Which must contain lots of pollutants. **Results** Due to the above mentioned experience,the author has developed the new concept to eliminate the contaminants in the seeds food by water washing the seeds food directly and then drying the washed seeds food in the degree not destroying nutrients in it.As the modern time, the author has not done something to eliminate the contaminants in the seeds food. By using the modern advanced technology, this concept must be easily to be made into automatization equipment. **Conclusion** The new technology for washing the seeds food to eliminate the contaminants in them is valuable to be referenced and further researched. So is to be applied in daily life of public and promoting the food safety and public health.

[Key words] Washing the seeds food;Contaminants;Food safety

A novel conception to diagnose arhythmia by monitoring impulse of radical artery and brachial artery

XU Hanyou

International Liasom Hospital in Anji, Huzhou 313399, China

[Abstract] **Objective** To diagnose arhythmia by monitoring impulse of radical artery and brachial artery. **Methods** Summarized clinical experience and created the novel method to diagnose the arhythmia for further rapidly and effectively applying in clinical practices. **Results** Though the conception is only a idea or a strategy. But there are lots of facts or experiences of clinical practices can support the creating of the conception. For the great inventions are usually created in the labor practices. **Conclusion** The novel strategy method is valuable to be referenced and further researched. So is to be applied.

[Key words] Radical artery;Brachial artery;Cardiac impulse;Arhythmia;Diagnosis

Direct bilirubin to adverse outcome among patients with acute coronary syndrome after percutaneous coronary intervention

LYU Feng TAO Yuan

Shengzhou People's Hospital, Shaoxing 312499, China

[Abstract] **Objective** Based on GRACE score, to explore the clinical value of initial blood bilirubin levels in evaluating the prognosis of patients with acute coronary syndrome(ACS) after coronary intervention. **Methods** Selected patients with acute coronary syndrome who were diagnosed and treated with coronary intervention in the cardiology department of our hospital from January 2019 to June 2020. According to the inclusion and exclusion criteria, 293 patients with acute coronary syndrome were finally included.All selected patients' heart rate, blood pressure, age, renal function, cardiac function, cardiac events (cardiac arrest on admission, ECG ST changes, myocardial necrosis marked as elevated),and other relevant clinical data on admission were Collected. The fasting [total bilirubin (TBIL), direct bilirubin (DBIL), and indirect bilirubin (IBIL)]were checked within 24 hours of admission, and they were all divided into elevated and normal groups according to the reference value of our hospital.The GRACE scoring system software was used to calculate the patient's in-hospital death risk score and the 6-month out-of-hospital death risk score.The risk score was compared between the elevated initial bilirubin group and the normal group. And The optimal boundary value of bilirubin were calculated based on GRACE score. **Results** After grouping by initial bilirubin, there was a statistically significant difference in the 6-month death risk score of DBIL (t=7.18, P < 0.05), and there was a trend of difference in the hospital death risk score. There was no statistical difference in the scores of TBIL and IBIL.The optimal cut-off value of DBIL for the risk of death for 6 months outside the hospital was 4.05 μmol/L (The area under the ROC curve is 0.616, P < 0.05). **Conclusion** The initial serum DBIL level is significantly correlated with the 6-month out-of-hospital mortality risk score of patients with acute coronary syndrome undergoing coronary intervention,which suggested that it have clinical predictive value for the long-term prognosis in these patients.

[Key words] Acute coronary syndrome(ACS);Percutaneous coronary intervention;Direct bilirubin

Predictive value of inflammation–based glasgow prognostic score, platelet–lymphocyte ratio, and global registry of acute coronary events score for major cardiovascular and cerebrovascular events during hospitalization in patients with acute myocardial inf

ZHU Houyong　XU Xiaoqun　HUANG Jinyu

The Affiliated Hangzhou First People's Hospital, Zhejiang University School of Medicine, Hangzhou 310006, China

[Abstract] **Objective** To evaluate the predictive ability of the Glasgow prognostic score (GPS) , platelet–to–lymphocyte ratio (PLR), The global registry of acute coronary events (GRACE) score and combined diagnostic models for the major adverse cardiovascular and cerebrovascular events (MACEs)in patients with acute myocardial infarction (AMI). **Methods** In this retrospective cohort study, eligible patients were required to meet the third global definition of myocardial infarction. The primary outcome of this study was the occurrence of MACEs during hospitalization. Receiver operating characteristic (ROC) curve analysis was performed to assess the predictive ability of the GPS, PLR, GRACE scores, and joint diagnostic models for primary outcomes, univariate and multivariate logistic regression analyses were performed. Subgroup analysis were completed according to the type of percutaneous coronary intervention (PCI), the type of AMI, and the presence or absence of acute infection. **Results** A total of 175 patients were enrolled. The results of the univariate ROC curve analysis for the incidence of MACEs during hospitalization showed that the AUC was 0.780 (95%*CI*:0.696–0.864) for the GPS, 0.766 (95%*CI*:0.682–0.850) for the redefined GPS (RGPS), 0.561 (95%*CI*:0.458–0.664) for the PLR score (PLRS), and 0.793 (95%*CI*:0.706–0.880) for GRACE. Multivariate ROC curve analysis showed that the AUC value was 0.809 (95%*CI*:0.726–0.893) for the GPS combined with GRACE, 0.783 (95%*CI*:0.701–0.864) for the GPS combined with the PLRS, 0.794 (95%*CI*:0.707–0.880) for GRACE combined with the PLRS, and 0.841 (95%*CI*:0.761–0.921) for the GPS combined with GRACE and the PLRS. The combined diagnostic model including the GPS plus GRACE and the PLRS had a higher AUC value than the GPS, RGPS and GRACE models (all $P < 0.05$ respectively). The multivariate logistic regression model showed that the odds ratio for hospitalized MACEs was 5.573 (95%*CI*:1.588–19.554) for GPS scores of 2 versus 0, and the GRACE score was also an independent risk factor for MACEs, with an odds ratio of 1.023 (95%*CI*:1.009–1.036). The results of all subgroup analyses were similar to the whole cohort. **Conclusion** The diagnostic model combining the GPS plus GRACE and the PLRS has better predictive ability for the MACEs during hospitalization than each single score. Thus, the use of a combined GPS plus GRACE and PLRS model will be of clinical benefit in a broad group of individuals with AMI.

[Key words] Glasgow prognostic score;Global registry of acute coronary events;Myocardial infarction

Comparing outcomes of self–expanding and balloon–expandable Valves for transcatheter aortic valve replacement: a meta of randomized controlled trials and propensity score matching studies

ZHU Gangjie　LIU Xianbao　Fan Jiaqi　Wang Jian'an

The Second Affiliated Hospital Zhejiang University School of Medicine, Hangzhou 310009, China

[Abstract] **Objective** Transcatheter aortic valve replacement (TAVR) is a feasible and safe option for treatment of aortic stenosis (AS). There are two main bioprosthetic valves for TAVR, self–expanding valves (SEV) and balloon–expandable valves (BEV). However, clinical outcomes of two valves were varying. **Methods** A comprehensive search was conducted through Pubmed, Embase and Cochrane library from inception up to September 2020. The study used both MeSH terms and text words for search, including ''Transcatheter Aortic Valve implantation'', ''Transcatheter Aortic Valve Replacement'',''balloonexpanding'',''balloon expanding'',''balloon expandable'',''balloonexpandable'',''selfexpanding'',''self expanding'',''selfexpandable'' and ''self expandable''. No language limitation was imposed for the search. Two reviewers screened literatures, selected eligible studies and extracted valuable data independently. **Results** A total of 937 reports were searched from Pubmed, Embase and Cochrane library and final 6 trials (8 reports) were enrolled in this study. Among included trials, 3 trials were RCTs and 3 trials were PSM studies, with 18 097 patients (9 052 in self–expanding valve group, 9 045 in balloon–expandable valve group). All–cause mortality in the BEV group was significantly lower than SEV group (*OR*=1.35, 95%*CI*:1.18–1.55) in 30 days. However, two groups were comparable in the RCTs subgroup analysis (*OR*=1.7, 95%*CI*:0.84–3.45). There was no significant difference between 2 groups in cardiovascular death. Comparing with SEV group, BEV group had less ⩾ moderate paravalvular regurgitation (*OR*=2.66, 95%*CI*:1.82–3.87), which was consistent with the results in the subgroup analyses. Stroke in two groups wasn't significantly different. However, the results of stroke were contradictory in the two subgroups. In terms of new PPM implantation, there was lower incidence in BEV group (*OR*=1.64, 95%*CI*:1.08–2.49). **Conclusion** BEV was associated with lower all–cause mortality, less paravalvular regurgitation of moderate or severe degree and less new PPM implantation in 30 days.

[Key words] Transcatheter aortic valve replacement;Aortic stenosis;Self–expanding valves

LMK235 attenuates cardiac dysfunction and increasing risk of ventricular arrhythmia post–myocardial infarction through inhibition of ventricular remodeling

PIAO Zhehao　LYU Fangzhou　JIN Li　LIN Jiafeng

The Second Affiliated Hospital of Wenzhou Medical University, Wenzhou 325000, China

[Abstract] **Objective** Aimed to determine the impact of LMK235 on ventricular remodeling and its underlying mechanisms. **Methods** After being anesthetized by intraperitoneal injection of 2% sodium pentobarbital (50 mg/kg), the rats were mechanically ventilated. The left anterior descending (LAD) coronary artery was ligated with a 6–0 suture line after thoracotomy. First, the study performed a preliminary experiment. Non–infarcted and infarcted left ventricles at 7, 14, and 21 days were collected from 20 rats and examined by western blotting. Then, 22 rats were divided into four groups.Sham group (*n*=4), which underwent sham operation and received a daily intraperitoneal injection of vehicle

(1 mL) for 21 days as control.Sham+LMK235 group (n=4), which underwent sham operation and received a daily intraperitoneal injection of LMK235 (5 mg/kg) for 21 days to exclude the potential influence of latent cardiac toxicity. MI group (n=4), which underwent thoracotomy and LAD ligation and received a daily intraperitoneal injection of vehicle (1 mL) for 21 days,and MI+LMK235 group (n=4), which underwent thoracotomy and LAD ligation and received a daily intraperitoneal injection of LMK235 (5 mg/kg) for 21 days. The remaining 6 rats were euthanized and excluded from the experiment. Data are expressed as mean ± SD. The remaining 6 rats were euthanized and excluded from the experiment. The vehicle was produced in accordance with the instructions of MCE and Choi et al. **Results** The major findings of the present study were as follows.HDAC5 expression was gradually increased and HDAC5 underwent phosphorylation–dependent nuclear export post–MI. LMK235 attenuated cardiac dysfunction post–MI and inhibited pathological cardiac hypertrophy and interstitial fibrosis in the border zone. LMK235 ameliorated electrophysiological disorder post–MI and reversed MMP7–dependent Cx43 degradation in the border zone. LMK235 promoted feedback upregulation of HDAC5 and suppressed pro–hypertrophic transcriptional factor MEF2A but had little effect on phosphorylation–dependent nuclear export of HDAC5 and histone acetylation after MI, indicating that the potential mechanism underlying the cardioprotective effects of LMK235 may be transcriptional repression mediated by HDAC5, rather than regulation of histone acetylation. **Conclusion** LMK235 can improve cardiac function and electrophysiology, attenuate cardiac hypertrophy and interstitial fibrosis, Its salutary effect may be due to feedback upregulation of HDAC5, rather than regulation of chromatin remodeling. Specifically, inhibition of class IIa HDAC activity and enhancement of HDAC5 transcriptional repression may hold promise as a future therapeutic strategy in ventricular remodeling.

[Key words] LMK235;Cardiac dysfunction;Ventricular arrhythmia

NOX4 is core target for baicalin and quercetin in treatment of atherosclerosis: based on network pharmacology, transcriptomics and experimental validation

LI Mingshuang MAO Wei

Zhejiang Traditional Chinese Medicine Hospital (The First Affiliated Hospital of Zhejiang University of Traditional Chinese Medicine), Hangzhou 310003, China

[Abstract] Objective Aimed to compare the differences in the mechanisms of baicalin and quercetin in treatment of arteriosclerosis (AS) by integrating network pharmacology and transcriptomics. **Methods** The chemical structures and ADME (absorption, distribution, metabolism and excretion) parameters of baicalin and quercetin were obtained from PubChem and TCM Systems Pharmacology (TCMSP), respectively. Then targets of two compounds and disease were identified from related public databases, and the same were considered to be compound–disease targets. Subsequently, differentially expressed genes (DEGs) of microarray dataset GSE57691, downloaded from GEO database, were selected to validate compound–disease targets. The study used CIBERSORT website to analyze immune cell subtypes that were abundant in AS patients, and performed Pearson correlation analysis with the aim of gaining relationships between targets and leukocyte subtypes. Finally, the core gene was validated by RT–qPCR. **Results** The study identified 45 baicalin–AS targets and 34 quercetin–AS targets. Functional enrichment analysis demonstrated that most targets were involved in inflammation related pathways. After validation by DEGs, three common targets (NOX4, IL6 and IL1B) and two common targets (NOX4 and MAOA) were identified as core targets of baicalin and quercetin, respectively. Immune infiltration analysis showed that monocytes and naive B cells were abundant in AS samples. Through Pearson correlation analysis, the study found that the expression of all core targets had strong correlation with monocytes infiltration.

Through RT–qPCR, the study found that intervention with baicalin and quercetin can alter NOX4 expression in AS model. **Conclusion** The study results indicate that NOX4 is core target for baicalin and quercetin in treatment of AS. These two different flavonoids modulate similar biological processes and signaling pathways to exert therapeutic effects on AS.

[Key words] Arteriosclerosis;NOX4;Network pharmacology

Left atrial appendage closure following the optimized workflow via intracardiac echocardiography guidance

DU Xianfeng ZHUO Weidong HE Bin SHEN Caijie FENG Mingjun YU Li
LIU Jing FU Guohua WANG Binhao CHU Huimin
Ningbo First Hospital, Ningbo 315010, China

[Abstract] Objective To investigate the efficacy and safety endpoints of the left atrial appendage closure (LAAC) procedure following the intracardiac echocardiography (ICE)–guided, optimized workflow and compare its procedural and clinical outcomes to those following the minimalistic approach. **Methods** Eighty–nine patients with nonvalvular atrial fibrillation [female 32.6%, aged (71.8 ± 9.1) years, mean CHA_2DS_2–VASc score (4.5 ± 1.5),mean HAS–BLED score (2.9 ± 0.7)]were enrolled into the optimized group to undergo LAAC procedures. The LAA size and its closure results were assessed following the orthogonal tri–axial workflow under the ICE– and fluoroscopic guidance. Intraprocedural and follow–up outcomes were compared retrospectively to those from another 179–patient cohort (minimalistic group) who underwent the LAAC procedures following the minimalistic approach. **Results** Baseline characteristics were comparable between groups. The fluoroscopy time [(5.6 ± 2.9) min vs. (7.0 ± 3.2) min], fluoroscopy exposure [(103.1 ± 61.7) mGy vs. (139.4 ± 102.3) mGy] and contrast volume [(73.8 ± 58.7) mL vs (103.5 ± 44.7) mL] were significantly lower in the optimized group within similar procedure time(all $P < 0.05$). No difference of peri–procedural safety endpoints was recorded. However, higher incidence of device–related thrombus (DRT, 5.6% vs 0.6%,$P < 0.05$) was detected in the optimized group during follow–up. **Conclusion** Optimized workflow following the orthogonal triaxial assessment using ICE and fluoroscopy could reduce the radiation exposure and contrast consumption during the LAAC procedure, however, sufficient anticoagulation should be recommended concerning the higher DRT incidence.

[Key words] Atrial fibrillation;Left atrial appendage closure;Intracardiac echocardiography;Radiation exposure

The association between CD99 expression on neutrophils and coronary artery disease in China: a prospective study

LIN Xiaoxiao GAO Beibei HUANG Jinyu
Hangzhou First People's Hospital, Hangzhou 310006, China

[Abstract] Objective To investigated the expression levels of CD99 on neutrophils in coronary artery disease (CAD) patients. **Methods** Between July 2013 and July 2014, a total 498 patients including 305 with significant CAD and 113 with mild CAD who underwent coronary angiography were admitted to the Department of Cardiology, Affiliated Hangzhou First People's Hospital, Zhejiang University School of Medicine. We evaluated the severity of CAD by standard coronary angiography (CAG). All angiograms were prospectively evaluated at our cardiac catheterization laboratory.

Significant CAD were defined as > 50% stenosis in any vessel with a diameter ⩾ 2.0 mm. Mild CAD were defined as ⩽50% stenosis in all vessels. The following measurements were collected for each patient: gender, age, body mass index(BMI), left ventricular ejection fraction(LVEF), Triglyceride(TG), total cholesterol(TC), HDL–cholesterol(HDL–C), LDL–cholesterol(LDL–C), Serum creatinine(SCr), high–sensitive C–reactive protein (hsCRP), Fasting glucose(FBG), hyperlipidemia, hypertension, diabetes mellitus, current smoking and medications. Percentage of neutrophils expressing CD99 were enumerated by flow cytometry. SPSS 25 was used for statistical analysis. Categorical variables were defined as percentages. Student t–test was used to compare continuous variables. Categorical variables were compared with Chi–square test. Binary logistic regression was used to identify independent predictors of CAD. **Results** Significant CAD patients showed a higher prevalence of hypertension, diabetes mellitus, dyslipidemia and current smoking rate. The frequencies of significant CAD patients under medications of ACE–I/ARB, statins, beta–blockers, aspirin, CCB, diuretics and clopidogrel were all significantly higher than these of mild group. Sujects with significant CAD showed no significant difference in body mass index (BMI), Fasting glucose (FBG), LDL–cholesterol (LDL–C), HDL–cholesterol (HDL–C), total cholesterol (TC) and high–sensitive C–reactive protein (hsCRP) between patients with mild CAD. Percentage of neutrophils expressing CD99 was significantly higher in patients with significant CAD when compared with mild CAD (0.95% vs. 0.72%, $P < 0.05$). Binary logistic regression analysis revealed that percentage of neutrophil expressing CD99 was associated with CAD (*OR*= 1.514; 95%*CI*: 1.014–2.260,$P < 0.05$). **Conclusion** The data indicated that increased CD99 levels on neutrophils were observed in patients with significant CAD when compared with patients with mild CAD, an increased percentage of CD99 level on neutrophils may be associated with psychopathology of coronary artery disease and more further research is needed.

[Key words] Coronary artery disease;Risk factors;CD99;Neutrophil;Dyslipidemia

Prognostic value of CA125 serum levels in female patients with acute coronary syndrome

LUO Yanhong CHENG Yongran ZHANG Xiaofu WANG Mingwei YANG Zhiqiang ZHANG Xingwei PAN Chunqi

The Affiliated Hospital of Hangzhou Normal University, Hangzhou 310015, China

[Abstract] Objective To determine the short–term and long–term prognostic value of Carbohydrate antigen 125 (CA125) serum levels in female patients with acute coronary syndrome (ACS). **Methods** A total of 131 consecutive female patients with ACS were retrospective enrolled. Their CA125 levels, B–type natriuretic peptide (BNP) level, and biochemical parameters were measured, and echocardiography was performed at admission. All–cause mortality during hospitalization and two–year follow–up was investigated for the prognosis. **Results** The median value of CA125 serum level in the entire ACS patients was 13.85 U/mL. Patients in Killip Ⅲ had the highest values of CA125 level, followed by Killip Ⅱ and then Killip Ⅰ ($P < 0.05$). However, no statical difference was observed between Killip Ⅳ and Ⅰ–Ⅲ groups respectively ($P > 0.05$). The CA125 serum levels showed weak positive correlation with left ventricular end–diastolic diameter (LVEDD) (r=0.3,$P < 0.01$) and a weak negative correlation with left ventricular ejection fraction (LVEF) (r= –0.23, $P < 0.01$). A receive operating characteristic (ROC) curve analysis showed that the AUC of CA125 in predicting acute heart failure (AHF) in ACS patients during hospitalization was 0.912, exhibiting higher sensitivity and specificity than BNP (0.846). The optimal cut–off value for CA125 in predicting AHF was 16.4 U/mL with a sensitivity of 0.916 and specificity of 0.893. The Kaplan–Meier survival analysis demonstrated that patients with high values of CA125 level had a poor overall survival than those with low values of CA125 level (log–rank, $P < 0.05$), whether during hospitalization or long–

term follow–up. **Conclusion** Elevated CA125 level can be used to predict AHF in female ACS patients. Patients with elevated CA125 levels had higher mortality in short–term and long–term than those with low CA125 levels.

[Key words] Carbohydrate antigen 125;Acute coronary syndrome;Acute heart failure;Mortality

Galectin–3 in predicting mortality of heart failure: a systematic review and meta–analysis

WU Chenxia MAO wei

The First Affiliated Hospital of Zhejiang Chinese Medical University, Hangzhou 310006, China

[Abstract] Objective To define galectin–3 in predicting mortality of heart failure. **Methods** PubMed, Embase, and the Cochrane Library were searched. A total of 1 540 studies were identified, and of these studies, 19 involving 9 217 patients were included in our meta–analysis. **Results** The diagnostic hazard ratios of galectin–3 in predicting mortality in chronic heart failure patients was 1.13(95%*CI*:1.07–1.21) and 2.17 (95%*CI*:1.27–3.08) in acute heart failure (HF) patients. **Conclusion** The meta–analysis shows that elevated levels of galectin–3 are associated with higher mortality in both acute and chronic heart failure patients.

[Key words] Galectin–3;Heart failure;Review;Meta–analysis

Activation of extracellular signal–regulated kinase 1/2 and Sp1 may contribute to the expression of tissue inhibitor of metalloproteinases–1 induced by transforming growth factor–β 1 in human pulmonary arterial smooth muscle cells

YANG Jinxiu

The First Affiliated Hospital of Zhejiang Chinese Medical University, Hangzhou 310006, China

[Abstract] Objective Tissue inhibitor of metalloproteinases–1 (TIMP–1) is important in the development of pulmonary arterial hypertension (PAH). However, the molecular regulatory mechanisms of TIMP–1 in the pulmonary arteries were not very clear, especially in the human pulmonary arterial smooth muscle cells(HPASMCs). The present study investigated the signaling pathway involved in the regulation of TIMP–1 in HPASMCs induced by transforming growth factor (TGF)–β 1. **Methods** Cultured HPASMCs were incubated with different concentrations of TGF–β 1 (0~40 ng/mL) for 24 h, or with 10 ng/mL TGF–β 1 for different time (1–48 h). Western blot, real–time PCR and ELISA analysis showed that TGF–β 1 time– and dose–dependently enhanced the expression and secretion of TIMP–1. Furthermore, TGF–β 1 could phosphorylate two of the three mitogen–activated protein kinases (MAPK), extracellular signal–regulated kinase 1/2 (ERK1/2) and p38, but not c–Jun NH2–terminal kinase (JNK). **Results** Of these kinases, only the inhibition of ERK 1/2 by U0126, which was a specific inhibitor of MAPK/ERK kinase1/2, effectively blocked the TGF–β 1–induced expression of TIMP–1. Mithramycin, an inhibitor of Sp1 transcription factor, also significantly inhibited the expression of TIMP–1. Additionally, EMSA showed that TGF–β 1 could up–regulate the DNA–binding activity of Sp1, and that U0126 and mithramycin could effectively inhibit these events. **Conclusion** TGF–β 1 could time– and dose–dependently stimulate the expression and secretion of TIMP–1 in HPASMCs, and ERK1/2 and Sp1 signaling pathways might be

involved in these activities.

[Key words] Human pulmonary arterial smooth muscle cells;Tissue inhibitor of metalloproteinases–1;Transforming growth factor – β 1;Extracellular signal–regulated kinase 1/2;Sp1

Catheter ablation versus medical rate control for persistent atrial fibrillation in patients with heart failure:a PRISMA–compliant systematic review and meta–analysis of randomized controlled trials

ZHOU Bin

The First Affiliated Hospital of Zhejiang Chinese Medical University, Hangzhou 310006, China

[Abstract] Objective The effectiveness of restoring the sinus rhythm by catheter ablation relative to that of medical rate control for persistent atrial fibrillation (AF) patients with heart failure(HF) remains to be defined. Methods The study systematically searched Embase, Pubmed, the Cochrane Library, and ClinicalTrials.gov for articles that compared the outcomes of interest between catheter ablation and medical rate control therapy in persistent AF patients with HF and left ventricular systolic dysfunction (LVSD). The primary endpoint was the change in the left ventricular ejection fraction (LVEF) following catheter ablation or medical rate control therapy relative to baseline. Other endpoints included changes in cardiac function and exercise capacity, including the New York Heart Association (NYHA) class, the brain natriuretic peptide (BNP) level, the peak oxygen consumption (peak VO2), the 6–minute walk test (6MWT) results, and quality of life (QOL). Results Three randomized controlled trials (RCTs) with 143 patients were included. At the overall term follow–up, catheter ablation significantly improved the LVEF (mean difference(MD):6.22%,95%*CI*:0.7 – 11.74,$P<0.05$) and peak VO2 (MD:2.81 mL/(kg·min),95%*CI*: 0.78 – 4.85, $P<0.05$) and reduced the NYHA class (MD: 0.9,95%*CI*: 0.59 – 1.21,$P<0.05$) and the Minnesota Living with Heart Failure Questionnaires (MLHFQ) scores (MD:11.05;95%*CI*:19.45–2.66, $P<0.05$) compared with the medical rate control for persistent AF patients with HF. Alterations in parameters, such as the BNP level, 6MWT, and Short Form–36 (SF–36) questionnaire scores also revealed trends that favored catheter ablation therapy, although these differences were not significant. Conclusion Catheter ablation resulted in improved LVEF, cardiac function, exercise capacity, and QOL for persistent AF patients with HF compared with the medical rate control strategy.

[Key words] Atrial fibrillation;Aatheter ablation;Heart failure;Medical rate control;Systematic review

Current status and considerations of clinical experience in the treatment of atherosclerosis from the perspective of phlegm

MA Lan

The First Affiliated Hospital of Zhejiang Chinese Medical University, Hangzhou 310006, China

[Abstract] Atherosclerosis is characterized by lipid core composed of atherosclerotic lipid and necrotic substance, and fibrous cap composed of focal fibrous thickening of intima. Phlegm is mostly formed by stagnation of fluid, which can be distributed throughout the body with the rise and fall of Qi. The phlegm production in the vascular tract is

closely related to the formation of atherosclerotic plaque and is the key driving factor in each link of its pathophysiology. Therefore, by reviewing the ancient and modern literature, the author analyzed the relationship between phlegm and different disease stages of atherosclerosis from the aspects of etiology, pathogenesis, clinical manifestations and treatment, so as to provide more theoretical basis for the treatment of atherosclerosis from phlegm.

[Key words] Phlegm; Retardance the vascular; Atherosclerosis; Staging; Chinese medicine

Cardiac–specific knockout of farnesyl pyrophosphate synthase induces cardiac remodeling and chronic heart failure by enhancing the activity of small GTP – binding proteins

WANG Xiying ZHANG Xuan CHEN Yuxiao

The First Affiliated Hospital, Zhejiang University School of Medicine, Hangzhou 310003, China

[Abstract] **Objective** To clarify the role of farnesyl pyrophosphate synthase (FDPS) in cardiac homeostasis, and provide more evidence for cardiovascular effects of the mevalonate pathway, knocked out FDPS in mouse cardiomyocytes and explored the relevant mechanisms. **Methods** The study used human samples and cardiac–specific FDPS knockout mice as models. Cardiac function was assessed by echocardiography at different age stages of mice and molecular biomarkers of cardiac remodeling was detected by real–time PCR. HE staining was used to observe structural changes in the heart, as well as sirius red staining for fibrosis. The contents of geranyl pyrophosphate (GPP), farnesyl pyrophosphate (FPP) and geranylgeranyl pyrophosphate (GGPP) in cardiomyocytes were determined by high performance liquid chromatography (HPLC). The activity of small G protein in the heart of mice was detected by pull–down method, and the changes of protein levels in the downstream pathways were detected by Western Blot. One–month–old FDPS knockout mice were randomized to receive FTI–277 (inhibitor of farnesyltransferase) or vehicle treatment for 4 weeks, six male age– and weight–matched wild type mice were housed as normal control, given an intraperitoneal injection of vehicle in same volume. Prior to tissue collection, cardiac function was assessed via echocardiography. **Results** The results showed that FDPS protein levels were downregulated in samples from cardiomyopathy patients. FDPS knockout mice exhibited spontaneous hypertrophy, fibrosis and develop cardiac dysfunction, along with enlargement of cardiomyocytes. This effect was associated with activation of Ras and Rheb, as well as their downstream extracellular signal–related kinase 1/2 (ERK1/2) and mTOR expression. Additionally, FDPS knockout led to deletion of FPP and accumulation of GPP which may be the reason about increased Ras and Rheb activity. Furthermore, administration of farnesyltransferase inhibitors attenuated cardiac remodeling and dysfunction in FDPS knockout mice. **Conclusion** These results indicated that FDPS plays a role in cardiac remodeling. The deletion of FDPS will activate the downstream complex signaling pathways and cause cardiac remodeling and dysfunction. From the perspective of clinical application, FDPS may be an important molecule to maintain cardiac homeostasis. We have observed changes in FDPS levels in patients with heart failure. For these patients, correcting their FDPS levels may have potential therapeutic significance.

[Key words] Cardiac–specific knockout;Farnesyl pyrophosphate synthase;Cardiac remodeling;Chronic heart failure;GTP

Left bundle branch pacing post–atrioventricular junction ablation for atrial fibrillation: a propensity score matching analysis

CAI Mengxing

The First Affiliated Hospital of Wenzhou Medical University, Wenzhou 325000, China

[Abstract] **Objective** Aimed to examine the long–term clinical feasibility, safety, and efficacy of left bundle branch pacing (LBBP) in atrial fibrillation (AF) patients post–atrioventricular junction (AVJ) ablation and provide a balanced comparison of LBBP versus His bundle pacing (HBP). **Methods** This study prospectively enrolled patients with AF and heart failure (HF) who underwent AVJ ablation and LBBP from July 2017 to December 2019. The control group patients were selected, by propensity score (PS) matching with a 1:1 ratio, among those HBP implantations performed in the years 2012–2019. **Results** A total of 99 patients were enrolled in this study, with successful permanent LBBP post–AVJ ablation in 100% of patients (primary LBBP:76,secondary LBBP:23).Significantly improvements were observed in left ventricular ejection fraction, tricuspid regurgitation, and mitral regurgitation at 1–year follow–up ($P<0.05$). The proportion of patients whose acute threshold < 1 V/0.5 ms was 97.9% (97/99) and only one patient had an increase in threshold ≥1 V/0.5 ms at 1–year follow–up. Further, patients with LBBP as an active group was compared to patients with HBP (control group) through PS matching with 170 successfully matched (PS–HBP n=85,PS–LBBP n=85). In the control group, the success rate of permanent HBP was 81.9% (176/215), which was lower than that with LBBP (100% vs. 81.5%, $P<0.05$). No significant differences in echocardiographic or clinical outcomes were observed between groups ($P>0.05$), while lower thresholds, greater sensed R–wave amplitudes, and less complication were observed in PS–LBBP group ($P<0.05$). **Conclusion** LBBP is feasible, safe, and effective in AF and HF patients post–AVJ ablation, which has comparable clinical benefit, higher success rate, better pacing parameters, and less complication than HBP.

[Key words] Left bundle branch pacing;Atrial fibrillation;His bundle pacing;Atrioventricular junction

Inhibition of the P2X7 receptor prevents atrial arrhythmias in a rat model of sterile pericarditis

YE Tianxin WANG Xingxiang

The First Affiliated Hospital, Zhejiang University School of Medicine, Hangzhou 310003, China

[Abstract] **Objective** Atrial fibrillation (AF) is the most common sustained arrhythmia, and inflammation–related fibrosis signals play a crucial role in the pathogenesis of AF. The purinergic receptor P2X7 (P2X7R), activated by ATP, is a ligand–gated cation channel that predominately mediates inflammation and cellular death. Post–operative AF is a common complication in patients undergoing cardiac surgery. Therefore, the study evaluated the effects of P2X7R inhibition on atrial arrhythmogenic remodeling in a rat model of sterile pericarditis (SP). **Methods** SP was induced in rats by the epicardial application of sterile talc. An intervention group received daily P2X7R inhibition Brilliant Blue G (BBG,30 mg/kg,i.p.) for 4 days, starting 1 day before pericardiotomy. AF susceptibility was assessed in vitro electrophysiology. Atrial histology was determined with Masson staining. The protein expression and gene–expression were analyzed respectively by western blot assays and rt–PCR/gene microarray. **Results** In vitro electrophysiology, burst pacing induced atrial tachyarrhythmias in 10% Sham rats vs. 80% SP–only rats, and only 11% BBG–treated SP rats ($P<0.05$ vs. SP–only). Atrial action potential duration (APD) and activation latency (AL) were significantly prolonged by SP, whereas atrial triangulation and effective refractory period (ERP)/APD90 ratio were reduced (all $P<0.05$). The above–

mentioned electrophysiological parameters were attenuated by BBG. SP caused atrial fibrosis. BBG strongly attenuated atrial fibrosis. SP increased atrium expression of inflammation– and fibrosis–related gene expression pathways on gene–microarray transcriptomic analysis, which was significantly attenuated by BBG. SP increased protein expression of P2X7R and caused significant increases in mRNA–expression of collagen–1, collagen–3, NLRP3, ASC, CASP1, IL–1β, TGF–β3, and α–SMA vs. Sham. BBG–treatment suppressed all these SP–induced alterations. **Conclusion** The P2X7R inhibition BBG prevents SP–induced atrial remodeling, while suppressing inflammatory changes and fibrotic/electrical remodeling, thus providing new insights into the relationship between P2X7R and atrial arrhythmias.

[Key words] Atrial fibrillation;P2X7;Sterile pericarditis

Preventive effect of Shenduning prescription combined with hydration therapy on contrast induced nephronpathy after elective percutaneous coronary intervention

JIANG Jiangang

Jinhua Hospital of Traditional Chinese Medicine, Jinhua 321000, China

[Abstract] **Objective** To explore the preventive effect of Shenduning prescription combined with hydration therapy on contrast induced nephronpathy (CIN) after elective percutaneous coronary intervention. **Methods** One hundred and fifty–nine patients undergoing selective coronary intervention were divided into simple hydration group, intensive statin group and Shenduning prescription group randomly, with 53 cases in each group. The simple hydration group received conventional drugs for coronary heart disease and preoperative routine hydration therapy. The intensive statin group received intensive treatment with atorvastatin calcium tablets on the basis of the simple hydration group, and the Shenduning prescription group received Shenduning prescription treatment on the basis of the hydration group. Serum creatinine(Scr), malondialdehyde (MDA), superoxide dismutase (SOD) and glomerular filtration rate (eGFR) were detected by blood samples at 24 h before and after operation, as well as 72 h after operation respectively. The primary endpoint event was the occurrence of CI–AKI. **Results** The Scr level of the intensive statin group and the Shenduning prescription group was significantly lower than that of the simple hydration group, while the eGFR level was significantly higher than that of the simple hydration group, which is of statistical significance ($P<0.05$). The incidence of CI–AKI was 15.1% in simple hydration group, 5.7% in intensive statin group and 3.8% in Shenduning prescription group respectively after operation ($P>0.05$), of which there was significant statistical difference between simple hydration group and Shenduning prescription group ($P<0.05$). After 72 h of the operation, MDA level in Shenduning prescription group was significantly lower than that in simple hydration group and intensive statin group, while its SOD level was significantly higher than that in simple hydration group and intensive statin group, which is of statistical significance ($P<0.05$). The proportion of abnormal liver function in intensive statin group and the Shenduning prescription group was 13.1% and 3.8%, respectively, and the difference was statistically significant ($P<0.05$). **Conclusion** The combination treatment of Shenduning prescription with hydration therapy may protect the patient's renal function after elective coronary interventional therapy, while reducing the incidence of CIN and the oxidative stress reaction caused by contrast agent, thus effectively reducing adverse reactions.

[Key words] Contrast induced nephronpathy;Shenduning prescription;Hydration therapy

Feasibility and clinical benefits of reimplantation of his–purkinje conduction system pacing lead

WU Shengjie

The First Affiliated Hospital of Wenzhou Medical University, Wenzhou 325000, China

[Abstract] **Objective** Aimed at evaluating the feasibility, safety, and clinical prognosis of the patients with chronically implanted his–purkinje conduction system pacing leads (HPCSP) after reimplantation. **Methods** Patients from February 2012 to April 2021 with HPCSP having lead revision were included. The primary outcomes were success rate, feasibility, safety, and clinical prognosis after reimplantation. **Results** There were 2005 patients using HPCSP, of which 31 patients having lead reimplantation met the criteria according to the current guideline. Four patients failed to reimplant due to high thresholds during the procedure, and were excluded from the study. Twenty seven patients [male 15,mean age (64 ± 11) years,23 HBP,4 LBBP] were included in this study. The indication for pacemaker was atrioventricular block (AVB) in 8, left bundle branch block (LBBB) in 10, atrial fibrillation (AF) with atrial ventricular junction ablation (AVJA) in 5, Sick sinus syndrome (SSS) in 3. One patient have both LBBB and AF with AVJA. The most common reason for lead reimplantation was high threshold (including 17 HBP, 1 LBBP). Early increased threshold happened in 6 patients due to not pacing beyond the block site. Four patients lost capture, 3 for lead–dislodgement and 2 for pocket infection. Medtronic 3830 leads planted in his bundle region or left bundle branch region were all successfully extracted. Tools were needed in 2 patients. The remaining 25 patients only used manual traction. The mean lead dwell time in patients with battery depletion was (2 106 ± 514) days and in the remaining was (535 ± 423) days.10 patients used HBP and 17 LBBP after revision. The baseline left ventricular ejection fraction (LVEF) was 45% ± 19%,and climbed to 52% ± 16% after 6 months follow–up. Before lead revision, LVEF was 49% ± 17%, while 6 months after revision, LVEF kept stable(50% ± 13%). LVEF in the LBBB group changed from 32% ± 6% at baseline, 43% ± 14% ($P < 0.05$) before reimplantation, to 44% ± 8 % ($P < 0.05$) after 6 months. While in the non–LBBB group, LVEF was 53% ± 20%, 53% ± 18%, 55% ± 14%, respectively. In the high thresholds group[(4.3 ± 1.3) V/0.5 ms], patients' thresholds dropped to [(0.5 ± 0.3) V/0.5 ms] after revision, and remained stable [(0.6 ± 0.3) V/0.5 ms] after 6–month follow–up. The sensing remained stable during the all operations. There were no serious complications during the procedure. **Conclusion** Lead extraction of HPCSP was safe and feasible, and HPCSP's success rate of reimplantation was high. The prognosis of these patients also remained sound or became better after lead revision.

[Key words] His–purkinje conduction system pacing leads;Left bundle branch block;Feasibility

CIDEC silencing attenuates diabetic nephropathy via inhibiting apoptosis and promoting autophagy

ZHENG Gaoshu

Qilu Hospital, Cheeloo College of Medicine, Shandong University, Ji'nan 250012, China

[Abstract] **Objective** To explore whether cell death–inducing DFF45–like effector C(CIDEC) plays an important role in the regulation of diabetic nephropathy (DN) and its potential mechanism. **Methods** High fat diet and low dose streptozotocin were used to establish type 2 diabetic rat model. The study investigate the role of CIDEC in the pathogenesis and process of DN through histopathological analysis, western blot and gene silencing. Meanwhile, the effect of CIDEC on renal tubular epithelial cells stimulated by high glucose was also verified. **Results** DM group

exhibited glucose and lipid metabolic disturbance, with hypertrophy of kidneys, damaged renal function, increased apoptosis, decreased autophagy, glomerulosclerosis and interstitial fibrosis. CIDEC gene silencing improved metabolic disorder and insulin resistance, alleviated renal hypertrophy and renal function damage, decreased glomerular and tubular apoptosis, increased autophagy and inhibited renal fibrosis. At the cellular level, high glucose stimulation increased CIDEC expression in renal tubular epithelial cells, accompanied by increased apoptosis and decreased autophagy. CIDEC gene silencing can improve autophagy and reduce apoptosis. At the molecular level, CIDEC gene silencing also decreased the expression of early growth response factor (EGR)1 and increased the expression of adipose triglyceride lipase (ATGL). **Conclusion** CIDEC gene silencing may delay the progression of DN by restoring autophagy activity and inhibiting apoptosis with the participation of EGR1and ATGL.

[Key words] Cell death-inducing DFF45-like effector C;Diabetic nephropathy;Early growth response factor

Evaluation of electrocardiographic and intracardiac electrogram characteristics for response to his-purkinje conduction system pacing in patients with left bundle branch block corrected by his bundle pacing

ZHENG Rujie

The First Affiliated Hospital of Wenzhou Medical University, Wenzhou 325000, China

[Abstract] Objective Aimed to evaluate the effect of electrocardiographic and intracardiac electrogram characteristics for response to His-Purkinje conduction system pacing (HPCSP) in patients with typical left bundle branch block (LBBB) which could be corrected by His bundle pacing (HBP) . **Methods** Consecutively enrolled patients with strictly defined LBBB and baseline LVEF ≤40% from January 2012 to June 2020 who were able to achieve LBBB correction during HBP and implanted HPCSP. Baseline QRS duration, paced QRS duration, ΔQRSd, H-QRSend and ΔQRSend/H-QRSend were measured during the implantation. The study population was divided into two groups based on value of the 1-year absolute increase in LVEF (ΔLVEF < 15%, ΔLVEF≥15%). Baseline patient characteristics, electrocardiographic, intracardiac electrogram characteristics and echocardiogram data were compared between two groups. **Results** A total of 123 patients were included in the study [mean age (68.2 ± 10.6) years,male 52.0%]. Baseline characteristics of patients with ΔLVEF≥15% (*n*=93) and ΔLVEF < 15% (*n*=30) were comparable except for larger ΔQRSend/H-QRSend [(0.42 ± 0.07)ms vs. (0.35 ± 0.08) ms, *P* < 0.05], smaller baseline QRS duration[(161.9 ± 15.5) vs. (172.3 ± 17.4)ms, *P* < 0.05] and paced QRS duration [(100.9 ± 14.9) vs. (110.5 ± 13.4) ms,*P* < 0.05] in patients with ΔLVEF≥15%. Receiver-operating characteristic curve analysis demonstrated that a cut-off value of 0.39 for ΔQRSend/H-QRSend presented a sensitivity of 77% and specificity of 76% (AUC=0.776) to predict super-response to HPCSP. At multivariate analysis, larger ΔQRSend/H-QRSend, smaller paced QRS duration and baseline QRS duration remained predictors of super-response after HPCSP. Patients with baseline LVEF < 30% and baseline LVEF≥30% had similar absolute increase in LVEF at 3 m, 6 m, and 1-year follow-up after HPCSP. However, the proportion of LVEF normalizing (final LVEF≥50%) was significantly lower in patients with baseline LVEF < 30% at 1-year follow-up. **Conclusion** HPCSP delivers favorable echocardiographic response in typical LBBB corrected by HBP. In typical LBBB, A larger ΔQRSend/H-QRSend, smaller baseline QRS duration and paced QRS duration are associated with a better response after HPCSP. ΔQRSend/H-QRSend is a novel and important predictor of LVEF increase.

[Key words] His-Purkinje conduction system pacing;Left bundle branch block;His bundle

The effect of farnesyl diphosphate synthase on endothelial autophagy of pulmonary arterial hypertension induced by monocrotaline

JIN Tingting　JIANG Dongmei　FU Guosheng

Sir Run Run Shaw Hospital, School of Medicine, Zhejiang University, Hangzhou 310020, China

[Abstract] **Objective** To observe the effects of these enzymes on the cardiovascular and pulmonary vascular systems in PAH models by directly interfering with their expression, and to clarify whether these enzymes can affect pulmonary arterial blood pressure by affecting endothelial function. However, there have been no reports from home and abroad. **Methods** PAECs were treated with monocrotaline pyrrole (MCTP) for 24 hours. The expression of farnesyl diphosphate synthase (FDPS) and autophagy - related proteins was determined. The proliferation of endothelium was measured by a trans-well assay. Ras-related C3 botulinum toxin substrate 1, Rac1(small G protein) activity was determined by pull-down assay. Moreover, Rac1 was activated with MCTP or inhibited by FDPS small interfering RNA (siRNA) to explore the role of FDPS in the modulation of endothelium function and autophagy. Meanwhile, autophagy was activated or blocked to observe the change in endothelium function. **Results** It was found that the protein expression of FDPS and autophagy - related proteins was increased. Inhibition of FDPS also recovered the reduced endothelium function induced by MCTP and inhibited Rac1 activated. **Conclusion** MCT-induced upregulated expression of FDPS and autophagy level in PAECs likely accounts for diverse alterations in endothelial cell signaling in this model of PH.

[Key words] Monocrotaline pyrrole;Farnesyl diphosphate synthase;Endothelial autophagy

Health-related quality of life after left bundle branch area pacing upgrade in patients of chroninc right ventricular pacing

YE Yang　WEI Lingling　FU Guosheng　JIANG Chenyang

Sir Run Run Shaw Hospital, School of Medicine, Zhejiang University, Hangzhou 310020, China

[Abstract] **Objective** To determine the health-related quality of life (QOL) after left bundle branch area pacing (LBBAP) upgrade in patients after chronic long term right ventricular pacing (RVP). **Methods** Patients referred for pulse generator change with long term RVP of larger than 40% attempted for LBBAP upgrade were included. The measures of cardiovascular health and quality of life were compared before, 3 months and 12 months post-LBBAP. The Clinical evaluation, cardiothoracic ratio, echocardiographic and electrocardiographic assessments were recorded at baseline and during the follow-up. Leads parameters and complications were also assessed. **Results** Permanent LBBAPupgradewas successful in 17 of twenty patients and were followed up for 12 months. Improvements in QOL parameters including physical functioning,physical problems, general healthand vitality on the MOS SF-36 Health Survey were seen after 12-month follow up(all $P<0.05$). The QRS duration (QRSd) was shortened to (114.8 ± 10.3)ms by LBBAP from (160.3 ± 24.7) ms by RVP ($P<0.05$). Their left ventricular ejection fraction (LVEF) was increased from baseline [(51.8% ± 15.3%) to (64.9% ± 11.9%) ($P<0.05$, $n=17$)] with left ventricular end of systolic volume was from [(139.8 ± 24.0) mL to (130.2 ± 20.2) mL ($P<0.05$)].Cardiac function status assessed by New York Heart Association (NYHA) functional class were all improved [from (2.7 ± 0.8) to (1.9 ± 0.6), $P<0.05$, $n=17$]. The LBBAP threshold was (0.8 ± 0.3) V/0.4 ms at implant

and remained stable during the 12 month–follow–up. **Conclusion** The health–related QOL was improved by LBBAP upgrade in patients by long term RVP irrespective of LVEF. LBBAP could reverse electrical synchrony and structural remodeling by chronic RVP.

[Key words] Left bundle branch area pacing; Right ventricular pacing; The quality of life; Electrical synchrony

The association between increased visceral adipose tissue and atherosclerosis in type 2 diabetes patients with a normal body weight

XU Kun ZHANG Jingyuan DU Changqing

Zhejiang Chinese Medical University, Hangzhou 310053, China

[Abstract] Objective To investigate the relationship between increased visceral adipose tissue (VAT) and the atherosclerosis in type 2 diabetes (T2D) patients with a normal body weight in China. **Methods** Data of patients with T2D who were admitted to the Second People's Hospital of Yuhuan and Jiangsu Sheyang County Diabetes Hospital were collected from the National Metabolic Management Center (MMC) database. The study used brachial ankle pulse wave velocity (baPWV) as indicator of atherosclerosis, and the the dual–bioelectrical impedance analysis was used to measure visceral fat area(VFA). Patients were classified into four groups according to the cutoff values of VFA and body mass index (BMI): BMI ⩽ 23.9 kg/m^2 and VFA < 100 cm^2 [OB(–)VA(–)], BMI > 23.9 kg/m^2 and VFA < 100 cm^2 [OB(+)VA(–)], BMI⩽23.9 kg/m^2 and VFA⩾100 cm^2 [OB(–)VA(+)], BMI > 23.9 kg/m^2 and VFA⩾100 cm^2 [OB(+)VA(+)]. The binary logistic regression analysis were performed to access the association of VFA and BMI with atherosclerosis. **Results** A total of 8 839 patients with T2D were enrolled in this study [51.7%(*n*=4 567) males, mean age (56.41 ± 10.39) years]. Among these patients, 3.7%(*n*=327) was classified as OB(–)VA(+), and 24.6%(*n*=2 171) , 25.2%(*n*=2 225), 46.6%(*n*=4 116) were classified as OB(–)VA(–), OB(+)VA(–), OB(+)VA(+). The OB(–)VA(+) patients had the highest baPWV(*P* < 0.05) among these four groups. In binary logistic regression analysis, significantly association were observed between the OB(–)VA(+) patients and atherosclerosis in multivariable adjustment model(*OR*=1.444, 95%*CI*:1.048–1.988, *P* < 0.05). **Conclusion** The increased VAT was associated with the incidence of the atherosclerosis in Chinese T2D patients with a normal body weight. Prospective studies should be performed to better characterize the relationship between the two.

[Key words] Visceral adipose tissue;atherosclerosis;Type 2 diabetes;BMI;Brachial ankle pulse wave velocity

CXCR4 blockade in macrophage promotes angiogenesis in ischemic hindlimb by modulating autophagy

MA Qunchao

The Second Affiliated Hospital, Zhejiang University School of Medicine, Hangzhou 310009, China

[Abstract] Objective Chemokine receptor CXCR4 plays a crucial role in leukocyte recruitment and inflammation regulation to influence tissue repair in ischemic diseases. However, the contribution of macrophagic CXCR4 in the ischemic hindlimb is not fully understood. **Methods** Using myeloid–specific CXCR4 knockout (MKO) mice, the effect of macrophagic CXCR4 on angiogenesis was assessed in limb ischemia mice model. RNA sequencing was used to

explore the role of CXCR4 on macrophage phenotype and function. **Results** Inflammatory cells were increased in the ischemic muscles of hindlimb, and CXCR4 was highly expressed in the infiltrated macrophages but not in neutrophils. Myeloid–specific CXCR4 knockout attenuated macrophage infiltration and subsequently reduced inflammatory response in the ischemic hindlimb, resulted in better blood reperfusion and higher capillary density as compared with that in wild–type (WT) mice. Similar outcomes were also observed in WT mice reconstituted with bone marrow cells from MKO mice. Gene ontology cluster analysis reviewed that Decorin, a negative regulator of angiogenesis, was reduced in CXCR4–deficient macrophages. CXCR4–deficient macrophages were less inducible into M1 polarization and more favorable for M2 polarization. Enhanced autophagy flux was detected in the CXCR4– deficient macrophages, which was associated with less expression of both Decorin and the inflammatory cytokines. **Conclusion** The data highlight the negative role of CXCR4 on macrophages for angiogenesis. Targeting at macrophagic CXCR4 may be a potential therapeutic strategy for ischemic diseases.

[Key words] CXCR4; Ischemic hindlimb;Modulate autophagy

Spinal cord stimulation attenuates neural remodeling, inflammation and fibrosis in myocardial infarction

HE Yuxian

The First Affiliated Hospital, Zhejiang University School of Medicine, Hangzhou 310003, China

[Abstract] Objective Spinal cord stimulation (SCS) is an established treatment regulating multiple levels of cardiac autonomic system. However, the biological mechanism of SCS produces therapeutic effects on myocardial infarction (MI) remains unclear. **Methods** New Zealand male rabbits were divided into five groups: SCS–MI (voltage of 0.5 v, pulse width 0.2 ms, 50 Hz, 10 min on, 30 min off; 2 weeks, *n*=5), MI (*n*=5), sham SCS–MI (voltage of 0 v; 2 weeks, *n*=5), sham MI (*n*=5) and the blank control group (*n*=5). MI was established by permanent left anterior descending artery (LAD) ligation. SCS–MI and sham SCS–MI rabbits received corresponding intervention 24 hours after MI surgery. Heart morphology was assessed by hematoxylin–eosin (HE). Autonomic remodeling was evaluated by enzyme–linked immunosorbent assay (ELISA) and immunohistochemistry(IHC). Inflammation and myocardial fibrosis were assessed via IHC, Western blotting, quantitative Polymerase Chain reaction(qPCR), Masson staining and immunofluorescence colocalization. **Results** SCS rebalanced systemic sympathetic and parasympathetic tone. Cardiac norepinephrine (NE) decreased after MI, and was not affected by SCS. SCS increased cardiac acetylcholine (Ach) compared with the MI group while no difference was observed among the MI, sham SCS–MI, sham MI and the blank control group. GAP43 and TH increased while ChAT decreased in the MI group compared with the blank control group, which were ameliorated by SCS. SCS inhibited inflammation, inhibiting the ratio of p–Erk to Erk and promoting the ratio of p–STAT3 to STAT3 compared with the MI group. Myocardial fibrosis was attenuated by SCS. **Conclusion** SCS rebalanced systemic sympathetic and parasympathetic tone, and improved cardiac parasympathetic tone in MI heart, leading to anti–inflammatory effects and the reactivation of STAT3 as well as the inhibition of Erk. Besides, SCS attenuated myocardial fibrosis. The study provided a preliminary basis for future research on biological mechanisms of SCS protecting the heart.

[Key words] Spinal cord stimulation;Myocardial infarction;Neural remodeling

Cofilin–1 controls mechanosensing in MSCs adhesion maturation

ZHU Dan　CHENWei　HU Xinyang　WANG Jian'an

The Second Affiliated Hospital of Zhejiang University School of Medicine, Hangzhou 310009, China

[Abstract] **Objective** To investigate heart stiffness variation after myocardial infarction, the role of stiffness on mesenchymal stem cells (MSCs) engraftment and its underlying mechanism. **Methods** The study used atomic force microscopy to probe heart stiffness in the setting of myocardial infarction and demonstrate a progressive increase in heart rigidity around the infarct region. Interestingly, MSCs engraftment is positively related to the stiffness. To investigate its underlying mechanism, the study use different polyacrylamide (PAA) gels to mimic variable heart stiffness and test its effect on MSCs adhesion. The study show that stronger adhesions form on stiffer gels and larger force generation on stiffer substrates is responsible for the formation of stronger adhesions. Here traction force microscopy was used to measure force generated by cell on different substrate. The study further investigated the origination of larger force on stiffer substrates. **Results** Consistent with a role of stress fibers in generating force, the study found more stress fibers formed on stiffer substrates. F–actin and myosin are the two main components of stress fiber. By labeling F–actin with lifeact and investigating them under time lapse microscopy, the study are able to find an increase of F–actin delivery from the lamellipodium to the lamella on stiffer substrates. In addition, the study found a stiffness dependent redistribution of tropomyosin between the lamellipodium and the lamella, which is another key structural component of stress fiber. As lamella is the main site of stress fiber formation, tropomyosin redistribution to the lamella may be responsible for increased F–actin delivery and stress fiber formation on stiffer substrate. Furthermore, the study found that redistribution of tropomyosin on stiffer substrates is regulated by cofilin–1 activity, and inhibition of cofilin–1 activity abolished the redistribution. Inhibition of cofilin–1 activity also disrupted focal adhesion formation and force generation on stiffer substrates. As cofilin–1 activity is suppressed by its phosphorylation state, the study confirmed its role on stiffness sensing by investigating its phosphorylation level on different substrate stiffness. The study result showed that phosphorylation of cofilin–1 decreased with an increasing stiffness. **Conclusion** These results indicate that heart stiffness is a major regulator of MSCs engraftment after myocardial infarction. In vitro mimic of stiffness by PAA gels shows that force generated from increased stress fiber promotes adhesion formation on stiffer substrate.

[Key words] Cofilin–1;Mesenchymal stem cells;Polyacrylamide

Cardiac fibroblastic LRP1–dependent endocytosis of liver angiotensinogen promotes sepsis induced myocardial dysfunction via NLRP3 inflammasome pathway

RONG Jiabing　XU Yinchuan　Wang Jian'an

The Second Affiliated Hospital of Zhejiang University School of Medicine, Hangzhou 310009, China

[Abstract] **Objective** Sepsis combined with cardiac dysfunction leads to a significant increase in mortality. The renin–angiotensin system (RAS system) plays an important role in the development of sepsis induced myocardial

dysfunction (SIMD). Angiotensinogen (AGT) is the only known precursor and substrate of the RAS system, and its effects on SIMD has not been illuminated. Meanwhile, locally synthesized AGT which was independent of systemic AGT was detected in end-organs, like kidney, heart, and adipose tissue. To investigate whether circulated or cardiac locally synthesized AGT was responsible for myocardial function during sepsis process and explored its potential mechanism, and then tried to provide a novel theoretical basis and potential intervention target to protect heart function after sepsis. **Methods** Male C57BL/6 mice were intraperitoneally injected by either lipopolysaccharide (LPS) or an equal volume of PBS and taken down 6 hours later. Cardiac function pre- and post-injection was evaluated by Vevo 2100 imaging system. The survival rate was monitored every hour for a 72-h period. Plasma AGT and angiotensin II (Ang II) levels were measured by ELISA, while hepatic and cardiac AGT expression level was determined by Western Blot. Cardiac hypertrophic markers expression and proinflammatory cytokine production were assessed by RT-qPCR while plasma levels of proinflammatory cytokines were detected by ELISA. Cardiomyocytes and cardiac fibroblasts were isolated by an enzymatic dissociation method. Combination of AGT and its receptor, low density lipoprotein receptor related protein1 (LRP1), was confirmed by ligand blotting. Furthermore, RNA sequencing of cardiac tissue was performed to uncover the role of hepatic AGT on hearts after LPS challenge. **Results** Intraperitoneal injection of LPS significantly activated AGT expression both in liver and heart and elevated plasma AGT level 6 hours later. We further generated hepatocyte-specific AGT-deficient (hepAGT-/-) mice and cardiomyocyte-specific AGT-deficient (carAGT-/-). Interestingly, the study found that hepatic conditional AGT deletion in mice triggered resistance to septic cardiac dysfunction and lethality. Contrarily, cardiac deficiency of AGT in mice had a similar phenotype as wild-type (WT) littermates. Depressed plasma AGT and AngII concentrations accompanied with less Interleukin 1 beta (IL-1β) level hinted hepatic elimination of AGT may functioned via circulated AngII-dependent manner. However, WT mice infused with an AT1R antagonist, losartan, partially protected from cardiac dysfunction compared to hepatic AGT deficiency, which implied that liver-secreted AGT may have an another effect on heart via an AngII-independent pathway. Furthermore, the study found cardiac AngII content of hepAGT-/- mice was comparable with WT littermates while IL-1β mRNA level in heart was lower, which proved there exited a pathway which IL-1β was involved in while AngII was not. Then, we discovered that hepatic AGT knock-out led to a distinct reduction of AGT expression in liver but heart showed a remarkably decreased AGT protein level with a compensatory augment of mRNA level. However in carAGT-/- mice, cardiac AGT expression was restrained in mRNA level but had no change in protein level, while hepatic AGT remained unchanged compared with their wild-type littermates. These facts implied that cardiac AGT is mainly derived from circulation rather than synthesized locally. Furthermore, the study identified liver derived AGT entered cardiac fibroblast rather than cardiomyocytes via LRP1 mediated endocytosis, which in turn activated NLRP3 inflammasome and improved IL-1β production. **Conclusion** Hepatocyte-specific deficiency of AGT ameliorates SIMD via preventing cardiac fibroblastic LRP1-dependent endocytosis and then decreasing NLRP3 inflammasome assembly, which alleviates IL-1β releasing. These findings provide potential therapeutic targets in liver to treat SIMD.

[Key words] NLRP3;Sepsis induced myocardial dysfunction;Angiotensinogen

Long non-coding RNA LUCAT1 influences the survival ability and therapeutic effect of MSCs and related mechanisms exploration

TAO Yue　WU Rongrong　HU Xinyang　WANG Jian'an

The Second Affiliated Hospital of Zhejiang University School of Medicine, Hangzhou 310009, China

[Abstract] **Objective** Myocardial infarction is a major hazard disease to human health. Bone marrow mesenchymal stem cells (MSCs) transplantation is one of the most promising treatment for myocardial tissue repair, but low survival rate of engrafted MSCs mainly limits the therapeutic effect of MSCs in the infarct-ed myocardium. Illustrating mechanism of stem cells survival and improving the therapeutic effect of engrafted cells are primary issues remained to be resolved. In this study, long non-coding RNA was used to improve the anti-apoptotic ability of MSCs and the mechanism involved was explored. **Methods** From 0.5% O_2、5% CO2、37 ℃ and 5% O2、5% CO2、37 ℃ culture environment after 24 hours, respectively, MSCs were under the screening process of lncRNA sequencing, filtered for lncRNA LCUAT1. By lentivirus editing LUCAT1 level of MSCs and injecting the modified MSCs into the border zone of the infarcted heart, we aimed to find out whether LUCAT1 influences the apoptosis of MSCs and the therapeutic effect of MSCs for myocarial infarction. GFP staining 3 days after myocardial infarction, echo detection 28 days after myocardial infarction and Masson staining 28 days after myocardial infarction were conducted. Furthermore, through mass spectrometry analysis of proteins that were co-precipitated by LUCAT1 and RNA immunoprecipitation (RIP) experiment, the study screened regulatory proteins in the nucleus which LUCAT1 could bind to. Synthesis of the results from mass spectrometry and transcriptome sequencing of MSCs after LUCAT1 knocking down, the study singled out the specific target gene which can be regulated by LUCAT1. With chromatin immunoprecitation(CHIP) assay and luciferase experiment, the study explored LUCAT1 may manipulate the apoptosis of MSCs by recruiting regulatory protein to target gene promoter. **Results** The study found that knock down of LUCAT1 decreased cell apoptosis resistance while over expression of LUCAT1 showed the opposite results. GFP staining showed that survival rate of the MSCs that knock down of LUCAT1 was reduced in 3 days post injection, and the echo results in 28 days after the myocardial infarction indicated that the cardiac function was worse than control group. In addition, the Masson staining results after 28 days showed that the scar area of heart was increased. Overexpression of LUCAT1 can enhance the anti-apoptotic ability of cells and the therapeutic effect after myocardial infarction. It was found that LUCAT1 could bind to a lot of regulatory proteins in the nucleus. RIP results showed LUCAT1 had strong binding ability with JMJD6. Through transcriptome sequencing of MSCs after LUCAT1 knock down, the expression of FOXQ1, an anti-apoptotic protein, was significantly decreased compared with control group. When LUCAT1 was overexpressed, FOXQ1 expression increased significantly. Lentivirus knockdown of JMJD6 in mesenchymal decreased FOXQ1 expression, but overexpression had no effect on FOXQ1 expression. Luciferase experiment verified that JMJD6 could bind to the promoter region of FOXQ1. CHIP assay detected that JMJD6 acted in FOXQ1 promoter region on the methylation sites H3R2me2a and H4R3me2s reported. It was also found that the methylation level of these two sites increased when LUCAT1 was knocked down, while the methylation enrichment of H4R3me2s decreased when LUCAT1 was overexpressed and H3R2me2a showed no significant change. **Conclusion** LUCAT1 can improve the viability of MSCs, and enhance the therapeutic effect of MSCs for myocardial infarction by recruiting JMJD6 to the promoter of the anti-apoptotic protein FOXQ1, affecting the methylation enrichment level of H4R3me2s in the promoter region and thus changing FOXQ1 expression level.

[Key words] Bone marrow mesenchymal stem cells;Myocardial;Infarction;LUCAT1;JMJD6;FOXQ1;H4R3me2s;H3R2me2a

Exosomal microRNA–486–5p promotes the angiogenic response to myocardial infarction by targeting matrix metalloproteinase 19 in fibroblasts

LI Qingju XU Yinchuan LYU Kaiqi HU Xinyang WANG Jian'an

The Second Affiliated Hospital of Zhejiang University School of Medicine, Hangzhou 310009, China

[Abstract] **Objective** The potency of mesenchymal stem cells (MSCs) for treatment of myocardial infarction (MI) in nonhuman primates (NHPs) can be significantly improved by culturing the cells under hypoxic conditions before administration, and most of the improvement is likely caused by increases in the cells' paracrine activity , which are often transported to their target cells by exosomes. thus, exosomes have a key role in mechanisms that regulate apoptosis, inflammation, angiogenesis,4 and many other biological processes that protect and repair the heart after myocardial injury. we have shown that the potency of allogeneic MSCs for myocardial repair and angiogenesis in nonhuman primates (NHPs) can be significantly improved by culturing the cells under hypoxic conditions before administration. The study results also suggested that the improvement is likely mediated by increases in the paracrine activity of the hypoxia–preconditioned cells,9but the molecular factors that contributed to this increase were not identified. **Methods** In a murine MI model, cardiac function, infarct size, vascular density were measured by echocardiography, Masson staining and immunofluorescence. Aortic ring and tube formation were performed to evaluate angiogenic activity. Microarray and RNA sequencing were applied to determine the difference between exosomes from hypoxia–preconditioned MSCs (hpEXOs) and normoxia–cultured MSCs (nEXOs) and with these treated heart tissue. **Results** Cardiac function, infarct size, and vascular density were significantly greater in mice treated with hypoxia–preconditioned MSCs (hpMSCs) than with normoxia–cultured MSCs (nMSCs) and with hpEXOs than with nEXOs. miR–486–5p levels were significantly greater in hpEXOs than in nEXOs, which also confirmed to play a central role in exosomal mediated cardiac repair. Matrix metalloproteinase 19 (MMP19) levels were significantly lower in tissues from hpEXO–treated than nEXO–treated hearts and significantly greater in cardiac fibroblasts (CFs). miR–486–5p interacted with the 3' untranslated region of MMP19, and downregulated MMP19 expression in CFs, while both miR–486–5p upregulation and MMP19 silencing (MMP19 siRNA) in CFs increased the angiogenic activity of ECs cultured in the CF–conditioned medium. MMP19 silencing in CFs also reduced the cleavage of extracellular vascular endothelial growth factor (VEGF), and MMP19 cleaved VEGF in solution, while miR–486–5p upregulation significantly increased the potency of nEXOs for myocardial recovery and angiogenesis in an NHP MI model. **Conclusion** In summary, the results presented in this report show that exosomal miR–486–5p is one of the primary pro–angiogenic paracrine factors produced by MSCs, and that it functions by downregulating MMP19 expression in fibroblasts and the cleavage of extracellular VEGFA. Furthermore, the exosomes produced by miR–486–5p–overexpressing MSCs significantly improved measures of cardiac function, infarct size, and angiogenesis when delivered to the infarcted hearts of NHPs without increasing the occurrence of arrhythmic complications. Collectively, these observations support additional investigations of the role of miR–486–5p, as well as the exosomes produced by other stem–cell populations, in myocardial regeneration.

[Key words] Mesenchymal stem cells;Exosomal miR–486–5p;Angiogenesis; Myocardial infarction

TANK–binding kinase 1 improves myocardial ischemia/reperfusion injury via TBK1–OPTN regulated mitophagy

LYU Ping　WANG Lihong　ZHENG Hao

Zhejiang Provincial People's Hospital, People's Hospital of Hangzhou Medical College, Hangzhou 310009, China

[Abstract] **Objective** Myocardial ischemia/reperfusion (MI/R) injury, a complicated pathophysiological process, is regulated by lots of signaling pathways. TANK–binding kinase 1 (TBK1) is an IKK–related serine/threonine kinase, and its role in MI/R injury is not that clear. Here in our present study, we examined the function of TBK1 in MI/R injury and try to illuminate the underlying mechanisms. **Methods** Mice or neonatal rat cardiomyocytes (NRCMs) were subjected to I/R surgery or hypoxia/reoxygenation (H/R) injury, respectively. Cardiac function was detected by echocardiography and cardiac infarct size was measured by Evans Blue and TTC staining. Cardiomyocyte apoptosis was measured by TUNEL staining while TEM or a laser confocal microscope was used to observe the mitochondria and mitophagy. Western Blotting was used to detect the levels of related proteins. **Results** The results indicated that TBK1 was decreased in mice subjected to MI/R injury. However, after overexpressing TBK1 through an intramyocardial injection of TBK1 adenovirus, TBK1 overexpression improved cardiac function detected by echocardiography, decreased infarct size detected by Evans Blue and TTC staining, reduced cardiomyocyte apoptosis measured by TUNEL staining and increased mitophagy detected by TEM or a laser confocal microscope in response to MI/R injury. Consistently, TBK1 overexpression ameliorated mitochondrial oxygen consumption rate (OCR) in NRCMs in response to H/R injury. Also, cardiomyocyte apoptosis in vitro was rescued by TBK1 overexpression through TUNEL staining. Mechanistically, MI/R or H/R injury disturbed the colocalization of TBK1 and OPTN by downregulating TBK1. Therefore, phosphorylated OPTN by TBK1 was reduced, leading to decreased mitophagy in response to MI/R or H/R injury. However, TBK1 overexpression could rescue mitophagy through increasing the colocalization of TBK1 and OPTN and subsequently phosphorylated OPTN. **Conclusion** Our findings uncovered a pivotal function of TBK1 in MI/R injury through regulating the mitophagy by recruiting and phosphorylating OPTN for the first time, which might represent a promising target in treating MI/R patients in the future.

[Key words] Myocardial ischemia/reperfusion (MI/R) injury;TANK–binding kinase 1;Function

Serum irisin level as a biomarker for pure aortic stenosis and aortic valve calcification

CHEN Han　WANG Shanshan　LI Jiamin

The Second Affiliated Hospital, Zhejiang University School of Medicine, Hangzhou 310009, China

[Abstract] **Background** Irisin is a myokine mainly secreted by skeletal and cardiac muscles, and it is actively involved in cardiovascular diseases such as heart failure and atherosclerosis. However, whether irisin is associated with valvular heart disease remains unknown. The study examined serum irisin level in a cohort of patients who underwent transcatheter aortic valve implantation (TAVI). **Methods** Two hundred and ninety–three patients with severe aortic stenosis (AS) who underwent TAVI were enrolled in this study. The median follow–up period was 35 months. Blood samples were collected before TAVI procedures. The structural and hemodynamic parameters of aortic valves were evaluated by echocardiogram and Computed Tomography (CT). Enzyme–linked Immunosorbent Assay (ELISA)

was applied to measure the irisin levels. The patient population was divided into 2 groups (high versus low) based on median serum irisin level readings. Correlation analysis, linear regression analysis, logistic regression analysis, and survival analysis were performed to explore the association of serum irisin level with clinical characteristics and outcomes. **Results** The median age of the entire population was 77 years and 58% were male. The median irisin levels was 13.70 ng/mL (10.95,17.96).The severity of aortic valve calcification (in terms of calcification grading) is negatively associated with serum irisin levels ($P<0.01$). High irisin level is significantly associated with pure aortic stenosis (*OR*=2.868, 95%*CI*:L 1.729–4.755, $P<0.01$). Multivariate logistic analysis adjusting age, BMI, history of peripheral vascular disease, and creatinine level demonstrated that high irisin level was independently associated with pure aortic stenosis (*OR*=3.015, 95%*CI*: 1.775–5.119, $P<0.01$). ROC curve analysis showed a strong prognostic value of irisin level for pure aortic stenosis (AUC=0.647, 95%*CI*: 0.582–0.711, $P<0.01$). Kaplan–Meier survival analysis indicated that there were similar death rates of all–cause or cardiovascular mortality rates between patients in the irisin dichotomous group during follow–up (LogRank $P>0.05$). **Conclusion** Serum irisin level is negatively associated with the severity of aortic valve calcification, and high serum irisin level is an independent predictor for pure aortic stenosis. These findings imply an important role of irisin in aortic stenosis.

[Key words] Serum irisin level;Aortic valve calcification;Pure aortic stenosis

Prognostic value of fragmented QRS complexes in patients with AMI treated with percutaneous coronary intervention

CHEN Zhangqiang

Jiangxi Provincal People's Hospital, Nanchang 330006, China

[Abstract] Objective To evaluate the prognostic value of fragmented QRS complexes in patients with acute myocardial infarction treated with percutaneous coronary intervention. **Methods** A total of 200 In–patients with acute myocardial infarction treated with percutaneous coronary intervention were included from January 2018 to April 2021 in this retrospective study. Patients were divided into 2 groups according to the presence or absence of fragmented QRS complex at discharge. Fragmented QRS complexes refer to various RSR' patterns (⩾1 R' or notching of S wave or R wave) with or without Q wave in 2 or more contiguous leads corresponding to a major coronary artery territory on the routine 12lead electrocardiograms (ECGs). **Results** The follow–up period was similar in both groups ($P>0.05$). During the 1year follow–up,the incidence of major composite endpoint event was significant difference between the two groups in this study ($P<0.01$). The rate of all–cause death was 8% for the fragmented QRS complex group and 1% for the nonfragmented QRS complex group, there were significant difference between the two groups in this study ($P<0.05$). Cardiac death rate was 6% in the fragmented QRS complex group and 1% in the nonfragmented QRS complex group, there were also significant difference between the two groups($P<0.05$). The incidence of acute coronary syndrome and coronary artery revascularization were similar between the two groups during 1–year follow–up($P>0.05$ and $P>0.05$, respectively). The incidence of heart failure was 15% in the fragmented QRS complex group and 6% in the nonfragmented QRS complex group, there were also significant difference between the two groups($P<0.05$). **Conclusion** In patients with acute myocardial infarction who underwent percutaneous coronary intervention,the incidence of major composite endpoint event was significantly higher in patients with fragmented QRS complex than those without fragmented QRS complex. The all–cause mortality rate and Cardiac death rate as well as incidence of heart failure were significantly increased in patients with fragmented QRS complex compared with without fragmented QRS complex.

[Key words] QRS complex;Fragmented;Acute myocardial infarction

The combined effect of patient activation and relational aspects on the quality of life with in atrial fibrillation patients

WANG Jie SUN Guozhen BAO Zhipeng GAO Min

Nanjing Medical University, Nanjing 225000, China

[Abstract] **Objective** This study mainly explored the degree of influence of patient activation (PA) and relational aspects on the quality of life (QoL) and then provided a basis for improving PA and QoL in patients with atrial fibrillation (AF). **Methods** A cross-sectional study was undertaken in 2021 among 190 AF patients in Nanjing, China. The study measures comprised a self-designed general information questionnaire, the patient activation measure (PAM), the atrial fibrillation effect on quality of life (AFEQT). The data analysis was performed using IBM SPSS, version 25 and comprised Spearman correlation analysis, a multiple linear regression model, and Wilcoxon rank-sum tests. **Results** The average AFEQT score for the 190 AF patients was (69.32 ± 14.52). Results about the distribution of activation levels where 13.7%, 47.4%, 34.2% and 4.7% were in activation Levels 4, 3, 2, and 1, respectively. The multiple linear regression analysis revealed that patient activation, work status, and cardiac rehabilitation of AF patients predicted AF-related QoL (β = 0.270, –0.205, and 0.183, respectively; all $P < 0.05$). The influence of PA on sub-dimensions of AF- related QoL were as follows: symptoms, daily activities and treatment concern. **Conclusion** The level of QoL of patients with AF was moderate. PA level positively affected symptoms, daily activities and treatment concern and the whole QoL. In light of our findings, we suggest that medical workers should encourage AF patients to take actively participation in cardiac rehabilitation and disease self-management, foster progression of PA level. Future research is warranted to develop tailor-made interventions aimed at activation level.

[Key words] Atrial fibrillation;Quality of life;Combined effect

Sealing behaviour in transcatheter bicuspid and tricuspid aortic valves replacement through patient-specific computational modeling

FAN Jiaqi LIU Xianbao WANG Jian'an

The Second Affiliated Hospital of Zhejiang University Schoool of Medicine, Hangzhou 310009, China

[Abstract] **Objecive** Patient-specific computer simulation of transcatheter aortic valve replacement (TAVR) can provide unique insights in device-patient interaction.This study was to compare transcatheter aortic valve sealing behaviour in patients with bicuspid aortic valves (BAV) and tricuspid aortic valves (TAV) through patient-specific computational modeling. **Methods** Patient-specific computer simulation was retrospectively performed with FEops HEARTguide for TAVR patients. Simulation output was compared with postprocedural computed tomography and echocardiography to validate the accuracy. Skirt malapposition was defined by a distance larger than 1mm based on the predicted device-patient interaction by quantifying the distance between the transcatheter heart valve (THV) skirt and the surrounding anatomical regions. **Results** In total, 43 patients were included in the study. Predicted and observed THV frame deformation showed good correlation ($R^2 \geqslant 0.90$) for all analysed measurements (maximum diameter, minimum diameter, area, and perimeter). The amount of predicted THV skirt malapposition was strongly linked with the

echocardiographic grading of paravalvular leakage (PVL). More THV skirt malapposition was observed for BAV cases when compared to TAV cases (22.7% vs. 15.5%, $P<0.05$). A detailed analysis of skirt malapposition showed a higher degree of malapposition in the interleaflet triangles section for BAV cases as compared to TAV patients (11.1% vs. 5.8%, $P<0.05$). **Conclusion** Patient-specific computer simulation of TAVR can accurately predict the behaviour of the Venus A-Valve. BAV patients are associated with more malapposition of the THV skirt as compared to TAV patients, and this is mainly driven by more malapposition in the interleaflet triangle region.

[Key words] Transcatheter aortic valve replacement;Bicuspid aortic valves;Tricuspid aortic valves

LncRNA CPhar attenuates pressure-overload induced cardiac pathological hypertrophy via regulating C/EBP β

WU Xiaodong

The Second Affiliated Hospital, Zhejiang University School of Medicine, Hangzhou 310009, China

[Abstract] Objective As great changes in lifestyle and diet, incidence of heart failure worldwide has been significantly elevated. However, specific treatment with high efficiency is still in lack. So further investigation is still in urgent need. At present, exploring of medication treatment to heart failure is focus on attenuating pathological remodeling, and hypertrophy occupied vital role in cardiac remodeling. LncRNA refers to RNAs that are longer than 200 nucleotides and lack the potentiality to encode a protein, which has been involved in cardiovascular disease progression. In our previous study, we demonstrated a novel lncRNA, named cardiac physiological associated regulator (CPhar, Acession ID: FR236703), which participated in exercise-induced cardiac physiological hypertrophy (PMID: 34015936). But its role in cardiac pathological hypertrophy is still unclear, the purpose of this study is to clarify effect of CPhar on cardiac pathological hypertrophy. **Methods** The study isolated primary mouse cardiomyocytes (NMCM). Phenylephrine (PE) was used to induce cardiomyocyte hypertrophy and CPhar over-expression or knockdown Adv was involved in study to determine if CPhar affected the occurrence of cardiomyocyte pathological hypertrophy.And in in vivo study, Ang II or transverse aortic constriction (TAC) was exposed to mouse to induced cardiac pathological hypertrophy and dysfunction. One week prior to Ang II pump or TAC surgery exposure, tail vein injection of CPhar over-expression or knockdown AAV9 was performed. At endpoint of experiment, echocardiograph was used to evaluate the influence of CPhar on cardiac function, followed by adequate detection on cardiac pathological hypertrophy.After proving the role of CPhar in cardiac pathological hypertrophy, we further found C/EBP β functions as the downstream transcriptional factor of CPhar, and CPhar exerts its effect via inhibiting C/EBP β. **Results** The in vitro study demonstrated CPhar decreased expression of PE induced ANP、BNP in cardiomyocytes, and attenuated cardiomyocyte pathological hypertrophy resulted from PE stimulation. And CPhar protected mice from Ang II or TAC caused cardiac pathological hypertrophy and cardiac dysfunction. But after CPhar knockdown, the stimulation did not further deteriorate the phenotypes both in in vitro and in vivo experiments. Subsequently, we found C/EBP β acts as the down-stream transcriptional factor of CPhar and CPhar develops anti-hypertrophic effect via inhibiting C/EBP β. And basic on our previous study, DDX17 functions as RNA binding protein to CPhar, and there is direct interaction between DDX17 and C/EBP β, and CPhar knockdown can attenuate their interaction. Thus, CPhar exerts its effect on cardiac pathological hypertrophy via regulating C/EBP β. **Conclusion** LncRNA (CPhar) attenuated the progression of cardiac pathological hypertrophy and showed a beneficial effect on cardiac dysfunction both in in vitro and in vivo experiments. And CPhar develops its impact by regulating C/EBP β via recruiting DDX17.

[Key words] LncRNA;Cardiac pathological hypertrophy;C/EBP β

Sirt3 is a novel target to treat sepsis induced myocardial dysfunction by acetylated modulation of critical enzymes within cardiac tricarboxylic acid cycle

XU Yinchuan ZHANG Shujing RONG Jiabing LIN Yao WANG Yi ZHANG Zhaocai

The Second Affiliated Hospital, Zhejiang University School of Medicine, Hangzhou 310009, China

[Abstract] Sepsis induced myocardial dysfunction (SIMD) results in high morbidity and mortality. However, the effective therapeutic strategies for SIMD treatment remain limited. Sirt3 is the main mitochondrial Sirtuin member and is a key modulator of mitochondrial metabolism and function. In this study, we aimed to investigate the effect and mechanism of Sirt3 on SIMD. SIMD was induced by 20 mg/kg Lipopolysaccharides (LPS) injection for 6 h in mice. Sepsis could induce the reduction of cardiac Sirt3 expression and global deficiency of Sirt3 exacerbated cardiac function. Quantitative acetyl-proteomics and cardiac metabolomics analysis revealed that loss of Sirt3 led to hyper-acetylation of critical enzymes within cardiac tricarboxylic acid (TCA) cycle and generation of lactate and NADH, subsequently promotion of cardiac dysfunction after sepsis. Additionally, to evaluate whether Emodin could be utilized as a potential Sirt3 modulator to treat SIMD, male wild type mice (WT mice) or global Sirt3 deficient mice ($Sirt3^{-/-}$ mice) were intraperitoneally injected with 40 mg/kg Emodin for 5 days followed by 20 mg/kg LPS administration for another 6 h and observed that exogenous administration of Emodin could attenuate myocardial dysfunction in septic WT mice. However, septic $Sirt3^{-/-}$ mice can not gain benefit on cardiac performance from Emodin infusion. In conclusion, this study presented the protective role of Sirt3 targeting SIMD, which may provide a potential novel approach to maintain normal cardiac performance after sepsis.

[Key words] Sepsis induced myocardial dysfunction;Cardiac tricarboxylic acid cycle;Sirt3

Myocardial integrin β1 overexpression protects against sepsis induced cardiac dysfunction in rats

XU Yinchuan LIN Yao RONG Jiabing ZHANG Zhaocai

The Second Affiliated Hospital, Zhejiang University School of Medicine, Hangzhou 310009, China

[Abstract] **Background** Cardiac dysfunction is one of the major complications in patients with sepsis, which leads to high mortality. However, the effective therapeutic strategies for sepsis induced myocardial dysfunction (SIMD) treatment remain limited. Integrin β1 is one of the dominant Integrin forms on cardiomyocytes and functioned as mechanotransduers, translating mechanical to biochemical information. The aim of this study was to investigate the effect and mechanism of myocardial Integrin β1 on SIMD. **Methods** In this study, the technique of intramyocardial delivery of lentivirus was applied to modulate cardiac Integrin β1 expression. Then the forty-four male SD rats were randomly assigned to six groups: PBS, PBS+LPS, lenti-Integrin β1Over+LPS, lenti-Integrin β1Si+LPS, lenti-Mock+LPS and lenti-Scramble+LPS group. Rats were treated with lipopolysaccharide (LPS) for 12 hours to induce sepsis model. The cardiac function, myocardial injury biomarkers, cardiac apoptosis, the expression of cardiac cytoskeletal proteins as well as cardiac cells membrane stability were assayed. **Results** The results demonstrated that improvements in cardiac function 12 hours after LPS injection were significantly greater in lenti-Inegrin β1Over -treated rats than in rats treated with lenti-Inegrin β1Si or lenti-Mock, whereas differences between the lenti-Inegrin β1Si and lenti-Scramble groups did not reach statistical significance. Furthermore, the observed improvements were accompanied by evidences of

attenuation of cardiac apoptosis, enhancement of myocardial cytoskeletal proteins expression as well as improvement of cardiac cells membrane stability. **Conclusion** The current study presented the investigation of SIMD treatment targeting Integrin β 1, which may provide a potential novel approach to maintain normal cardiac performance after sepsis.

[Key words] Myocardial Integrin; β 1 overexpression ;Sepsis induced cardiac dysfunction

Two–way interaction between cardiac adipose tissue and cardiomyocytes in the process of cardiac repair

LIN Yan

The Second Affiliated Hospital, Zhejiang University School of Medicine, Hangzhou 310009, China

[Abstract] Cardiomyocytes loss was mostly induced by myocardial ischemia or infarction, which ultimately results in irreversible myocardial damage, even heart failure. Myocardial ischemia or infarction is one of the most frequent cardiovascular diseases, causing millions of deaths per year worldwide. The prognosis of heart failure is also poor with 2% to 17% of patients dying during their first admission, 17% to 45% mortality within 1 year of admission, and > 50% mortality within 5 years. Although updated pharmacological and interventional therapies have made the mortality rates of MI decrease, there is hardly treatment available to repair massive loss of cardiomyocytes since they had poor capacity of regeneration. Therefore, numerous research efforts were in progress in search of alternative treatments.

[Key words] Cardiac adipose tissue;Cardiomyocytes;Cardiac repair

Next–generation sequencing identified novel KCNQ1 mutation associated with LQT syndrome

LIN Xiaoping

The Second Affiliated Hospital, Zhejiang University School of Medicine, Hangzhou 310009, China

[Abstract] **Background** Long QT syndrome (LQT) is one of the leading causes for sudden cardiac death (SCD). Recent studies have identified mutations in ion channels as key players in the pathogenesis of LQT. However, the specific etiology in individual families remains largely unknown. **Methods** A 12–year old boy presented with recurrent exertional syncope and seizure was recruited. Targeted next generation sequencing (NGS) was performed and validated by Sanger sequencing. **Results** The proband, a 12–year old boy presented with unexplained syncope and seizure after vigorous exercise. Following resuscitation, he was recruited to neurology department due to suspicion of epilepsy. However, EKG showed significantly prolong QTc up to 577ms. The boy was then treated with Propanolol, and remained asymptomatic. NGS revealed a novel heterozygous missense mutation (c.749T > C) in potassium voltage–gated channel subfamily Q member 1 (KCNQ1). The KCNQ1 c.749T > C led to a Leu substituted by Pro in 250th of amino acid sequence. Validation Sanger sequencing of the child's parents unveiled that his father also carried the same mutation KCNQ1 c.749T > C. Although his QTc was in the normal range in rest EKG (430–444 ms), exercise treadmill test revealed his QTc was significantly prolonged during recovery period, more than 500ms even after 8 min, fulfilling the diagnosis of LQT. **Conclusion** The novel KCNQ1 c.749T > C mutation was co–segregated with QT prolongation in this small family, thus was causal with LQT syndrome. Functional study is well underway to further explore the role of novel KCNQ1 mutation in LQT.

[Key words] Next-generation sequencing;Novel KCNQ1 mutation;LQT syndrome

Functional coordination of non-myocytes plays a key role in in de novo heart regeneration

MA Hong LIU Ziqing YANG Yuchen FENG Dong DONG Yanhan Tiffany A. Garbutt HU Zhiyuan WANG Li Cynthia D. Cooper LI Yun Joshua D. Welch QIAN Li LIU Jiandong

The Second Affiliated Hospital, Zhejiang University School of Medicine, Hangzhou 310009, China

[Abstract] Cardiac regeneration occurs primarily through proliferation of existing cardiomyocytes, yet the regenerative response also involves complex interactions between distinct cardiac cell types including not only cardiomyocytes, but also non-cardiomyocytes (nonCMs). However, the subpopulations, distinguishing molecular features, cellular functions, and intercellular interactions of nonCMs in heart regeneration remain largely unexplored. Using the LIGER algorithm, we assembled an atlas of cell states from 61,977 individual nonCM scRNA-seq profiles isolated at multiple time points during heart regeneration in both wildtype and mutant fish. This analysis revealed extensive nonCM cell diversity, including multiple macrophage, fibroblast and endothelial subpopulations with unique spatiotemporal distributions. Furthermore, this analysis suggested an important role for the inflammatory MC subpopulation in inducing the formation of the activated fibroblast subtype and endocardial endothelial cell subpopulation. Indeed, genetic and pharmacological perturbation of macrophage functional dynamics compromised the induction of these unique subpopulation cells, reduced cardiomyocyte proliferation, and caused defective cardiac regeneration. Furthermore, we developed a computational algorithm called Topologizer to map the topological relationships and dynamic transitions between functional states. Through this analysis, we uncovered dynamic transitions between macrophage functional states and identified factors involved in mRNA processing and transcriptional regulation associated with the transition. Together, our single-cell transcriptomic analysis of nonCMs during cardiac regeneration provides a blueprint for interrogating the molecular and cellular basis of cardiac regeneration.

[Key words] Functional coordination;Non-myocytes ;In de novo heart regeneration

Flavin containing monooxygenase 2 confers cardiac protection via unfolded protein response signaling modulated by disulfide bond catalysis

LIU Qingnian TAO Yue DING Hao XIAO Changchen ZHOU Yu NI Cheng KE Changle WANG Jingyi WU Rongrong FAN Lin WU Xianpeng ZHAO Jing WU Yan HU Xinyang WANG Jian'an

The Second Affiliated Hospital, Zhejiang University School of Medicine, Hangzhou 310009, China

[Abstract] **Introduction** Myocardial infarction (MI) is characterized by cardiac dysfunction and increased cardiomyocyte death, induced mainly by apoptosis. Using an unbiased transcriptome analysis, we identified flavin containing monooxygenase 2 (FMO2) as one of the top-ranked genes involved in the process of MI. The study investigate the roles of FMO2 in ischemic injury and its potential mechanisms.Hypothesis: FMO2 exhibits the cardiac

protection from MI injury. **Methods** Male SD rats receiving either adeno-associated virus serotype 9 containing FMO2 shRNA particles (AAV-shFMO2) or FMO2 (AAV-FMO2), and FMO2 knockout rats were subjected to myocardial infarction surgery. Cardiac function, fibrosis, and apoptosis were examined in these rats and related cellular and molecular mechanisms were investigated. **Results** Cardiac ischemia injury was associated with significant increases of FMO2 levels both in ex vivo and in vivo models. Loss of FMO2 significantly enhanced cardiomyocyte apoptosis and deteriorated cardiac function accompanied by augmented infarct size in infarcted rat hearts, while elevated expression of FMO2 exhibited the opposite results. Mechanically, located on the ER membrane, FMO2 inhibited activation of ER stress-initiated apoptotic proteins including caspase 12 and C/EBP homologous protein (CHOP), via down-regulating upstream unfolded protein response (UPR) pathway. Furthermore, we found that FMO2, as a novel chaperone in ER, directly catalyzed disulfide-bond synthesis to facilitate proteins folding. Finally, structure analysis of FMO2 revealed the active site GVSG for disulfide-bond catalysis, which was confirmed by the molecular docking experiment of GSH with FMO2. However, FMO2 with GVSG mutation failed to catalyze disulfide-bond formation and lost protection from ER stress or apoptosis in cardiomyocytes. **Conclusion** FMO2 confers cardiac protection from ischemic damage due to improved cardiomyocyte apoptosis through UPR pathway, which is mediated by disulfide-bond catalysis at GVSG active site. Our findings uncover a novel FMO2-involved regulatory mechanism which could serves as a potential therapeutic target for ischemic cardiovascular diseases.

[Key words] Flavin containing monooxygenase 2;Cardiac protection; Unfolded protein response;Disulfide bond catalysis

Meta-analysis of C242T polymorphism in CYBA genes: risk of acute coronary syndrome is lower in Asians but not in caucasians

HU Po

The Second Affiliated Hospital, Zhejiang University School of Medicine, Hangzhou 310009, China

[Abstract] Background A lot of studies have demonstrated that C242T polymorphism in CYBA genes may play an important role in the pathological process of acute coronary syndrome (ACS). However, the results are not consistent. To further evaluate this debate, we performed a meta-analysis to determine the relationship between C242T polymorphism and ACS. **Methods** We screened PubMed/MEDLINE, EBSCIO, and EMBASE research reports until Mar 2014 and extracted data from 10 studies involving 6102 ACS patients and 8669 controls. **Results** Subgroup analysis by ethnicity documented a significant decreased risk of ACS for C242T polymorphism in the Asian population under allelic comparison [odd ratio (*OR*)= 0.73; 95% confidence intervals (*CI*): 0.64 – 0.83], dominant model (*OR*= 0.71; 95%*CI*: 0.62 – 0.82), and homozygote comparison (*OR*= 0.57; 95%*CI*: 0.35 – 0.92). However, in the overall population and especially with Caucasians, no significant association was uncovered. Further meta-regression analysis revealed that the heterogeneity among studies was largely attributed to ethnicity. No publication bias was detected through a funnel plot and an Egger's linear regression test. **Conclusion** Taken together, our results suggest that the C242T polymorphism might be a protective factor against developing ACS in the Asian population. Further researches will be needed to identify the confounding factors which modified the protective effect of T allele among caucasians.

[Key words] Meta-analysis; C242T polymorphism;CYBA genes;Acute coronary syndrome

Longty pure paclitaxel coated balloon versus SeQuent Please drug coated balloon for the treatment of in-stent restenosis

JIANG Jun WANG Jian'an

The Second Affiliated Hospital, Zhejiang University School of Medicine, Hangzhou 310009, China

[Abstract] **Background** drug coated balloon (DCB) is an effective treatment for in-stent restenosis (ISR). The present study was designed to compare the angiographic efficacy, clinical safety, and effectiveness of the Longty pure paclitaxel-coated balloon (ZheJiang Barty Medical Technology Co., Ltd, Hangzhou, China) with SeQuent Please DCB (B. Braun, Melsungen AG, Melsungen, Germany) for the approval of the new device in China. **Methods** Longty ISR was a 212-patient randomized (1:1), single-blind prospective, non-inferiority trial conducted in 13 Chinese centers. Patients with first episode of coronary ISR received either Longty DCB or SeQuent Please DCBtreatment. The primary endpoint was in-segment late lumen loss at 9 months. **Results** There were no significant differences between both treatment groups regarding patient baseline, lesion, or procedural characteristics. At 9 months, in-segment late lumen loss in the LONGTY DCB group was noninferior to that of the SeQuent Please group (0.26 mm vs. 0.32 mm; difference: −0.06 mm with 95% *CI*: −0.17 −0.16; P for noninferiority < 0.01). The 9-months rate of binary restenosis and 12-month composite clinical event rates were not significantly different between 2 groups. **Conclusion** In a randomized trial of 212 ISR patients, angioplasty with Longty DCB was noninferior to the SeQuent Please DCB for the primary endpoint of 9-month in-segment late loss. **Results** The of 1-year clinical follow-up showed no significant differences between 2 groups in terms of target lesion failure, acute myocardial infarction, and cardiac death.

[Key words] Drug coated balloon;In-stent restenosis;SeQuent

The growth differentiation factor 11 is essential for maintain cardiac function after myocardial injury through autocrine and paracrine pathway

ZHU Jinyun ZHAO Yun ZHANG Ning WANG Yingchao LIU Qi

TANG Yaoliang WEBSTER Keith YU Hong

The Second Affiliated Hospital, Zhejiang University School of Medicine, Hangzhou 310009, China

[Abstract] **Background** Growth differentiation factor 11 (GDF11), a transforming growth factor β superfamily member. The roles of GDF11 in heart diseases and cardiomyocytes (CMs) remain unclear, and little is known about the physiological and pathological functions of GDF11 in cardiomyocytes and heart. **Objective** To elucidate the cell-specific roles of GDF11 in heart under physiological and pathological conditions. **Methods** Since the GDF11 global knockout in mice resulted in perinatal lethality, we used three cardiac specific Cre line mice (Nkx2.5-Cre, cTnT-Cre, and Myh6-MerCreMer) to identify the cardiac function of GDF11 in embryonic and adult period. Mice were subjected to pressure overload caused by transverse aortic constriction (TAC) and myocardial infarction (MI). Cardiac injury was evaluated using pathological analysis, echocardiograph, haemodynamics, transmission electron microscopy, calcium transient and molecular analysis. In vitro, neonatal and adult CMs of knockout mice were used. Knockdown or overexpression of GDF11 was achieved by siRNA or lentiviral transduction of GDF11 in CMs, respectively. CMs hypertrophy was induced by culturing CMs with phenylephrine (PE) (50 μmol/L) for 24 h. CMs under hypoxia and

serum deprivation condition were to mimic the microenvironment of MI. RNA–seq was performed to identify signaling pathway and downstream targets of GDF11 in CMs. Results GDF11 was mainly derived from CMs in the heart. GDF11 expression increased in patient's heart with dilated cardiomyopathy (DCM) and MI. It also increased in mouse's heart after TAC and MI. Under basal conditions, the knockout mice have normal left ventricular structure and function. In order to identify whether GDF11 deletion at the early stage of CMs development could affect embryonic survival and cardiac morphology, GDF11 floxed mice were crossed with Nkx2.5–Cre and cTnT–Cre Tg. GDF11 deletion in early stage of CMs development does not affect the birth rate at the expected Mendelian ratios, and all mice appeared normal and showed no significant perturbations in the cardiac development. However, deficiency of GDF11 accelerated cardiac dysfunction with left ventricular dilatation, impaired angiogenesis and more fibrosis after TAC and MI. Moreover, the conditioned medium derived from GDF11 overexpressed CMs had more VEGF expression. It also stimulated tube formation of HUVECs significantly as compared with the null–vector group. The stimulation would be reversed by adding VEGF neutralized antibody into the conditioned medium. In addition to the communication with endothelial cells, CMs overexpressed GDF11 could also influence fibroblast via the secretion of anti–fibrosis mediators.Furthermore, RNA–seq shown the activation of protein synthesis signaling pathways after overexpressed GDF11 in CMs. We testified that GDF11 enhances Smad2/3 signaling and AKT–mTOR activity in cultured CMs, contributing to VEGF production and anti–fibrosis mediators. In contrast, blockage of TGFβ–Smad pathway and AKT activity by TGF–β receptor inhibitor (SB431542), Smad3 inhibitor (SIS3) and AKT inhibitors (MK–2206) blunted GDF11 overexpression–induced paracrine effect of pro–angiogenesis. GDF11 overexpression in heart with AAV9–GDF11 during TAC rescued the detrimental cardiac function of CKO mice. **Conclusion** GDF11 is necessary for cardiac function after pathological injury, which actions as an autocrine/paracrine regulatory factor, possibly through the mechanism of activation of TGFβ–Smad and AKT–mTOR signaling axis.

[Key words] GDF11; Heart failure; Cardiomyocytes; Autocrine; Paracrine manner

Anemia and risk of periprocedural stroke detected by diffusion–weighted magnetic resonance imaging in patients undergoing transcatheter aortic valve replacement

ZHU Qifeng Ng Stella LIU Xianbao WANG Jian'an

The Second Affiliated Hospital, Zhejiang University School of Medicine, Hangzhou 310009, China

[Abstract] **Background** Anemia is found to be prevalent in patients undergoing transcatheter aortic valve replacement (TAVR) and has been linked to impaired outcome after the procedure. The study aim to evaluate the association of pre–procedural anemia and the risk of periprocedural silent cerebral injury detected by diffusion–weighted magnetic resonance imaging (DW–MRI) in patients undergoing TAVR. **Methods** The study prospectively collected 158 patients who received TAVR in our center.Anemia was defined according to the World Health Organization criteria as hemoglobin < 12 g/dL in women and < 13 g/dL in men. All patients underwent DW–MRI procedure before and within 4–7 days after TAVR, and the incidence, number, and volume of new ischemic lesions were analyzed. **Results** Anemia was present in 54% (85/158) of the patients with a mean hemoglobin level of 11.2 ± 1.3 g/dL in the anemic patients. Patients with anemia had an overall worse clinical profile with older age (80 ± 6 vs. 76 ± 6, $P < 0.01$), lower body mass index (21.55 ± 3.47 vs. 23.35 ± 3.04, $P < 0.01$) and a higher mean STS score (8.77 ± 4.73 vs. 5.32 ± 2.94, $P < 0.01$). Of the 158 patients who underwent TAVR, 126 (79.7%) patients were found to have 718 new DWI–positive lesions with a mean of 4.54 ± 5.26 lesions per patient. There was no significant difference in the incidence of new ischemic lesions among the

anemic and non–anemic patients (81.18 vs. 78.1, $P > 0.05$). Additionally, the number of lesions did not differ significantly between two groups (4.46 ± 4.735 vs. 4.64 ± 5.837, $P > 0.05$). Nonetheless, patients with anemia showed to have bigger total volume/lesions in the ACA/MCA and MCA regions compared to the non–anemic patients (0.032 vs. 0.017, $P < 0.05$ and 0.055 vs. 0.034, $P < 0.05$ respectively). **Conclusion** Multiple, clinically silent ischemic brain lesions were detected in 79.7% patients after TAVR procedure. Patients with anemia were shown to have bigger total volume/lesions in the ACA/MCA and MCA regions compared to the non–anemic patients. An independent association was found between NYHA functional class, anemia and aortic mean gradient and the volume/lesion in the ACA/MCA region. However, only anemia was independently associated with the volume/lesion in the MCA zone.

[Key words] Transcatheter aortic valve replacement; MRI; Periprocedural stroke

The effectiveness of cardiac magnetic resonance imaging in diagnosis of left ventricular hypertrophy

JIN Chunna

The Second Affiliated Hospital, Zhejiang University School of Medicine, Hangzhou 310009, China

[Abstract] Objective Left ventricular hypertrophy (LVH) is a common indication for cardiac magnetic resonance imaging (CMRI) test, while well identification of the etiology is critical for the clinical management. The aim of this study is to explore the CMRI pattern of cardiac function, left ventricular (LV) strain and feature of myocardium in different diseases. **Methods** Patients referred to our imaging center for LVH evaluation from January 2017 to December 2018 were retrospectively included. All the patients underwent a standardized CMRI protocol with contrast at 1.5–T. Comprehensive imaging analysis, including cardiac volumes and mass, LV strain, extra cellular volume by T1 mapping and late gadolinium enhancement (LGE) was performed. **Results** A total of 35 cases were finally enrolled, including 7 hypertensive heart disease, 18 hypertrophy cardiomyopathy and 10 infiltrative disease. Another 16 normal subjects were recruited for normal control. All the comparison data was listed in the table. Compared with normal control, hypertensive patients had similar cardiac volume, strain and ECV data. No LGE was found in both of these two groups. Hypertrophied patients had high mass and mass index, more myocardial tissue fibrosis in LGE, but significantly reduced 3D global longitudinal strain (all $P < 0.05$) when compared to normal. Besides mass, mass index, 3D global longitudinal strain as well as myocardial fibrosis, infiltrative disease also had lower 3D global radial strain and circumferential strain ($P < 0.05$). **Conclusion** CMRI is useful in distinguishing the etiology of LVH. Both hypertrophied and infiltrative diseases have more severe mass increment, while whole 3 layers myocardium impairment detected by 3D strain may be a critical factor indicating infiltrative diseases.

[Key words] The effectiveness;Cardiac magnetic resonance imaging;Diagnosis;Left ventricular hypertrophy

Surface–anchored nanogel masking improves the engraftment and reparative potency of transplanted mesenchymal stem cells in infarcted rat hearts

ZHANG Ling LIU Guowu LYU Kaiqi WANG Yingchao ZHAO Jing HU Wangxing XIN Jinxia XIAO Changchen ZHU Keyang NAN Jinliang FENG Ye ZHU Huaying CHEN Wei ZHU Wei ZHANG Jianyi HU Xinyang WANG Ben WANG Jian'an

The Second Affiliated Hospital, Zhejiang University School of Medicine, Hangzhou 310009, China

[Abstract] **Objective** The survival and engraftment rates of stem cells that have been transplanted into infarcted hearts are poor and believed to limit the effectiveness of cell therapy. A novel approach for improving the retention and survival of transplanted cells is needed to increase the therapeutic potency. We developed a novel technique for applying a single cell coating with surface–anchored nanogel and determined whether the coating protected bone marrow mesenchymal stem cells (MSCs) from hypoxic culture conditions and improved their engraftment and therapeutic potency in the infarcted rat hearts. **Methods** The study artificially synthesize poly(sialic acid)–based anchor molecule (PAAM) that can self–assemble in the phospholipid bilayer of bone marrow mesenchymal stem cell (MSCs) membrane and which concatenates with microbial transglutaminase (mTG) that can lead to catalytic formation of gelatin hydrogel on the surface of single MSCs. Then the cell survival after single cell surface nanogel coating was detected in the hypoxia and ischemia environment in vitro and in vivo, and the cardiac function and the infarct size after cell transplantation was investigated by echocardiography and Masson's trichrome staining. Furthermore, the underlying mechanism of cell protection against apoptosis by nanogel coating was explored by RNA–seq, binding–force assay and western blot. **Results** The single MSCs coating was applied to the cell surface by using a polysialic acid–based system to anchor microbial transglutaminase to the external surface of the cell membrane, where it catalyzed the crosslinking of hydrogel molecules. The cell surface nanogel coating did not alter the pluripotency or proliferation of cultured MSCs, induced only minor changes in cytokine production, and protected the cells from hypoxia–induced apoptosis. Meanwhile, it served as a barrier between cell and environment to block the excessive apoptotic cytokines such as TNFα binding to TNFR, which in turn maintained the mitochondrial integrity and protected MSCs from TNFα–induced apoptosis via IκB/NFκB/OPA1 and PGC–1α/MFN2 pathways. Furthermore, when MSCs engineered to express GFP and luciferase were administered to hearts after myocardial infarction (MI), measurements of engraftment, cardiac function, infarct size, and vascularity were significantly better in the rats treated with nanogel–coated MSCs than with uncoated MSCs. **Conclusion** The single cell coating with surface–anchored nanogel served as a barrier and protected MSCs from apoptosis partially through reducing the TNFα binding to TNFR which in turn maintained the mitochondrial fucntion and hence improved the reparative potency of transplanted MSCs in a rat MI model.

[Key words] Single cell surface coating; Cell therapy; Myocardial infarction; Stem cells

A novel long noncoding RNA lncAng promotes angiogenesis through SNF5–mediated GDF6 expression: the lncRNA LncAng promotes angiogenesis

WU Rongrong　HU Wangxing　WANG Yingchao　LI Qingju　Chen Jinghai
ZHANG Jianyi　HU Xinyang　WANG Jian'an
The Second Affiliated Hospital Zhejiang University School of Medicine, Hangzhou 310009, China

[Abstract] **Background** Angiogenesis is essential for tissue development and homeostasis. Enhancing angiogenesis is regarded as an important therapeutic target for the salvage of stressed myocardium to reduce adverse remodeling and preserve cardiac function by restoring sufficient blood supply to the heart. However, the roles of regulatory long noncoding RNAs (lncRNAs) in mediating angiogenesis remain under–explored. Pursuant to our observations that cardiac ischemia is preferably rescued by human embryonic stem cell–derived mesenchymal stem cells (hES–MSCs) through enhanced neovascularization compared with MSCs from human bone marrow (hBM–MSCs), the study uses hES–MSCs as a model to search for novel and functionally important proangiogenic lncRNAs, and investigate their biological roles and prevalence in human cardiovascular tissues. **Methods** Highly enriched lncRNAs in hES–MSCs were searched by RNA sequencing compared to hBM–MSCs. Molecular mechanisms were investigated by RNA sequencing, RNA pull–down and immunoprecipitation, mass spectrometry, several loss– and gain–of–function approaches, chromatin immunoprecipitation and luciferase assays in hES–MSCs. Human endothelial cells, and aorta tissues from dilated cardiomyopathy (DCM) patients were studied for lncRNA expression and function. Left ventricular (LV) tissues from DCM patients were studied for the involvement of lncRNAs in the compensatory vascularization/angiogenesis. **Results** The study described a previously unannotated lncRNA AC103746.1, here termed LncAng, as one of most highly expressed intergenic lncRNAs in hES–MSCs. LncAng knockdown significantly impaired proangiogenic potential and myocardial reparative functions of hES–MSCs, while elevated expression of LncAng in either hES–MSCs or hBM–MSCs exhibited augmented angiogenesis and cardiac function recovery. Mechanistically, LncAng was transcriptionally regulated by E2F1, and functionally interacted with and recruited a chromatin–remodeling protein SNF5 [the core subunit of SWItch/Sucrose NonFermentable (SWI/SNF) adenosine triphosphate (ATP)–dependent chromatin–remodeling complexes] to the growth differentiation factor 6 (GDF6) promoter, thereby initiating GDF6 expression. GDF6 secretion from hES–MSCs promoted endothelial angiogenesis by triggering non–canonical vascular endothelial growth factor receptor 2 (VEGFR2) activation and downstream Akt/endothelial nitric synthase (eNOS) signaling. Furthermore, we found that LncAng was also expressed in human endothelial cells, and aorta tissues from DCM patients. LncAng overexpression directly enhanced endothelial angiogenic function via up–regulating GDF6, indicating the biological prevalence of LncAng–GDF6 function in mediating proangiogenesis/angiogenesis. Finally, the LncAng–GDF6 axis and PECAM1 (CD31) were synergistically up–regulated in LV of DCM patients, suggesting a possible link between the LncAng–GDF6 axis and compensatory vascularization/angiogenesis of DCM. **Conclusion** The study uncover a novel lncRNA–involved regulatory mechanism for proangiogenesis/angiogenesis. The findings support further research into the therapeutic potential of the LncAng–GDF6 pathway for ischemic cardiovascular diseases. The insights obtained from this study further advance our understanding of the physiological roles of lncRNAs in general and the growing importance of these molecules in angiogenesis.

[Key words] LncAng; GDF6; Angiogenesis; Ischemic cardiovascular diseases

Nano–hydroxyapatite induces calcification of vascular smooth muscle cells by autophagic flux blockage

LIU Qi　YU Hong

The Second Affiliated Hospital, Zhejiang University School of Medicine, Hangzhou 310009, China

[Abstract] **Background** Cardiovascular disease is the leading cause of mortality worldwide. Calcification of the arterial wall is a common characteristic of aging, diabetes, chronic renal failure, and atherosclerosis.Vascular calcification (VC) is a physiological process that predominantly involves the apoptosis of vascular smooth muscle cells (VSMCs) and the phenotypic transformation of VSMCs into osteoblast–like cells. During calcification, cytoplasmic Ca^{2+} and Pi incorporate with alkaline phosphatase (ALP) into matrix vesicles, which bud off the plasma membrane and associate with extracellular proteins, such as collagen.Crystals initially form octacalcium phosphate[$Ca_8H_2(PO_4)_6 \cdot 5H_2O$], which reorganizes and stimulates the epitaxial growth of highly insoluble hydroxyapatite ([$Ca_{10}(OH)_2(PO_4)_6$],HAp); HAp then repeats nucleation and crystallization in the same approach and expands the deposition area. Studies have showed that nano–sized hydroxyapatite (nano–HAp) can induce vascular calcification, however the underlying mechanisms remain unknown. Recently, nanoparticles were defined as a novel class of autophagy inducers. And autophagy plays a role in vascular calcification according to previous studies.However ,there lacks evidence that nano–HAp could induce autophagy changes in VSMCs.Therefore, we aim to determine whether nano–HAp could promote extracellular calcification deposition of VSMCs through modulating autophagy pathway. **Methods** Primary mouse VSMCs were isolated from aorta of male, eight–week–old C57BL/6J mice as reported previously,and cultured in Dulbecco's Modified Eagle's Medium (DMEM), treated with nano–Hap (100 μg/mL) or not.Transmission electron–microscopy (TEM), X–ray diffraction with Cu–Kα radiation and Fourier transform infrared (FT–IR) spectroscopy were used to characterize nano–HAp. Intracellular distribution of nano–Hap was observed using laser scanning confocal microscopy (LSCM) and TEM. Cell viability was evaluated using Cell Counting Kit–8. Autophagy flux was measured through Western blot, mRFP–GFP–LC3 adenovirus, transmission electron microscopy and immunofluorescence. Alkaline phosphatase (ALP) activity was used to observe osteogenic differentiation. Other calcification–associated targets were measured by Western blot. **Results** Nano–HAp was identified as nano–sized (about 100 nm in length and 10 nm in width) and rod–like shaped with crystallinity demonstrated by electron diffraction. It was internalized into VSMCs via endocytosis, and mainly located in lysosomes and autophagic vacuoles observed under TEM. VSMCs treated with nano–HAp had less cell viability. ALP activity, the expression of calcification–related proteins (RUNX2 and OPN) were increased in nano–HAp treated cells compared with control cells,Consistently, nano–HAp treatment induced significant calcification deposition of VSMCs. To elucidate the mechanism of nano–HAP on osteogenic differentiation, the osteogenic signaling pathways were examined. Nano–HAp stimulated phosphorylation of c–Jun N–terminal kinase– (JNK–) in VSMCs, and the inhibitor of JNK (sp600125) significantly attenuated ALP activity,Runx2 and OPN expression,and calcification induced by nano–HAp.What'more,we found that nano–HAp increased the number of autophagosomes in VSMCs by TEM. Western blotting revealed increased LC3II and p62 expression, indicating impairment of autophagic degradation induced by nano–HAp. Both colocalization of LC3 with Rab7,and LC3 with LAMP1 revealed nano–HAp didn't affect fusion of autophagysome and lysosome.Next,CTSD expression,Acridine Orange staining , mRFP–GFP–LC3 adenovirus,and EGFR degradation experiments demonstrated that nano–HAp impaired acdification and degradation ability of lysosome. What'more, autophagy stimulator rapamycin and autophagy inhibitor chloroquine both aggravated calcification of VSMCs induced by nano–HAp. **Conclusion** The internalized nano–HAp decreased cell viability.Nano–Hap promoted osteogenic differentiation VSMCs via activation of JNK pathway. Nano–HAp impaired autophagic flux through damaging lysosome acidification ability,which facilitated calcification caused by nano–HAp. This study will help elucidate the mechanism of

HAp-induced VSMC damage,and provide new insights into the understanding of vascular calcification development.

[Key words] Nanosized hydroxyapatite;Osteogenic differentiation;Calcification;JNK pathway;Autophagy

SRT1720 pretreatment improves survival of aged human mesenchymal stem cells in post-infarct non-human primate hearts by promoting mitochondrial biogenesis

ZENG Zhiru LIU Xianbao WANG Jian'an

The Second Affiliated Hospital, Zhejiang University School of Medicine, Hangzhou 310009, China

[Abstract] **Objective** Declined function of aged stem cells diminishes the benefits of autologous cell therapy for myocardial infarction. Mitochondrial dysfunction is associated with stem cell aging and it has received increasing attention as a target to restore aged stem cell function. Silent information regulator 1 (SIRT1) has a regulatory effect on mitochondrial dynamics. The authors have previously demonstrated SRT1720, a specific SIRT1 activator, protected aged human mesenchymal stem cells (hMSCs) against the extrinsic apoptotic pathway by upregulating FAIM1 and those cells pretreated with SRT1720 exihibited improved survival rate and achieved increased cardiac function in a rat model of myocardial infarction (MI). However, the role of mitochondria in SRT1720 mediated inhibition of apoptosis was not elucidated. The aim of the current study was to investigate the role of mitochondria in the anti-apoptotic effects of SRT1720 pretreatment of aged mesenchymal stem cells. Moreover, we evaluated the survival and therapeutic efficacy of SRT1720 pretreated aged hMSCs in non-human primate myocardial infarction models to provide evidence for future clinical application. **Methods** To study the effect of SRT1720 pretreatment on mitochondrial function, mitochondrial contents were evaluated by mitotracker staining, mtDNA measurements and expression of mitochondrial components and mitochondrial membrane potential was assessed by TMRM staining. Transmission electron microscopy was applied to assess mitochondrial morphology. As for in vivo studies, immunosupressed Cynomolgus monkeys were subjected to myocardial infarction and treated with vehicle treated or SRT1720 pretreated aged hMSCs cells or DMEM. Cardiac function, cardiac cell apoptosis, angiogenesis and aged hMSCs engraftment were evaluated. **Results** Here we report that SRT1720 protects aged hMSCs against mitochondria apoptosis pathway by increasing mitochondrial biogenesis and function. We showed that SRT1720 pretreated aged hMSCs has reduced release of cytochrome C and caspase9 activation when subjected to H_2O_2 treatment and mitochondrial morphology was better preserved indicated by transmission electron microscopy. Mitochondria contents were compared between young and aged hMSCs by quantifying mtDNA level. Consistent with previous reports, aged hMSCs had decreased mitochondrial numbers and reduced expression of PGC1α and TFAM. We found that SRT1720 increased mitochondrial biogenesis of aged hMSCs, reflected by enhanced mtDNA levels, mitotracker staining, and expression of mitochondrial components. This resulted in higher mitochondrial respiratory capacity and oxidative phosphorylation (OXPHOS) efficiency. At 3 days after transplanted in the infarcted non-human primate hearts, SRT1720 pretreated aged hMSCs had more retention rate than vehicle treated controls. And histological analysis showed that cardiac cell apoptosis was attenuated in the SRT1720 group at 3 days post MI whereas no effect of the vascular density was observed at 3 months. Concomitantly, the recovery of cardiac contractile function at 3 months post MI in the SRT1720 group tended to be better than that in the vehicle group. **Conclusion** SRT1720 promotes survival abilities of aged hMSCs in infarcted non-human primate hearts by increasing mitochondrial biogenesis and function. Although further research on the efficient strategies to rejuvenate aged hMSCs is required, the present study demonstrates that regulation of mitochondrial function through enhancing mitochondrial biogenesis is a potentially effective, low-cost, and stable treatment method to improve aged mesenchymal

stem cell survival.

[Key words] SRT1720 pretreatment;Mesenchymal;Stem cells

CCL7 blockade alleviates Ang II–induced abdominal aortic aneurysm by attenuating macrophage recruitment

XIE Cuiping YE Feiming XIE Xiaojie

The Second Affiliated Hospital, Zhejiang University School of Medicine, Hangzhou 310009, China

[Abstract] **Objective** Chemokine–mediated monocyte/macrophage recruitment contributes to the pathogenesis of abdominal aortic aneurysm (AAA). Due to the capacity to bind to multiple leukocyte receptors, the chemokine C–C motif ligand 7(CCL7) has been demonstrated to play a role in cardiovascular disease via attracting and regulating monocytes/macrophage function. However, the mechanisms underlying CCL7 importance in AAA have not yet been explained. Our study focused on the potent cytokine CCL7 involved in the recruitment of macrophages, which contributes to AAA formation. **Results** 8–10 weeks–old apo $E^{-/-}$ mice were infused with Ang II (angiotensin II) at 1000ng/kg/min for 4 weeks via osmotic minipumps to build Ang II–induced AAA. After 28 days, abdominal aortas and plasma were obtained to detect the expression level of CCL7. To test the role of CCL7 in AAA formation, CCL7–neutralizing antibody (CCL7–nAb), IgG antibody, or PBS were administered via intraperitoneal injections at baseline (before Ang II minipump implanted), and every three days after Ang II minipump implanted until the endpoint. Ang II infusion up–regulated CCL7 both in mRNA and protein level, which was accompanied by increased macrophage accumulation in abdominal aortas of $apoE^{-/-}$mice. Administration of CCL7–nAb attenuated Ang II–induced macrophage infiltration and AAA formation. In addition, in vitro data indicated CCL7 significantly contributed to the activation of M1–polarized macrophages by binding to CCR1 and activating the Jak2/STAT1 pathway. **Conclusion** Blockade of CCL7 alleviates Ang II–Induced AAA development by inhibiting macrophage recruitment and M1 polarization.

[Key words] CCL7;Blockade;Abdominal aortic aneurysm

C–X–C motif chemokine receptor 4 promotes the diastolic dysfunction in heart failure with preserved ejection fraction by enhancing macrophage recruitment and secretome

ZHANG Ning XIE Xiaojie

The Second Affiliated Hospital, Zhejiang University School of Medicine, Hangzhou 310009, China

[Abstract] **Background** Nearly half of all heart failure (HF) patients suffer from Heart failure with preserved ejection fraction (HFpEF), carrying a dismal prognosis without effective targeted therapies. However, the precise pathogenesis responsible for the HFpEF remains unknown. Studies have suggested that HFpEF correlates with macrophage activation and excessive secretion of pro–inflammatory cytokines, which drive left ventricular remodeling and diastolic dysfunction by stiffer cardiomyocytes and interstitial fibrosis. Furthermore, the chemokine CXCL12 and its receptor CXCR4 have been confirmed playing an important role in promoting the infiltration of macrophages into damaged tissues, and then activating the inflammatory cascade. However, whether CXCR4 in macrophages promotes fibrosis in HFpEF is uncleared. **Methods and Results** SAUNA (unilateral nephrectomy and a continuous infusion of d–aldosterone (0.30

μg/h) via osmotic minipumps (Alzet) and salty (1% NaCl) drinking water)was administrated to wild-type (WT) mice and myeloid-specific CXCR4-deficient mice or bone marrow (BM) reconstituted chimeric mice for 30 days. Loss of the myeloid cells-expressed CXCR4 in mice (MKO) markedly reduced cardiac inflammation, hypertrophy, fibrosis and diastolic dysfunction of HFpEF. These alterations were macrophage dependent because MKO compared with WT mice show decreased infiltration of macrophages but not neutrophils into the hearts at 30 days after SAUNA, whereas bone marrow transplantation from WT mice into MKO mice rescued the diastolic dysfunction and vice versa. In vitro, We first detected macrophage migration and cytokines secretion after HMGB1 treatment and explored the role of CXCR4 and Lyn interaction in macrophages. Then, we evaluated the paracrine effect from activated macrophages on fibroblasts through co-cultured with macrophage and fibroblasts. Consistent results were seen in vivo, suppressed Lyn phosphorylation contributed to impaired migration and cytokine secretion in CXCR4 KO macrophages. Additionally, primary fibroblasts co-cultured with CXCR4 knockout macrophages showed repressed differentiation of cardiac fibroblasts into myofibroblasts and blocked the synthesis of extracellular matrix (ECM), confirming that macrophages influence cardiac fibrosis in a CXCR4-dependent paracrine manner through TGFβ-smad2/3 signal pathway. **Conclusion** Our findings elucidate that CXCR4 in macrophages can affect left ventricular diastolic dysfunction by increasing macrophage infiltration and enhancing inflammatory secretion, and resulting in inflammation response and interstitial fibrosis.

[Key words] C-X-C motif chemokine receptor 4;Diastolic dysfunction;Heart failure

Improvement of cardiac and systemic function in old mice by agonist of growth hormone-releasing hormone

XIANG Pingping Andrew V Schally YU Hong

The Second Affiliated Hospital Zhejiang University School of Medicine, Hangzhou 310009, China

[Abstract] Background By binding to its receptor (GHRH-R) on the pituitary cellular membranes, GHRH stimulates the production of growth hormone (GH) and consequently insulin-like growth factor 1 (IGF-1). Synthetic GHRH agonists with much higher activity and increased stability compared to native GHRH peptide have been utilized to treat experiment myocardial infarction (MI), vascular calcification, diabetes mellitus, and lung damage in animal models. agonists of growth hormone-releasing hormone (GHRH) exhibit several favorable effects on heart function and remodeling. However, the GHRH agonists' effect on aging-related heart failure has not be tested. **Methods** Here we assessed whether GHRH agonist MR409 can modulate heart function and systemic parameters in old mice. Starting at the age of 15 months, mice were injected subcutaneously with MR409 (10 μg/mouse/day, *n*=8) or vehicle (*n*=7) daily for a total of 6 months. Echocardiography and body weights were measured at baseline and 5 months after treatment. Cardiac function, exercise capability and chronic inflammation in vivo and beta-gal staining and senescence-related protein P21 and reactive oxygen species in vitro were tested. **Results** Mice treated with MR409 showed improvements in exercise activity, cardiac systolic and diastolic function, survival rate, immune function, and hair growth in comparison with controls. More stem cell colonies could be grown out of the bone marrow recovered from the MR409-treated mice. In addition, there are fewer CD68+ macrophages in the heart of old mice treated with MR409 than those in the control mice. Mitochondrial oxidative phosphorylation functions of the hearts of mice treated with MR409 were also significantly improved with more mitochondrial fusion proved by electron microscope. The ratio of L-OPA1 to S-OPA1 was increased in MR409 treated mice. In vitro, fewer β-gal positive cells were observed in endothelial cells (ECs) after 10 passages with MR409. In Doxorubicin (DOX)-treated H9C2 cardiomyocytes, cell senescence marker p21 and reactive oxygen species were significantly reduced after cultured with MR409 in in Dox-treated H9C2, neonatal mouse CMs after one passage, and

HUVECs after 10 passages. MR409 also improved cellular ATP production and oxygen consumption rate in Dox–treated H9C2 cells. Mitochondrial protein OPA1 long isoform was significantly increased after treatment with MR409. Such effect could be blocked by GHRH antagonist MIA602 or PKA inhibitor H89, indicating the involvement of GHRH–R/cAMP/PKA pathway. **Conclusion** In short, GHRH agonist MR409 can reverse the aging–associated changes with respect of heart function, mobility, hair growth, cellular energy production and senescence biomarkers. The improvement of heart function may be related to a better mitochondrial functions through GHRH receptor/cAMP/PKA/OPA1 signaling pathway and relieved cardiac inflammation.

[Key words] GHRH agonist; OPA1; PKA; Senescence; Cardiac function; Exercise activity

GDF11 promote endothelial differentiation and paracrine functions of MSC on angiogenic therapy via TGFβ–R/ERK/EIF4E pathway

ZHANG Chi YU Hong

The Second Affiliated Hospital, Zhejiang University School of Medicine, Hangzhou 310009, China

[Abstract] Rationale Growth differentiation factor 11 (GDF11) is a member of the transforming growth factor–β super family. It has multiple effects on development, physiology and diseases. However, the role of GDF11 in the development of mesenchymal stem cells (MSCs) is not clear. The effectiveness of stem cell therapy for ischemia repair has been limited by the low cell survival rate, therefore, strategies for augmenting cell retention in the management of ischemia reperfusion are needed. **Objective** To explore the effects of GDF11on MSC differentiation into endothelial cells (ECs) and their proangiogenic activities in angiogenic therapy. **Methods and Results** Mouse bone marrow–derived MSCs were engineered to overexpress GDF11 along with green fluorescent protein (GFP) (MSC^{GDF11}), then exposed to hypoxia and serum deprivation for 48 hours to test cell viability, mobility, differentiation capacity and paracrine effect. Limb ischemia mice were introduced via femoral artery ligation, then received 50 μL saline buffer or MSCs or MSC^{GDF11} (1×10^6 cells) at the muscle of ischemic limb. MSC^{GDF11} showed markedly enhanced viability, mobility, and angiogenic paracrine in vitro as compared with control MSC. Meanwhile,real–time polymerase chain reaction,Western blot,flow cytometry and immunofluorescence were performed to detect the expression of EC marker during endothelial differentiation of MSCs induced by VEGF165 recombinant factor more in MSC^{GDF11} group. Expression of EC markers CD31 and VEGFR2 in both mRNA and protein levels were significantly higher in MSC^{GDF11} than the control MSCs when the cells were induced for endothelial differentiation by VEGF165. More tube formation was observed in GDF11–overexpressed MSCs in comparison with the controls. In vivo, MSC^{GDF11} had higher retention rate, resulted in better blood reperfusion, and limb salvage function after ischemic surgery for 21 days than the control MSCs. Significantly more vasculature CD31+ and α–SMA+ cells were detected in ischemic muscles that received MSC^{GDF11}. At same time, we found more MSC^{GDF11} were differentiated into CD31+ ECs and better angiogenesis was observed as compared with the control MSCs in a Matrigel plug that was implanted into mice. GDF11 activated ERK and EIF4E by enhancing their phosphorylation. The inhibitors of either TGF–β receptor or ERK can reverse the effect of GDF11 on MSC. In addition, the positive effect of GDF11 on differentiation of MSCs into ECs can be blocked by ERK inhibitor On the other hand,phosphorylation of ERK and EIF4E proteins was tremendously reduced when GDF11 in MSC was knocked down by transfection with siRNA. **Conclusion** Preconditioning MSCs with GDF11 significantly enhance endothelial differentiation and angiogenic ability in vitro and in vivo. GDF11 enhances the survival of MSCs, increases the secretion of proangiogenic factors, and augments the therapeutic potential of MSCs to promote angiogenesis. The study shed lights on the function of GDF11

to improve therapeutic angiogenesis in hindlimb ischemia with MSCs by enhancing their differentiation capability into ECs,viability, mobility, and paracrine angiogenic ability via TGF β –R/ERK/EIF4E pathway.

[Key words] GDF11;MSC;Angiogenic therapy;TGF β –R/ERK/EIF4E pathway

A comparative study of cardiac computed tomography angiography measurement for optimal sizing of the watchman device on the left atrial appendage closure

YE Jian FAN Youqi

The Second Affiliated Hospital, Zhejiang University School of Medicine, Hangzhou 310009, China

[Abstract] **Objective** To evaluate the assessment of cardiac computed tomography angiography (cCTA) for Watchman device size selection in patients on the percutaneous left atrial appendage (LAA) closure. **Methods** 51 patients underwent the Watchman device implantation were included in this retrospective study. They both received pre–procedural measurements of LAA ostium and landing zones by TEE, cCTA. cCTA measurements (CTlanding, CTdepth, CTmax, CTmin, CTmean), and TEE measurement (TEEmax) were determined for each patient, and correlated with the final device size. Clinical, procedural, and imaging data collection were analyzed. **Results** All the patients (mean age :(69 ± 8.5) years,49%female, CHA_2DS_2–VASc score of (3.8 ± 1.6) and HAS–BLED score of 2.8 ± 1.2) had successful LAA closure based on cCTA/TEE. CTmean, showed strongest correlation with the final Watchman device size (Spearman's rho is 0.615, $P < 0.01$), and CTmean–predicted Watchman device sizing showed no significant difference with the final deployed size ($P > 0.05$). Only 2 patients of population (4.9%) had a mild peri–device leak at post–procedure follow up. **Conclusion** cCTA based LAA device size selection of patients was more accurate method compared to TEE based measurement of Watchman device. A standardized pre–procedural cCTA protocol for assessment of Watchman device–size selection might be improve the long–term outcomes in the LAA device implantation.

[Key words] A comparative study;Cardiac computed tomography angiography; Measurement

Long noncoding RNA Cfast regulates cardiac fibrosis

ZHANG Feng FU Xuyang Masaharu Kataoka LIANG Tian GAO Feng LIU Ning DONG Xiaoxuan HU Xiaoyun ZHU Wei YU Hong HU Xinyang WANG Jian'an WANG Dazhi CHEN Jinghai

The Second Affiliated Hospital, Zhejiang University School of Medicine, Hangzhou 310009, China

[Abstract] **Objective** Cardiac fibrosis occurs in most cardiac disease, reduces cardiac muscle compliance, impairs both systolic and diastolic heart function and ultimately leads to heart failure. Long noncoding RNAs (lncRNAs) are recently emerging as important regulators of a variety of biological processes. However, little is known about the expression and function of lncRNAs in cardiac fibrosis. We aimed to identify cardiac fibroblasts (CFs)–enriched lncRNAs and investigate their role in regulation of cardiac fibrosis and heart function. **Methods** The study performed microarray–based transcriptome profiling on mouse infarcted heart and from Microarray analysis the study found a cardiac fibroblasts– enriched lncRNA, namely Cfast. The study used lentivirus system to knockdown Cfast expression to investigate the functional regulation of Cfast in cardiac fibrosis in vivo and vitro. The study further performed

RNA pull down to find its downstream target protein for elucidating the molecular regulation of Cfast in cardiac fibrosis. **Results** The study identified Cfast is a cardiac fibroblast–enriched lncRNA and is up–regulated after myocardial infarction. Knockdown of Cfast in cardiac fibroblast, resulted in a significant down regulation in both mRNA and protein expression of fibrotic ECM–related gene. At the same time, the study observed a significant decrease of α–SMA positive cells and a noticeable attenuation of the migratory ability of Cfast–silenced fibroblasts. We next tested the therapeutic potential of Cfast inhibition in treatment of cardiac fibrosis in mouse hearts by loss–of–function approach. After 28 days of MI, the study found that mice with Cfast depletion exhibited significantly improved cardiac function. Immunohistochemical analysis showed that scars of Cfast knockdown mice contained more cardiomyocytes compared with control hearts. Histological analysis revealed that Cfast inhibition significantly reduced scar formation in infracted heart as well. To better understanding of the therapeutic effect of Cfast depletion on cardiac fibrosis, the study employed another chronic pathological model with modest induction of cardiac fibrosis by daily injection of isopropanol (30mg/kg) for 21 days in wide type mice. The study found that Cfast depletion significantly prevented isopropanol–induced cardiac pathological fibrosis in the heart. This protective evidence was also supported by the impact on expression of the molecular marker genes, as a significant reduction of Nppa, Nppb, and Myh7 and of cardiac fibrosis associated genes, Col1a1, Col3a1, Eln, and α–Sma upon Cfast depletion. Finally, we performed RNA pull–down assay to elucidate the molecular mechanism.Among analyzed lncRNAs binding partners, five proteins were detected as specifically interacted with Cfast. Nevertheless, considering the subcellular localizations and documented reports, we speculated COTL1 can act as a functional binding protein because COTL1 involves in TGFβ signaling pathway. To confirm the mass spectrometry data, we performed independent batch of Cfast RNA pull–down assay, and then used western blotting experiment to detect COTL1 after the lncRNA pull–down. The binding of COTL1 was clearly observed in Cfast pull–down but not in the control samples. The association of COTL1 with Cfast was further confirmed by RNA immunoprecipitation. Co–immunoprecipitation assays indiated that COTL1 competitively binds with TRAP1, leads to abrogate the interaction of TRAP1 with SMAD4 and thus suppresses the formation of SMAD2/3/4 complex. **Conclusion** The study identified a novel cardiac fibroblast–enriched lncRNA, named Cfast, as an important regulator in the process of cardiac fibrosis. Cfast depletion clearly exhibits protective effects from pathological fibrotic remodeling and improves cardiac function upon pathological stress.Cfast exerts its function via binding COTL1 and consequently affects TRAP1/SMAD mediated down cascades of fibrotic signal. The study indicates that Cfast may represent a potential target in antifibrotic RNA therapy in heart diseases.

[Key words] Long noncoding;RNA;Cfast

TPP1 enhances therapeutic efficacy of aged mesenchymal stem cells in myocardial infarction

YU Kaixiang ZENG Zhiru CHENG Si HU Wangxing GAO Chenyang LIU Feng CHEN Jinyong Qian Yi XU Dilin ZHAO Jing LIU Xianbao WANG Jian'an

The Second Affiliated Hospital Zhejiang University School of Medicine, Hangzhou 310009, China

[Abstract] Backgrounds Poor cell survival after transplantation restricts the therapeutic potential of mesenchymal stem cell (MSCs) transplantation into infarcted hearts, especially in aged individuals. TPP1, a component of the Shelterin complex which is involved in telomere protection, is highly expressed in young MSCs, but declines in aged MSCs. Here, we aimed to explore whether TPP1 overexpression in aged MSCs could improve cell viability both in vivo and in vitro. **Methods** Aged MSCs overexpressing TPP1 were injected into the peri–infarct area of heart after left anterior

descending coronary artery ligation in the mouse. In parallel, to evaluate the effects at the cell level, H_2O_2 was applied to MSCs in vitro to mimic the microenvironment of myocardial injury. **Results** In vivo, transplantation of aged MSCs overexpressing TPP1 resulted in improved cell survival, enhanced cardiac function and reduced fibrosis as compared to unmodified aged MSCs. In vitro, TPP1 overexpression protected aged MSCs from H_2O_2–induced apoptosis and enhanced DNA double–strand break (DSB) repair. In addition, the phosphorylation of AKT and the key DSB repair protein MRE11 were both significantly upregulated in aged MSCs overexpressing TPP1. **Conclusion** The results reveal that TPP1 can enhance DNA repair by the AKT/MRE11 pathway, thereby improving the therapeutic effects of aged MSC transplantation and offering great potential in the clinical application of autologous transplantation in aged patients.

[Key words] TPP1 enhances;Therapeutic efficacy;Mesenchymal stem cells; Myocardial infarction

Knockdown of estrogen–related receptor α inhibits valve interstitial cells calcification in vitro via regulating heme oxygenase 1

HU Wangxing WU Rongrong GAO Chenyang LIU Xianbao WANG Jian'an

The Second Affiliated Hospital, Zhejiang University School of Medicine, Hangzhou 310009, China

[Abstract] **Background** Calcific aortic valve disease (CAVD) is the most common valvulopathy in developed countries and is characterized by inflammation, extracellular matrix (ECM) remodeling and calcification, leading a narrowing of the valve and the consequential obstruction of the cardiac outflow. A lot work has shown that valve interstitial cells within the aortic valve cusps when stimulated could differentiate toward an osteoblast–like cell and deposit bone–like matrix that leads to leaflet stiffening and calcific aortic valve stenosis. However, the mechanisms that promote pathological phenotypes in valve interstitial cells are still not clear. Nuclear receptors (NRs) regulate the transcription of genes involved in mitochondrial biogenesis in a tissue–specific manner. Accumulating evidence has suggested that NRs make contributions to calcific vascular and valvular disease. Estrogen–related receptor α (ERRα and NR3B1 (ESRRA)) is an orphan nuclear hormone receptor capable of regulating transcription of genes involved in multiple cellular and physiological processes. However, the role of ERRα in valve calcification has not been investigated to date. The aim of the present study was to examine the role of ERRα in aortic valve calcification. **Methods** Aortic valve leaflets were collected from CAVD patients (*n*=10) undergoing aortic valve replacement, and Control samples (no calcified aortic valve tissue) were taken from age–matched patients who had severe insufficiency without calcification (*n*=7) and patients who underwent heart transplantation due to late stage of cardiomyopathy (*n*=3). We compared the protein level of ERRα by Western blot and immunohistochemistry between the non–calcific valve and the calcific ones. In vitro study, valve interstitial cells (VICs) were isolated from the control aortic valve cusps and cultured in calcifying medium to induce calcification. Treated with 10 uM XCT790 or ERRα small interfering RNA silencing to inhibit ERRα or overexpression of ERRα by lentivirus, the samples were assessed for calcium nodule formation, and calcific markers using alizarin red staining, ALP enzyme activity assay, Western blot and qPCR. The effect of ERRα on osteoblastic transdifferentiation and its downstream pathway were also studied. **Results** This study had found that the protein level of ERRα is upregulated in CAVD samples versus the controls; moreover, during osteogenic differentiation of hVICs, the expression of ERRα is increased as the cultural time increased. Furthermore, the study found that inhibition of ERRα prevented OM–induced upregulation of Runx2 and ALP. The ALP activity was markedly attenuated by ERRα silencing. Alizarin red staining revealed that shRNA–mediated ERRα knockdown markedly suppressed calcified nodules formation. Meanwhile, the content of calcium was significantly reduced. The study also proved that ERRα overexpression enhances osteogenic

potential of hVICs. In addition, RNA sequencing results suggested that heme oxygenase-1 (Hmox1) was a downstream target of ERRα and it was further confirmed by western blot. Additionally, the study also found that downregulation of Hmox1 with shHmox1 efficiently reversed the inhibition of calcification induced by ERRα shRNA in hVICs. ChIP-qPCR and luciferase assay indicated that Hmox1 was negatively regulated by ERRα. **Conclusion** The present results indicate that knockdown of ERRα could impair the osteoblastic transdifferentiation of VICs, suggesting that inhibition of ERRα is a potential therapeutic strategy for the prevention of aortic valve calcification.

[Key words] ERRα;Impair;Prevention

Role of Piezo1 in heart failure progression via regulation of Ca^{2+} handling

SU Sheng'an ZHANG Yuhao XI Yutao LI Wudi MA Hong XIANG Meixiang

The Second Affiliated Hospital, Zhejiang University School of Medicine, Hangzhou 310009, China

[Abstract] Background Heart failure (HF) is a complex syndrome associated with an aggressive activation of mechanical stress that leads to deleterious cardiac remodeling including both structural and electrical remodeling. However, the underlying mechanisms of this syndrome are poorly understood. Piezo1 is a newly recognized ion channel sensitive to mechanical cues while its role in HF is unclear. **Objective** This study evaluated the role of Piezo1 in HF progression. **Methods** Piezo1 was examined in human failing myocardium and in a post-myocardial infarction (PMI) HF model evaluated in wild-type (wt-PMI) and myocardium Piezo1 conditional knockout mice ($Myh6^{cre+}Piezo1^{fl/fl}$-PMI). Meanwhile, human induced-pluripotent stem cell derived cardiomyocytes (hiPSC-CMs) were employed to assess the effect of Piezo1 in cardiomyocyte electrical activity. **Results** Piezo1 was up-regulated in human and murine failing myocardium. Compared with wt-PMI, hearts from $Myh6^{cre+}Piezo1^{fl/fl}$-PMI mice had better cardiac function and attenuated structural remodeling. $Myh6^{cre+}Piezo1^{fl/fl}$-PMI mice showed significantly fewer ventricular arrhythmias and lower mortality after isoproterenol administration. Ameliorated cardiac function in $Myh6^{cre+}Piezo1^{fl/fl}$-PMI mice was associated with prevention of $Ca2^{+}$ dynamic impairment linked to HF, including smaller and longer intracellular $Ca2^{+}$ concentration transients and a up-regulation of the sarcoplasmic reticulum $Ca2^{+}$ adenosine triphosphatase pump. Similar results were also witnessed in hiPSC-CMs. Piezo1 activation via specific agonist Yoda1 led to aggravated beating rate of hiPSC-CMs, as well as the dramatically increased risk of arrhythmia. **Conclusion** Piezo1 modulated intracellular $Ca2^{+}$ mishandling in HF, emerging as a new target for HF therapy.

[Key words] Piezo1;$Ca2^{+}$;Heart failure

Angiotensin II type 2 receptor as a novel modulator in the function of human umbilical vascular endothelial cells

BIAN Chang

The Second Affiliated Hospital, Zhejiang University School of Medicine, Hangzhou 310009, China

[Abstract] Objective To clarify the effect of AT2R on the expression of NO, PAF, MCP-1 and Claudin-5 in the cultured HUVECs. **Methods** With the use of Ang II, AT1R antagonist losartan, AT2R specific agonist C21and its specific antagonist PD-123319, the expression of NO, PAF, MCP-1 was measured, and the function of Claudin-5 was tested

in cultured HUVECs. **Results** Losartan could attenuated Ang II's effect on the expression of NO, PAF, MCP-1. When AT2R agonist C21 was added, the expression could be further decreased to normal value which could be reversed by PD-123319. However, there is no obvious effect with Claudin-5. **Conclusion** Our study suggests that Ang II could change the expression of NO, PAF, and MCP-1. The effect could be annulated by AT1R antagonist losartan. AT2R specific agonist C21could further attenuated the effect by Ang II, which could be reversed by PD-123319.

[Key words] Angiotensin II type 2 receptor;Modulator;Human umbilical vascular endothelial cells

SGLT2i promotes advanced atherosclerotic plaque regression in non-diabetic ApoE$^{-/-}$ mice through activating PPAR

CHEN Haibo

The Second Affiliated Hospital, Zhejiang University School of Medicine, Hangzhou 310009, China

[Abstract] Previous studies demonstrated that application of sodium-glucose cotransporter 2 inhibitor (SGLT2i) significantly decreased the incidence of AS-related cardiovascular events, which is mainly through reducing inflammation. Meanwhile, studies have showed that SGLT2i could promote AS plaque regression and relieve inflammation. However, the underlying signaling pathway remains unclear.

[Key words] SGLT2i;Promote;Advanced atherosclerotic plaque regression

Canagliflozin inhibits stenosis after arterial intima injury through AMPK-HuR pathway

SHEN Jian ZHU Linjun JIANG Jun

The Second Affiliated Hospital, Zhejiang University School of Medicine, Hangzhou 310009, China

[Abstract] **Objective** To investigate the role of sodium-glucose cotransporter 2 (SGLT-2) inhibitor canagliflozin (CANA) in inhibiting the stenosis after intima injury. **Methods** Smooth muscle cells were cultured under growth medium with or without the addition of CANA and were evaluated by CCK8 to assess the rate of proliferation, and trans-well assay was applied to assess the ability of migration of the cells. HuR was measured by western blot and immunohistochemical staining to evaluate the partten of sub-location. In vivo, mice were suffered internal carotid artery injury by wire, and CANA was oral fed for 4 weeks. **Results** CANA inhibits the proliferation and migration of smooth muscle cells in vitro. The inhibitory effects of CANA was time and concentration related, which peeked at the concentration of 10nM and at the time of 48 hours. Cell cycle assay showed that SMCs were blocked in the G2/M phase after treated with CANA. Mechanically, CNAN promote HuR transplant from plasma to nucleus, which lead to the unstable of mRNA of cyclin A. Simultaneously, the protein level of cyclin A was significantly down regulated after CANA treatment. Technically, the translocation of HuR was AMPK dependent. By the inhibition of AMPK via Dorsomorphin or siRNA of AMPK, the effects of CANA is blocked. In vivo, in the CANA treated group, the area of lumen was around 0.13 mm^2, while in the control group, the area is about 0.05 mm^2 ($P<0.05$). **Conclusion** CANA significantly inhibits SMCs proliferation after artery injury. By the phosphorylation of AMPK, CANA promote HuR transplant to the nucleus, and reduced cyclin A. These results indicate that SGLT2 is a potential new strategy for the treatment of stenosis after intima injury.

[Key words] Canagliflozin;Inhibits stenosis;Arterial intima injury;AMPK-HuR pathway

Validation study of angio–based fractional flow reserve during coronary angiography

LI Changling JIANG Jun HE Jingsong XIA Yongqing LENG Xiaochang
DONG Liang SUN Yong XIANG Jianping WANG Jian'an
The Second Affiliated Hospital, Zhejiang University School of Medicine, Hangzhou 310009, China

[Abstract] **Objective** Non–wire fractional flow reserve (FFR) has been increasingly used in the clinical workflow to assist clinical decision–making for PCI intervention. This clinical study aims to evaluate the diagnostic performance (accuracy, sensitivity and specificity) of newly developed Angio–based FFR compared to wire–based fractional flow reserve (FFR) using retrospectively collected data from patients with stable angina. **Methods** 2D–QCA was performed by using anigogram vendor–integrated QCA software (Allura Xper FD20/10; PHILIPS Medical Systems, the Netherlands). Angio–based FFR was computed with the AccuFFRangio V1.0 software (ArteryFlow Technology, Hangzhou, China) by participated physicians and technicians who were blinded to FFR. Two angiographic images with projections > 25° apart at the end–diastolic frame were selected for 3D reconstruction for the segmented vessel. In this x–ray angiography system, an effective and robust calibration method is accomplished. Three physiological mates of points need to be defined for this calibration. To simplify the geometry calibration procedure and achieve a reliable correspondence in centerline points 3D reconstruction, the study have found that identifying three pairs of reference points is sufficient to approximate eliminate the isocenter offset and rotational angle parameter errors.The central premise of the estimated FFR value is the determination of reference vessel diameter. This reference has a direct impact on stenosis recognition□more specific relative narrow or long stenosis resulting in larger pressure drop and lower estimated FFR. The technique for determining a reference vessel diameter is denoted as interpolated percent diameter stenosis measurement. The blood vessel diameter curve is filtered by high frequency, and the linear interpolation is used to initially determine the reference blood vessel diameter slope. After offset transformation is made, to obtain a reference diameter line, that 80% points are below the reference radius line.Then the contrast frame count was performed in an angiographic run to calculate the flow velocity. Based on the segmented vessel, calculated velocity and input aortic pressure, AccuFFRangio distribution can be calculated through the pressure drop equation. In general, pressure drop from proximal to distal are caused by two factors. Viscous pressure drop, this term is related to friction. Briefly, longer and slimmer blood vessels cause a larger pressure drop. Expansion pressure drop term is mainly because of the rapid change of radius, which usually is the character of stenosis. **Results** In all, 300 patients with 300 vessels who underwent ICA were included in the statistical analysis. Comparison of AccuFFRangio with pressure wire–derived FFR as reference resulted in an AUC for AccuFFRangio of 0.935 (per–vessel, $P < 0.01$). Accuracy for AccuFFRangio was 92.3% in this preclinical study. Overall sensitivity, specificity, positive predictive value and negative predictive value for per–vessel were 85%, 95%, 86.1% and 94.6%, respectively. Whereas, overall accuracy, sensitivity, specificity, positive predictive value and negative predictive value for 2D–QCA were 63.3%, 42.5%, 70.9%, 34.7% and 77.2%, respectively. **Conclusion** This clinical study demonstrates that AccuFFRangio is clinically feasible and the performance is superior to angiographic assessment by 2D–QCA for evaluation of coronary artery stenosis when using FFR as a reference. The accuracy, sensitivity and specificity of AccuFFRangio in identifying hemodynamically significant coronary stenosis using 300 patient data are 93.7%, 90% and 95%, respectively. AccuFFRangio bears the potential of improving angio–based identification of functionally significant stenosis during coronary angiography procedure. We also need to notice the limitations for this clinical study. Firstly, this is a retrospective study. Secondly, the study is limited at one single center. Third, this study is an observational study. In the future, prospective, multi–center and follow–up studies will be performed in the post–market clinical studies.

[Key words] Validation study ;Angio–based;Fractional flow reserve;Coronary angiography

Left ventricle segmentation from CT based on deep neural network

SUN Yong LI Changling SONG Xiangfen ZHAO Xing FENG Li HU Tao
ZHANG Yuchen JIANG Jun WANG Jian'an Xiang Jianping
The Second Affiliated Hospital, Zhejiang University School of Medicine, Hangzhou 310009, China

[Abstract] **Objective** Cardiovascular disease is a common disease that seriously threatens human life and health. Cardiac CT angiography (CTA) has become a clinically important method for diagnosing cardiovascular disease due to its non–invasive and simple operation. Left ventricle segmentation is a key step in quantifying clinical indices such as ejection fraction (EF), left ventricular mass (LVM), wall thickening (WT), and wall motion abnormalities (WMA) etc. derived from the diastolic and systolic left ventricular volume for analysis of the cardiac function and then diagnosis and treatment of cardiovascular disease. Manual segmentation of the left ventricle is tedious and time–consuming, and is susceptible to subjective factors, thus is not feasible in clinical practice. To fully and accurately segment the left ventricle, we propose a segmentation method of left ventricle from CT based on deep neural network. **Methods** The method was based on the prototype 4–layer U–Net, deepening the network to eight layers to improve the recognition capability of left ventricle, incorporating residual blocks to better optimize the gradient flow, and introducing deep supervision mechanism and attention mechanism to further improve segmentation accuracy. The method included nine encoding blocks and eight decoding blocks, the blocks from the same layers were concatenated according to the channel dimension. The residual blocks were incorporated into each blocks and the deep supervised branches were introduced before first seven decoding blocks. The attention mechanism was added after the deep supervised branches and the main branch. This attention contained channel–wise attention and spatial–wise attention. Feature maps from different channels were multiplied by different weights to enhance the attention of the key channel domain, and feature maps from different spatial locations were multiplied by different weights to enhance the attention of the key spatial domain. The channel attention mechanism globally averaged the feature maps in each channel which ignored the spatial information, and the spatial attention mechanism could provide different weights to the different regions of feature maps in the channel. The channel attention mechanism and the spatial attention mechanism complemented each other and automatically learned the weights to pay more attention to key features for further improvement in segmentation performance. The study collected 2 901 cardiac CTA images, including training set of 2 301 and testing set of 600. Online data augmentation composed of sequential random rotation, scaling, and shear transformation was performed during the training process to improve the generalization and robustness of our method. **Results** Compared with the segmentation results from testing set of the prototype U–Net, Dice similarity coefficient (DSC) of 0.938 ± 0.144, precision of 0.941 ± 0.144, sensitivity of 0.961 ± 0.058, our method achieved DSC of 0.964 ± 0.033, precision of 0.960 ± 0.043, sensitivity of 0.970 ± 0.040, which demonstrated that our method has higher segmentation accuracy and robustness. In addition, compared with other existing studies on left ventricle segmentation from CT, our method has a competitive advantage. **Conclusion** The method based on deep neural network can accurately and effectively segment the left ventricle in cardiac CTA images, which is expected to become a reliable segmentation tool for evaluating cardiac function in the future.

[Key words] Left ventricle segmentation;CT ;Deep neural network

Diagnostic performance of fractional flow reserve derived from coronary CT angiography

XIANG Jianping　LI Changling　LENG Xiaochang　JIANG Jun　FENG Li
XIA Yongqing　JIANG Wenbing　HU Tao　SUN Yong　WANG Jian'an
The Second Affiliated Hospital, Zhejiang University School of Medicine, Hangzhou 310009, China

[Abstract] **Objective** We described the feasibility and accuracy of a novel technique to noninvasively compute FFR from coronary CTA images, termed as AccuFFRct, to detect lesion-specific ischemia of coronary artery stenosis. **Methods** In order to evaluate the diagnostic performance of AccuFFRct for exploring ischemia-causing stenosis, 76 patients with 105 vessels were retrospectively enrolled in this study to compute AccuFFRct value for each lesion and compare with the wire-measured invasive FFR value as reference. The 3D patient-specific coronary tree geometry, including aorta, was extract from CTA images using semi-automatic method. First, initial aorta images were segmented using fast marching algorithm while coronary artery images were segmented with colliding fronts method. Then, with initial segmented images, level-set algorithm was applied to find the optimal borders of the coronary tree. Finally, the study use marching cubes algorithm to extract the geometry model. In addition, the myocardium of the left ventricle was constructed automatically using the deep-learning method.Three-dimensional segmented geometries were then cleared. The blood flow and pressure of the coronary artery tree were simulated by using CFD analysis based on finite volume method and the resting flow was estimated from the myocardium mass. Myocardial demand at rest is determined by the mass of left ventricle myocardium, derived from the volume of which with the hypothesis of the constant density of myocardium. The coronary supply meets the myocardial demand at rest. To simulate blood flow rate at hyperemic state, the mean flow was increased 400% compared to baseline value. Meanwhile, the diameters of the outlets were computed and the blood flow distribution was determined by the Murry's law $Q \propto D\hat{}3$; The arterial wall was assumed to be rigid with no-slip boundary condition. To perform FFR-CT(AccuFFR®ct, version 1.0, ArteryFlow) calculation, volume mesh was generated based on the anatomic model. The flow distribution and pressure distribution of the coronary can be acquired by solving steady-state incompressible Navier-Stokes equation through a finite volume approach on a standard desktop (Intel Core i7 processors, 8 cores). While simulating blood flow in the three-dimensional coronary, blood was modeled as a Newtonian fluid (ρ=1058 kg/m^3, μ=0.0035 Pa·s). The AccuFFRct value is calculated as the pressure ratio of the distal pressure located at the measuring point of FFR to the mean aortic pressure. Currently coronary CTA image segmentation takes around 0.5 hour, while the core FFR calculation for AccuFFRct using finite volume method takes around 5 minutes. **Results** Data collected between January 2016 and September 2017 of 76 patients (62% male) with 105 vessels were retrospectively enrolled in this study to compute AccuFFRct value for each lesion and compare with wire-measured invasive FFR values as reference. Average patient age was 66 ± 8 years and body mass index was (24 ± 3) kg/m^2. The average calcification score for the CTA data was 502 ± 445. Using FFR≤0.8 as reference, we evaluated AccuFFRct performance by its accuracy, sensitivity, specificity, positive predictive value (PPV) and negative predictive value (NPV). Diagnostic accuracy, sensitivity, specificity, PPV, and NPV for AccuFFRct for per-patient basis were 92.1%, 90%, 93.5%, 90% and 93.5%, respectively; and those of AccuFFRct for the per-vessel were 89.5%, 90%, 89.3%, 77.1% and 95.7%, respectively. Direct correlations between computed AccuFFRct and measured FFR were 0.69 for per-patient and 0.61 for per-vessel basis, respectively. AUC values of AccuFFRct for per-patient and per-vessel basis were 0.94 and 0.91, respectively. **Conclusion** AccuFFRct computed from coronary CTA images could be an accurate and time-efficient computational tool for detecting lesion-specific ischemia of coronary artery stenosis. Further validation is required in a large prospective multicenter study.

[Key words] Diagnostic performance;Fractional flow reserve;Coronary CT ngiography

All-trans retinoic acid increase peripheral $CD4^{-}CD25^{+}Foxp3^{+}$T cells and inhibit the expression of the NFκB-p65 signal in early stage of atherosclerotic plaque of rats aorta

CHEN Zhangqiang

Jiangxi Provincal People's Hospital, Nanchang 330006, China

[Abstract] **Objective** To investigate the effect of all-trans retinoic acid on regulatory T lymphocytes and the NF-κB in the early stage of atherosclerotic plaque of rats. **Methods** Fifty SD rats were randomly divided into normal control group, high fat model group, immunized model group, immunized high fat model group and all-trans retinoic acid treated group, every group was five SD. Immunized model group, immunized high fat model group and All-trans retinoic acid treated group were treated with immunization method and/or high fat method to establish atherosclerosis model. All-trans retinoic acid treated group was given all-trans retinoic acid at the basis of immunized high fat model group, the rest of the non-treatment group fed with volume of saline. Collect peripheral blood and aortic tissue after 16 weeks. The frequency of $CD4^{+}CD25^{+}Foxp3^{+}$T cells in peripheral blood was measured by flow cytometry. The changes of cytokines in serum were detected by enzyme-linked immunosorbent assay (ELISA). The expression of NFκB-p65 was detected by Western blotting. **Results** Compared with the control group, the degree of atherosclerosis in the high-fat model group and the high-fat immunized model group was significantly increased; The frequency of $CD4^{+}CD25^{+}Foxp3^{+}$ T cells in the peripheral blood of the immunized model group and the high-fat immunized model group were significantly decreased ($P<0.05$), the levels of IL-1β and IL-6 were significantly increased, the levels of IL-10 and TGF-β were significantly decreased, and the expression of NFκB-p65 protein in the aorta was significantly increased ($P<0.05$). Compared with the immunized model group and the high-fat immunized model group, The frequency of $CD4^{+}CD25^{+}Foxp3^{+}$T cells increased significantly ($P<0.05$), and the levels of IL-1β and IL-6 were significantly decreased in all-trans retinoic acid-treated patients ($P<0.05$), and the expression of NFκB-p65 was also significantly decreased ($P<0.05$). **Conclusion** All-trans retinoic acid may inhibit the expression of NFκB-p65 signal in early stage of atherosclerotic plaque and increase the protective effect of atherosclerotic plaque by up-regulating the ratio of peripheral regulatory T cells and the level of anti-inflammatory cytokines.

[Key words] All-trans retinoic acid; $CD4^{-}CD25^{+}Foxp3^{+}$T cells; NFκB-p65 signal

Application of balloon dilation in pregnant women of rheumatic heart disease with mitral stenosis:our experience

CHEN Zhangqiang

Jiangxi Provincal People's Hospital, Nanchang 330006, China

[Abstract] **Objective** To explore the efficacy and safety of balloon dilation in pregnancy women of rheumatic heart disease with mitral stenosis. **Methods** Forty pregnancy women suffered from rheumatic heart disease with mitral stenosis included in our hospital, 20 cases of moderate, 20 cases of severe stenosis, mitral valve area of an average of (0.9 ± 0.3) cm^2. mean (7.6 ± 2.5 months) of pregnancy. during procedure patients' lower back with anti-radiation lead mat pad. expansion of the end of the left atrial pressure decreased more than 50%, or the average left atrial pressure below 15mmHg, diastolic murmur of mitral valve area disappeared or significantly reduced. **Results** 40 cases of pregnant

patients after balloon dilation, mitral valve area of an average of (1.8 ± 0.3) cm^2 increased significantly compared with the preoperative an average of (0.9 ± 0.3) cm^2 ($P < 0.01$). Postoperative left atrial diameter (40.5 ± 5.5) mm, compared with the preoperative (48.5 ± 5.8) mm significantly reduced ($P < 0.01$). The average postoperative left atrial pressure (19.5 ± 6.5) mmHg significantly reduced compared with preoperative (27.4 ± 6.5) mmHg ($P < 0.01$). Postoperative left atrioventricular valve MTPG (6.8 ± 2.5) mmHg significantly reduced compared with the preoperative (14.4 ± 3.5) mmHg ($P < 0.01$). Pulmonary artery pressure decreased significantly after procedure ($P < 0.01$). Left ventricular ejection fraction appeared no significant change ($P > 0.05$). **Conclusion** Percutaneous balloon dilatation is an effective treatment for pregnant patients suffered from severe rheumatic mitral stenosis and can reduce symptoms, improve quality of life, improve the prognosis of pregnancy.

[Key words] Application;balloon dilation;Pregnant women;Rheumatic heart disease;Mitral stenosis

●病例分析

心脏永久起搏器植入术后应激性心肌病 1 例

叶士勇　吕玲春　施振华

作者单位：323000　丽水市中心医院

慢性活动性 EB 病毒感染致大量心包积液 1 例

叶士勇　吕玲春　徐浩翔　毛卫波　金陽缙

作者单位：323000　丽水市中心医院

心房颤动伴心功能不全的护理体会 1 例

顾丽君

作者单位：315000　宁波市第一医院

以腹痛为首发表现的心肌梗死心肺复苏后溶栓 1 例

郑杨剑　林韩立

作者单位：316100　舟山普陀医院

急性心肌梗死合并肝硬化凝血功能异常 1 例

阳泽文　陈小芳　王晓艳　骆高江

作者单位：322000　义乌市中心医院

腰椎间盘突出患者并发主动脉夹层 1 例

薛捷文

作者单位：750004　宁夏医科大学总医院

心房颤动伴左束支传导阻滞 1 例

刘小青

作者单位：310006　杭州市第一人民医院

33 次电除颤抢救急性心肌梗死致电风暴患者的护理 1 例

高岭燕

作者单位：325000　温州医科大学附属第二医院（温州医科大学附属育英儿童医院）

心房颤动、心房扑动射频导管消融术后房性心动过速 1 列

张琪

作者单位：322000　义乌，浙江大学医学院附属第四医院

频发室性期前收缩 1 例

葛久欣

作者单位：322000　义乌，浙江大学医学院附属第四医院

体表胸导 55 导联心电图评价扩张型心肌病心肌纤维化 1 例

董瑞庆　夏灵　陈弹　周亚峰　杨翠微　邓冬东

作者单位：215000　苏州大学附属独墅湖医院

造影剂脑病 1 例

范媛媛

作者单位：100191　北京大学第三医院

心电图类似于左主干病变的中间支病变 2 例

陈多学

作者单位：233600　安徽省亳州市人民医院

非诺贝特致慢性肾脏病患者横纹肌溶解 1 例

贾益仑

作者单位：310006　杭州，浙江省中医院（浙江中医药大学附属第一医院）

Wellens 综合征 1 例

赵博文

作者单位：310006　杭州，浙江省中医院（浙江中医药大学附属第一医院）

卵圆孔未闭封堵 2 例

李心怡

作者单位：310006　杭州，浙江省中医院（浙江中医药大学附属第一医院）

三尖瓣重度反流患者行导管三尖瓣置换术的围术期护理 1 例

余东鹤

作者单位：310000　杭州，浙江大学医学院附属第二医院

室性心动过速电复律后心肌致密化不全伴扩张性心肌病患者的护理 1 例

何杰

作者单位：310000　杭州，浙江大学医学院附属第二医院

急性心肌梗死合并心源性休克患者的护理 1 例

张晶晶

作者单位：310000　杭州，浙江大学医学院附属第二医院

心肌梗死患者行经皮冠状动脉介入术后并发失血性休克的护理 1 例

曹金

作者单位：310051　杭州，浙江大学医学院附属第二医院

右心室心肌病合并反复右心血栓形成 1 例

魏渠成

作者单位：310009　杭州，浙江大学医学院附属第二医院

急性心肌梗死并发心脏破裂患者护理 1 例

管敏芳

作者单位：315010　宁波市第一医院

国产 CTO 导丝应用 2 例

毛晓波

作者单位：311399　杭州，华中科技大学同济医学院附属协和医院

药物快速控制、治愈长期频发室性期前收缩 1 例

徐汉友

作者单位：313399　湖州市安吉联生医院

高尿酸血症诱发中学生运动性哮喘 1 例

徐汉友

作者单位：313399　湖州市安吉联生医院

非诺贝特致慢性肾脏病患者横纹肌溶解 1 例

贾益仑

作者单位：310003　杭州，浙江省中医院（浙江中医药大学附属第一医院）

沙库巴曲缬沙坦治疗射血分数降低的心力衰竭伴终末期肾病血液透析患者 1 例

刘生华　傅路红

作者单位：322118　金华文荣医院

钩端螺旋体病引起的心肌损伤及多脏器功能衰竭 2 例

朱佳贞

作者单位：325000　温州医科大学附属第一医院

左冠状动脉起源右冠状窦致急性心肌梗死 1 例

包程鸿

作者单位：321300　金华市中心医院

经导管主动脉瓣置换术治疗白塞病合并重度主动脉瓣反流 1 例

蒋巨波　刘先宝　高峰　范嘉祺　林心平　蒲朝霞　孔敏坚　董爱强　徐勇　周琦晶　王建安

作者单位：310009　杭州，浙江大学医学院附属第二医院解放路院区

生物瓣衰败经导管行双瓣中瓣置换术的护理配合 1 例

温红梅　许娇阳　甘婉瑜　钟伟琼　卞洋洋

作者单位：361004　厦门大学附属心血管病医院 (厦门市心脏中心)

植入永久起搏器术后并发囊袋感染的救治和护理 1 例

陈洁莹

作者单位：310009　杭州，浙江大学医学院附属第二医院

急性 ST 段抬高型心肌梗死合并三度房室传导阻滞的救治和护理 1 例

邵翠梅

作者单位：310009　杭州，浙江大学医学院附属第二医院

经皮心包穿刺行心外膜室性期前收缩射频导管消融术的护理体会 1 例

姚晓芳

作者单位：310009　杭州，浙江大学医学院附属第二医院解放路院区

心动过速性心肌病并发心源性休克 2 例并文献复习

郑杨剑　吴亚楠

作者单位：316100　舟山市普陀区人民医院

Burgada 综合征合并间歇性右束支传导阻滞植入式心律转变复除颤器电风暴 1 例

潘小宏

作者单位：310009　杭州，浙江大学医学院附属第二医院

超级横位心经导管主动脉瓣植入术 1 例

陈毓文

作者单位：310009　杭州，浙江大学医学院附属第二医院解放路院区

Systemic embolism with left atrial thrombus occurred 4 years after left atrial appendage occlusion in atrial fibrillation: a case report

ZHAO Zhihong

Shanghai Pudong New Area Zhoupu Hospital, Shanghai University of Medicine & Health Sciences Affiliated Zhoupu Hospital, Shanghai 201318, China

Rumpel–Leede Sign after coronary angiography: a case report

GUI Yang

Zhejiang Provincial People's Hospital, People's Hospital of Hangzhou Medical College, Hangzhou 310014, China

An intramural left ventricular fistula caused by left ventriculography: a case report

GE Wenjun

Hospital of Chengdu University of Traditional Chinese Medicine,Chengdu 610072,China

The evolvement of de Winter pattern related with stenosis of left main coronary artery: a case report

YANG Lingfeng

The First Affiliated Hospital of Zhejiang Chinese Medical University, 310006 Hangzhou, China

Specific medication combined with percutaneous balloon mitral valvotomy for treatment of the lutembacher syndrome with pulmonary hypertension: a 14–patient case series

CHANG Xiaoxin　ZHOU Daxin　XU Yawei
Shanghai Tenth People's Hospital of Tongji University,Shanghai 200000, China

Apex–to–femoral rail technology for horizontal aorta in transcatheter aortic valve replacement

DAI Hanyi　LIU Xianbao
The Second Hospital Affiliated to Zhejiang University School of Medicine, Hangzhou 310009, China

A successful case of post–TAVR His bundle pacing

LYU Fei　PAN Xiaohong　FAN Jia　WANG Lihan　YANG Dandan　LIN Xinping
LI Huajun　ZHU Qifeng　LIU Xianbao　WANG Jian'an
The Second Affiliated Hospital, Zhejiang University School of Medicine, Hangzhou 310009, China

Doxorubicin induced delayed heart failure with preserved EF: a brief report

LYU Fei　YANG Dandan　PAN Xiaohong
The Second Affiliated Hospital, Zhejiang University School of Medicine, Hangzhou 310009, China

Myocardial infarction caused by a leukemic clot: a case report

LI Jing　DONG liang
The Second Affiliated Hospital, Zhejiang University School of Medicine, Hangzhou 310009, China

Alcohol septal ablation for the treatment of obstructive hypertrophic cardiomyopathy in a patient with prior transcatheter aortic valve replacement

LIN Xinping　LIU Xianbao
The Second Affiliated Hospital, Zhejiang University School of Medicine, Hangzhou 310009, China

中国标准连续出版物号：ISSN 2095-3933 CN 33-1377/R　　国内邮发代号：32-61　　国内定价：25.00 元